AD-A114 957   EG AND G WASHINGTON ANALYTICAL SERVICES CENTER INC R--ETC F/G 13/10
               VALIDATION OF COMPUTER MODELS OF CABLE SYSTEM DYNAMICS.(U)
               APR 82 D B DILLON   N68305-80-C-0020
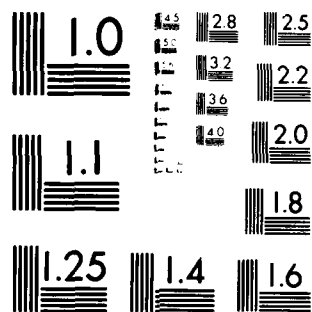UNCLASSIFIED   NCEL-CR-82.015   NL

MICROCOPY RESOLUTION TEST CHART

NATIONAL BUREAU OF STANDARDS 1963 A

REPORT DOCUMENTATION PAGE		READ INSTRUCTIONS BEFORE COMPLETING FORM
1. REPORT NUMBER CR 82.015	2. GOVT ACCESSION NO. AD-A114 957	3. RECIPIENT'S CATALOG NUMBER
4. TITLE (and Subtitle) Validation of Computer Models of Cable System Dynamics		5. TYPE OF REPORT & PERIOD COVERED Final May 1980 - May 1981
		6. PERFORMING ORG. REPORT NUMBER
7. AUTHOR(s) David B. Dillon		8. CONTRACT OR GRANT NUMBER(s) N68305-80-C-0020
9. PERFORMING ORGANIZATION NAME AND ADDRESS EG&G Washington Analytical Services Ctr., Inc. 2150 Fields Road Rockville, MD 20850		10. PROGRAM ELEMENT. PROJECT, TASK AREA & WORK UNIT NUMBERS PE62759N YF50.556.091.01.402
11. CONTROLLING OFFICE NAME AND ADDRESS Naval Civil Engineering Laboratory Port Hueneme, CA 93043		12. REPORT DATE April 1982
		13. NUMBER OF PAGES 188
14. MONITORING AGENCY NAME & ADDRESS(if different from Controlling Office)		15. SECURITY CLASS. (of this report) Unclassified
		15a. DECLASSIFICATION DOWNGRADING SCHEDULE

16. DISTRIBUTION STATEMENT (of this Report)

Approved for public release; distribution unlimited.

17. DISTRIBUTION STATEMENT (of the abstract entered in Block 20, if different from Report)

18. SUPPLEMENTARY NOTES

19. KEY WORDS (Continue on reverse side if necessary and identify by block number)

Mooring; Cables; Ropes; Mathematical models; Dynamics; SEADYN;
SNAPLOAD; Mooring design; Mooring dynamics; Cable dynamics;
Dynamic models

20. ABSTRACT (Continue on reverse side if necessary and identify by block number)

Comparisons are made between measurements taken during
four series of dynamic cable experiments and simulations of the
experimental events using two computer models, SEADYN and SNAP-
LOAD, under the sponsorship of the Naval Civil Engineering
Laboratory. Three of the experiments were conducted in labora-
tory water tanks using an elastically stiff nylon cord and a

DD FORM 1473 EDITION OF 1 NOV 65 IS OBSOLETE
1 JAN 73

soft silicon rubber cable.

The first experiment used cables 6 feet long. Five distinct geometries were measured, including simulation of the anchor-last deployment of a single mooring leg, the relaxation of a subsurface mooring from a displaced condition, and the response of a load suspended along a cable fixed at one end and moved around a circle at the other. The deployment and relaxation simulations were repeated in the second experimental series using cables 60 feet long. The tension was measured during the third series while a weight suspended from the nylon or rubber cable was paid out or reeled in from a small winch. The winch base could be oscillated vertically to simulate wave action.

The fourth experiment was the deployment of a full-size instrumented subsurface mooring in 2,500 feet of water off Kauai, Hawaii as part of the joint Mooring Dynamics Experiment (MDE) conducted in late 1976.

SEADYN is a general three-dimensional model of the dynamic response of cable networks to environmental changes using a nonlinear finite element techniques in the time domain. SNAPLOAD uses the lumped parameter method to model the dynamics of serially connected cables suspended in a vertical plane. Both models are shown to reproduce all the significant motions and forces in the modeled events, but tension are introduced in both models by the inaccurate hydrodynamic drag coefficients that they use.

Material damping caused by elastic hysteresis in the cable material is found to play a significant part in smoothing the computation of cable tension, enen though it has little overt relation to the overall event. Small amounts of material damping are sufficient to prevent undersirable oscillations between model nodes; larger values enable SEADYN to accurately model the forced oscillation of the anchor as the length of the suspension cable was varied through resonance.

The laboratory experiments were restricted to serially connected cables and special buoys or anchors suspended in a vertical plane in still water in order to make the data useful for comparing simple computer models as well as stances by comparing equilibrium and steady-state conditions to results obtained from elementary theory. The data from all four experiments are available for evaluating other models.

ACKNOWLEDGEMENT

v

TABLE OF CONTENTS

LIST OF ILLUSTRATIONS

LIST OF ILLUSTRATIONS (Cont'd)

LIST OF ILLUSTRATIONS (Cont'd)

LIST OF ILLUSTRATIONS (Cont'd)

LIST OF TABLES

LIST OF TABLES (Cont'd)

SECTION I

INTRODUCTION

1.1 BACKGROUND.

Large rigid structures are supported by foundations resting deep in the earth. This obvious convenience is manifest in most land based civil engineering. When the environment restricts access to suitable foundation supports, other design concepts must be used. Suspension bridges are one method to simplify construction when foundation supports are difficult to access: concentrate the rigid structure at a few points. In the ocean, not only the remoteness of the foundation, but also the large overturning moments produced by the drag from ocean current militate against rigid structures.

Cable structures in the ocean provide a compliant response to hydrodynamic forces, varying their geometry to provide more "leverage" against the flow. In addition, the flexibility of cables facilitates undersea "construction" by compact storage on shipboard winches and deployment through sheaves. Since cable must be loaded in tension, gravity must be counteracted by a support at the top of the structure. This supporting force is nearly always provided by hydrostatic buoyancy. Anchors represent the vestigial remains of the sophisticated foundations used to support rigid structures.

When the purpose of the structure includes the need for accurate, consistent relative position of parts, the cost of rigid structures in the ocean may be accepted, as in the offshore oil industry, but in deep water, cable systems are virtually always used.

Sophisticated computer models have been developed to analyze the stress and deflection of rigid structures. These models can use the nearly linear response and small deflection inherent in most rigid structural materials to simplify the solution of large algebraic matrices. Computer models of ocean cable systems, however, must contend with the large deflections that these structures exhibit, as well as the nonlinear response of many cable materials. Only in recent years have the mathematical and procedural difficulties posed by the solution of the response of even simple cable geometries to the dynamic ocean environment been successfully addressed (Reference 1).

The Civil Engineering Laboratory (CEL), under the sponsorship of the Naval Facilities Engineering Command, has engaged in a major program to develop techniques for the static and dynamic analysis of oceanic cable structures. This program is divided, on the one hand, into a series of small- and large-scale experiments to measure the response of cable structures to their environment, and on

the other hand, to develop and evaluate computer programs which attempt to predict that response.

The series of experiments was devised to provide data by which computer models of cable systems can be evaluated. The data from these experiments provide not only a standard for measuring the accuracy of model predictions, but also a severe test of the "robustness" of the computer algorithms used by the model.

Separate reports have already been issued describing each experiment in detail; other reports compare computer model results with the experimental data. These reports are listed in the References. This report brings the results of all these comparisons together in summary form.

The series of experiments was devised to test various aspects of the models. The experiments ranged in size from a 6-foot laboratory scale to a 2,500-foot prototype mooring in the ocean. The small-size experiments should not be considered as scale models of large cable systems, but as full-size events of their own. This is because all the parameters of a cable system cannot be scaled simultaneously. The parameters for each size experiment can be specified independently in the computer model. It is valid, therefore, to require that a computer model small-size events as well as large ocean cable systems.

1.2 CABLE GEOMETRIES.

The first experiment in the series used thin elastic nylon or rubber strands about 6 feet long (Reference 2). The second experiment used a 60-foot length of the rubber material (Reference 3). A third experiment (Reference 4) used both the nylon string as well as the rubber material in the 6- and 60-foot experiments. The length of the cable was a variable in this experiment; the length was varied between about 6 and 60 feet by a small winch. The fourth experiment in the series was a full scale mooring set in 2500 feet of water (Reference 5).

The experiments included several cable geometries. The sketches on Figure 1-1 show the cases that were studied. The geometries are simple, consisting of serial cable systems with no Y connections, in order to simplify computer modeling. The presumption is that more computer programs will be able to model simple geometries, and that the causes of model aberrations from the data will be more easily identified if the geometry is simple. Nevertheless, these cases exhibit many of the dynamic processes that affect actual cable structures in the ocean.

1.2.1 THE DROPPED PENDULUM. Figure 1-1(a) is a sketch of the dropped pendulum. One end of a cable is fixed at or near the water surface. A weight is attached to the other end and supported at approximately the same elevation as the fixed end, but displaced from it, so that the cable hangs in a catenary arc. When the cable is released, it drops, jerks the cable taut, then swings under the fixed suspension. At the end, the cable hangs vertically.
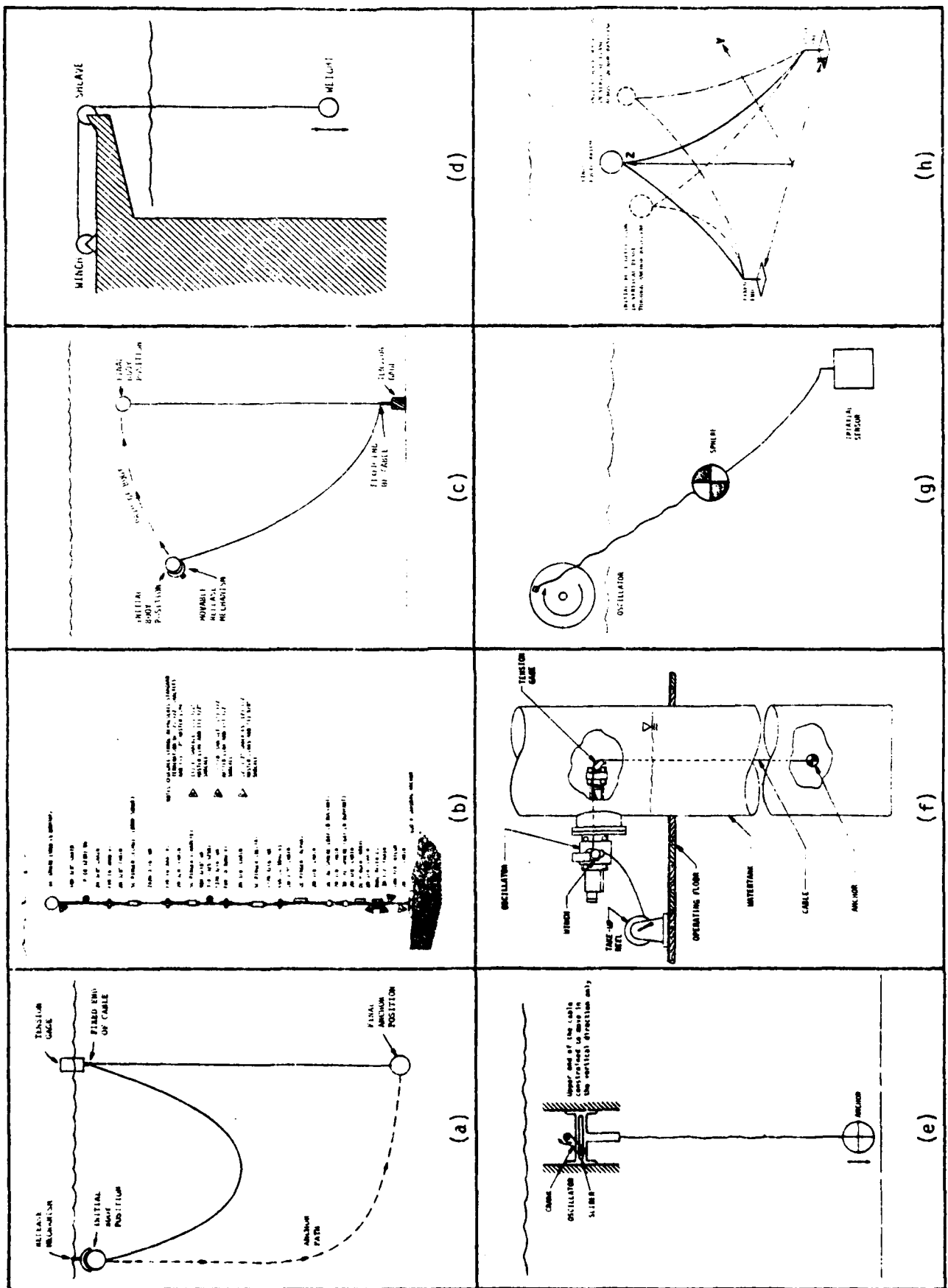
Figure 1-1. Geometry of Experiments

Some of the events a computer model should replicate for this geometry are the static, elastic catenaries that describe the inital and final states of the cable, the "gooseneck" that forms in the cable just after the weight is dropped, the occurence of slack cable at the vertex of the initial catenary shortly after the weight is dropped, the impact of the weight as the cable comes taut, and the damping of the swing towards the final vertical shape.

Although the final configuration of this case suggests that it represents a measurement system suspended from a drifting surface float, these systems are not deployed with such brusque abandon. It is instead an approximation of the technique used to deploy the mooring sketched in Figure 1-1(b).

1.2.2 <u>ANCHOR LAST MOORING DEPLOYMENT</u>. In this technique, the buoy that supports a mooring leg is towed in the water behind a ship by means of the mooring wire. As the ship steams over the desired site, the anchor is dropped into the water. It falls to the bottom dragging the buoy behind it. If the mooring wire is shorter than the water depth and the anchor is heavy enough, the buoy is submerged. Figure 1-1(b) is a sketch of a mooring deployed by the author-last technique.

Computer models of this case should depict the initial towing "catenary", the horizontal deceleration after the anchor is dropped, the "gooseneck", the anchor speed and trajectory, the buoy speed and trajectory (especially the growth of tension that ultimately submerges the buoy of a subsurface mooring), and the response of the mooring to the anchor impact as well as the final mooring configuration under the influence of the prevailing ocean currents.

1.2.3 <u>SINGLE LEG MOORING RELAXATION</u>. If a system is mathematically linear, then its response to an abrupt disturbance is an important measure of its dynamic charateristics. Some mooring models are based on linearized mathematics, in which dynamic effects are treated as small, linear disturbances about a series of equilibrium states that are updated non-linearly every so often. The mooring relaxation experiments sketched in Figure 1-1(c) provide a step-function input to a single leg mooring.

In the sketch, one end of a cable is shown anchored to the bottom of the test tank or ocean with the other end supported by a subsurface buoy. The buoy is displaced from its equilibrium position, held until equilibrium is re-established, then abruptly released. The buoy floats back to the original equilibrium.

1.2.4 <u>SIMPLE PAYOUT</u>. Winches are commonly used to deploy and recover cables at sea. Most cable models to date require fixed cable lengths, but a few can solve the variable length cable problem. Figure 1-1(d) shows a weight being lowered or raised on a cable.

1.2.5 <u>SIMPLE OSCILLATOR</u>. Figure 1-1(e) shows another common event when cables are used at sea: a weight is suspended from a floating object that heaves in the seaway.

1.2.6 PAYOUT WITH OSCILLATOR. This case combines (d) and (e) in a more realistic scenario: using a winch on a heaving ship. Figure 1-1(f) shows the concept. The experiment is deceptively simple. Resonant interactions between the oscillator frequency and the varying cable length may be masked in the experiment by fluid and material damping, but present an imposing obstacle to a computer algorithm.

1.2.7 OBLIQUE OSCILLATOR WITH SUSPENDED LOAD. Figure 1-1(g) shows a cable with one end fixed and the other end constrained to move in a vertical circle. A load is attached at some point along the cable. The load may be heavy or buoyant. This case represents the problem of a ship anchored in a seaway or a cable system being installed from a cable laying ship.

1.2.8 TWO LEG MOORING RELAXATION, TRANSVERSE DEFLECTION. Figure 1-1(h) shows a variation of the relaxation experiment described in part 1.2.5 above. The buoy supports two mooring cables in this case, and the initial deflection is along the bisector of the anchor baseline.

1.2.9 TWO LEG MOORING RELAXATION, PARALLEL DEFLECTION. The last sketch shows the two leg mooring, but in this case the initial defection is in the plane of the mooring. The first case represents the loading that results in maximum deflection and holding power. This case gives minimum deflection per unit load, but all the load is held by one leg.

Not every configuration shown on Figure 1-1 was tested at every scale. Table 1-1 summarizes the runs for each experiment.

The experimental data may be used to evaluate many computer models of cable systems. The results from two programs are described in this report. SEADYN is a general model for networks of cables in three dimensions, SNAPLOAD models serially connected cables hanging in a vertical plane.

1.3 COMPUTER MODELS.

1.3.1 SEADYN. SEADYN (Reference 6) uses finite element techniques to analyze three dimensional networks of cables. The finite element method divides the continuous cable into segments (elements) whose properties are uniform. Spatially varying forces are assumed to be constant on an element. The solution obtained for each element is required to align with the solution obtained for adjacent elements.

SEADYN is partitioned into several kinds of analyses, including static networks (no acceleration of cable or fluid), time dependent dynamics, resonant vibrations (standing wave shape), and harmonic analysis in the frequency domain. The cable network may include discrete bodies such as buoys, anchors, and winches that pay out or reel in cable. External point loads, non-steady three dimensional current fields, surface waves or spectra, and wind forces are accepted.

Although the finite element technique originated in the analysis of linear or nearly linear systems, the SEADYN algorithm accepts the nonlinearities that result from large deflection, large strain, fluid drag, and hyper-elastic materials with

TABLE 1-1. SUMMARY OF EXPERIMENTAL CASES

Experiment	Dropped Pendulum (Run)	Anchor-Last Deployment (Run)	Single-Leg Relaxation (Run)	Simple Winch (Run)	Simple Oscillation (Run)	Winch + Oscillation (Run)	Oblique Oscillation (Run)	Two Leg Relaxation (Run)
6 Foot Laboratory	32-47		1-28		6797		133 142	50-58# 50-65+
60 Foot Laboratory	1-6 14, 15		7, 8 10-12		16-20			
2,500 Feet At Sea		2*	4-8					
Variable Length Laboratory				1-6 13-18 25-38 75	76-97	7-12 19-24 39-74		

\# In-Plane Deflection.

\+ Out-of-Plane Deflection.

* Run = Force Vector Recorder Burst Number.

hysteretic damping. The internal stress distributions produced by bending and torsion are not modeled.

1.3.2 <u>SNAPLOAD</u>. SNAPLOAD (Reference 7) is a lumped parameter model of serial cable systems that hang in a vertical plane. This implies that wind, current, and wave forces are also aligned in that plane. The lumped parameter method replaces the continuous cable and its partial differential equations with a series of "lumps" where all forces act, connected by massless springs. The algebraic equations of motion for the "lumps" are then solved. If the parameters of the lumps are properly chosen, the response of the lumps converges to the response of corresponding points of the cable.

Inasmuch as serially connected two dimensional cable systems is the largest class of applications, SNAPLOAD has broad applicability. Like SEADYN, SNAPLOAD provides for momentarily slack cables, as well as variable length cables. Environmental forces from surface waves and depth-dependent ocean currents are accepted. For the class of problems that it solves, SNAPLOAD is usually more economical than SEADYN.

SECTION 2

EXPERIMENTS

2.1 THE SIX FOOT EXPERIMENTS.

2.1.1 CONFIGURATIONS. Five simple types of experiments were made.

2.1.1.1 Single Point Mooring Relaxation. In single point mooring relaxation, one end of a cable is fixed to the tank floor and a buoy is attached to the free end. The buoy is displaced a specified distance horizontally and then released, allowing it to return to the original, or equilibrium position, as illustrated in Figure 2-1. The variable for this kind of experiment is the initial position (vertical and horizontal displacement) of the buoy relative to the fixed end of the cable prior to release; this determines the initial configuration and tensions (degree of slackness) in the system. Twenty-six of the experiments were of this type.

2.1.1.2 Simulated Anchor-Last Deployment. In simulated anchor-last deployment, the fixed end of the cable is positioned just below the surface of the water and an anchor is attached to the free end. The anchor is raised to a height equal to the fixed end and displaced a specific distance horizontally, then allowed to fall, and return to the vertical equilibrium position as shown in Figure 2-2. This experiment simulates the free-fall anchor-last deployment procedure frequently used for single point moors. The test variable is the horizontal separation of the fixed end of the cable and the anchor. Sixteen simulated anchor-last experiments were made.

2.1.1.3 Bi-moor Relaxation. In a bi-moor relaxation, one end of each of two cables is attached to a common point on a buoy; the other ends are fixed to separate positions on the tank floor as shown in Figure 2-3. As with the previous types of experiments, the test variable is the spatial position of the buoy prior to release. For this test, the buoy was displaced from equilibrium either in the vertical plane passing through the anchors or perpendicular to this plane, and allowed to relax to the original or equilibrium position. The latter provided the only three-dimensional experiments in this series. Nine in-plane (two-dimensional) and seven out-of-plane experiments were made. The horizontal separation of the fixed cable ends was 5.5 feet.

2.1.1.4 Single Cable Suspended Load. In the single cable suspended load tests, an anchor is suspended from a single cable fixed to a load measuring device and vertically oscillating point as shown in Figure 2-4. The frequency and amplitude of the oscillating end of the cable were varied to provide a laboratory simulation of wave-induced ship or platform motion. Seven suspended load experiments were made.

2-1

RELEASE
MECHANISM

TENSION
GAGE

INITIAL
BUOY
POSITION

FIXED END
OF CABLE

ANCHOR
PATH

FINAL
ANCHOR
POSITION
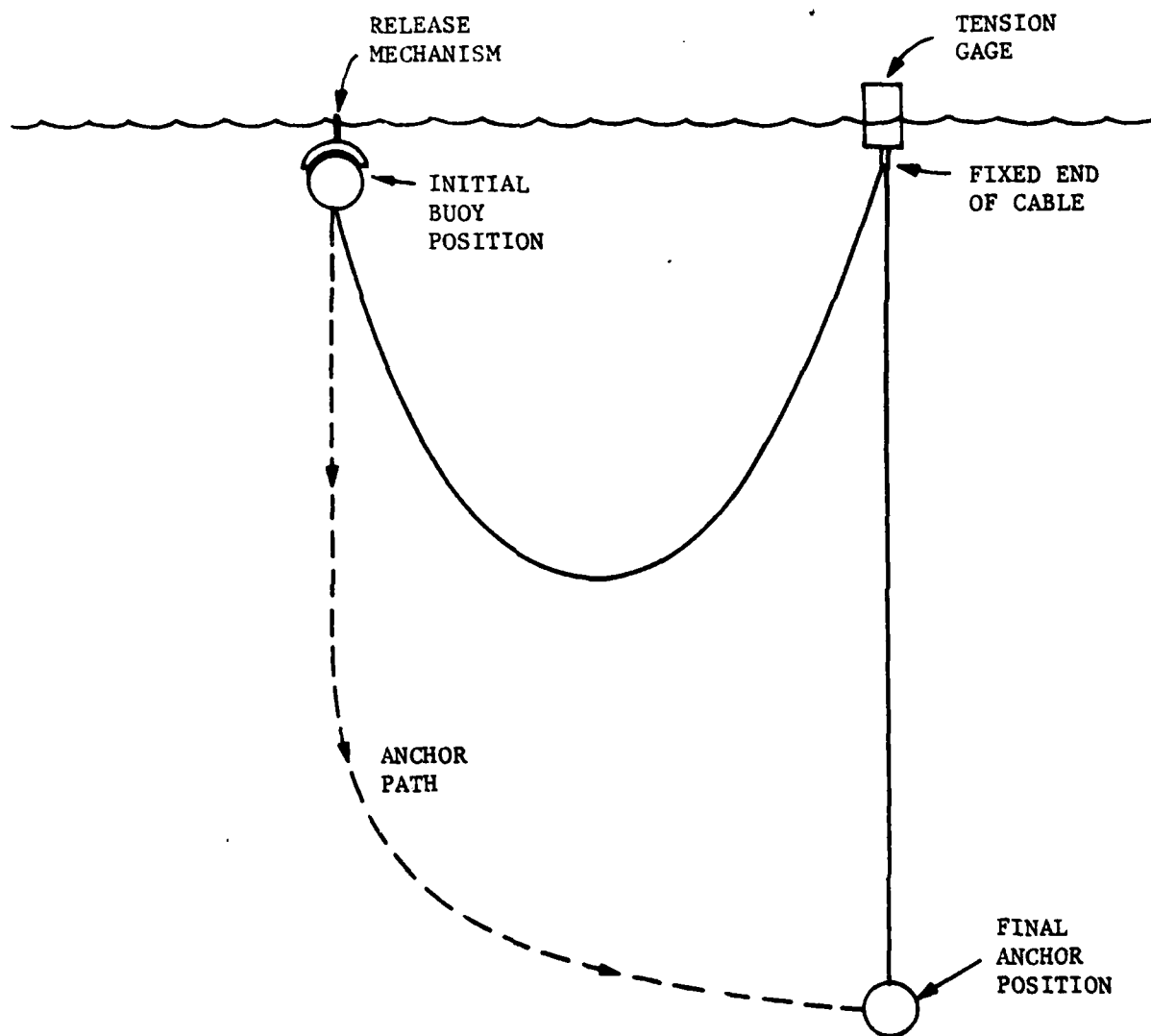
Figure 2-1. Diagram of Simulated Anchor-Last Deployment Experiment
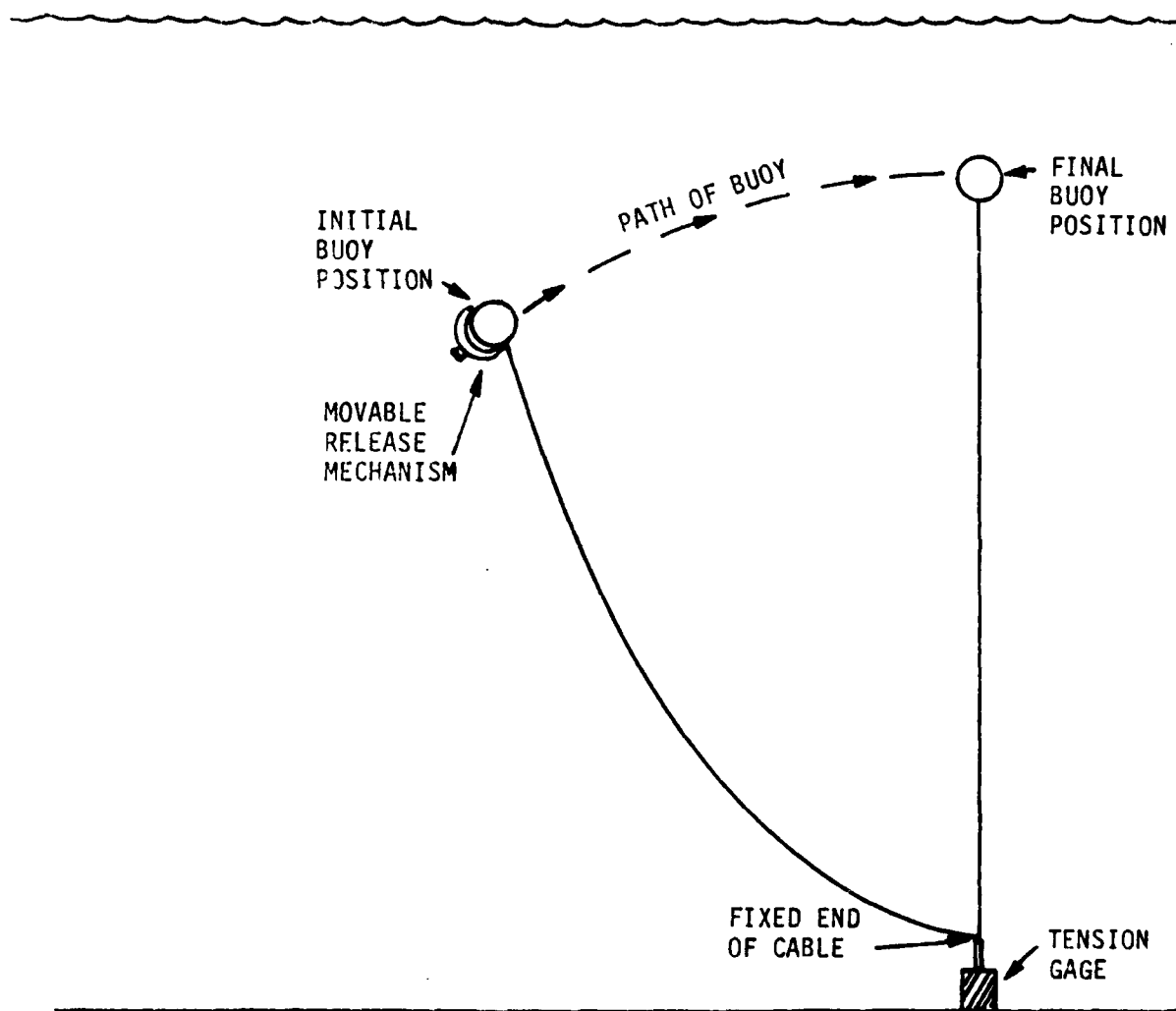
Figure 2-2. Diagram of Single Point Mooring Relaxation Experiment
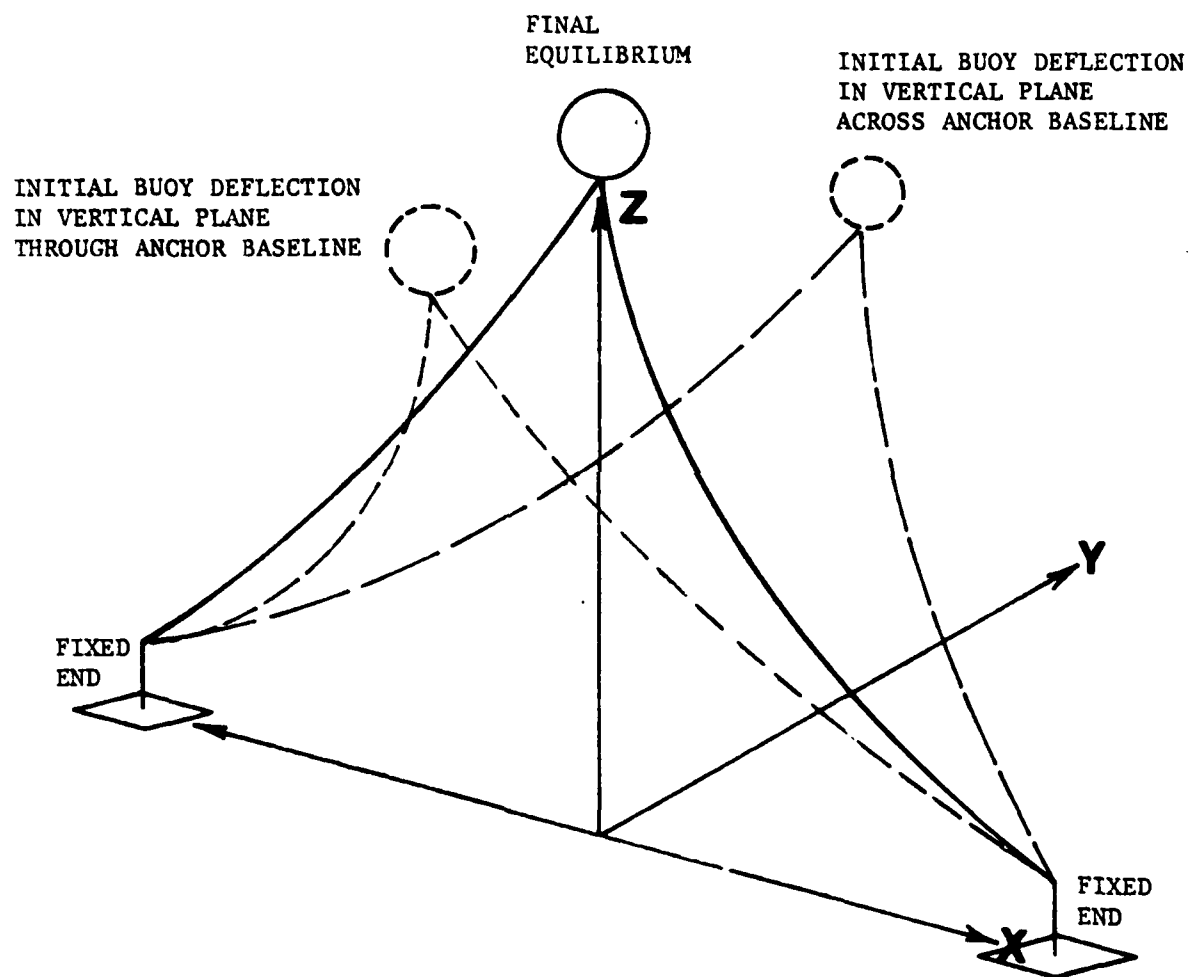
Figure 2-3. Diagram of Bi-Moor Relaxation Experiment

2-4

SCOTCH
YOKE
MECHANISM

TENSION GAGE

CABLE ATTACHMENT

ELECTRICAL
LEADS

VERTICAL

Figure 2-4. Single Cable Suspended Load Oscillator

2-5

2.1.1.5 <u>Dual Cable Suspended Load</u>. In dual cable suspended load, one end of each of two cables is attached to opposite sides of an anchor or buoy and the remaining ends are attached one to an oscillator, the other to a load measuring device fixed on the tank floor as shown in Figure 2-5. The vertical and horizontal separation of the cable ends was 4.0 and 3.5 feet. The oscillating end is moved in a circular motion at a predetermined amplitude and frequency. Two of these dual cable tests were performed.

2.1.2 <u>MATERIALS</u>. Three types of cable were used in these experiments, a nylon line and two silicon rubber cables used to absorb shock in sonobuoys[1]. The nylon line was inelastic[2] whereas the rubber cables were considerably more elastic. One of the sonobuoy cables was solid rubber. The other included two fine copper wires wound as shown in Figure 2-6. The latter cable is identical to that used in the 60-foot experiments and was tested in the present experiments to provide an assessment of scale effects. The physical properties of all of the cables are given in Table 2-1 and the elastic behavior is plotted in Figures 2-7, 2-8, and 2.9. All the cables exhibit significant hysteresis in their elastic properties. The data shown were measured after the cables had been stretched to 15 percent of their original length five times each; care was taken during the experiments to insure that the cables were not stretched beyond this initial prestretch. The black rubber cables were marked at approximately 6-inch intervals with contrasting bands of white silicon ink; the ink did not change any of the cable properties.

The buoys and anchors used in these experiments were fabricated from 2-inch diameter hollow plastic spheres[3]. The surfaces of the spheres were smoothed and painted for the experiments. The hollow spheres were used directly as buoys; the anchors were made by lining the interior of the spheres concentrically with lead shot to the desired total weight. Thus the diameters and surface conditions (and drag coefficients) of all the buoys and anchors were the same. The physical properties of the buoys and anchors are presented in Table 2-1.

Complete assemblies of buoys or anchors and cables were made up before the experiments were begun. All of the cables were mounted on the tension transducers by a threaded ferrule; a pin in each ferrule provided an index for installation on the force transducers to give a common zero point for the length measurements. The distance from the center of the pin to the center of the buoys or anchors was 1.3 inches.

2.1.3 <u>EXPERIMENTAL ARRANGEMENT</u>. The experiments were conducted in the Controlled Atmosphere Launching Tank of the California Institute of Technology (CIT) Hydrodynamics Laboratory during October 1976. The tank is a horizontal cylinder 13 feet in diameter and 30 feet long (Figure 2-10). Camera ports are precisely located

---

[1] Marsh Industries, Mt. Clemens, Michigan 48403

[2] Inasmuch as all real materials deflect under load, no material is literally "inelastic". The word is used in this report in a relative sense. Materials that deflect slightly under a force are inelastic when compared to materials that deflect greatly under the same force.

[3] Emerson and Cuming, Canton, Massachusetts 02021
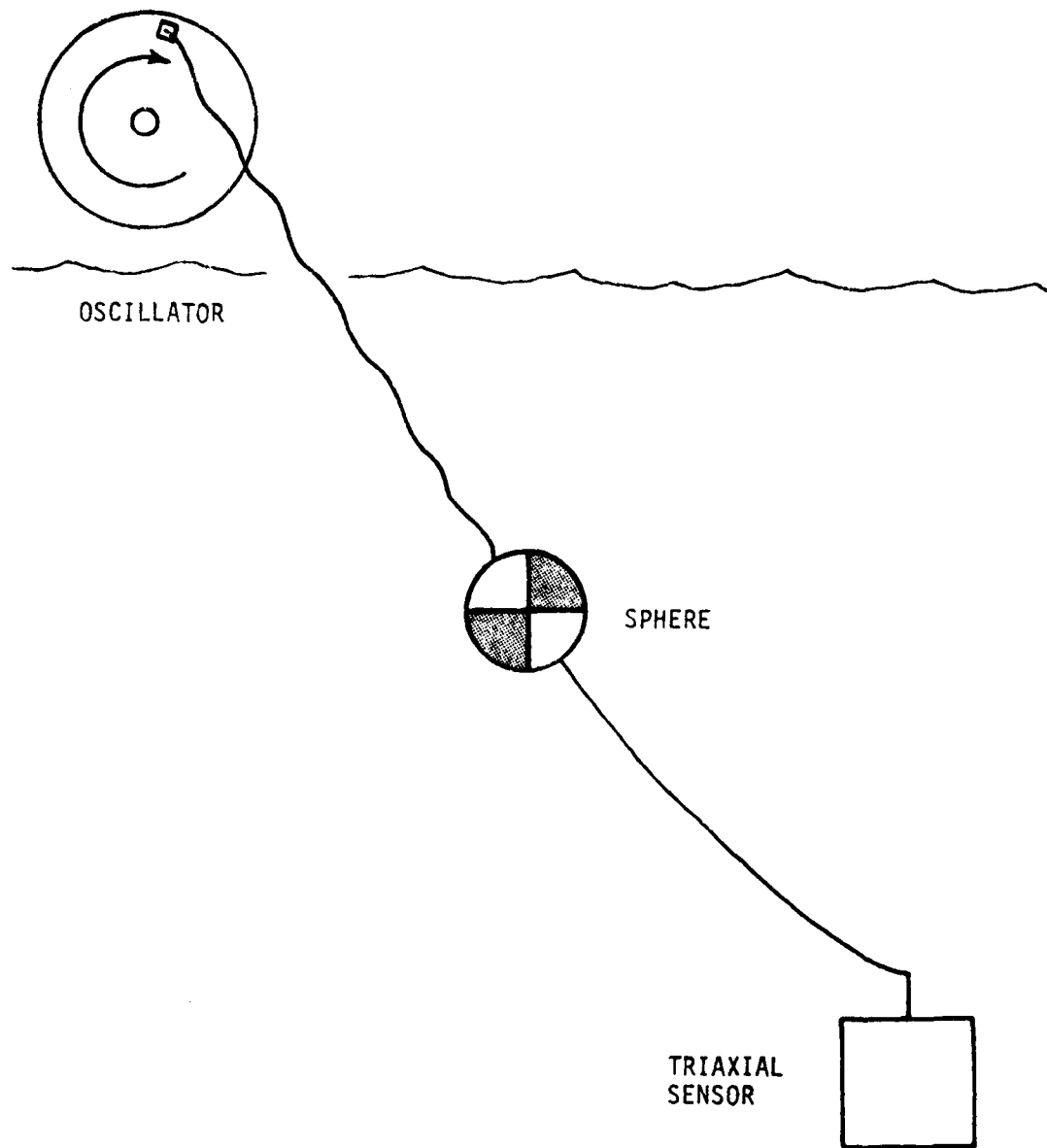
Figure 2-5.   Diagram of Dual Cable Suspended-Load Experiment

SILICON RUBBER CORD

ELECTRICAL CONDUCTERS
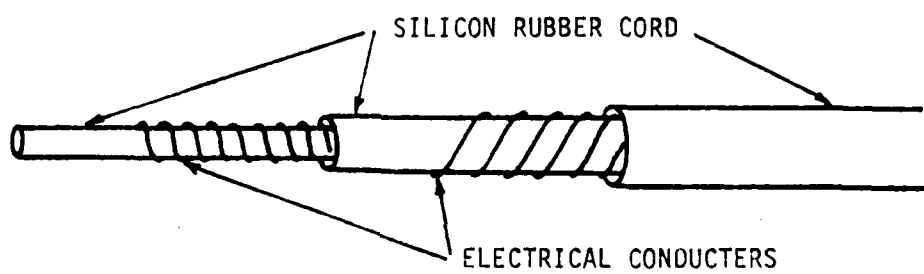
Figure 2-6.   Construction of Silicon Rubber Cable with Conductors

TABLE 2-1. MATERIAL PROPERTIES FOR LABORATORY EXPERIMENTS

ITEM	TEST SERIES	DIAMETER (in)	WEIGHT IN AIR (lb)	WEIGHT IN FRESH WATER (lb)
Small Buoy	6 ft	2.0	0.025	-0.121
Large Buoy	60 ft	2.9	0.047	-0.406
Light Anchor	6 ft, 60 ft	2.0	0.246	0.108
Heavy Anchor	6 ft, 60 ft	2.0	0.398	0.252
Suspended Load	Variable	2.0	1.16	1.003
			(lb/ft)	(lb/ft)
Silicon		0.163	8.979×10^{-3}	1.075×10^{-3}
Silicon, wired				
Sample 1	60 ft	0.175	12.8×10^{-3}	2.00×10^{-3}
Sample 2	60 ft	0.168	12.8×10^{-3}	2.40×10^{-3}
Sample 3	6 ft	0.163	11.4×10^{-3}	2.38×10^{-3}
Silicon	Variable	0.159	9.2×10^{-3}	5.82×10^{-4}
Nylon	6 ft	0.10	$3.73 \times 10^{-3}6$	1.057×10^{-3}
Nylon	Variable	0.059	0.792×10^{-3}	5.73×10^{-4}

LENGTH OF LINE (INCHES)

LOAD (GRAMS)

○ AFTER INITIAL 24-HOUR SOAK

□ AFTER 30-MINUTE RESOAK

◇ AFTER SECOND 30-MINUTE RESOAK

LOADING CURVE

UNLOADING CURVE
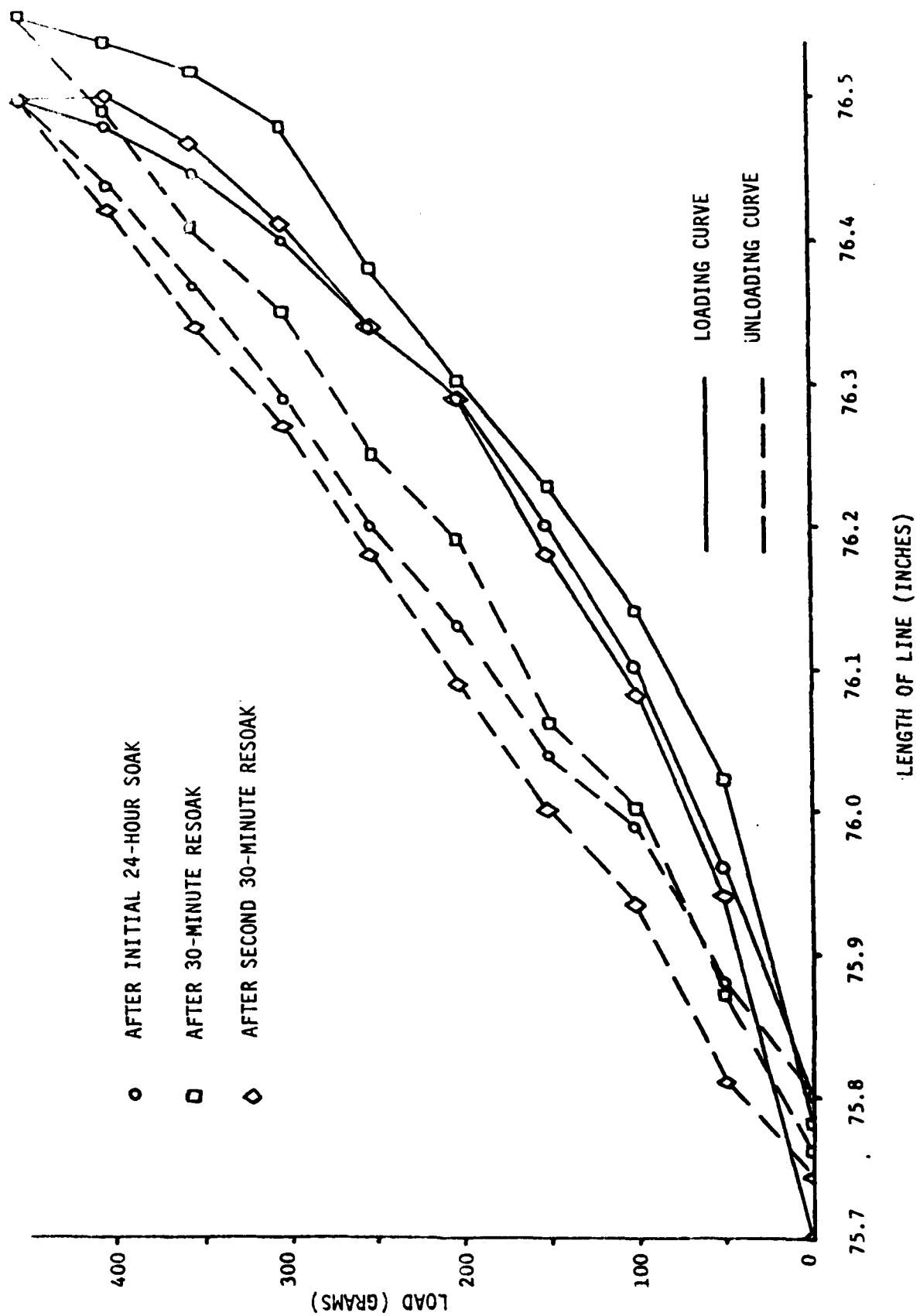
Figure 2-7. Elastic Characteristics of Nylon Cord
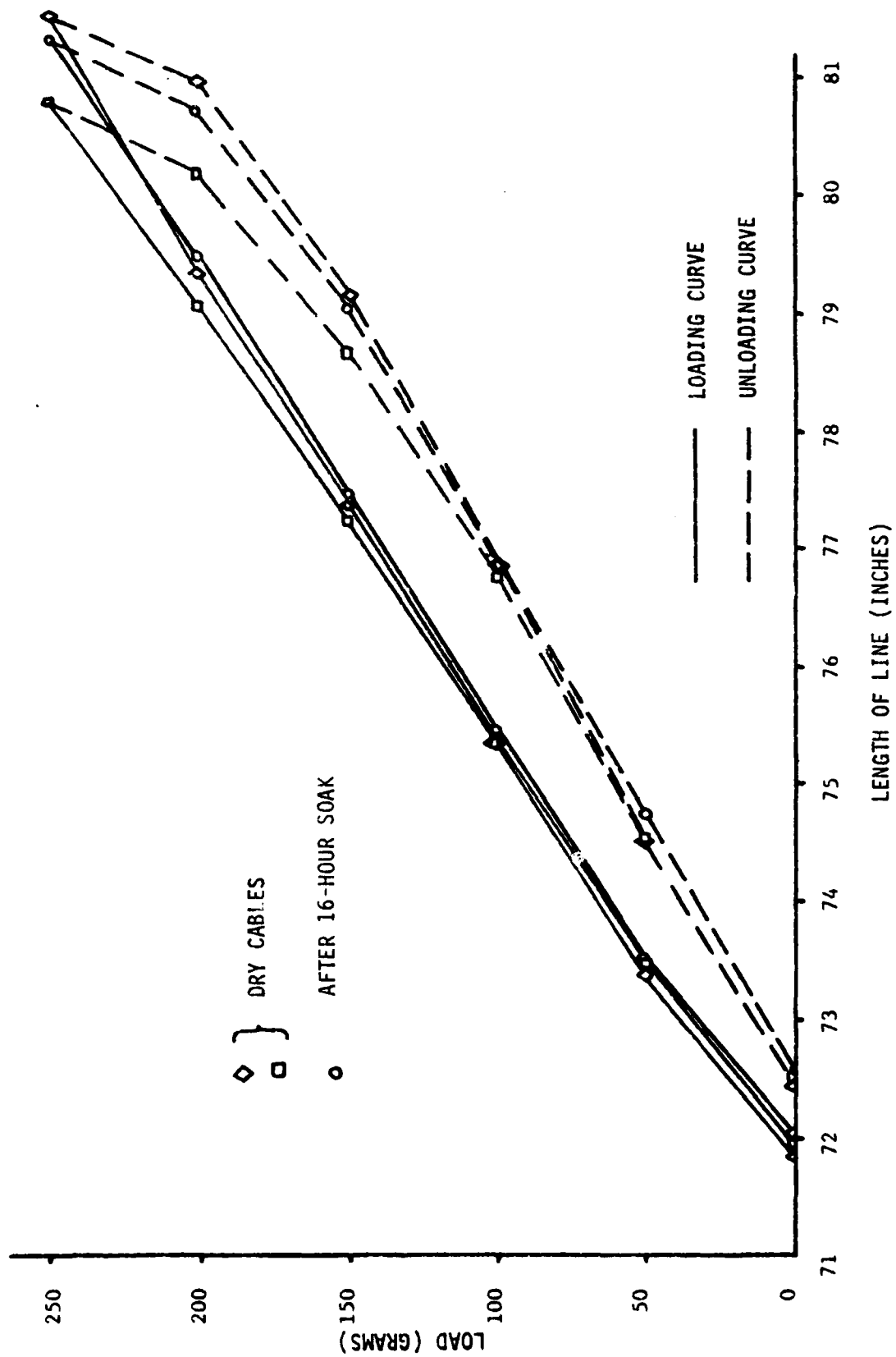
Figure 2-8. Elastic Characteristics of Solid Silicon Rubber Cable
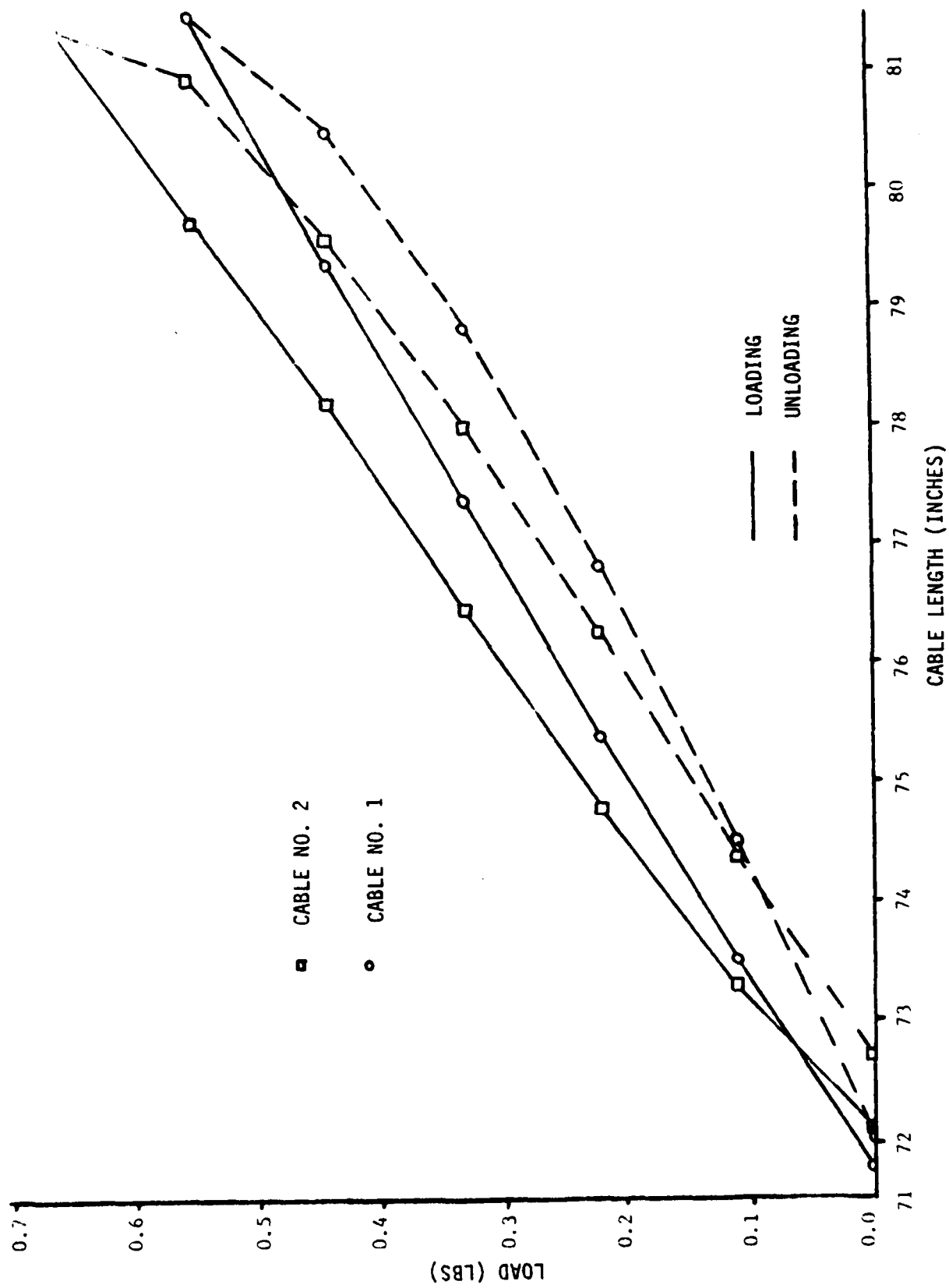
Figure 2-9. Elastic Characteristics of Silicon Rubber Cable with Conductors

2-12
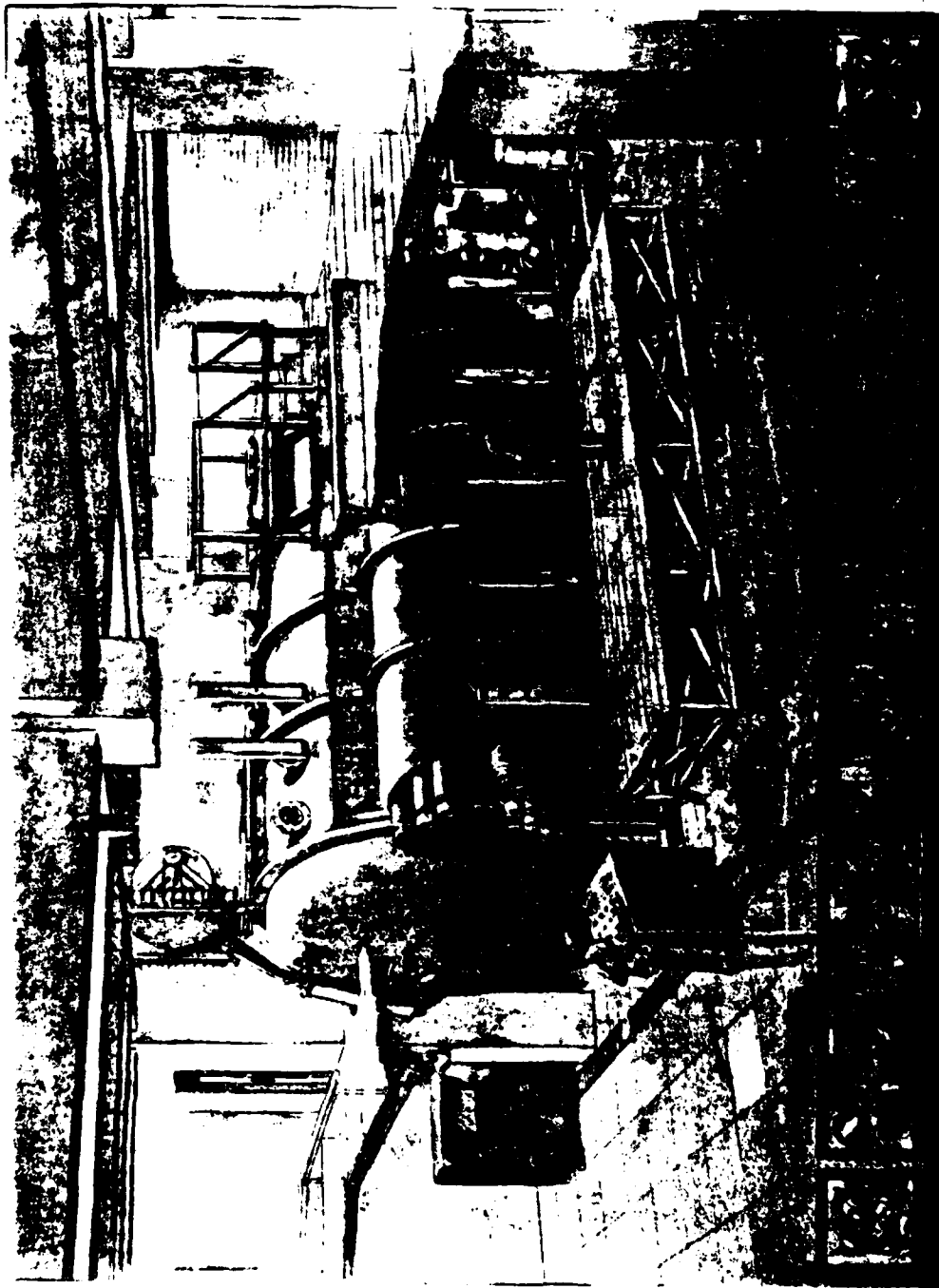
Figure 2-10. Six-Foot Experiment Test Facility

along one side and at both ends. The water in the tank is treated and filtered for optical clarity. The water in the tank was 8 feet deep for these experiments.

Tensions at fixed ends of the cables were measured by Kistler-Morse Model 113 triaxial strain gage deflection sensors. Deflection along any axis produces a voltage proportional to the force component along the axis. The sensors were calibrated before and after the experiments and were found to be linear within 0.05 percent of full scale, with no drift of the instruments observed. The cross-axis interaction of the sensors was also measured and found to be less than 1 percent.

Position time histories of points on the cables were measured by three pulsed-frame instrumentation cameras. The cameras were modified for synchronized operation (on-off and frame rate) for these experiments. The fields of view for the cameras were arranged to overlap in the area in the tank where the experiments were conducted. The cameras were operated without shutters at 10 frames per second. Xenon quartz flash lamps keyed to the frame rate provided an effective shutter speed of 200 microseconds at precise intervals.

A special mechanism was used to release the buoy or anchor in the relaxation and anchor-last experiments. In operation, the sphere is held on the mechanism by a slight vacuum. At the specified release time, the vacuum line is switched to a low-pressure air source to relieve the suction holding the sphere. The air pressure was carefully adjusted to avoid giving the sphere an initial impulse. The release mechanism was mounted on a pan-and-tilt head; for each run, the angle of the sphere was adjusted to miminize the initial rotation when the sphere was released (Figure 2-11).

A variable frequency and amplitude oscillator was used to simulate ship motion. The frequency was controlled by changing the speed of the driving motor and was set between 0.16 and 1.7 Hz. The amplitude was adjusted to either 1, 3, or 6 inches by varying the radius of the crank pin in a Scotch Yoke mechanism, as shown in Figure 2-4. The cable attachment was free to swivel, so that only tension was induced at the oscillator end of the cable.

Figure 2-12 is a photograph of a buoy relaxation experiment rigged in the empty tank. Figure 2-13 shows a dual-cable suspended load set-up using the oscillator with the Scotch Yoke mechanism removed.

The experiment was controlled through a CIT Graduate Aeronautical Laboratories' minicomputer system. The computer synchronized the cameras, flash lamps, triaxial force transducers and buoy/anchor release mechanism and provided a common time base for all the data and events during an experiment. The computer also controlled data acquisition and displayed raw or processed data for "quick looks" during the experiments.

Tension data were recorded for all of the experiments. Photographic position data were recorded for the relaxation and anchor-last tests.
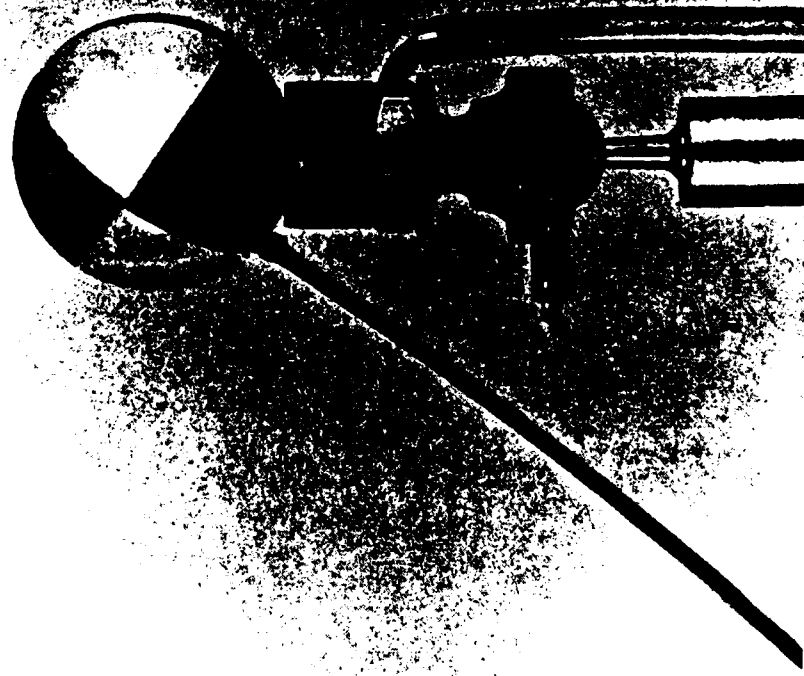
Figure 2-11. Model Buoy with Nylon Cord on Adjustable Release
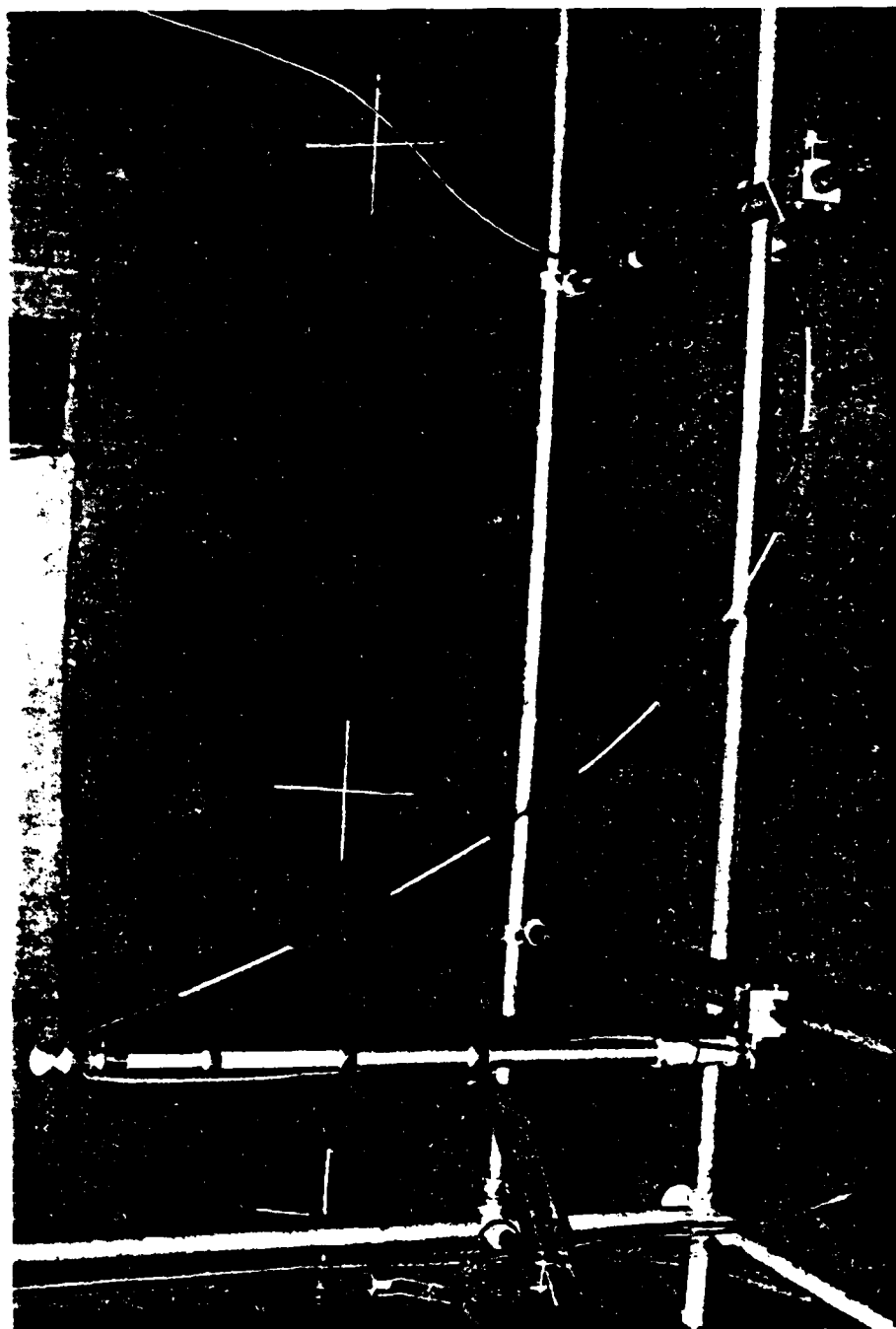
Figure 2-12. Rigging for a Buoy Relaxation Trial
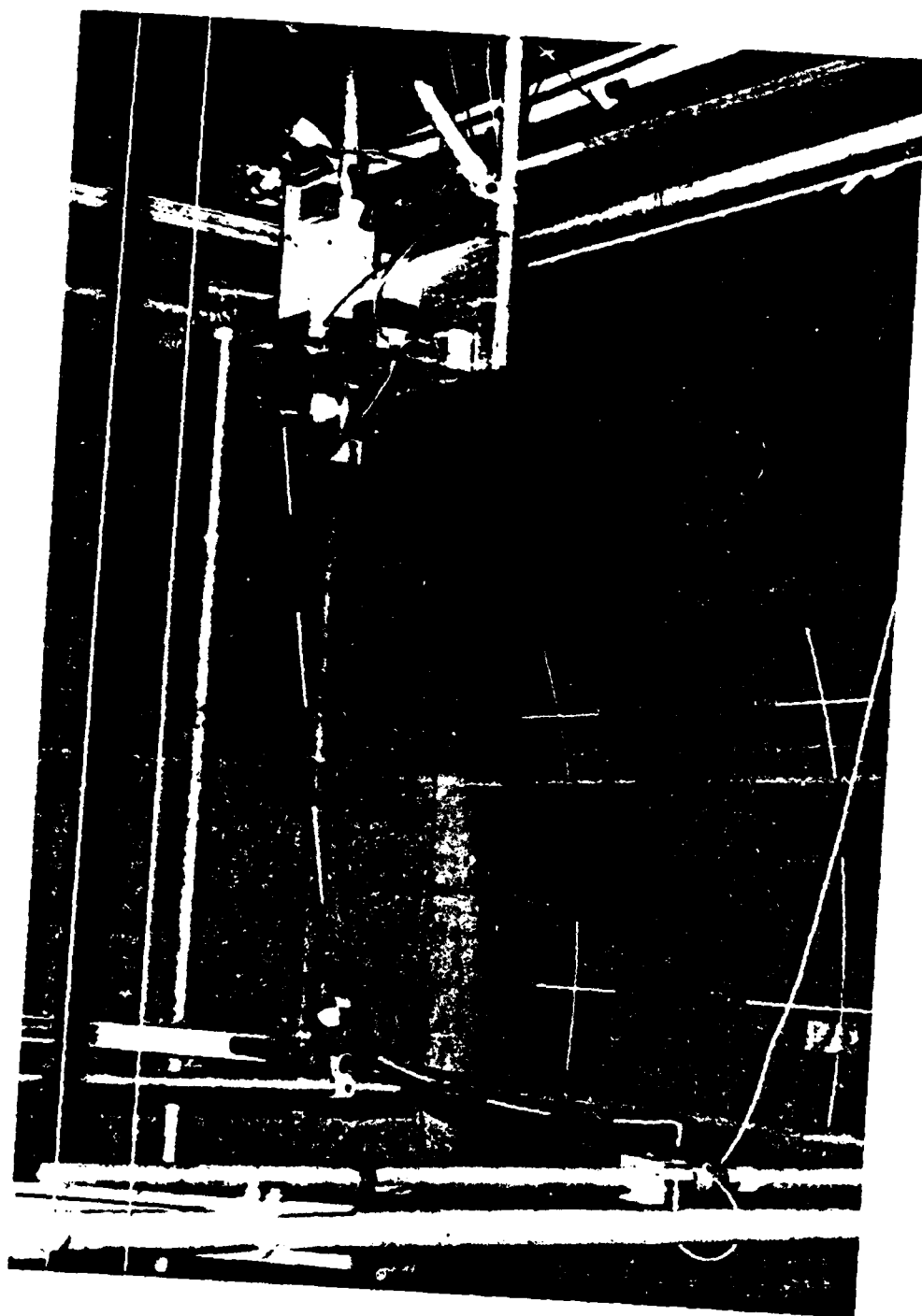
Figure 2-13. Dual-Cable Suspended Load Rigged in Tank

2.1.4 **DATA ACQUISITION.** Photographic data were recorded at 10 frames per second. Each channel of the triaxial force gages was sampled and digitized every 10 microseconds; ten samples were averaged and recorded every 0.1 second. The data were averaged to reduce noise, while the sampling rate was chosen to avoid aliasing in the oscillator experiments.

2.1.5 **DATA REDUCTION.** The photographic data from these experiments were reduced by the Computer Services Branch of the Naval Air Test Center, Patuxent, MD. The cable shape on each frame was digitized visually using a film reader which produced punched cards of the results. The three-dimensional nodal positions were computed from the cards using photogrammetry.

The nodal positions were merged with the tension data at CEL. The zero-time reference was determined visually from the photographic data by observing the initial separation of the sphere from the release mechanism. Velocity and acceleration at a node were estimated by differentiating a parabolic function fit to three consecutive position measurements.

2.1.6 **RESULTS.** The data collected in this experiment are suitable for comparison to numerical models. This is true for both the tension and photographic data.

The accuracy of the data in the tension and nodal displacement histories are dependent on the errors in the measured variables and the time. In both cases, the largest source of error is in the time estimate which is limited by the camera sampling period (0.1 second). The actual time-zero could occur anywhere within the sampling period, with a corresponding shift in time for the remaining data. This undetermined shift could cause significant differences between the experimental results and numerical predictions for the first few points. As time increased the relative error in the time estimate would decrease.

The accuracy of the tension measurements is considered very good. This judgement is supported by comparing the results of calibrations performed before and after the experiments.

The errors in the calculated nodal displacements are estimated to be approximately 1/2 inch in the X, Y, and Z directions. The velocities and accelerations should be used as estimates only, since they were numerically derived.

2.2 **THE 60 FOOT EXPERIMENTS.**

2.2.1 **CONFIGURATIONS.** Two simple types of experiments were made:

   a.   "Anchor-Last," in which the fixed end of the cable is positioned
        near the surface of the water and an anchor is attached to the free
        end. These are described in Section 2.1.1.2 and shown in Fig-
        ure 2-1. This experiment simulates the anchor-last deployment pro-
        cedure frequently used for single point moors.

   b.   "Buoy Relaxations," in which one end of a cable is fixed to the tank
        floor and a buoy is attached to the free end. These cases repeat,
        on a larger scale, the 6-foot experiment described in Section 2.1.1.1
        and sketched on Figure 2-2.

2.2.2 MATERIALS. Both types of experiments were made with simple cable systems, with only a single cable and a single buoy or anchor. The experiments were also two-dimensional, with little or no out-of-plane motion. The intent in these experiments was to minimize the complexity of the situation to be simulated by the computer models, while retaining the essential features of the dynamic behavior of cable systems.

2.2.3 EXPERIMENTAL ARRANGEMENT. The experiments were conducted in fresh water in the Hydroballistics Tank at the Naval Surface Weapons Center (NSWC), White Oak, Silver Spring, Maryland. The tank is 100 feet long x 35 feet wide x 75 feet deep and has windows on the walls and ends of the tank for observation or photography. The water depth in the tank for these tests was 65 feet. The water is filtered and treated for optical clarity.

The models consisted of 0.17-inch diameter silicon rubber shock mitigation cord, a 2.9-inch diameter hollow plastic buoy, and 2.0-inch diameter hollow plastic spheres concentrically weighted with lead shot for anchors. Properties of these models are presented in Table 2-1 and Figure 2-9. The silicon rubber cord had two contrahelically wound fine wire conductors which provided power for small light bulbs spaced at approximately 6-foot intervals along the cord.

For the 6-foot experiments, the cable was illuminated by high speed Xenon flash lights and photographed one frame per flash. The 60-foot experiments were conducted in darkness. A single photographic plate was exposed for each run, the camera shutter opened at the start of the run and not closed until the run was complete. Once a second during the run the small lights wired to the cable were flashed. The images of these lights define the shape of the cable at those instants.

For each run a buoy (or anchor) was attached to the free end of the cable. The fixed end was attached to a Kistler-Morse Model 113 triaxial deflection sensor as described for the 6-foot experiment. The sensor was calibrated before and after the experiments and was found to be within 0.05 percent of the full-scale used. The cross-axis interaction of the sensor was measured and found to be within 1.0 percent.

Photographic coverage of the tests was obtained by running the tests at one end of the 100-foot tank and placing cameras at the opposite end. Three cameras were used; one provided a close-up view of the initial release of the buoy or anchor, one showed half coverage in the central area, and the other showed full coverage of the cable motion. Camera and test apparatus positioning are shown in Figure 2-14.

At the end of the tank, opposite the cameras and directly behind the test area, small lights were placed in five of the view ports. These light positions provided references on the photographic plates for use in constructing grids for photo data reduction.

The Kistler-Morse triaxial sensors were wired directly to an analog-to-digital converter; x, y, and z forces were displayed on a strip chart and digitally recorded.
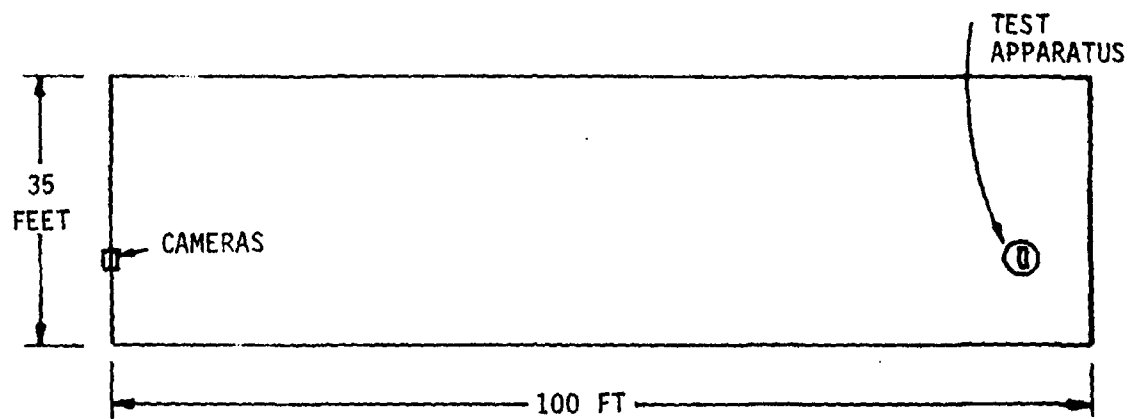
TOP VIEW
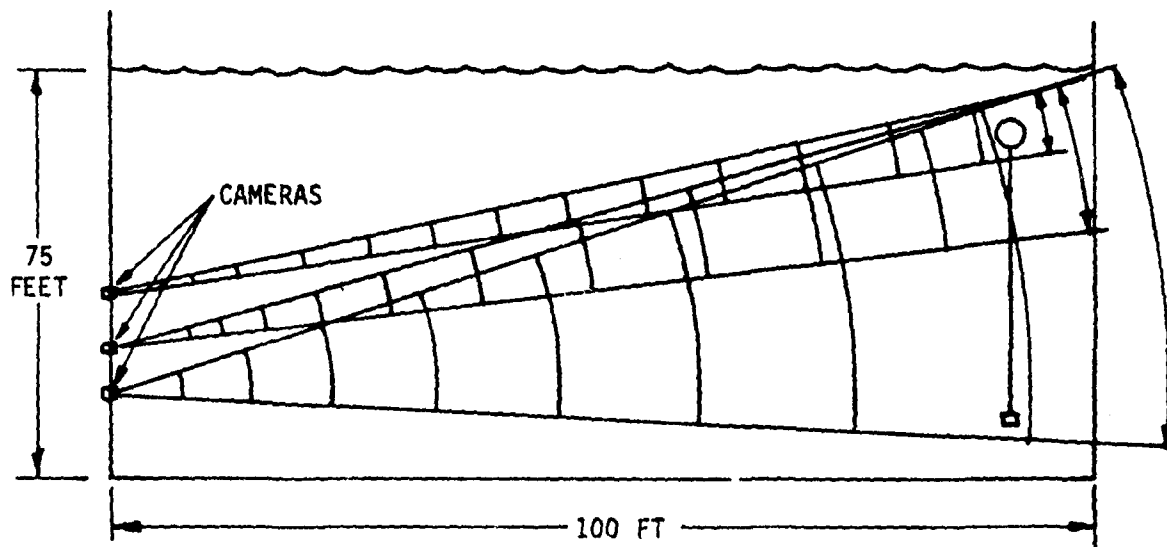
SIDE VIEW

Figure 2-14. Camera Positions for 60 Foot Experiments

2-20

2.2.4 DATA ACQUISITION. All recording equipment was turned on and running and the pulsing of the lights commenced prior to opening the camera shutters. When the camera shutters were opened the lights continued to pulse in their initial positions for a few seconds prior to buoy/anchor release. The cable system was then released and allowed to return to an equilibrium position. The camera shutters were then closed, providing a time lapse photograph of the dynamic sequence on a single plate.

2.2.5 DATA REDUCTION. All of the data photographs were enlarged to 8- x 10-inch size. A photograph of the five known position lights was also enlarged to 8-x 10-inch size and used to create a data reduction grid. The grid was then aligned over the reference lights on each data photograph. The position of the flashing lights was read from the grid and punched on computer cards manually.

The triaxial force data were transferred from magnetic tape to punched computer cards mechanically. The position cards and triaxial data cards were then entered into one computer program and the data reduced to position, velocity, acceleration, and tension vs time to be presented both in graphic and tabular form. The velocity and acceleration were calculated from the measured position-time data.

During the data reduction process various problems became evident. The cable rotated slowly about its axis while moving through the water, at times obscuring the pulse lights from the camera. The one-second pulse was slower than optimum during high velocity displacement and faster than optimum during slow velocities. The blanks in the photographs, due to obscuring of the lights, and the running together of the pulse, due to low velocities, were filled in manually where the separation was clear enough for reasonable estimates. In other portions the data were omitted.

2.2.6 RESULTS. Fifteen cases were run. Each run began and ended with the mooring line in a static condition. Since the static shape and tension distribution of a flexible, elastic line can be expressed by relatively simple formulae, the quality of the dynamic data gathered during a run can be inferred by comparing the initial and terminal measurements of cable shape and tension to the static calculation. Several runs were examined. Of these, three were selected for analysis by SEADYN and SNAPLOAD.

2.2.6.1 Run 6: Anchor-Last. The positions of seven points along the cable were recorded prior to releasing the anchor and compared to the static elastic catenary formulae. The mean radius from a measured point to the corresponding point along the catenary was 0.5 feet with a standard deviation of 0.4 feet. The mean radial error is about 1 percent of the length of the cable.

The cable force on the load cell was calculated to be 0.068 pound at 81.8 degrees below horizontal. The output of the load cell was 0.058 pound at an angle of 76.7 degrees. The standard deviation of the load cell calibration is 0.007 pound.

The remainder of the discrepancy must be accounted in the standard deviations of the measured cable weight and elasticity used in the catenary formulae.

By 90 seconds after the anchor was released, the mooring had virtually stabilized: drag forces were negligible. The elastic catenary equations were solved using the measured weight and horizontal displacement of the anchor as boundary conditions for this case. The mean distance between the measured and calculated node positions at t = 90 seconds was 0.7 feet with a standard deviation of 0.5 feet. This corroborates the 1 percent error noted for t = 0.

The immersed weight of the cable and anchor in Run 6 is about 0.240 pound. The load cell output was 0.221 pound at the end of the run, 100 seconds after the anchor was dropped. The load cell recorded the cable angle as about 5 degrees from vertical. This reflects an exponential approach to vertical equilibrium.

2.2.6.2 Run 11: Buoy Relaxation. At the start of Run 11, the mean radius between the calculated and measured locations of seven points along the cable was 0.8 feet, with a standard deviation of 0.4 feet. The initial tension was calculated to be 0.027 pound at 12.9 degrees below horizontal. The load cell output was only 0.0013 pound at 37.7 degrees below horizontal. The tension after 100 seconds was measured as 0.271 pound at 9.2 degrees from vertical. The tension due to weight and buoyancy was 0.308 pound.

The measured state of this mooring at t = 90 seconds was compared with the state calculated for a static, elastic catenary, using the buoyancy and displacement of the buoy as boundary conditions. The mean radius from a measured mode position to its theoretical position was 3.3 feet, but the standard deviation of the position difference was only 0.2 feet. These values are not consistent with corresponding values from Runs 6 and 15. Run 11 was accepted for comparison because the nodes follow a smooth trajectory through the relaxation. The question will be addressed again in Section 4.

2.2.6.3 Run 15: Large Anchor-Last. The seven points compared for this run averaged 0.8 feet difference between measured and calculated location prior to anchor release. The standard deviation was 0.3 feet.

The comparison at the end of Run 15 is as good or better. The mean distance is 0.6 feet with a standard deviation for eight nodes of 0.4 feet.

The calculated initial tension was 0.068 pound at 82.0 degrees from horizontal. The load cell read 0.060 pound at 80.1 degrees from vertical. The combined cable and anchor weight for this case is 0.384 pound.

2.3 VARIABLE LENGTH EXPERIMENTS.

2.3.1 CONFIGURATIONS. The variable length experiments model the effects of handling loads suspended from a ship in a seaway.

Simple payout involves lowering a load on an elastic line deployed from a fixed winch. Included in payout is the closely related case of simple recovery. Simple oscillation has the load suspended on a fixed length of line from a winch

that is heaving in simple harmonic motion. Both the 6-foot and 60-foot experiments included a few cases with simple oscillation. The variable length experiment combined simple payout on reel in with oscillation.

2.3.2 MATERIALS. Two model assemblies were tested. One used an elastic cable to support a small anchor, and the other used an inelastic cable to support the same anchor.

2.3.2.1 Anchor. The model anchor was a 2-inch sphere weighing one pound in water. The outside of the sphere was painted in a black and white pattern. The cables ended in a swivel which clipped into a stud on the anchor.

2.3.2.2 Cables. The dynamic response of a compliant system was simulated through the use of a soft rubber cable attached to the anchor. The mechanical properties of this cable are included in Table 2-1. A plot of the elastic characteristics is provided on Figure 2-15. The response of an inelastic system was simulated through the use of a braided nylon line attached to the anchor. This cable had approximately four times the axial stiffness of the rubber cable. Mechanical properties of this cable are listed on Table 2-1. The results of load-deflection tests conducted on a 6-foot specimen of nylon line are shown as Figure 2-7.

2.3.3 EXPERIMENTAL ARRANGEMENT. The series of tests was conducted in the High Speed Water Tunnel of the Graduate Aeronautical Laboratories at CIT in late 1977. The water tunnel pumps were not used during the exercise.

One of the vertical sections of the tunnel thus formed a tank 5 feet in diameter and 65 feet deep. A large port in the pipe gave access above the water surface. A mechanism for winching and oscillating the sample cables protruded through the port, as sketched in Figure 2-16.

The traction winch mechanism outside the tank and the right angle sheave cantilevered over the water rode on vertical tracks (Figure 2-17). A Scotch Yoke mechanism (Figure 2-18) moved the entire assembly in simple harmonic vertical motion along the tracks. A strain gauge measured the cable tension around the right angle sheave (Figure 2-19). Oscillation amplitudes of one tenth and one inch were available at frequencies continuously variable up to three cycles per second. The winch could reel in or out at speeds up to 2 feet per second. Its acceleration was also controllable up to a maximum of 4 feet per second-squared.

2.3.4 DATA ACQUISITION. Strip chart recorders gave real time verification that the apparatus was functioning as desired. The permanent record of the experimental data was made on analog magnetic tape. Five parameters were measured:

    a.   The length of cable deployed,

    b.   The winch speed,

    c.   The winch acceleration,

    d   The tension of the right-angle sheave, and

    e.   The phase angle of the oscillator.
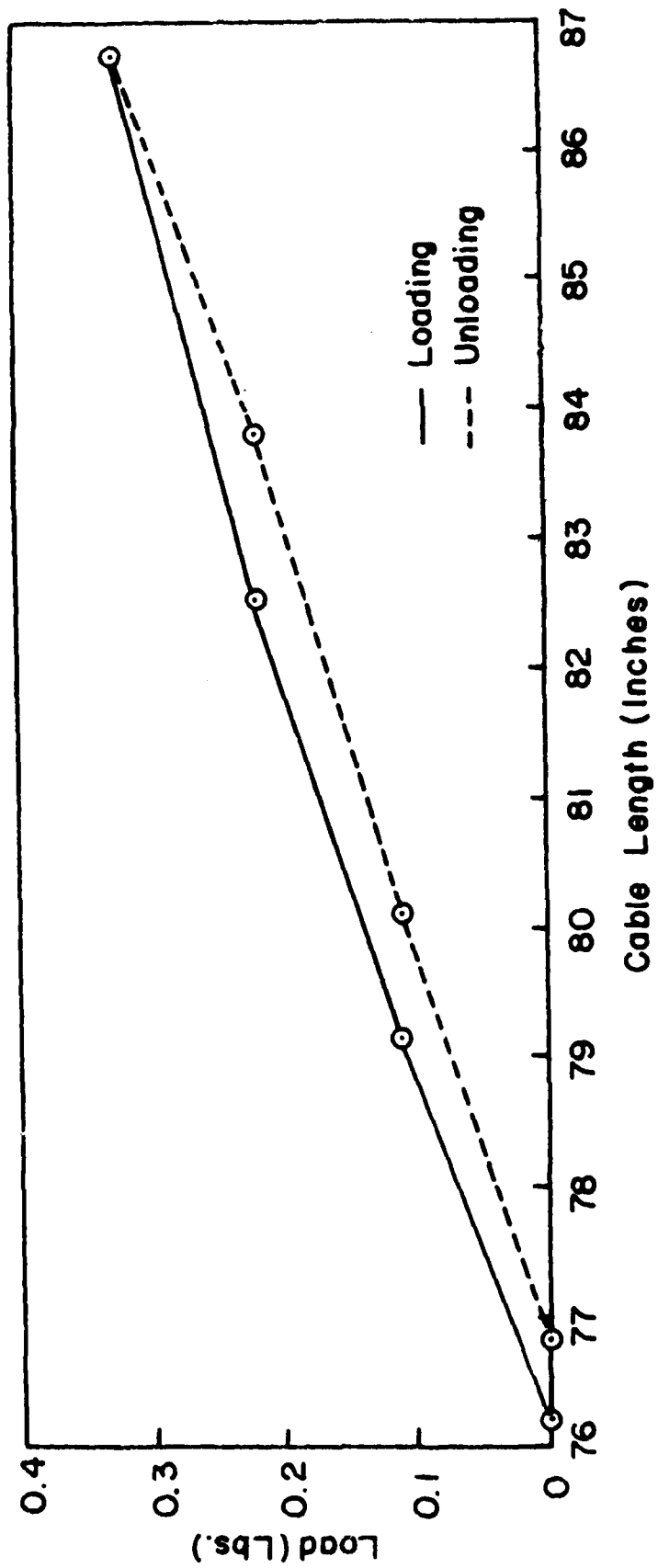
Figure 2-15. Elastic Characteristics of Solid Rubber Cable
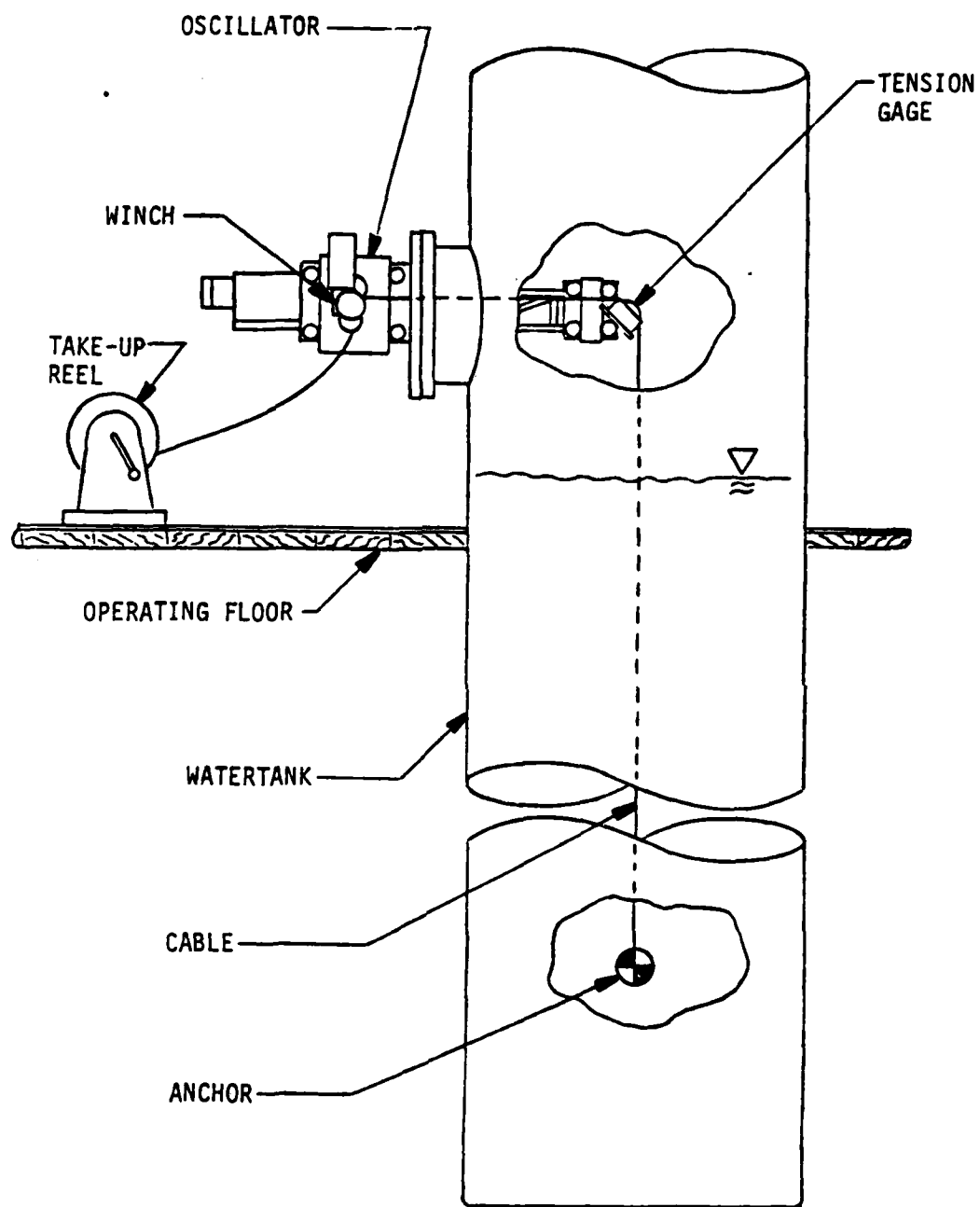
Figure 2-16. Variable Length Experiment Arrangement
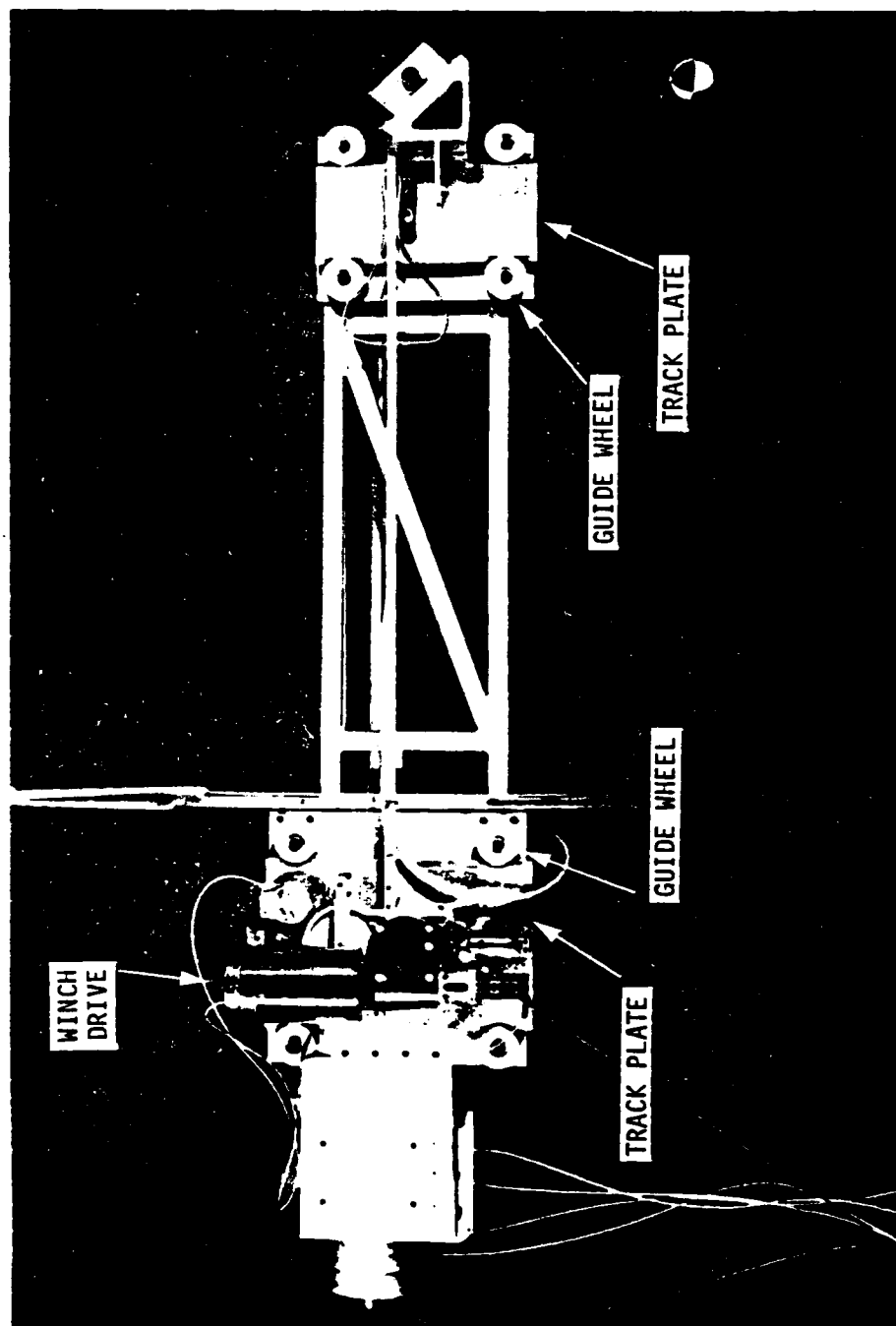
Figure 2-17. The Variable Length Winch with Oscillator
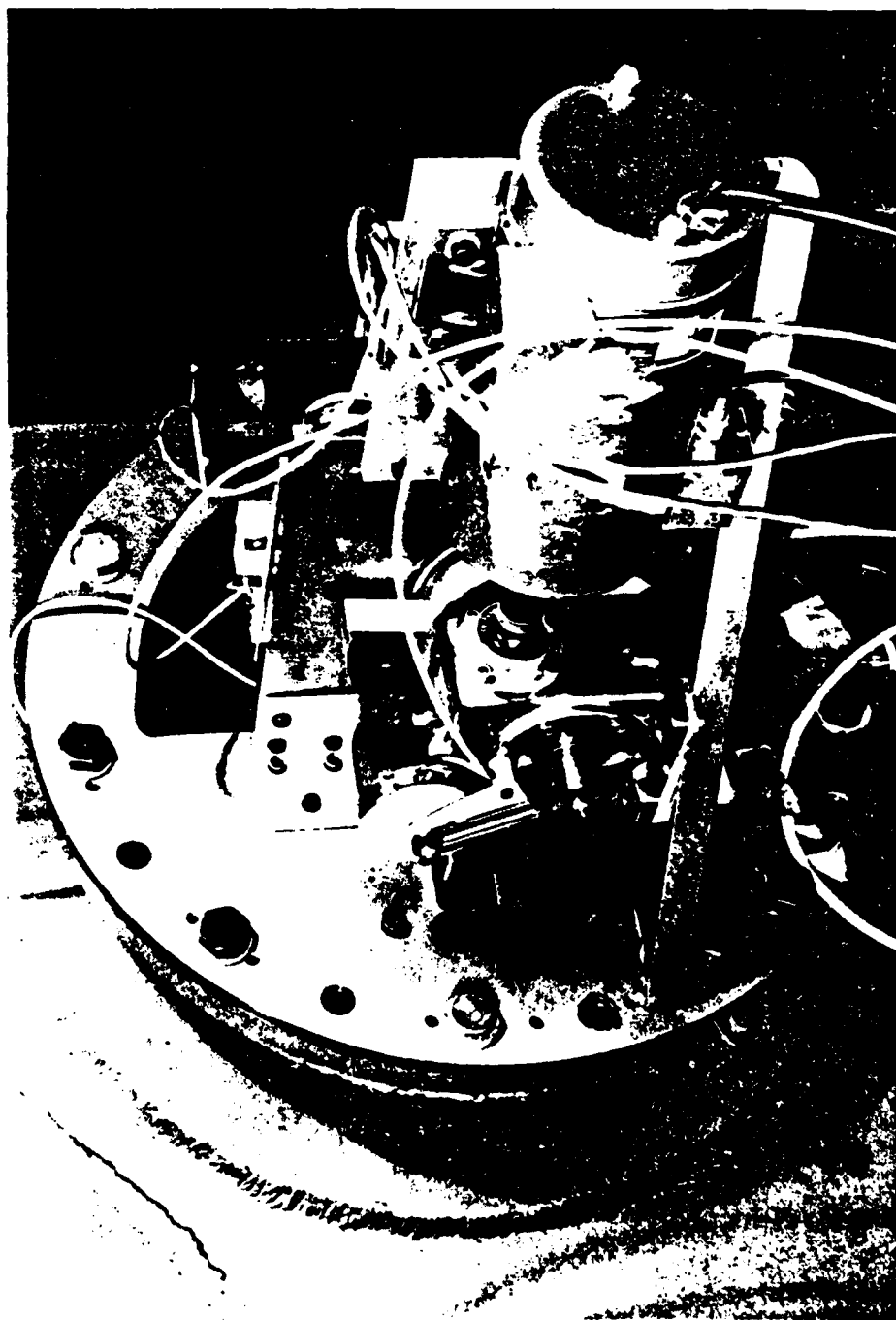
Figure 2-18. Variable Length Oscillator Drive
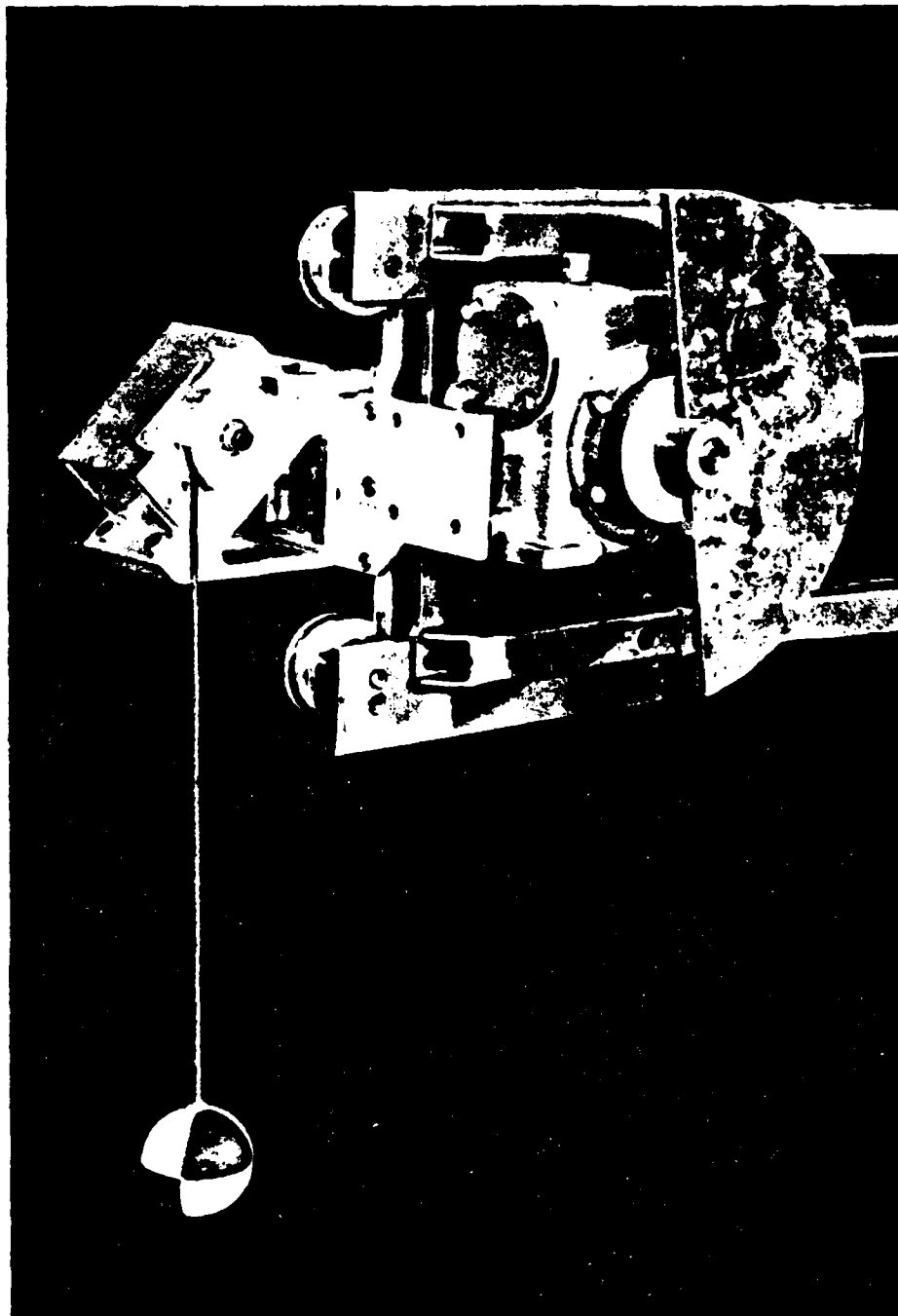
Figure 2-19. Right Angle Sheave and Oscillator
Follower with Counter Weight

The cable was metered by rolling it between a 1-foot circumference wheel and the winch capstan. A tachometer on the capstan drive provided winch velocity. Its signal was differentiated to give the acceleration of the winch. A strain gauge on the sheave support cantilevered over the water provided a tension signal. The oscillator phase angle was measured by a rotary potentiometer coupled to the Scotch Yoke crank. A voice log and a run-in-progress signal used the remaining two channels on the analog tape recorder.

The data acquisition system and cable oscillator were started about 10 seconds before engaging the winch and continued to record about 10 seconds after the winch was stopped. Normally the winch was started and stopped with a constant acceleration "ramp function," but occasionally the winch was abruptly braked to simulate an emergency stop. The cable meter wheel offset the actual cable length by a total of 7.2 feet. Of this bias, 2.2 feet account for the horizontal span from the meter wheel to the tension sheave, 2.0 feet represent the distance to the water, and 3.0 feet represent the initial depth of the "anchor" sphere.

In some cases, motion pictures of the anchor were taken through a view port in the tank wall.

2.3.5 DATA REDUCTION. The analog tapes were played through an analog to digital converter and recorded on digital tape at a rate of 1000 samples per second. The digital tape record consisted of values corresponding to the sensor output voltages. Calibration of the digital tape record to engineering units is accomplished by a second post processing computer program. This program also smooths and tabulates the data for time increments longer than 0.001 second. For the data comparisons in this report, the smoothing interval was 0.01 second.

2.3.6 RESULTS. Ninety-seven cases were completed, of which 55 used the nylon cord and 42 used the rubber line. Thirty-seven each of payout and reel-in cases were included, with 22 fixed length oscillating cases, and one purely static case with no excitation whatever. Thirteen of the payout cases, 13 reel-in cases had no oscillatory excitation.

Time was not recorded during the experiment, except on the strip chart recorder. Slight drift in the analog recorded speed between the test and digitizing is negligible as is the inaccuracy of the time base used to trigger the analog to digital conversion.

The tension data lie within about 0.01 pound of the local common trend. Occasional values may deviate by as much as 0.05 pound. These points are obscure in tabular listings or graphic plots unless an expanded scale is used. These errant points have negligible influence on the overall data. Computer programs used to process the data may need extra statements to ignore these points.

Cable length was measured to within about 0.1 feet. The metering wheel rolled along the relaxed length on payout, but measured stretched length on reel-in. This is an imperceptible difference with metallic cables, but amounted to several feet in cases using the elastic rubber line.

The winch velocity was monitored to within 2 percent. The acceleration, electronically differentiated from the velocity signal, is estimated to be accurate to 5 percent. The oscillator phase angle is measured within 2.5 degrees.

The four cable excitation channels may also have occasional aberrant values much larger than these error estimates.

2.4 ANCHOR-LAST DEPLOYMENT AT SEA.

2.4.1 CONFIGURATIONS. The dynamic response of a 2,500-foot long single point sub-surface scientific mooring was measured at sea during nine events including the anchor-last deployment of the mooring itself. The term "scientific" is used to distinguish the mooring from a ship mooring which would use much heavier components. This mooring was fifth in a series of six moorings deployed for the Mooring Dynamics Experiment (MDE) at the Pacific Missile Range Facility, Barking Sands, Kauaii, Hawaii in October 1976 (Reference 8). The sixth mooring supported an array of current meters nearby.

Figure 2-20 is a chart of the MDE environment. It shows the location of each mooring as well as the deployment track for the CEL mooring. Figure 2-21 is a sketch of the CEL mooring.

The deployment proceeded from the top down. That is, the main buoy at the top of the mooring was made up to the mooring line and towed afloat behind the USNS DE STEIGUER, steaming slowly along the deployment track. The mooring line was deployed, with instruments attached at appropriate intervals, until the entire mooring except the anchor was undertow. The anchor, a large clump of sandbags, was made up to the mooring on a chute. It was dumped overboard at the drop site and plummeted to the bottom, eventually pulling the entire mooring below the surface. Later, the mooring was recovered by abandoning the anchor using acoustically controlled release devices.

The mooring tension was recorded by instruments at four locations along the cable. The positions of "pingers" attached near the tensiometer were tracked using the hydrophone array of the missile range. At two of the positions, water temperature and hydrostatic pressure (depth) was also recorded.

2.4.2 MATERIALS. Wire rope composed most of the mooring line. A 3/16-inch rope (3 x 19 construction) with a polyurethane jacket was used. Short lengths of 3/8-inch galvanized open-link chain were used to insert the instrument packages. One-half-inch chain and 33 feet of 3/4-inch nylon line linked the acoustic release assembly to the sand bag anchor. Table 2-2 summarizes the material properties.
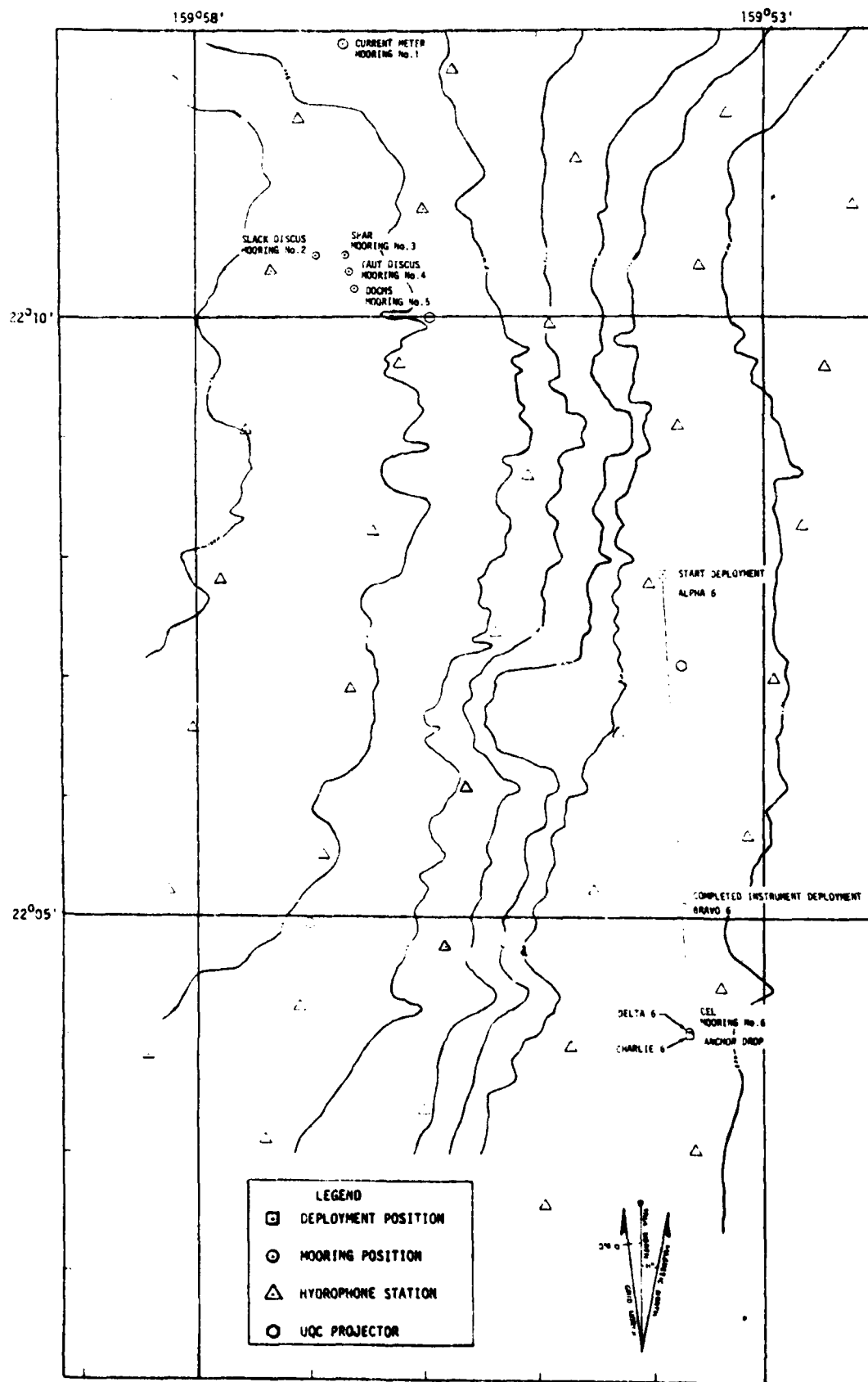
Figure 2-20. Ship Track and Experiment Location for CEL Mooring

LEGEND

▢ DEPLOYMENT POSITION

⊙ MOORING POSITION

△ HYDROPHONE STATION

○ UQC PROJECTOR

44" SPHERE (1050 LB BUOYANT)

10M 3/8" CHAIN

T/P (0-123M) 90

2M 3/8" CHAIN

FVR (0-3000 #)

2M 3/8" CHAIN

SC PINGER (ECHO) (DROP SONDE)

242M 3/16" WR

FVR (0-3000 #)

2M 3/8" CHAIN

SC PINGER (CHARLIE)

96M 3/16" WR

T/P (325-525M)

137M 3/16" WR

FVR (0-3000 #)

2M 3/8" CHAIN

SC PINGER (DELTA)

177M 3/16" WR

FVR (0-3000 #)

2M 3/8" CHAIN

DC PINGER (ALPHA)

2M 3/8" CHAIN

38" AL SPHERE (847 LB BUOYANT)
2M 3/8" CHAIN
38" AL SPHERE (847 LB BUOYANT)
2M 3/8" CHAIN
DC PINGER (BRAVO)
2M 3/8" CHAIN
DUAL RELEASES
3M 1/2" CHAIN

10M 3/4" NYLON
2M 1/2" CHAIN

2600 # SANDBAG ANCHOR

NOTES: O DEGREE SYMBOL REPRESENTS STANDARD
TERMINATION OF (2) 1/2" SHACKLES
AND (1) 1/2" MASTER LINK

A : (1) 1" SHACKLE, (1) 1/2"
MASTER LINK AND (1) 1/2"
SHACKLE

B : (1) 5/8" SHACKLE, (1) 1/2"
MASTER LINK AND (1) 1/2"
SHACKLE

C : (2) 1/2" SHACKLES, (2) 1/2"
MASTER LINKS AND (1) 5/8"
SHACKLE

Figure 2-21. Schematic Drawing of the CEL Mooring

2-32

2.4.3 EXPERIMENTAL ARRANGEMENT.

2.4.3.1 Mooring Description. The primary flotation element was a 44-inch diameter sphere producing 1050-pounds buoyancy in seawater. A Xenon flash lamp and radio beacon were mounted on top as recovery aids. The mooring line was 3/16-inch diameter 3 x 19 jacketed steel wire rope with an overall diameter of 0.390 inch. As shown in Figure 2-21, short lengths of chain and nylon line were used for assembly convenience and to resist chafing. Two Temperature/Pressure (T/P) Recorders, four FVRs and five acoustic pingers were installed on the mooring as shown. Two 38-inch aluminum spheres provided 847 pounds emergency buoyancy in the event the primary buoyancy failed. These two relatively large spheres were used on the CEL mooring in order to simplify the mooring as much as possible for numerical simulation. Dual AMF acoustic releases were used to improve system reliability. The anchor on the CEL mooring was made of sandbags lashed together and held in a cargo net (donated by PMRF). A photograph of the anchor is shown in Figure 2-22. The sandbag anchor was used to reduce the possibility of damage to the range hydrophone cables on the sea floor. A 1500-foot length of 1/4-inch polypropylene line with a small surface float was attached to the main buoy. It was used to displace the mooring during the relaxation experiments.

2.4.3.2 Instrumentation. The mooring was instrumented with two T/P recorders and four FVRs developed by Charles Stark Draper Laboratories (CSDL, Reference 9). Five acoustic pingers supplied and maintained by the Naval Torpedo Station Detachment, Hawaii were used. The position of these pingers was tracked by the PMR hydrophone array and computer.

Two types of T/P recorders were used during the MDE, differing primarily in the data sampling rate. Both types used calibrated thermistors for temperature measurement and strain-gauged diaphragms for pressure measurements. The instruments are battery-powered and self recording; the data are digitized in the instrument and are recorded on a data tape cassette. The low-frequency T/P (LFTP) instruments sampled temperature, pressure and time every 3.75 seconds, but recorded only every 64th sample (i.e., every 4 minutes). The high-frequency instruments (HFTP) recorded temperature every 2.08 seconds and pressure every 0.52 seconds so that four pressure words are recorded with each temperature word. For the CEL experiment, a burst lasted 28 minutes, 50.56 seconds, repeated every 43 minutes, 41.44 seconds. Ranges and scaling of the instruments used in the MDE are given in Table 2-3.

The Force Vector Recorder (FVR) is a self-contained motion and tension sensing package. The battery-powered instrument records digitized data on an internal tape cassette. The FVR has six sensor channels, including three mutually orthogonal servo accelerometers, two magnetometers for azimuth reference and a strain-guage load cell for tension measurement. For the MDE, tension cells with a full-scale
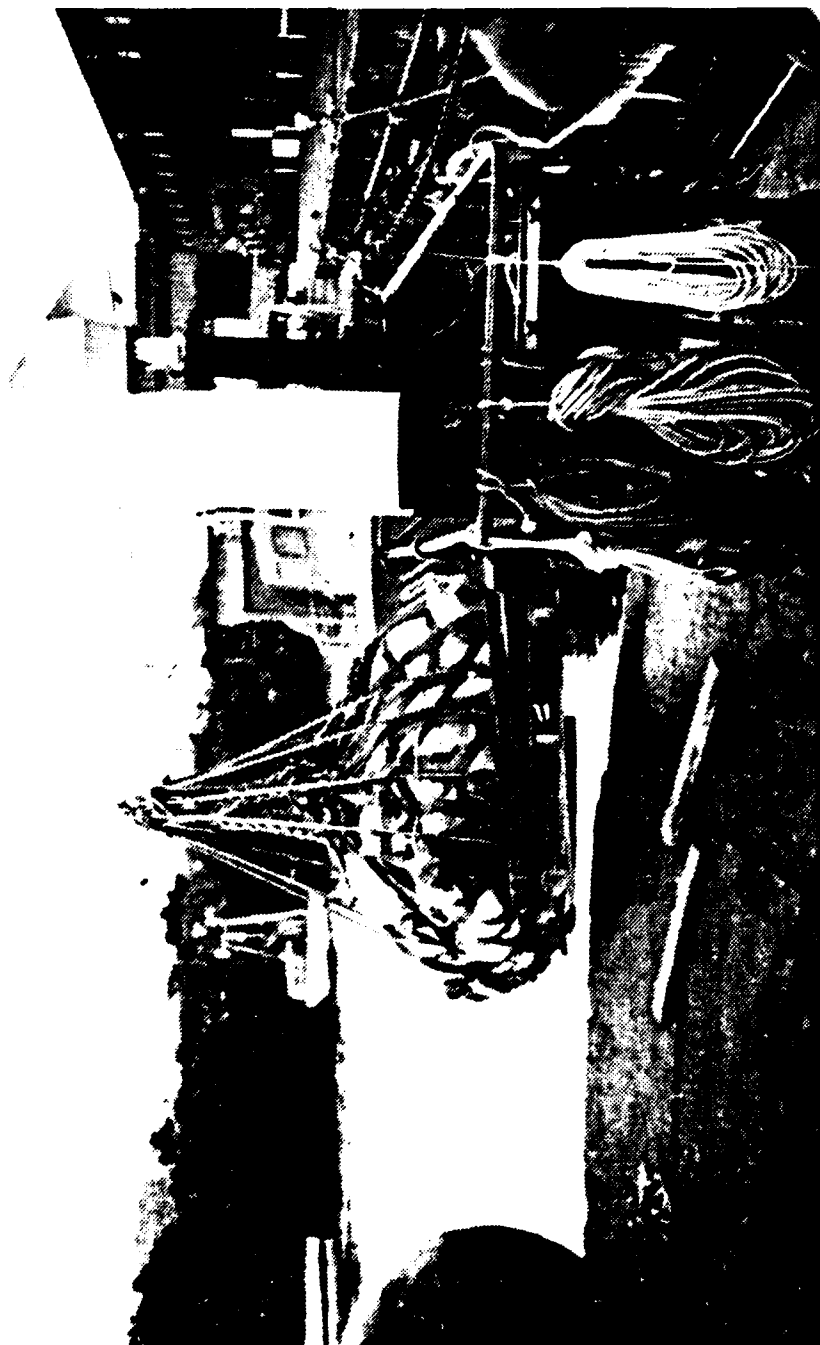
Figure 2-22. The Sandbag Anchor

TABLE 2-2. MOORING COMPONENTS AND PHYSICAL DATA

Item	Component	Material	Form	Attachment	Diameter in. (mm)	Air Wt. lb/ft (Kg/M)	Seawater lb/ft (Kg/M)	*	Ea lb (N)	In Line Length Ft (M)
1	Chain	Steel	Open-link	in-line	0.375 (9.52)	1.768 (2.660)	1.554 (2.313)	H	8.97×10^5 (3.99×10^6)	Variable
2	Chain	Steel	Open-link	in-line	0.500 (12.7)	3.154 (4.694)	2.743 (4.082)	H	1.26×10^6 (5.59×10^6)	Variable
3	Wire Rope	Steel Polyurethane	3/16-3x19 Jacketed	in-line	0.390 (9.9)	0.0549 (0.0817)	0.0469 (0.0698)	H	3.12×10^5	Variable
4	Line	Nylon	Braided	in-line	0.750 (19.1)	0.150 (0.223)	0.017 (0.025)	H	non-linear	32.8 (10.0)
5	Main Buoy	Aluminum	Sphere	in-line	44.0 (1118.)	Lbs (Kg) 360 (163)	Lbs (Kg) 1050 (477)	B	-	3.67 (1.12)
6	Reserve Buoy	Aluminum	Sphere	in-line	38.0 (965)	360 (163)	847 (384)	B	-	3.17 (9.65)
7	Anchor	Sand	Bags piled in 5'x5' square	Cargo net	60 (1524)	-	2600 (1180)	H	-	4 (1.2)
8	T/P Recorder	-	Sphere	Clamp-on	11.5 (292)	6.51 (29.5)	20.0 (9.1)	H	-	1.33 (0.406)
9	FVR	-	Sphere	in-line	19.0 (483)	130 (59.0)	4.0 (1.8)	B	-	1.85 (0.575)
10	SUB CAN Pinger	-	16.5 inch cylinder	in-line	10.0 (254)	98.9 (44.8)	44.3 (20.1)	H	-	3.51 (1.07)
11	DEEP CAN Pinger	-	26.0 inch cylinder	Clamp-on	12.2 (260)	143 (64.9)	75.9 (34.4)	H	-	-
12	Acoustic Release	-	41.0 inch cylinder	Clamp-on	7.5 (190)	130 (59.0)	70.0 (31.7)	H	-	5.0 (1.5)

* H = "Heavy" in Seawater
  B = Buoyancy in Seawater

TABLE 2-3. NOMINAL RANGES AND SCALING OF TEMPERATURE-PRESSURE RECORDERS
EMPLOYED IN MOORING DYNAMICS EXPERIMENT

	High Frequency Temperature - Pressure Recorder (HFTI)				Low Frequency Temperature - Pressure Recorder (LFTI)		
Instrument Serial Number (S/N)	90	91	92	93	15	84	85
Temperature Range (°C)	2.86-30.31	2.86-30.31	2.86-30.31	10.68-29.67	0-20	10-26	0-20
Temperature Least Significant Bit, LSB_T (°C)	.027	.027	.027	.019	.02	.015	.02
Pressure Sensor Full Scale Capability (Meters of Water)	127	229	127	58.3	1703	683	683
Pressure Sensor Range (Meters)	0-127	60-229	60-100	0-20	1167-1667	120-320	325-525
Pressure Sensor Least Bit Significant Bit, LSB_p (cm)	12.7	16.9	4	2	50	20	20

range of 3,000 pounds were used. In addition, an internal clock provides a reference time. The instrument can be used in a burst or sample mode; for the MDE the burst mode was used, with a burst duration of 14 minutes, 41.2 seconds and a burst repetition period of 87 minutes, 22.88 seconds. The data channels are sampled every 0.52 seconds. The instrumentation electronics are housed in a 13-inch diameter pressure shell which weighs 85 pounds in air and 45 pounds in water. In use, the pressure shell is surrounded by a 19-inch diameter syntactic foam flotation shell which renders the unit neutrally buoyant in seawater, with an air weight of 130 pounds. The mooring attachments are aligned with the centerline of the unit. Characteristics of the FVRs are summarized in Table 2-4.

The T/P and FVR instruments are switched on by the removal of an external magnet. All of the instruments (T/P's and FVR's) were synchronized to a common time base by CSDL.

Five acoustic pingers were installed on the mooring to give position data using the PMRF acoustic tracking range facilities. The pingers operated at frequencies between 13 and 24 kHz and were pulsed-coded for identification. The pulse repetition rate was 1 pulse per second.

2.4.4 DATA ACQUISITION. Two types of experiments were made on the CEL mooring during the MDE. The first of these was the anchor-last deployment of the mooring; and the other, termed a "relaxation" experiment, involved pulling the mooring to one side, releasing it and allowing it to return to equilibrium. Only data from the deployment are presented in this report.

The anchor-last technique is a common method for deploying single-point oceanographic moorings. In this procedure, the following sequence of operations is followed. First, the main buoy is released with the mooring line attached. The ship steams slowly away from the buoy, paying out mooring line, with any instruments or distributed flotation attached. The line is paid out at approximately the same rate as the ship speed until only the anchor remains on the ship. The anchor is then released and falls to the sea floor, pulling the mooring line and buoy into the equilibrium configuration. During the anchor descent, significant transient forces act on the mooring line. The present experiment was intended to measure these forces and the trajectories followed by the anchor, mooring line and buoy during the deployment.

The CEL mooring was set from USNS DE STEIGUER (T-AGOR-12) on 1 November 1976, at 22°04' 1.4" N, 159°53" 38.4" W. The track followed by the ship during the deployment is shown in Figure 2-20. The points shown on the ship track correspond to the operations in the deployment sequence as follows:

ALPHA 6   Main flotation buoy released

BRAVO 6   All mooring line and instruments deployed
               (Ship towing entire mooring with anchor on deck)

2-37

TABLE 2-4. FORCE VECTOR RECORDER CHARACTERISTICS

Measurement	Sensor	Maximum Ranges	Sensor* Frequency Response	Maximum+ Resolution (10 bit word)
Acceleration - 3 mutually orthogonal axes	Force Balance Accelerometer	±2g	48 Hz	0.001 x Full Scale (e.g., 0.004g for ±2g unit)
Azimuth Reference - 2 axes orthogonal to mooring line	Magnetometer	0-360°	N.A.	~0.1° (Max)
Tension	Strain Gage Bridge Load Cell	0-3,000 pounds	~0-10 kHz	0.001 x Full Scale = 3 pounds
Pressure	Strain Gage Bridge	0-10,000 psi	0-10 kHz	0.001 x Full Scale

General Capabilities: Pressure: 10,000 psi maximum external pressure on case, 5,000 psi on load cell, 3,400 psi on flotation shell.

Life: To approximately 6 months on internal battery package.

Data Recording: Burst or continuous mode at 2,6-word scans/sec (10 bit words).

* Overall FVR frequency response is limited to Nyquist frequency of $f_{Ny} = \frac{1}{2\Delta t} = 0.96$ Hz

+ Resolution of least significant bit may be increased by reducing sensor range. Select Full Scale output for optimum accuracy and range in any application.

CHARLIE 6   Anchor deployed

DELTA 6   Anchor position on bottom

It will be noted that the mooring location is approximately in the center of the triangle formed by three of the range hydrophones. The current meter mooring location is shown in the upper left hand corner of the figure.

The anchor was released at 7:14 a.m.; it reached the bottom about 9 minutes later. The weather during the deployment was excellent; the wind and sea were nearly calm, with a 2-foot swell.

2.4.4.1 Data Acquisition. The data coverage for the CEL experiment is summarized in Table 2-5. This figure shows the instrument burst times and the timing of the several events of the experiment. The anchor deployment, the relaxation experiments and the firing of the acoustic release were timed to coincide with FVR bursts. The data recovery rate for the CEL experiment was exceptionally high. The FVR's and T/P's provided a 100 percent data recovery throughout the experiment.

Pinger ALPHA was tracked during the deployment, but thereafter its signal was lost, apparently because it was mounted so close to the bottom. Acoustic "track" was never established on pinger BRAVO.

Pinger CHARLIE seemed to be tracked during the experiment, but further processing afterwards revealed several large gaps in the data. Pingers DELTA and ECHO were tracked more reliably, with only occasional "holidays" in their records.

2.4.4.2 Current Meter Data for MDE Experiment 5. Currents in the MDE area were measured by a vertical array of WHOI Vector Averaging Current Meters (VACM's) mounted on a separate mooring nearby. The current meter mooring location is shown on Figure 2-20. The data were reduced by the Pacific Marine Electronics Laboratory (PMEL) of NOAA. Current data are presented in Appendix C of Reference 5. In general, current speed was less than 0.2 knots.

2.4.4.3 Temperature/Presure Recorder Data. A low frequency temperature and pressure recorder was installed on the CEL mooring 1179 feet below the buoy at a nominal depth of 1385 feet. This device recorded a sample each 4 minutes continuously throughout the entire MDE. Figures 2-23 and 2-24 show the temperature and depth data recorded during the CEL experiment plotted for a period from 2 hours before the first FVR burst until after the mooring was recovered. The depth plot, Figure 2-24, clearly shows the four relaxation experiments. The minimum depth which would be recorded by the instrument was 1066 feet.

A high frequency temperature/pressure recorder was installed on the CEL mooring 33 feet below the main buoy at a nominal depth of 244 feet. The burst repetition rate for the HFTP is twice that for an FVR. The instrument records four pressure readings in that interval. Figures 2-25 and 2-26 show the temperature and depth measured by the HFTP during the mooring deployment. The record for other bursts is plotted in Appendix D of Reference 5.

TABLE 2-5. DATA COVERAGE FOR MDE EXPERIMENT FIVE
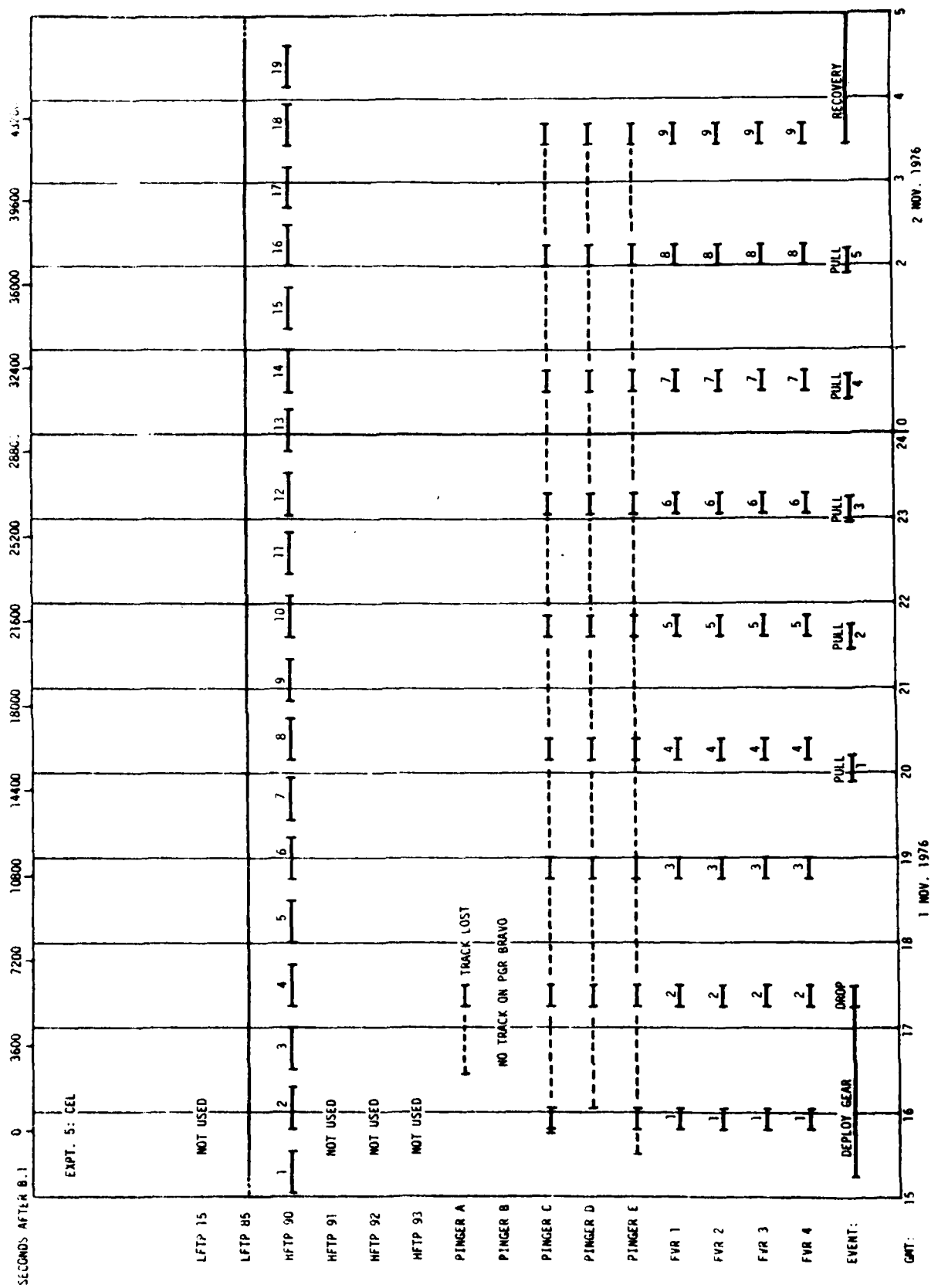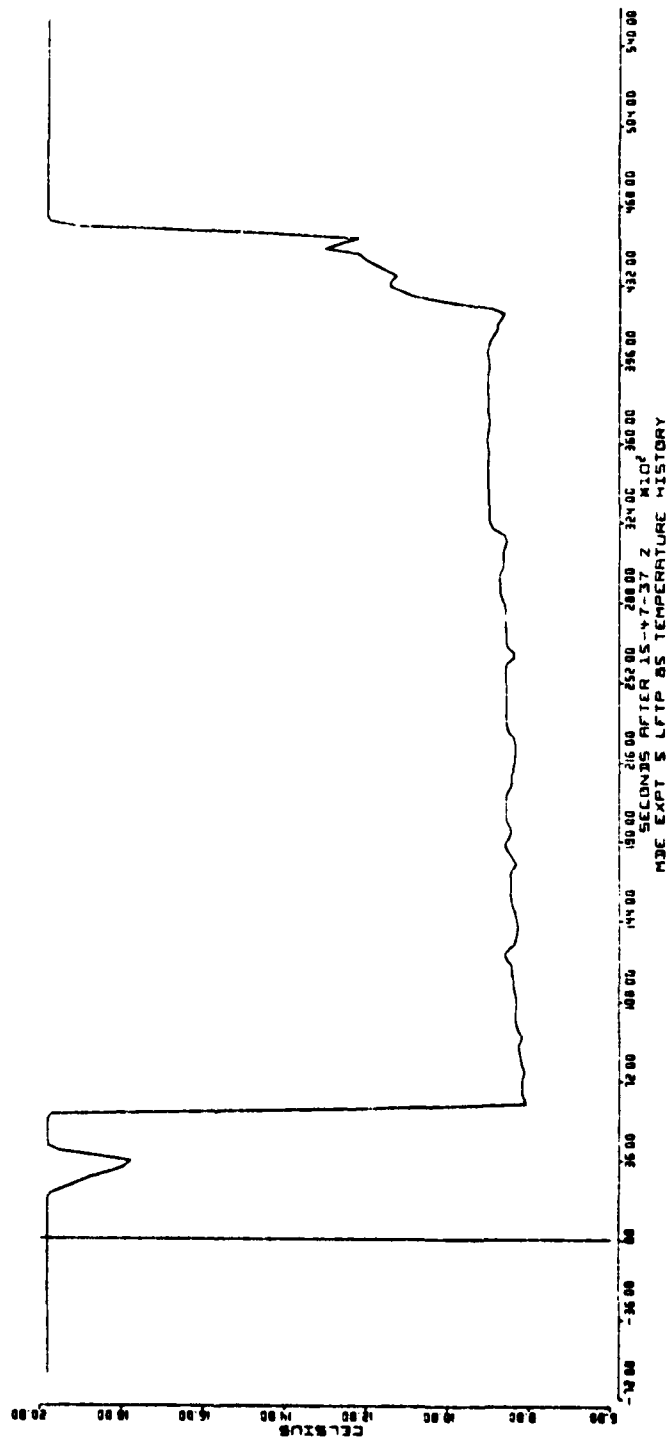
Figure 2-23. Temperature Data Recorded During the CEL Experiment

2-41
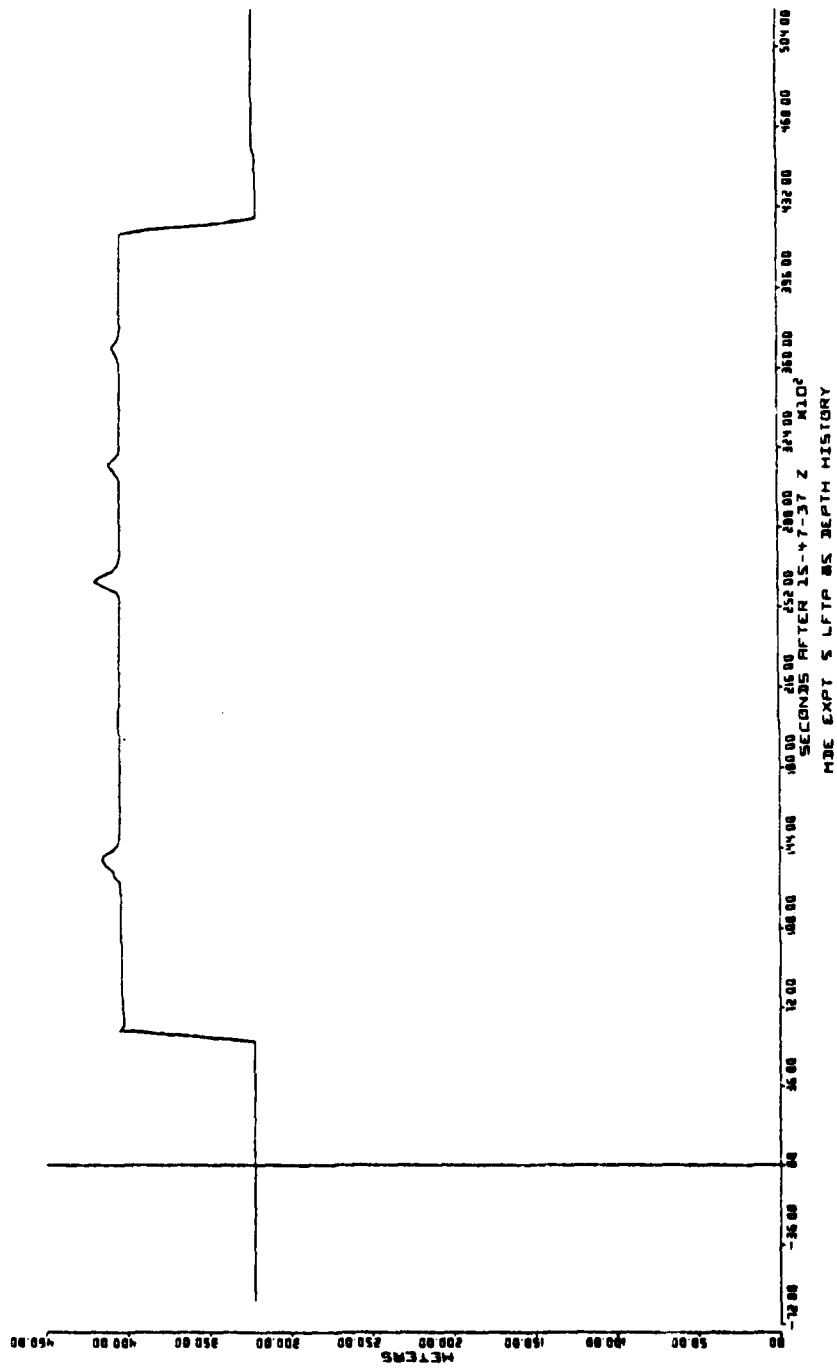
Figure 2-24. Depth Data Recorded During the CEL Experiment
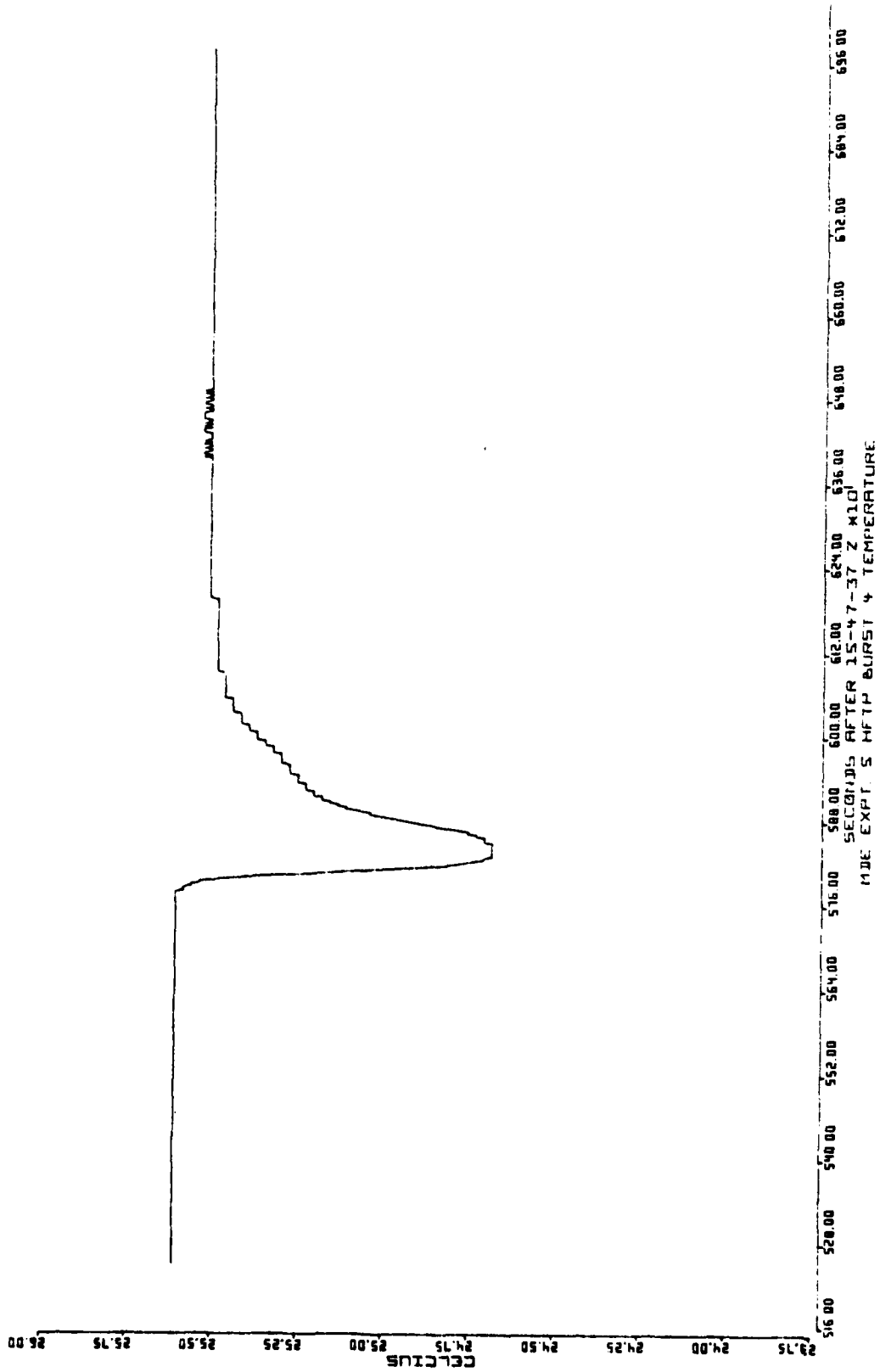
Figure 2-25. Temperature Measured by HFTP During the Mooring Deployment
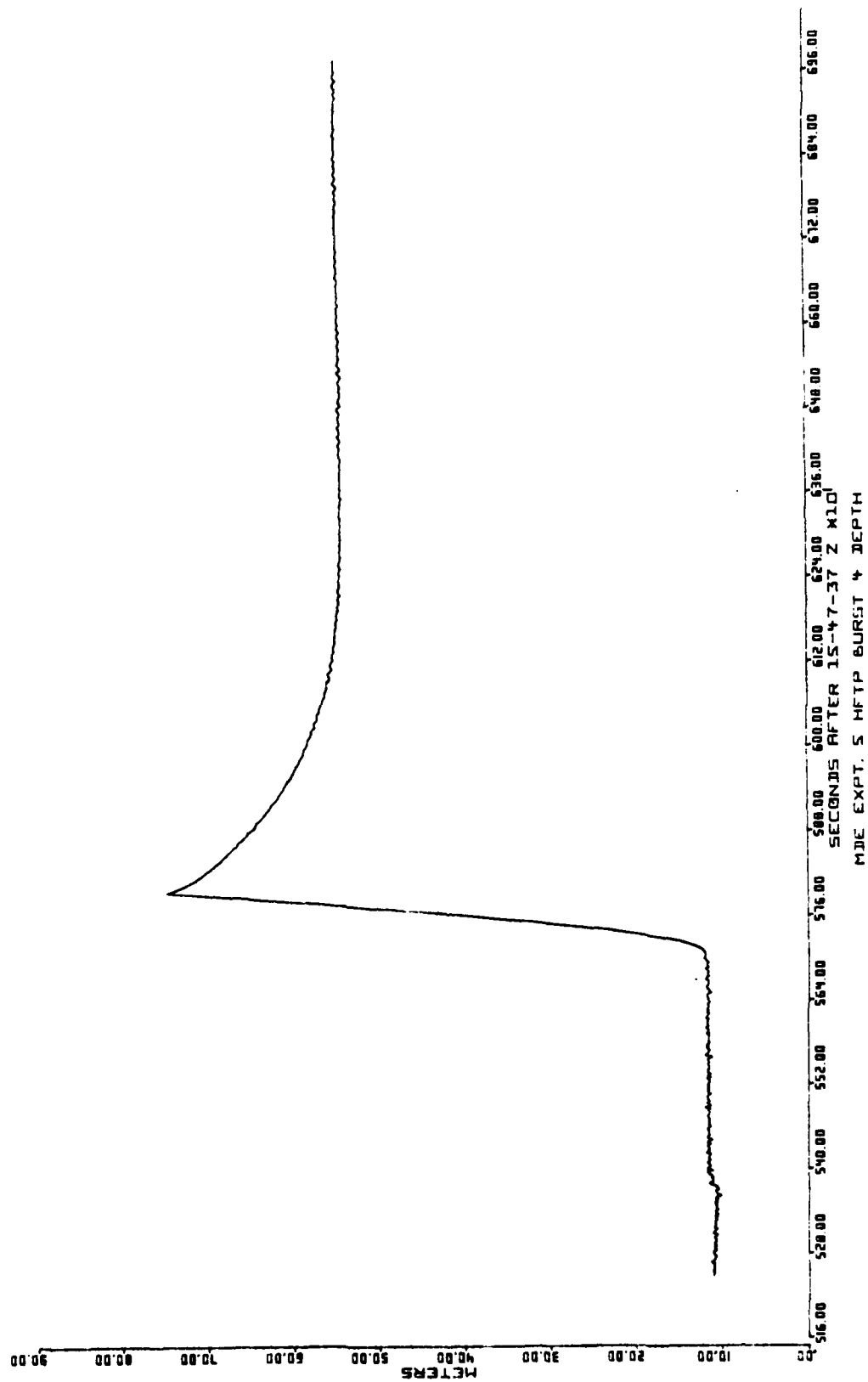
Figure 2-26. Depth Measured by HFTP During the Mooring Deployment

2.4.4.4 Force Vector Recorder Data for Deployment. Tensions measured by the FVRs during the deployment of the CEL mooring are plotted as Figures 2-27 through 2-30. The times shown are elapsed time after the start of the first FVR burst. The figures are in the order in which the instruments were installed on the mooring. The first plot is for FVR 1, installed nearest the top of the mooring, while the last plot is for FVR 4, nearest the anchor. These figures are reproduced because of the exceptional detail they present of a complex dynamic cable event. The FVR locations are shown on Figure 2-21.

2.4.4.5 Acoustic Position Data for Deployment. Five acoustic pingers mounted on the mooring were used to measure the positions of points on the mooring during the deployment. The range did not acquire a track on pinger BRAVO; position data for the other pingers are presented in Appendix F of Reference 5. Figure 2-31 shows the trajectories of the four pingers starting about 30 seconds before anchor release. Figure 2-32 shows the shape of the mooring at five times during the descent, as defined by pinger position.

2.4.5 DATA REDUCTION. The MDE was a major inter-agency program to measure the behavior of several deep-sea moorings. In addition to the CEL were the participants listed in Table 2-6. The experiment was extremely successful, with an exceptionally high data recovery rate. Each of the participating activities took responsibility to reduce, analyze, and report the data from their individual experiments and/or instruments.

The data, reduced to engineering units, were submitted to NDBO for distribution and storage on digital magnetic tape. PMR reduced the acoustic pinger tracking data. CSDL processed the data cassettes from the FVR's and T/P's. NOAA-PMEL reduced the current meter data.

2.4.6 RESULTS. The data gathered during the anchor-last deployment are of remarkably high quality. The current meter array confirmed that the currents during the entire deployed time of the CEL mooring were less than 0.2 knots, although varying direction markedly. These slow currents deflect the taut subsurface mooring only slightly.

The T/P recorders confirm the stability of the mooring, with deflections apparent only when the mooring was displaced deliberately.

The four FVR records show the anchor-last deployment in remarkable detail. The major events of the deployment are clearly portrayed, from before the anchor was released until the mooring has stabilized. Each plot sustains the closest scrutiny: relative tension according to position in the mooring; time of anchor release; time of anchor impact; distance from ship excitation vs distance from buoy excitation under tow; intensity of anchor impact, etc.

Two of the five acoustic pingers were tracked most of the time the CEL mooring was in the water. Another pinger could be tracked only intermittently. Of the two pingers near the anchor, one could not be tracked at all. The other was tracked during the anchor descent, but could not be tracked after the impact. It was probably just too close to the bottom.

2-45
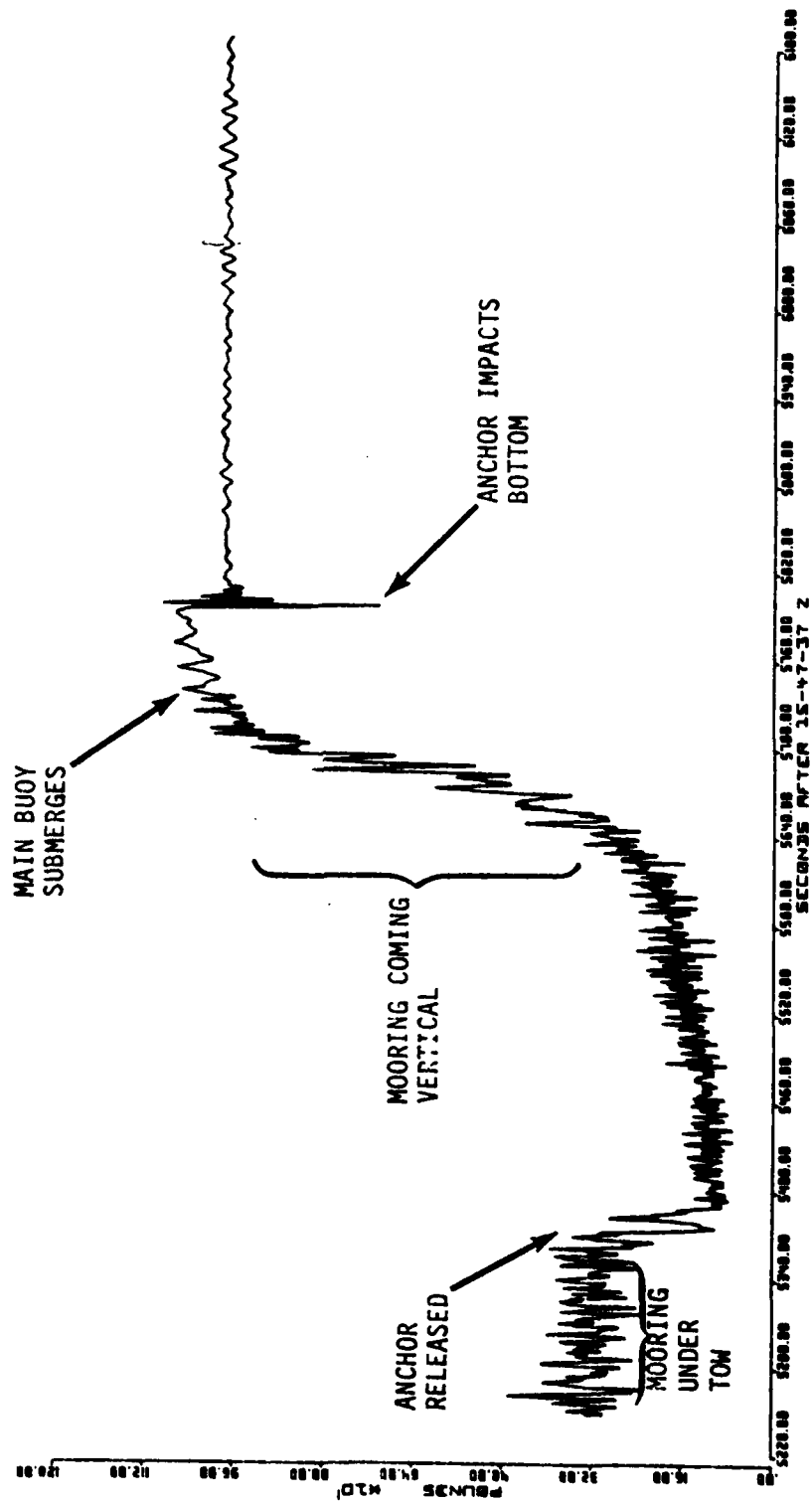
Figure 2-27. MDE Experiment 5 FVR 1, Burst 2: Deployment Tension History

2-46
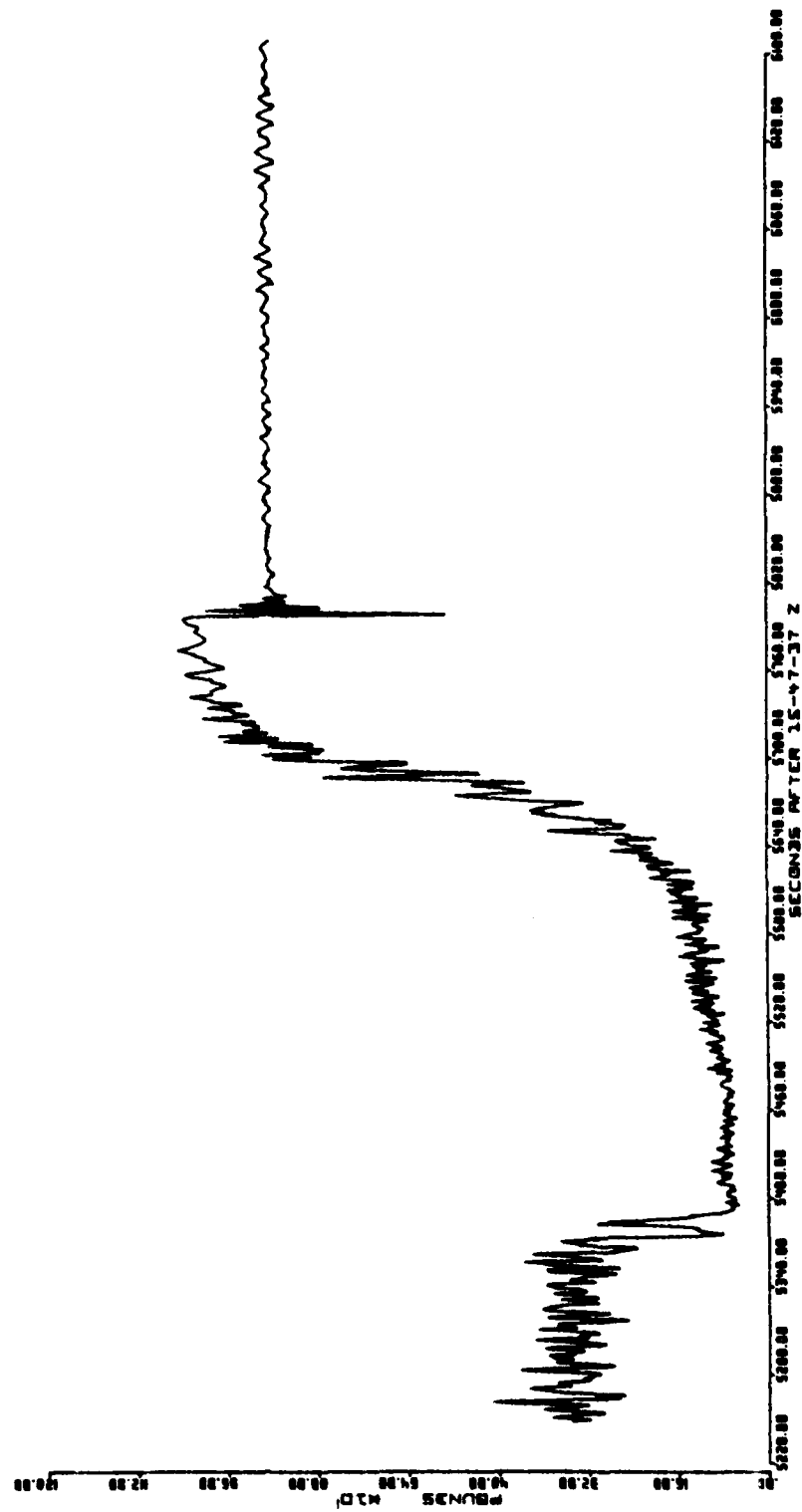
Figure 2-28. MDE Experiment 5 FVR 2, Burst 2: Deployment Tension History
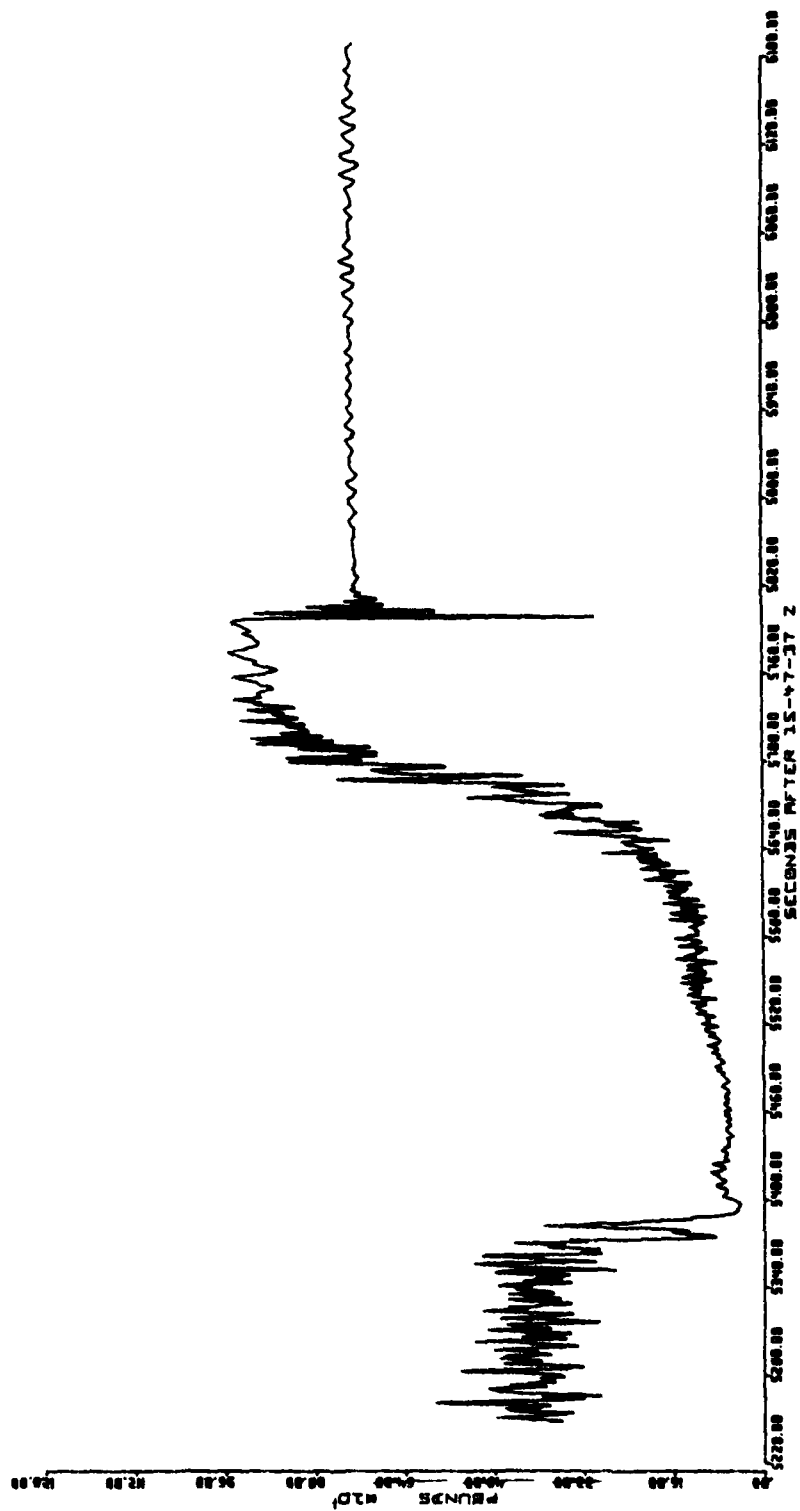
Figure 2-29. MDE Experiment 5 FVR 3, Burst 2: Deployment Tension History

2-48
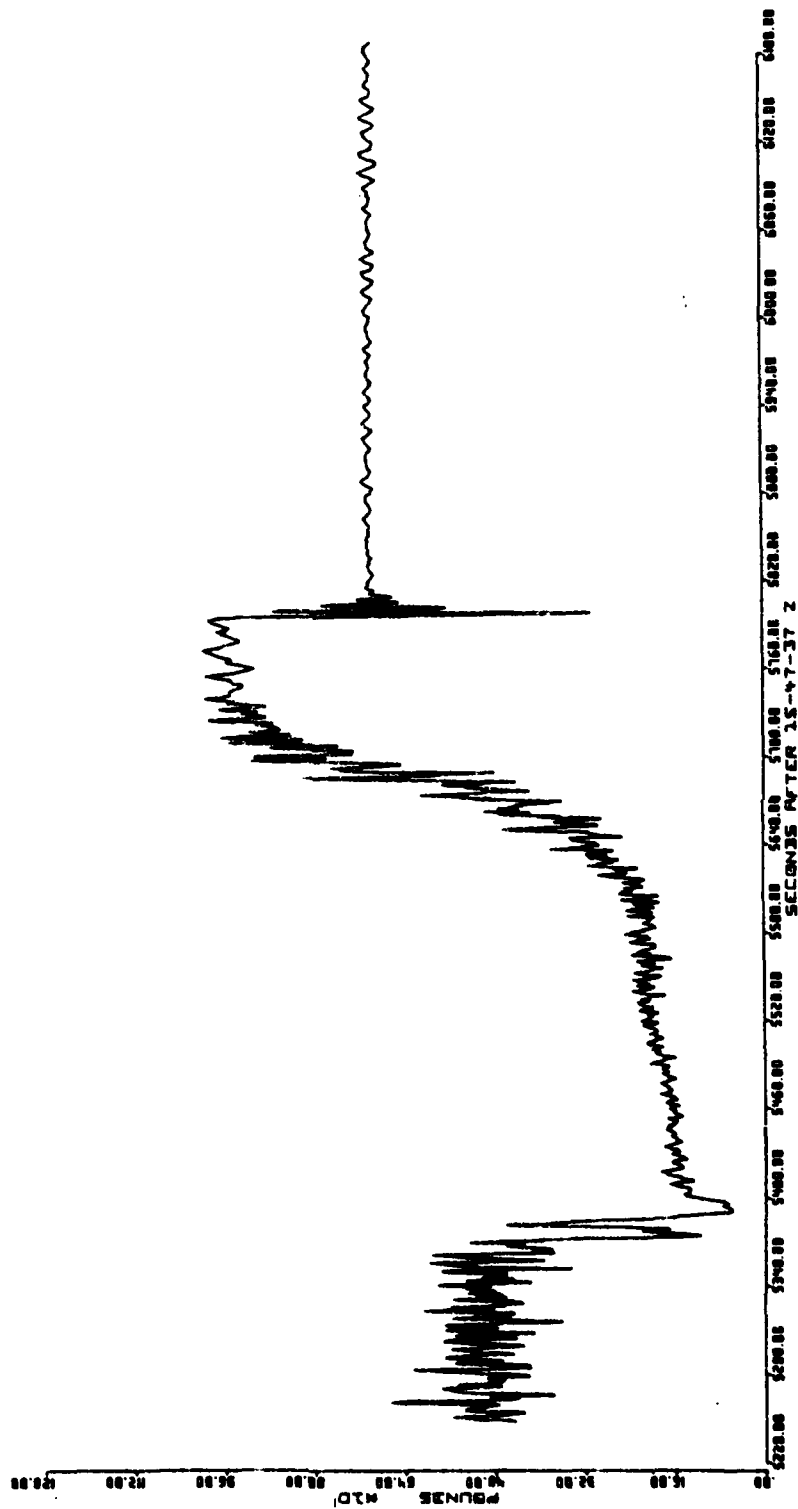
Figure 2-30. MDE Experiment 5 FVR 4, Burst 2: Deployment Tension History
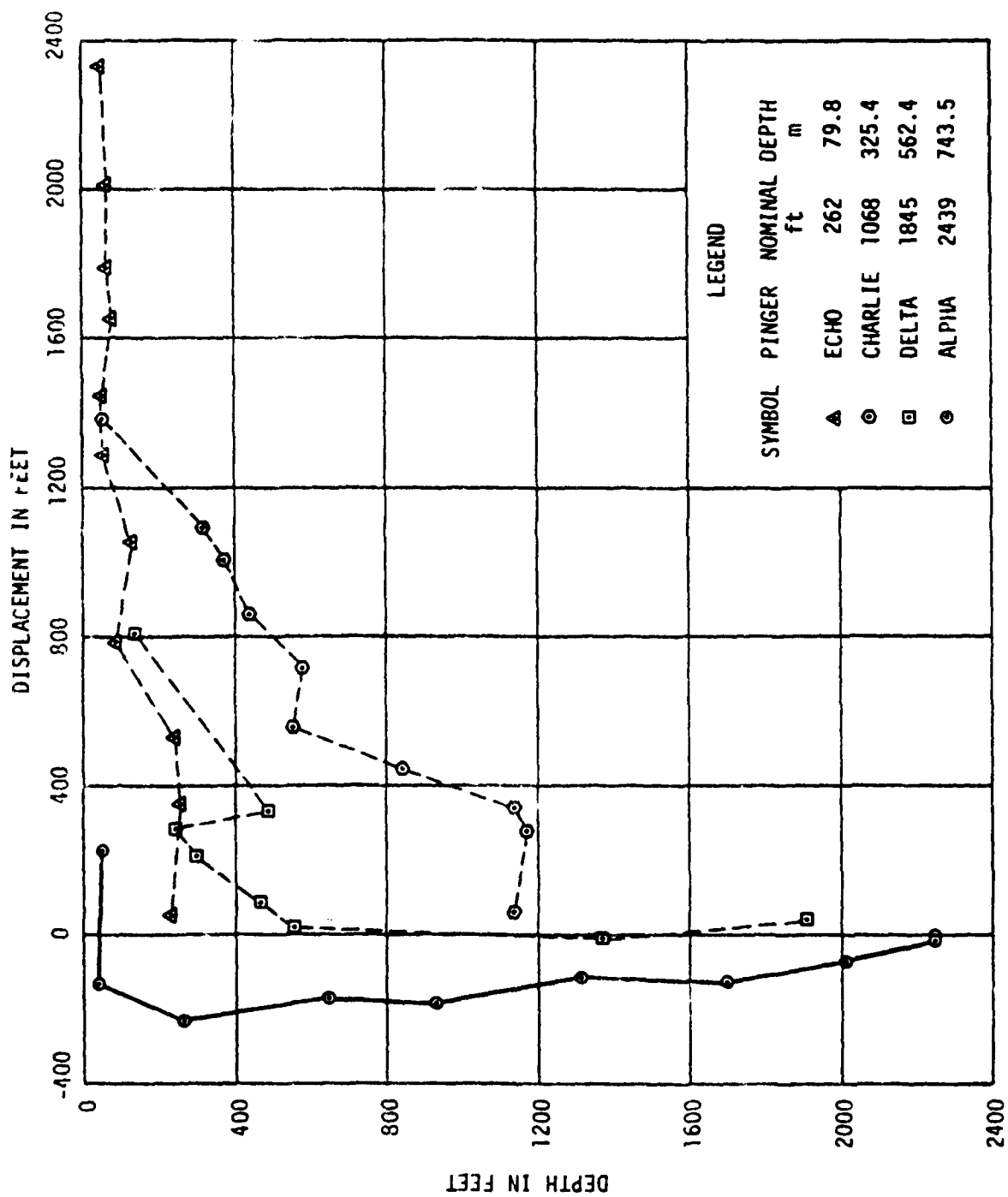
Figure 2-31. Deployment Trajectory for Pingers
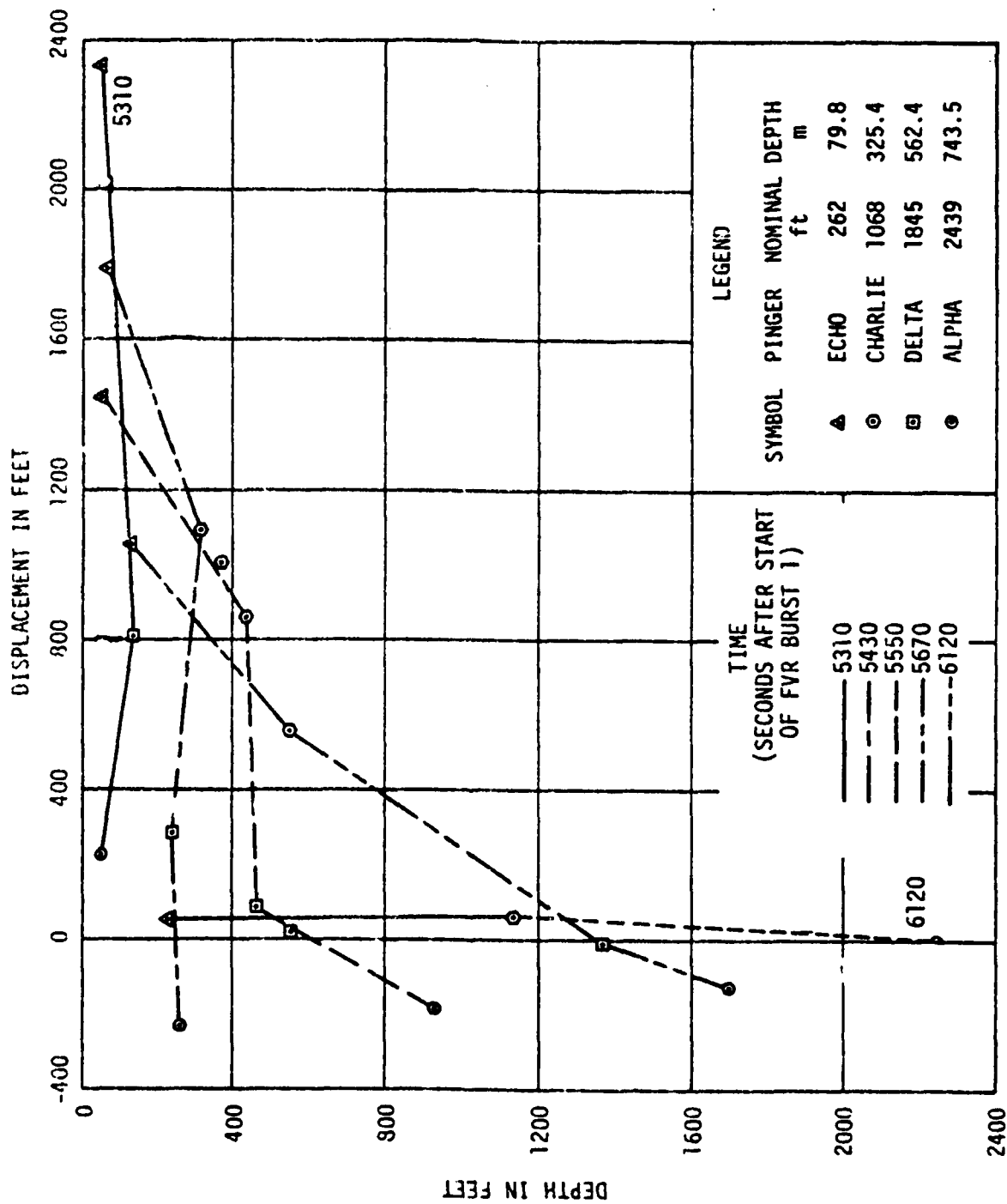
Figure 2-32. Deployment "Snapshots" of CEL Mooring

2-51

TABLE 2-6.   PARTICIPATION IN THE MOORING DYNAMICS EXPERIMENT

PARTICIPANT	RESPONSIBILITY
National Data Buoy Office	funding, buoy motion instrumentation, data archiving and dissemination
Office of Naval Research	funding, contract support
Woods Hole Oceanographic Institution	experiment coordination and direction; principal investigator
Charles Stark Draper Laboratories	manufacture, preparation and operation of mooring line motion and temperature/pressure instruments; data reduction from instruments
Pacific Missile Range Facility, Barking Sands	acoustic and radar range tracking facilities, logistic support
Naval Torpedo Station Detachment, Hawaii	acoustic pinger preparation and operation
Naval Oceanographic Office	current meter preparation and refurbishment, data reduction
Civil Engineering Laboratory	funding, mooring hardware, technician support
Naval Facilities Engineering Command	funding, current meters
Pacific Marine Environmental Laboratories, NOAA	current meter preparation and refurbishment, data reduction
EG&G Washington Analytical Services Center, Inc.	services, equipment

SECTION 3

COMPUTER MODELS

3.1 INTRODUCTION TO SEADYN.

This general, three-dimensional computer model of the static and dynamic re-
sponse of cable structures to the ocean environment uses the finite element method
of analysis (References 6 and 10). The system of continuous cables is divided into
a set of discrete elements joined at nodes. The equations of motion for each
element are solved subject to two conditions. First, the ends of all elements
attached to a common node must coincide at that node. Second, the forces acting at
a node must sum to zero.

3.1.1. OPTIONS AND CAPABILITIES.

SEADYN is capable of performing nonlinear ana-
lyses of both branch and series-connected submerged cable structures. Static, dy-
namic, nodal, and frequency domain analyses can be performed for complex systems
which include buoys, anchors, fixed points, different cable materials, and payout
or reel-in. An option exists to analyze mooring systems for surface ships. Load-
ings may result from point loads, non-steady three-dimensional current fields,
surface waves (or spectra) and wind loadings. Nonlinearities arising from large
displacements, large strains, velocity-squared drag, and position-dependent load-
ings, hyperelastic materials and constraints on the surface and bottom of the
current field are all treated. Bending and twisting effects are not modelled.

The program is a finite element model. Several solution techniques are
available. Three basic types of analyses can be performed:

- Static shape with gravity loads only,

- Equilibrium shape with current and point loads as well as gravity,

- Transient dynamic response of a system disturbed from initial
  equilibrium.

Additional options include:

- Calculating natural frequencies and mode shapes,

- Verifying a design for the holding capacity of its anchors, buoyancy
  of its floats, and strengths of its lines, and,

- Calculating the drag coefficient of strumming lines.

3-1

The SEADYN code has been under continual development during the time these components have been modeled. The chronological order for the model comparisons is: 6-foot; MDE; 7-foot; and Variable-length. Much of this development has been directed at the problem which plagues virtually all models of cable dynamics: converging to a solution. While this problem has not been entirely eliminated, the solution algorithm is substantially more versatile.

3.1.2 MODEL PARAMETERS. Inputs to SEADYN and SNAPLOAD fall into three categories. The first category describes the physical cable system, the ocean environment, and special loads. The computer model can not supply default values for these parameters. Furthermore, the computer models have only a limited repertoire of geometry-dependent factors; the user must adapt the literal geometry to one of these shapes. For example, the irregular clump of sandbags used to anchor the MDE mooring was modeled as a sphere.

A second type of input consists of parameters that describe the system response to excitation. Coefficients of drag, elastic clamping and added mass are examples. The computer model can supply default values for general cases. Table 3-1 indicates the default drag coefficients for SEADYN and SNAPLOAD. For most, if not all the parameters, certain cable systems and excitations will cause significant deviations from these default values. There is no substitute for sound ocean engineering judgement backed with selected engineering data in selecting these parameters, especially when significant penalties will result from wrong results.

The third category of input parameters consists of parameters for controlling the computer program itself. Some of these are useful and necessary. For example, parameters that specify optional features are essential to the concept of model flexibility. Selection of these parameters is facilitated by a clearly written manual. Other parameters, however, are a reflection of the mathematical difficulty in modeling cable dynamics. These are more difficult for the user to estimate. Ideally, they would be computed within the model. They are left for the user to estimate because suitable algorithms to compute them are not available. Manuals usually do not give explicit guidelines for selecting these parameters for the same reason. They are selected using prior experience as a guide.

3.2 INTRODUCTION TO SNAPLOAD.

SNAPLOAD (References 7 and 11) simulates nonlinear static and dynamic responses of two-dimensional, series-connected cable structures. The program can model dynamic tensions, including snap loads during transient conditions and/or payout/reel-in operations. Loadings can be from surface waves, steady ship velocity, or a nonuniform current profile. A lumped parameter model is used and solved by a finite difference technique. Because the model is less general than SEADYN, problems are more easily set-up and execution times are usually shorter.

The lumped parameter method replaces the system of cables with equivalent point masses (nodes) connected by springs. All forces are concentrated at the nodes. Differential equations describing the motion of the nodes are solved by any useful method; the SNAPLOAD equations, for example, are solved by an Adams-Bashforth predictor and Adams-Moulton corrector algorithm. In comparison, the

TABLE 3-1. DEFAULT DRAG COEFFICIENT

Model	Body Shape	Component	Coefficient	Reynolds Number		Velocity	Dimension	Drag Area
				Min.	Max.			
SEADYN	Sphere	Normal	0.000 $0.044 + 13.46/R^{0.50}$ 0.470 0.120	0.0 0.1 1000 10^5	0.0 1000 10^5 -	Total	Diameter	Frontal
	Cylinder	Normal	0.000 $0.450 + 5.93/R^{0.33}$ 1.270 0.300	0.0 0.1 400 10^5	0.1 400 10^5 -	Normal	Diameter	Frontal
	Cylinder	Tangential	0.000 $0.000 + 1.88/R^{0.74}$ 0.062	0.0 0.1 100	0.1 100 -	Tangential	Diameter	Frontal
SNAPLOAD	Sphere	Normal	None (mandatory input)	0.0	all	Total	Diameter	Frontal
	Cable	Normal	1.350	0.0	all	Normal	Diameter	Frontal
	Cable	Tangential	0.025	0.0	all	Tangential	Diamter	Frontal

node of a finite element system are simply joints; the equations of motion are solved for the elastic rods connecting the nodal joints. The classical analysis is based on the differential equations of an infinitesimal element of cable.

Snap loads occur when a transient tension reduction produces a momentarily slack cable. They are usually associated with impact events.

3.3 ACCURACY AND COEFFICIENT. There are three levels at which a model performs. First, just mentioned, the model must converge to a solution according to some criterion. Second, the solution obtained should reflect qualitatively the effects of the salient phenomena occuring during the event modeled. Third, the solution should be numerically accurate when compared to the experimental measurements.

It is important that this numeric accuracy be obtainable using characteristic parameters supplied either as default values by the program or by the user without reference to experimental data for the case at hand. (The purpose of computer models is to reduce the need for costly experiments.) In the case comparisons described below, most parameters are selected by default or on the basis of an a priori engineering decision. In a few cases, the parameters were adjusted to improve the comparison.

For example, the default drag coefficient of the anchor for the MDE mooring was selected for a spherical anchor shape. This gave a descent speed substantially too large. The drag coefficient was adjusted to give a terminal velocity equivalent to the measured descent of pinger ALPHA. This procedure is justified in order to show that given correct coefficients, SEADYN can give good results. In a design environment, the engineer must be sensitive to the need for pertinent design experiments. A "handbook" value was not an adequate representation for a clump of sandbags in a cargo net. Although the wrong coefficient allowed the modeled anchor to fall about twice as fast as its physical counterpart, the net effect was merely to compress the duration of the event. Other effects were slight.

Whenever parameters have been adjusted to improve the model "fit" to the data, it is noted in the text.

3.4 DIFFICULTIES.
There are three difficult areas that SEADYN shares with other dynamic cable models. Slack cable, inelastic[1] cable, and varying cable length pose problems that affect the efficiency and accuracy of computer models.

3.4.1 SLACK CABLE. The radius of curvature of a suspended cable varies directly with the tension. In most cases the radius of curvature is so large that bending moments, even in large wire rope, can be neglected. Virtually all cable models, SEADYN included, assume that the cable is flexible, that is, it does not produce internal stresses to resist bending.

---

[1] See note 2, page 2-6.

3-4

A flexible, suspended cable responds to low tension by bending more sharply in the direction that causes tension to increase. In real cables, very low tensions mean that bending moments are no longer negligible, and "zero" tension does not produce a "kink" in the cable shape.

Computer models discretize the cable into small straight segments. When the tension becomes so small that the radius of curvature is less than half a segment-length, the segments are unable to conform to flexible theory. The model response becomes "jerky", reflecting the difference between articulation and flexibilty. The problem is eased by using shorter elements.

SEADYN provides two options to approximate the behavior of slack cable. Both options allow elements to be shorter than their relaxed length. One option computes a compressive load for such elements, the other ignores the stress due to compressive strain.

3.4.2 INELASTIC CABLE. The elastic rigidity of a cable has a strong effect on the efficiency of a computer model. Changes in tension propagate along a cable at the speed of sound in the cable, which varies directly with its elastic rigidity. In general, the time step in a model must be less than the time for sound to traverse the length of the shortest element. Inelastic cables require short time steps because of the high speed of sound (15,000 ft/sec in steel wire).

Errors in the position of the ends of an element produce errors in the element tension according to the stress-strain function for the element. Inelastic elements produce large tension deviations for small nodal position errors. The problem of inelastic cables is alleviated by using short time steps and long elements. The latter technique conflicts with short elements used to avoid slack cable errors.

3.4.3 VARIABLE LENGTH. Cable systems that include winches add a third difficult area for computer models. In order to model the increasing length of cable, an element is allowed to increase its length up to some maximum, then a new node is inserted, dividing the element and creating a new sub-element. The new element then grows, and so on.

The discretization imposes a single tension value for each element, typically the average of the axial force at each end. When a new node divides an element, the resulting average tension is changed by the weight of the length transferred to the new element.

Each node insertion produces a small "jolt" that propagates through the system. These tremors do not materially affect the computed results unless the cable system itself is marginally stable (very near elastic resonance with inadequate damping). The node insertions may be visible on a tension plot. The problem is minimized by using short elements, frequent node insertions and short time steps/ near node insertions, but this adds to computation cost. The problem also occurs when nodes are removed.

The three factors - slack cable, inelastic cable, and variable length - should not be viewed as errors or inadequacies to be corrected, but rather as "facts of life" to be recognized and accommodated. In most cases the numerical effect is negligible. Failure to recognize them can increase the modeling cost substantially.

SECTION 4

MODEL COMPARISONS

4.1 SIX-FOOT EXPERIMENT COMPARISONS.

4.1.1 OVERVIEW OF COMPARISONS. A total of 17 tests were selected from the 67 six foot tests for comparison to the computer models. These tests were selected as representative of the full range of experimental conditions within each of the five types of tests. In some cases, tests were chosen because test results exhibited a distinctive behavior or phenomenon not found in other tests. Table 4-1 shows the major parameters of the selected cases. Table 4-2 summarizes the physical parameters used. Only spherical "anchors" and "buoys" were used in the 6-foot experiment in order to test the default drag coefficients used by the models.

4.1.2 SINGLE POINT MOORING COMPARISONS. Five cases were selected for comparison (Reference 12). Test 6 used a solid rubber cord, drawn as taut as its soft composition allows. Tests 7, 8, and 9 used the three cords, all starting from the same slack initial catenary. Test 19 used the rubber cord with embedded conductors, drawn even tighter than Test 6 relative to its elasticity.

4.1.2.1 Shape. Figure 4-1 shows the shape of the cable, as measured and modeled at several instants during the relaxation of the mooring. Similar plots for the other cases differ only in detail. The figure shows that the normal drag coefficients used in both models were too low, allowing the models to lead the data after the initial second.

4.1.2.2 Velocity. Figure 4-2 shows the velocity history of the buoy, as measured and as modeled by SEADYN and SNAPLOAD. The data show that when the buoy is released it bobs up quickly, initiating an impulse wave in the cord. The resonant period of the buoy and cable using elementary theory[1] is about 0.4 seconds, which seems to be supported by the velocity trace on Figure 4-2. During the first 1.5 seconds of the test, both models estimate excess buoy velocity. For the remainder of the test the models agree with the measured velocity. Referring to Figure 4-1 and comparing 5.1 seconds with 2.0 seconds shows that the models do not increase their "lead" perceptibly after about 2 seconds have elapsed.

4.1.2.3 Tension. SNAPLOAD models the gross build up of the tension, but smooths virtually all of the detail (Figure 4-3). This is because SNAPLOAD invokes extra, artificial damping for a short time after the start of a dynamic event in order to

[1] $t = 2\pi\sqrt{\dfrac{L(m+m')}{EA}}$

TABLE 4-1.   INDEX TO COMPARISONS

Type of Test	Test Number	Initial Position of Free-End X (in.)	Initial Position of Free-End Z (in.)	Free-End Oscillations Range (in.)	Free-End Oscillations Frequency (cycles/min)	Type of Cable[1]	Load[2]	Type of Comparison[3] Displacement	Type of Comparison[3] Velocity	Type of Comparison[3] Tension
Buoy Relaxation	6	51	51			SR	B	SEA, SN	SEA	SEA
	7	51	42			SR	B	SEA	SEA	SEA
	8	51	42			RC	B	SEA, SN	SEA, SN	SEA, SN
	9	51	42			N	B	SEA, SN	SEA, SN	SEA, SN
	19	42	58.4			RC	B	SEA, SN	SEA, SN	SEA, SN
Anchor-Last	32	66	0			SR	0.1A	SEA, SN	SEA, SN	SEA, SN
	35	66	0			N	0.25A	SEA, SN	SEA, SN	SEA, SN
	39	54	0			SR	0.1A	SEA, SN	SEA, SN	SEA, SN
	43	48	0			SR	0.25A	SEA, SN	SEA, SN	SEA, SN
	46	42	0			N	0.1A	-	-	SEA
Bi-Moor Relaxation	60	42	42			N	B	NR	NR	SEA
	61	42	42			SR	B	NR	NR	SEA
Single Cable Suspended Load	67			3	80	SR	0.25A	NR	NR	SEA, SN
	68			3	72	SR	0.25A	NR	NR	SEA, SN
	94			6	30	SR	0.1A	NR	NR	SEA, SN
Dual Cable Suspended Load	133			6	45	SR	0.1A	NR	NR	SEA, SN
	142			6	50	SR	B	NR	NR	SEA, SN

1 SR = Solid Rubber; RC = Rubber with Conductors; N = Nylon.

2 B = Buoy; 0.1A = 0.1 lb Anchor; 0.25A = 0.25 lb Anchor.

3 SEA = SEADYN; SN = SNAPLG; NR = No Experimental Results.

TABLE 4-2. BUOY, ANCHOR, AND CABLE PROPERTIES FOR THE
6-FOOT EXPERIMENTS MODELING

BUOYS

	Diameter	Weight in Air	Weight in Water
	2.0 in.	0.025 lb	-0.121 lb

ANCHORS

	Diameter	Weight in Air	Weight in Water
0.1 lb Anchor	2.0 in.	0.246 lb	0.108 lb
0.25 lb Anchor	2.0 in.	0.398 lb	0.252 lb

CABLES

	Diameter	Weight in Air	Weight in Water
Silicon w/Wire	0.163 in.	11.433×10^{-3} lb/ft	2.381×10^{-3} lb/ft
Silicon	0.163 in.	8.979×10^{-3} lb/ft	1.075×10^{-3} lb/ft
Nylon	0.1 in.	3.736×10^{-3} lb/ft	1.057×10^{-3} lb/ft
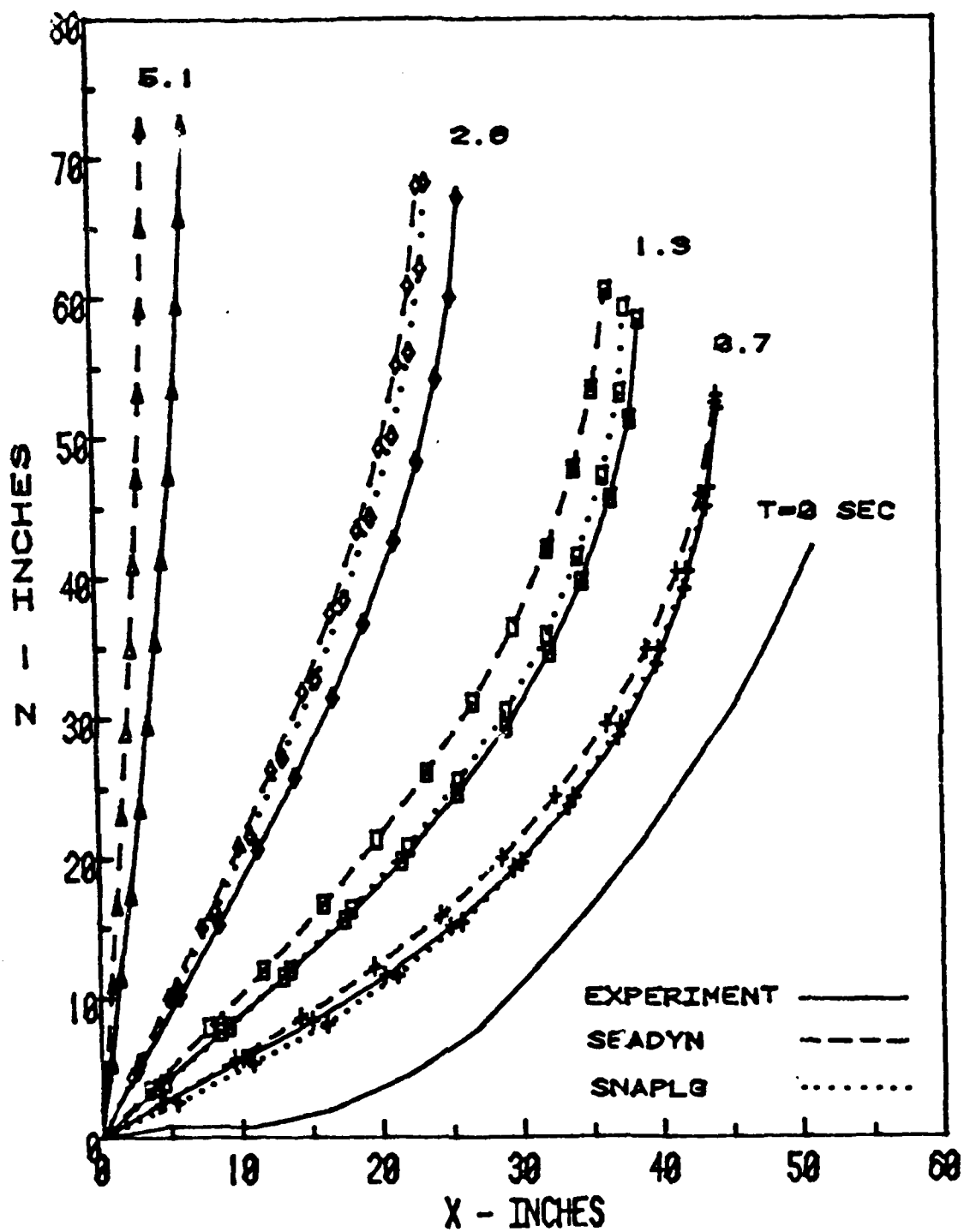
Figure 4-1. Displacement Comparison For Test 8

4-4
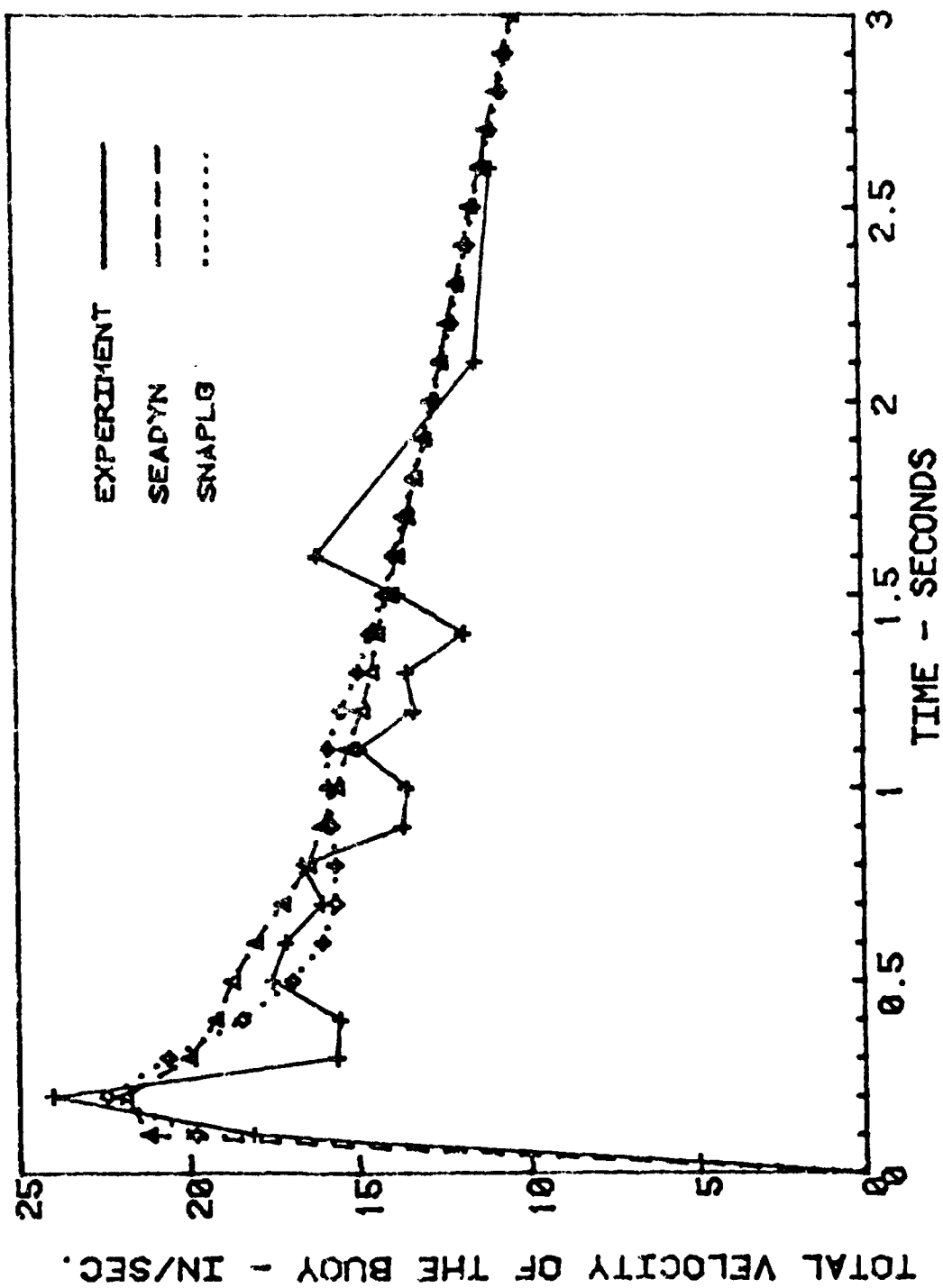
Figure 4-2. Buoy Velocity Comparison For Test 8
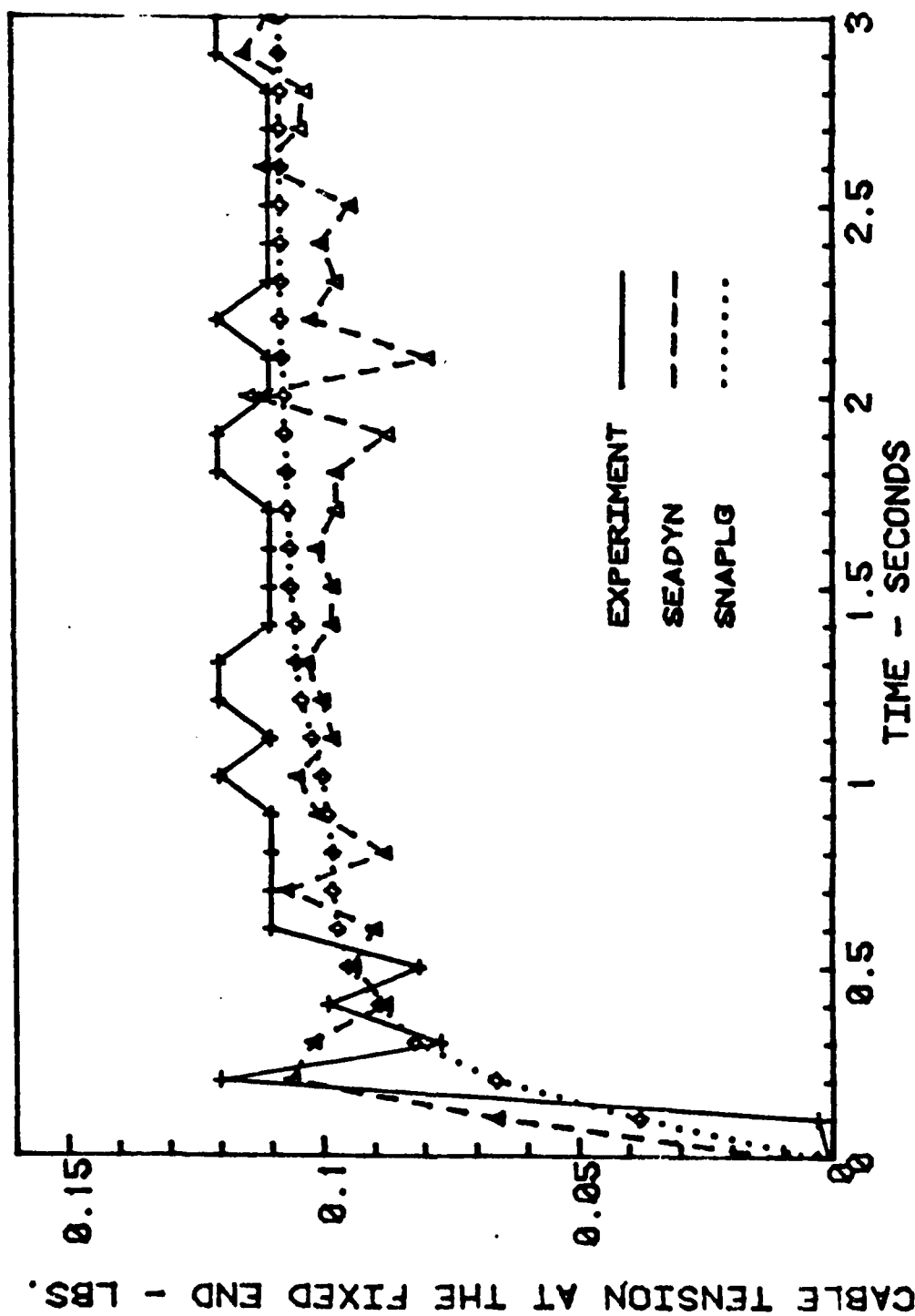
Figure 4-3. Tension Comparison For Test 8

maintain stable computation. It is not apparent whether SEADYN is modeling "real" tension impulses. The aberrations shown may be artifacts (inter-nodal resonance) that material damping would remove. Figure 4-4 shows what can happen to SEADYN when material damping is not used with a "stiffer" material. This is the tension history for Test 9, which used the nylon cord. The amplitude of "ringing" is virtually as great as the actual tension magnitude. As before, the artificial damping in SNAPLOAD has smoothed over all the detail.

4.1.3 SIMULATED ANCHOR-LAST DEPLOYMENT COMPARISONS. Anchor-last deployment simulation is a substantially more difficult modeling task. While the cases end like an inverted buoy relaxation, the initial curvature is opposite the final curvature, and the transition is accompnaied by quasi-impact conditions as the anchor pulls the slack out of the cable arc.

a. Test 32. This test began with a relatively taut initial shape, using the "softest" line material. These conditions were expected to produce the best model comparisons. Figures 4-5, 4-6, and 4-7 show the comparisons. Both models accurately portray the speed of the freely falling anchor, but then understate the cable drag. The predicted anchor motion is about 3 inches per second too fast during the middle part of the test. Both models accurately calculate the acceleration after the first second. SEADYN models the tension history fairly well, but SNAPLOAD misses the "impact" of the anchor as the cable comes taut.

b. Test 35. This test used the same initial shape, but substituted the inelastic nylon line for the soft rubber. The heavy anchor was used as well. SEADYN modeled this cases with the same strengths and weaknesses as Test 32. SNAPLOAD, however, lost control of the tension (Figure 4-8) and this spoiled the run. Perhaps this is because the resonant period for elastic motion, based on elementary theory, was about half the period for Test 32.

c. Test 39. In this test, the components of Test 32 were repeated, but the rubber was hung in a catenary twice as deep (Figure 4-9). Both models follow the gross motion at roughly the correct speed. SNAPLOAD has not handled the "gooseneck" that formed above the anchor just after release very well. SEADYN did better during that 2-second interval. Velocity and tension histories are shown on Figures 4-10 and 4-11.

d. Test 43. The initial catenary was even more slack for this case (separation = 2/3 line length). The heavy anchor was used. Elementary theory predicts a resonant period of 0.9 seconds for elastic motion. Figure 4-12 shows the measured period to be about 0.75 seconds. SEADYN was closer to the elementary theory, but neither model predicted the tension that actually occurred.
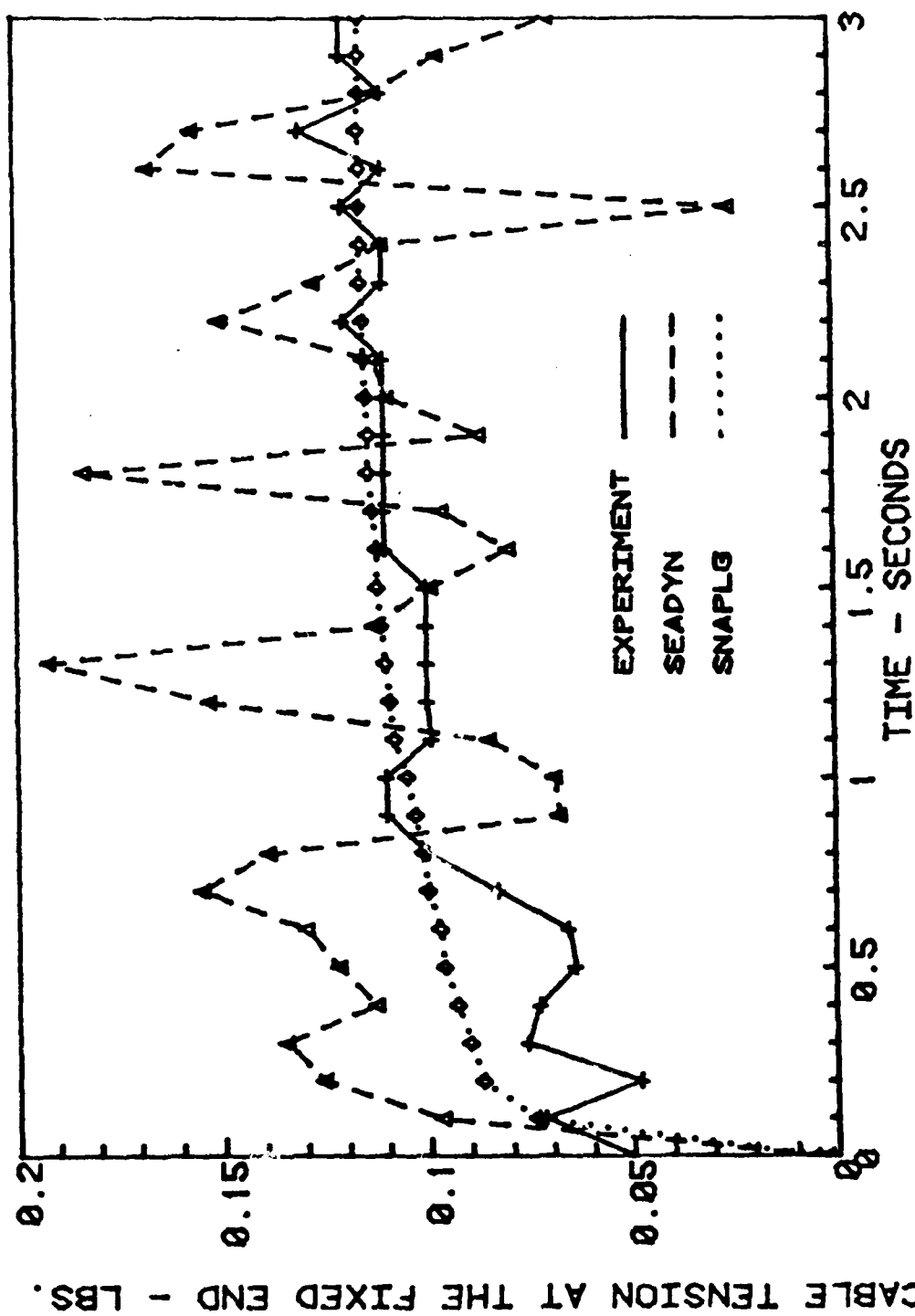
Figure 4-4. Tension Comparison For Test 9
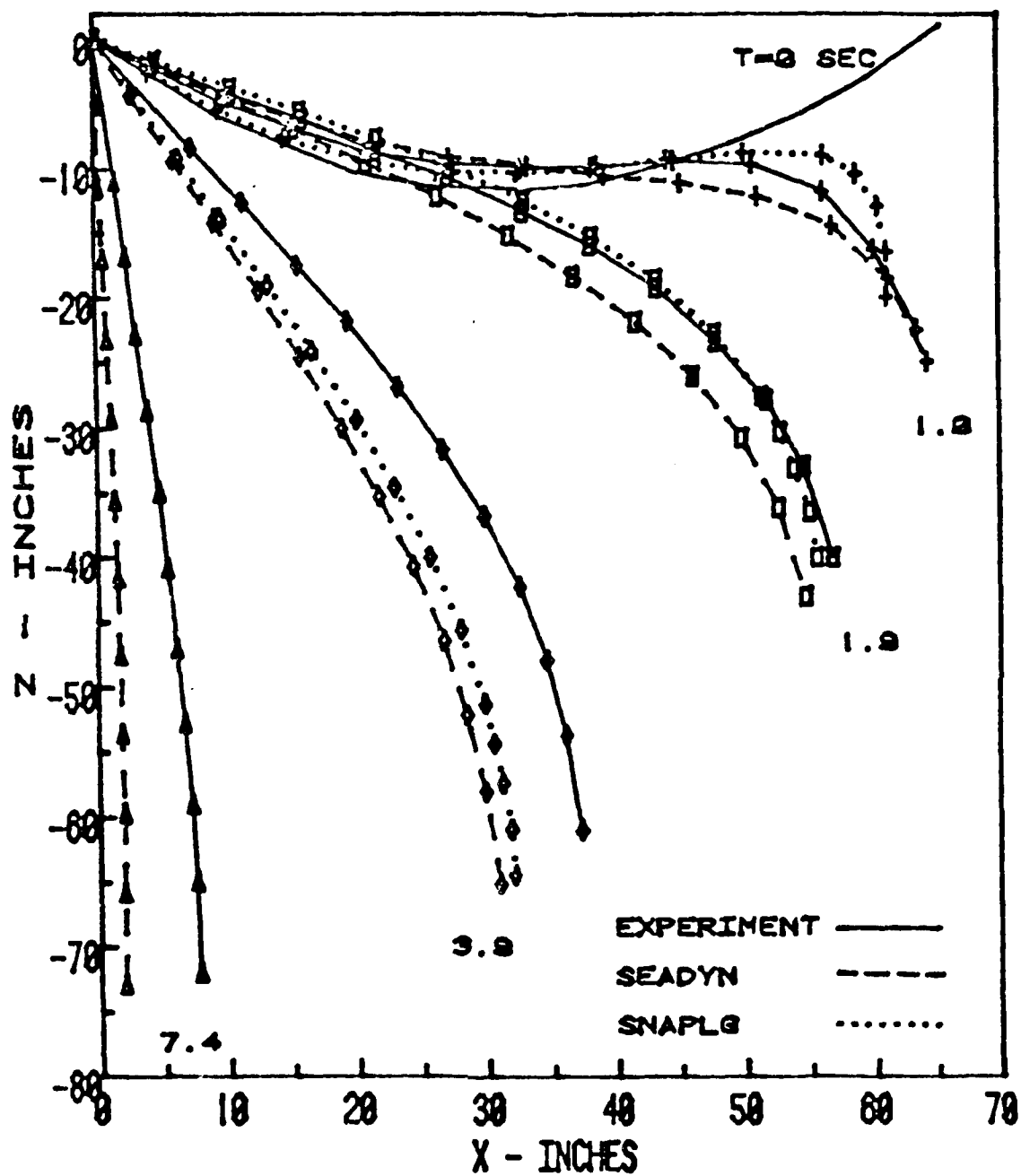
Figure 4-5.   Displacement Comparison For Test 32

4-9
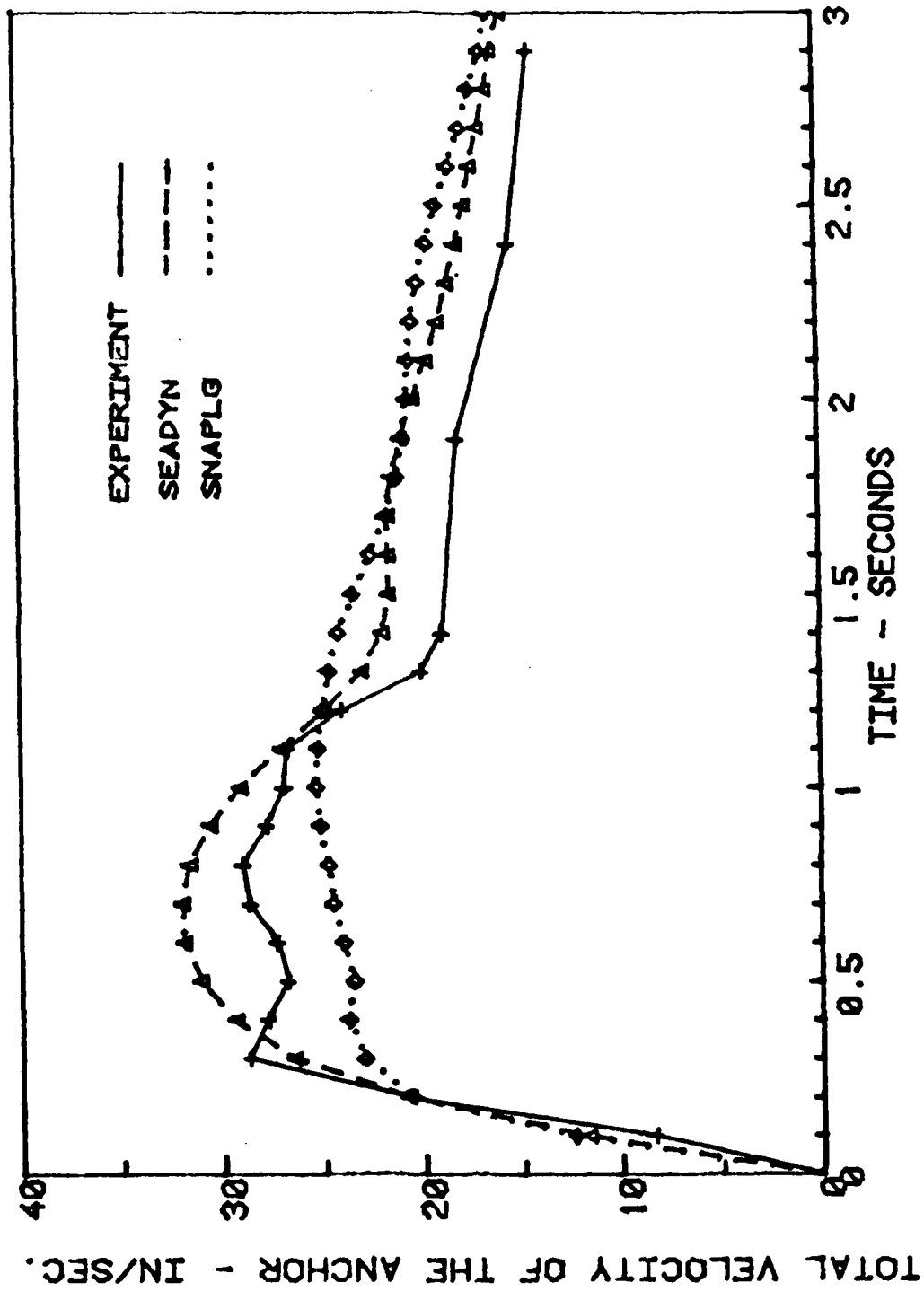
Figure 4-6. Anchor Velocity Comparison For Test 32
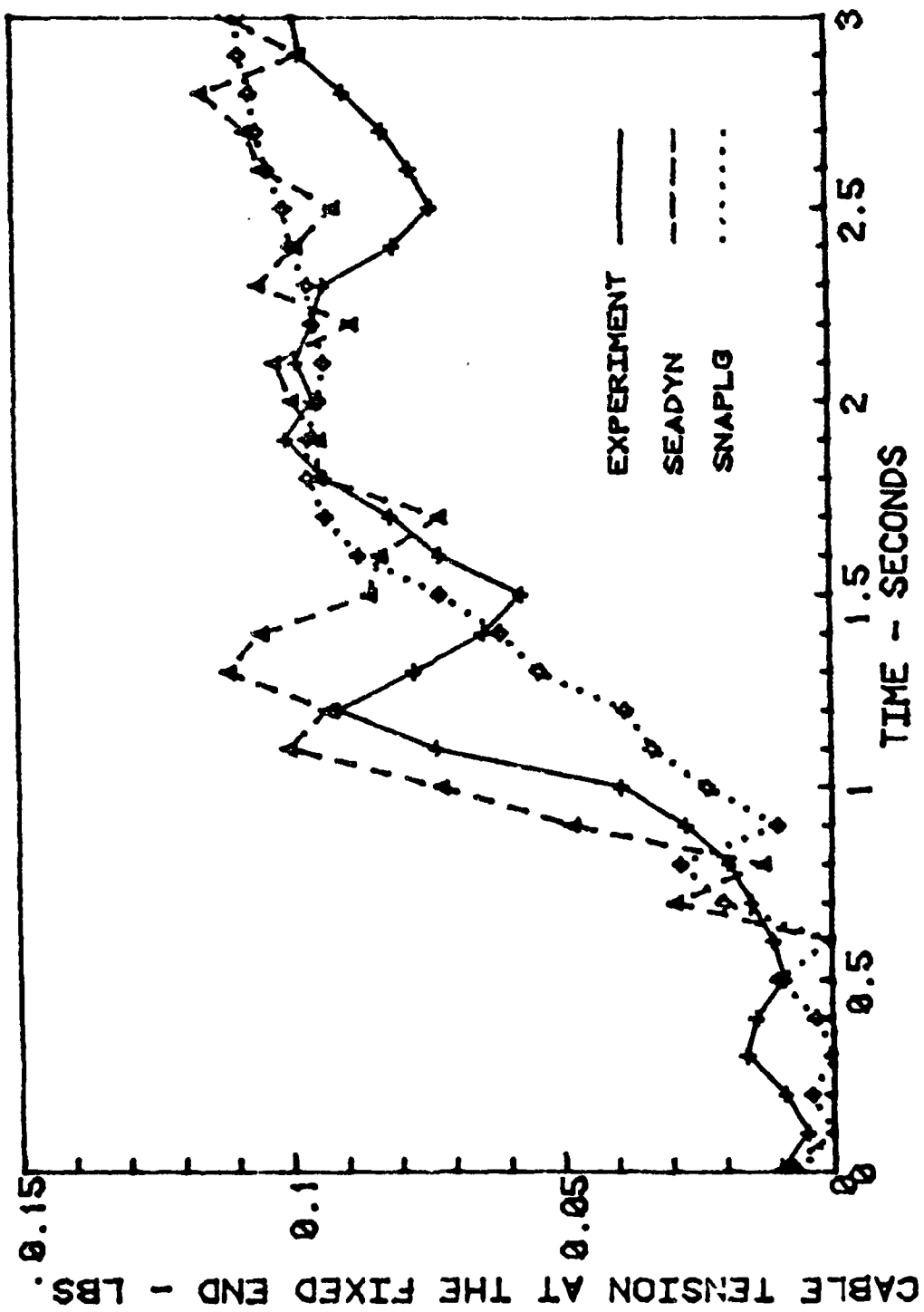
Figure 4-7. Tension Comparison For Test 32
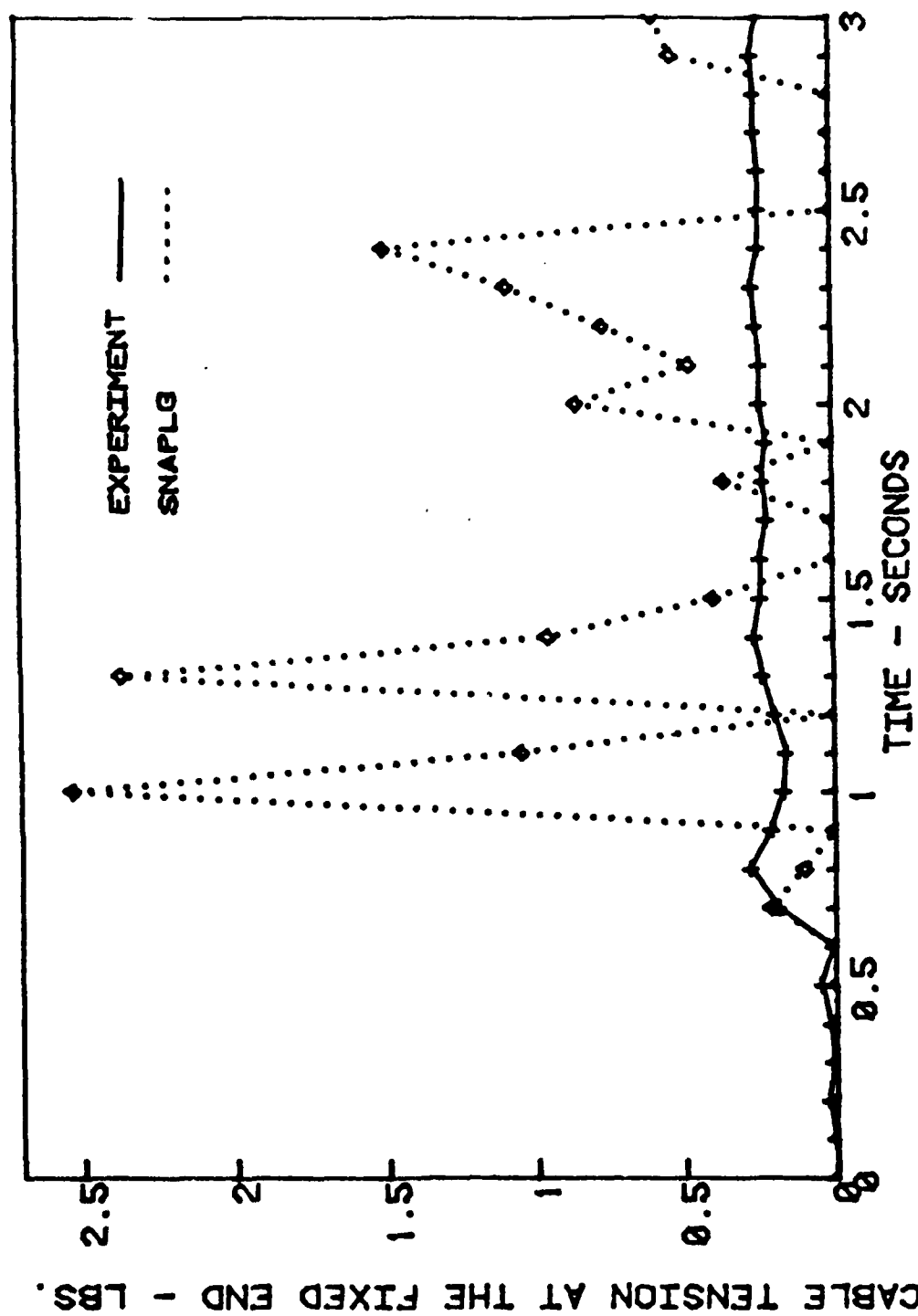
Figure 4-8. Tension Comparison For Test 35
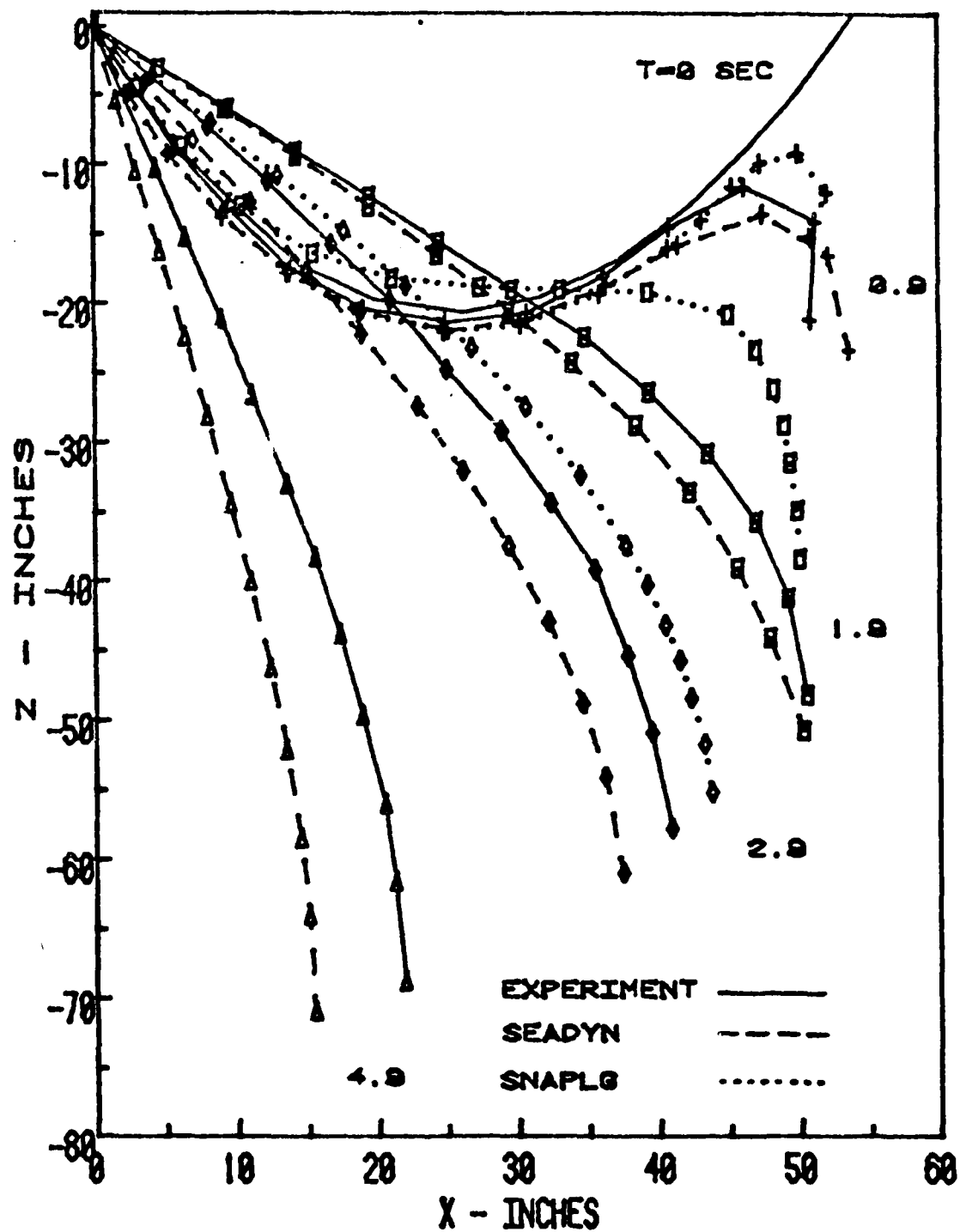
Figure 4-9. Displacement Comparison For Test 39
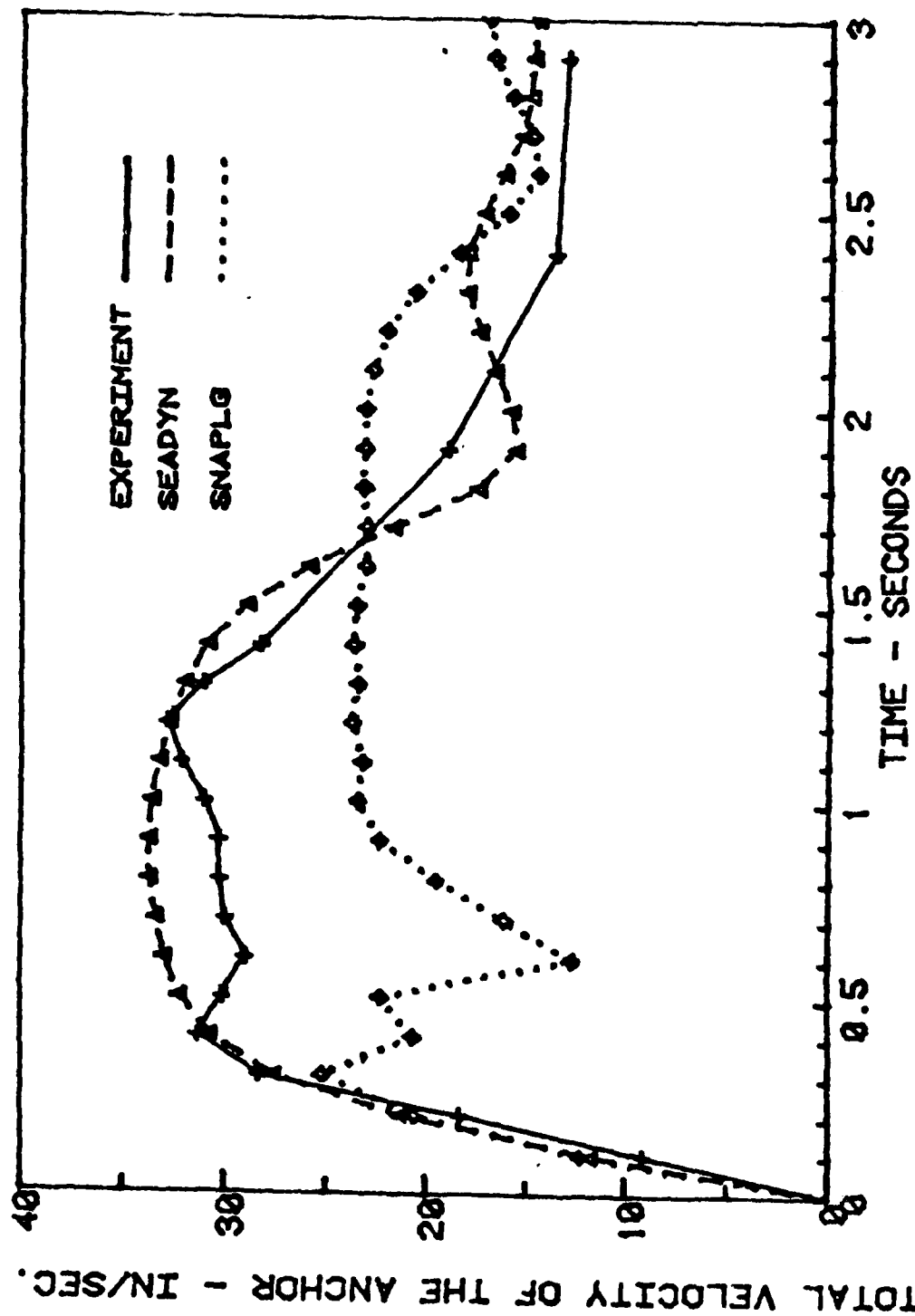
Figure 4-10. Anchor Velocity Comparison For Test 39
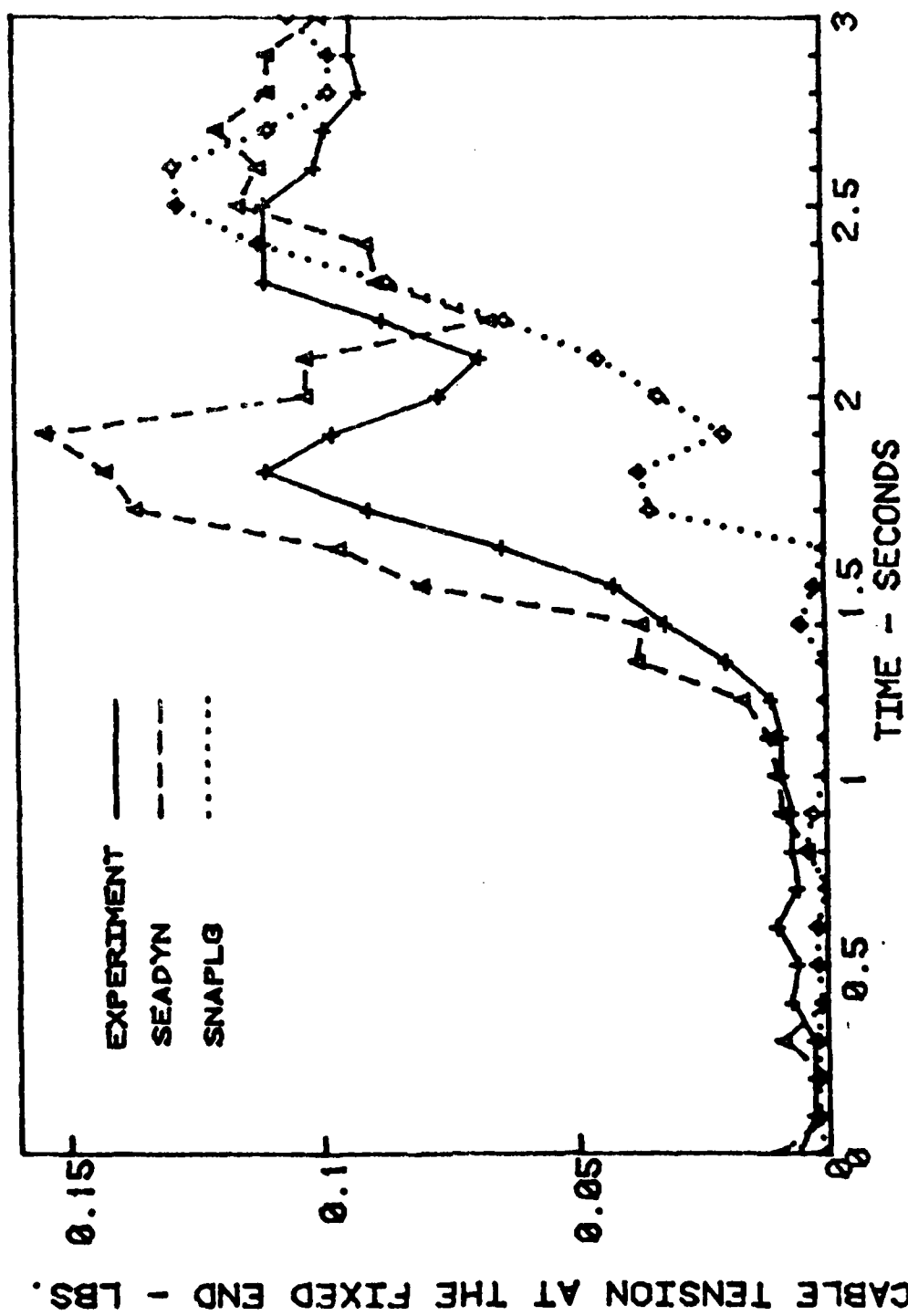
Figure 4-11. Tension Comparison For Test 39
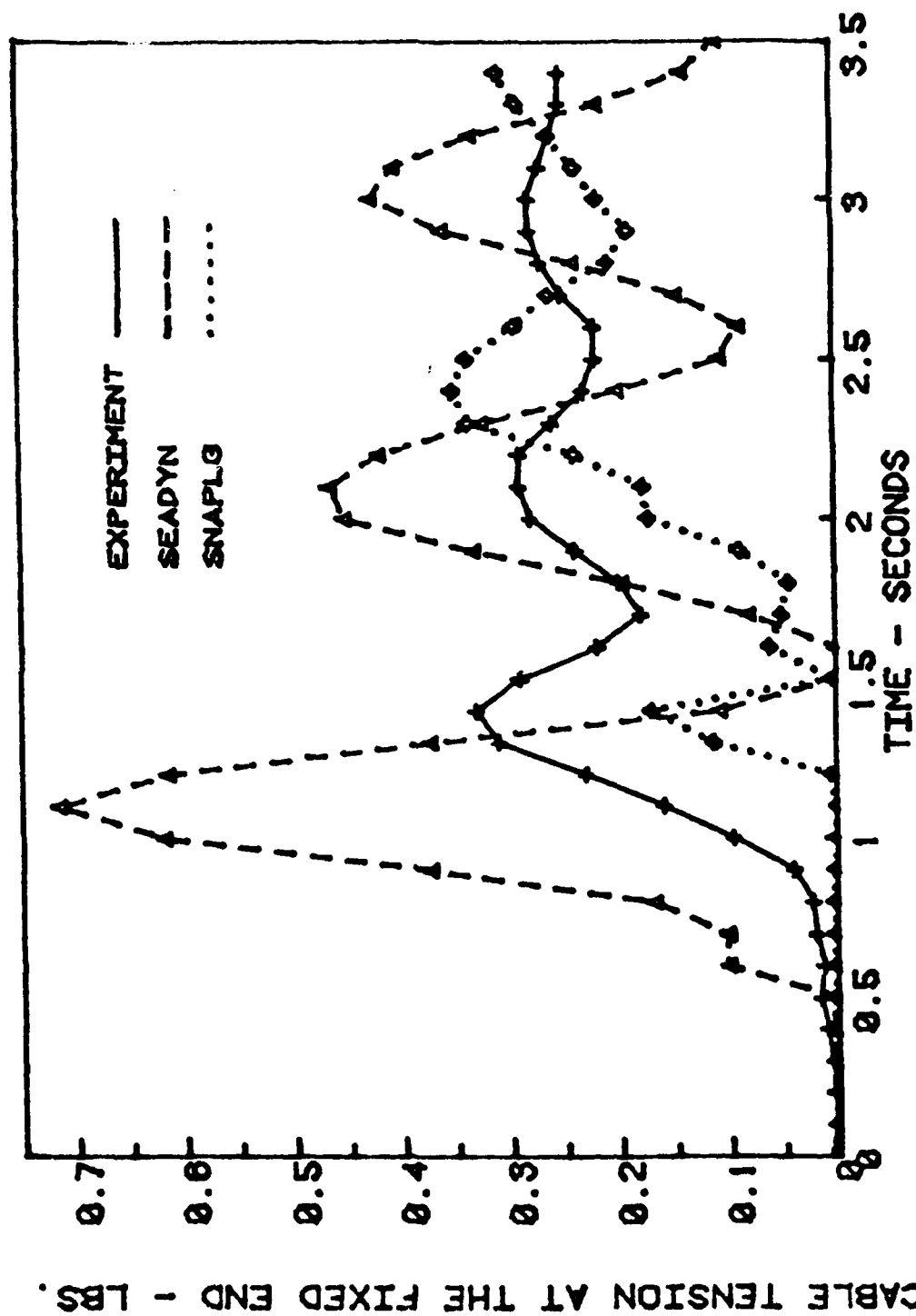
Figure 4-12. Tension Comparison For Test 43

e. <u>Test 46</u>. The initial separation between the anchor and fixed end was only 0.58 of the length. This allowed the anchor to fall freely over two-thirds of the total depth and produced an abrupt tension spike when the inelastic nylon line snapped taut. SNAPLOAD was not compared to this case. SEADYN produced unrealistic output.

To summarize, a total of five simulated anchor-last deployments were tested. As with the single point mooring relaxation tests, SEADYN and SNAPLOAD performed best for initially taut anchor-last deployments with soft cables. Neither model performed satisfactorily for the slack tests.

The cause of poor model performance in these slack tests has not been determined. These cases were modeled before the material damping algorithm had been implemented in SEADYN. That was found to have a pronounced smoothing effect on the tension model. SEADYN computed a tension impulse that was larger if the cable was hung initially in a slack bight (compare Figures 4-7, 4-11, and 4-12). This suggests that the default drag coefficients by SEADYN are too low. Low anchor drag gives excess terminal velocity; slack initial shape gives more free-fall time; low normal cable drag reduces the effectiveness of straightening the "gooseneck" as a smooth damper for the anchor impact.

It should be noted that the SNAPLOAD results for Test 35 represent the best results chosen from simulation runs. The initial SNAPLOAD model had lumped masses in the same locations as the nodes in SEADYN; this was the modeling technique followed in all the SNAPLOAD comparisons. This initial model did not produce realistic results - the anchor quickly dropped down and in too far, compared to the experimental data and SEADYN calculations. Further runs were made with SNAPLOAD with the final model using two additional "half" lumped masses at the end of the cable. The changes did not produce any significant improvements. Also, for the nylon cables in this and other tests, SNAPLOAD could not converge on the static solution, which probably accounted for much of the dynamic instabilities.

4.1.4 BI-MOOR RELAXATION COMPARISONS.

a. <u>Test 60</u>. This test was an out-of-plane test, and could not be modeled by the two-dimensional SNAPLOAD. Figure 4-13, however, shows the comparison between the experimental and SEADYN tension histories. The calculated tensions from SEADYN are extremely unstable, and show no tendency to stabilize even after 3.5 seconds. This instability is characteristic when inelastic cables are modeled without material damping.

b. <u>Test 61</u>. This test is similar to Test 60, except that a silicon rubber cable was used in place of the nylon cable. SEADYN tensions still show an oscillation about the steady-state value even for this softer cable material.

To summarize, only two bi-moor relaxation comparisons were made, and both were out-of-plane tests. Because these tests were three-dimensional, only SEADYN was compared.
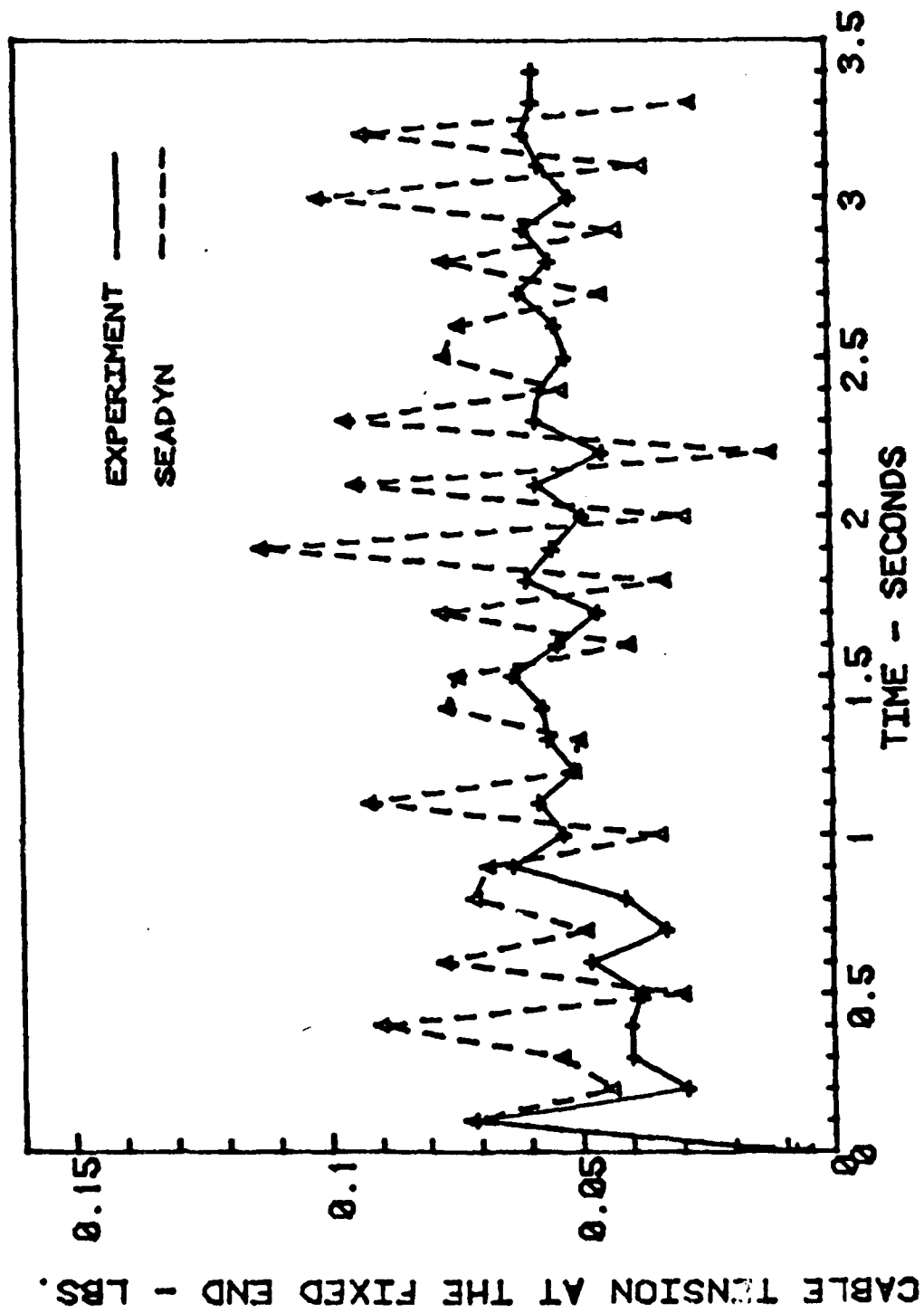
Figure 4-13. Tension Comparison For Test 60

The results were unexpected. A close fit between the experimental and SEADYN tensions was expected based on the simplicity and symmetry of the test, and the previous good comparisons for the single point mooring relaxation tests. This was not the case, however, as SEADYN never converged to a stable steady-state value.

These simulations demonstrate again that material damping is essential for good model results, because the program started form its own initial equilibrium shapes and maintained a symmetry of tensions and nodal positions in both legs at all times in the dynamic analyses. A small-time step was used in the dynamic analyses and was within the proper bounds, and was not the cause of any errors. Even small amounts of material damping markedly reduce these tension pulses.

4.1.5 SINGLE CABLE SUSPENDED LOAD COMPARISONS.

a. Test 67. For this and the remaining comparisons only steady-state tensions are given. Experimental results were taken only after a long delay to allow start-up transients to die out; likewise, the computer simulations were taken only after a delay of at least three periods of oscillation. A best fit comparison was found by shifting the computer tensions in time to best match the experimental tension history. The tension comparison for this test is shown in Figure 4-14. Both models calculated reasonable tensions compared to the actual values.

b. Test 68. The tension comparison for this test is shown in Figure 4-15. SEADYN tensions match the actual tensions extremely well; SNAPLOAD tensions do not show the regularity of the experimental tensions in either time or magnitude.

c. Test 94. Both models show good agreement with the experimental results as shown in Figure 4-16. Over this time span the results of SEADYN are slightly better than those of SNAPLOAD.

The results of these tests correlate strongly with the ratio of excitation frequency to the resonant frequency based on elementary theory:

Test No.	Frequency Ratio	Figure No.
67	1.19	4-14
68	1.07	4-15
94	0.37	4-16

Frequency was the only parameter changed between runs 67 and 68. The experimental results on Figure 4-14 and 4-15 are essentially equal, save the frequency difference. In each case, two of the four cycles plotted are "clipped" to zero
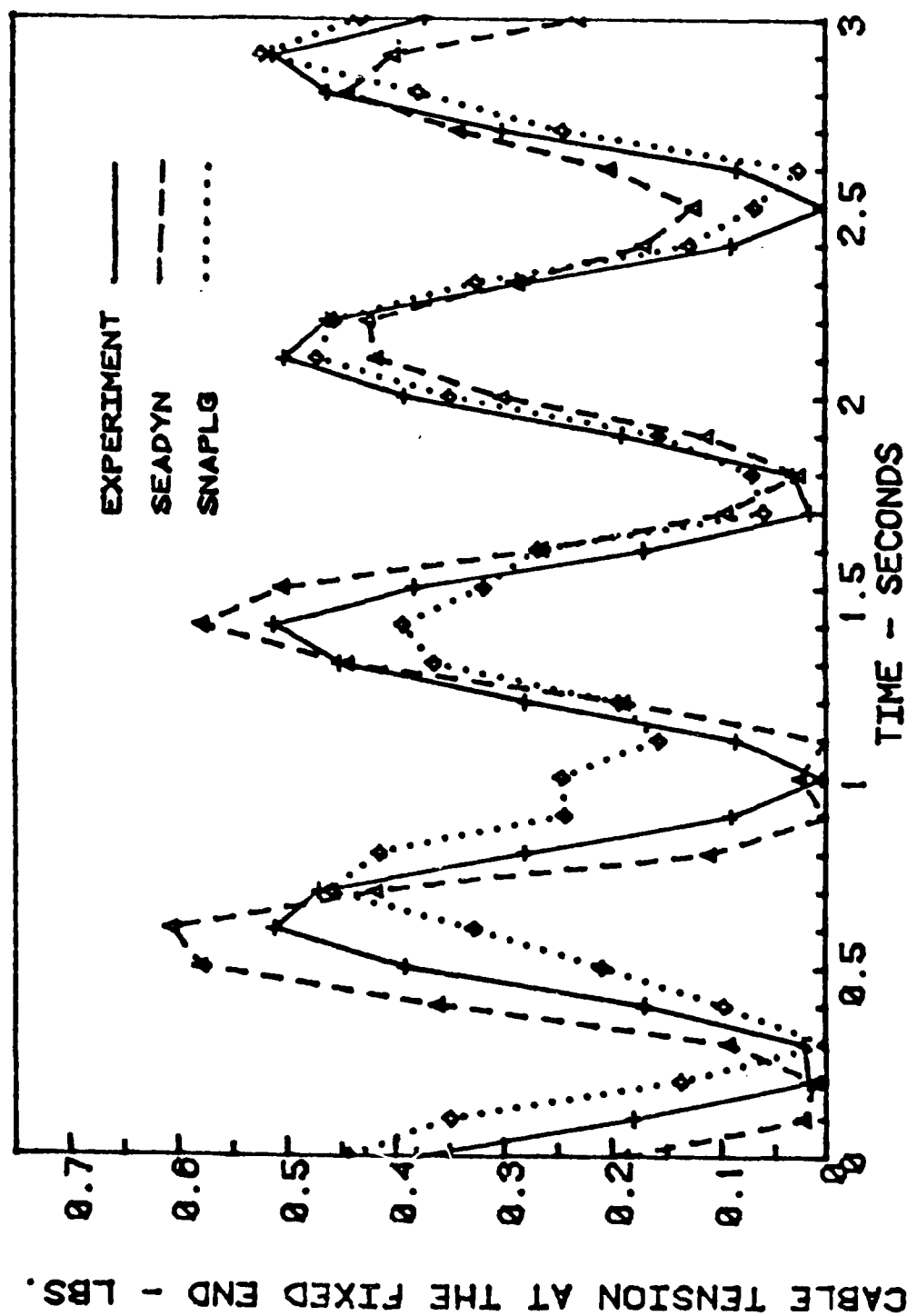
Figure 4-14. Tension Comparison For Test 67
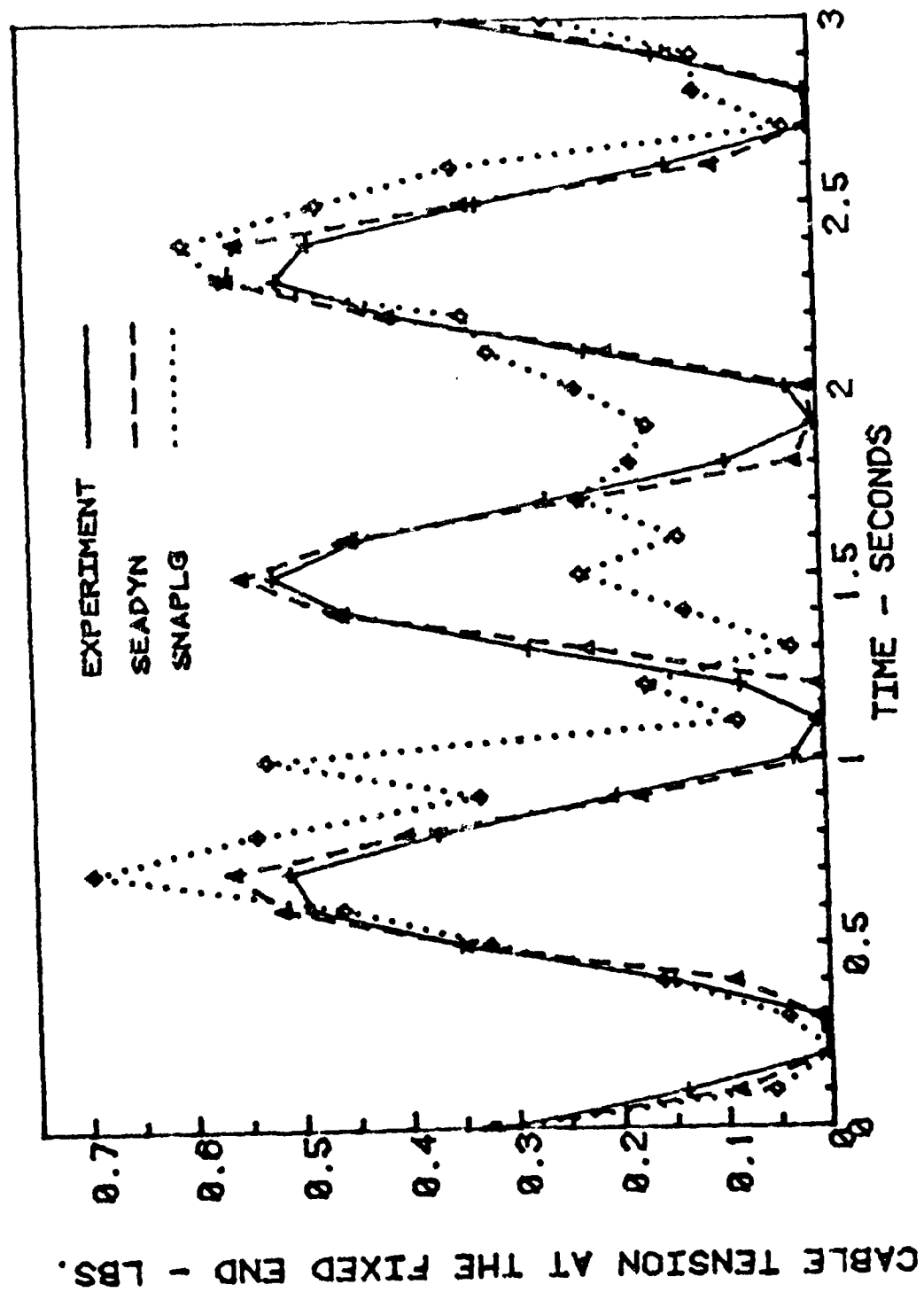
Figure 4-15. Tension Comparison For Test 68

1.0	4.5	2.8	2.5
1.1	3.2	2.2
	3.6	
	4.0	2.0
		1.8
1.25	1.4	1.6

MICROCOPY RESOLUTION TEST CHART

NATIONAL BUREAU OF STANDARDS 1964 A
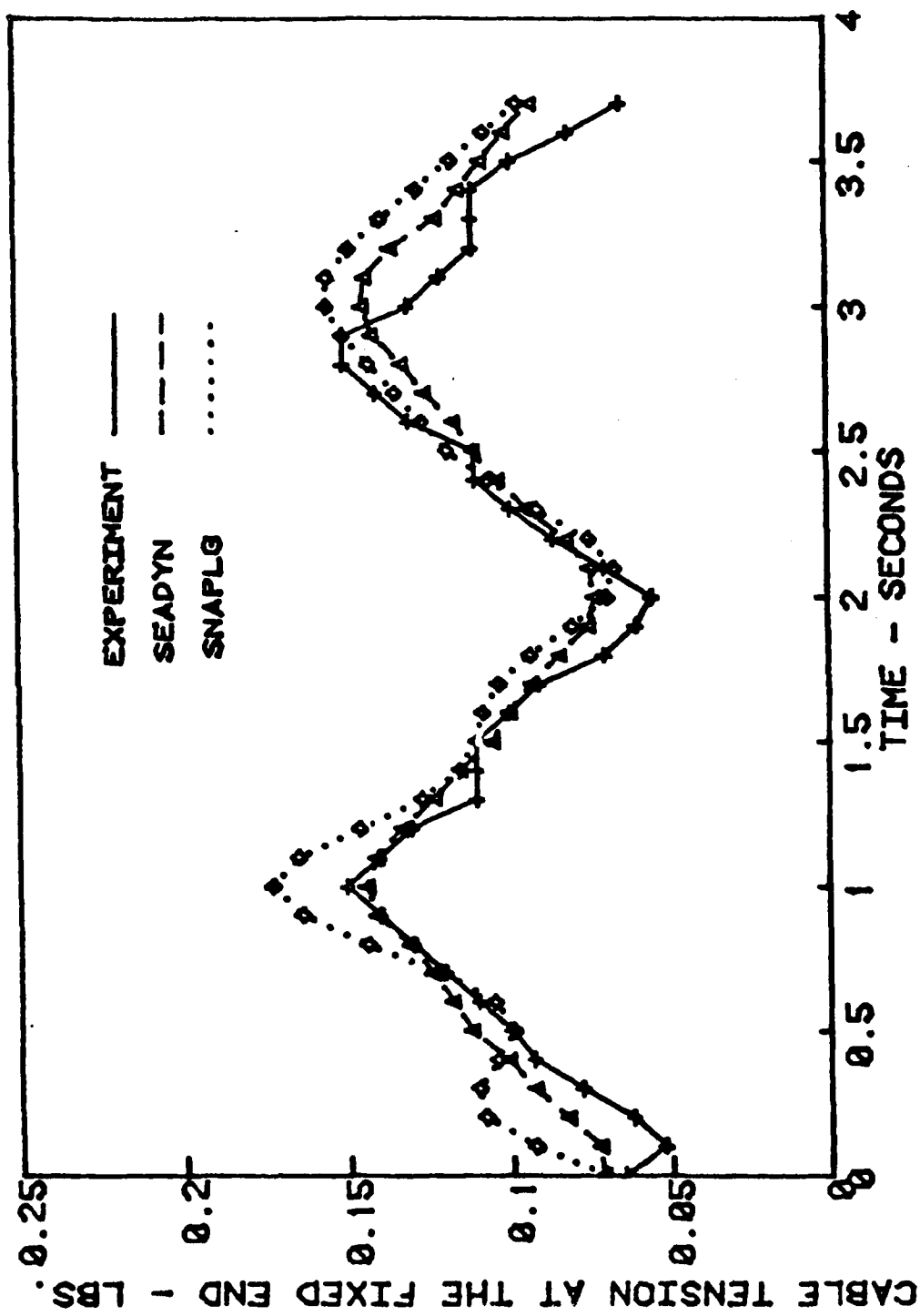
Figure 4-16. Tension Comparison For Test 94

tension, and the other two may in fact be clipped was well. SEADYN had not achieved a steady state on Figure 4-14; the trend was to under-predict the amplitude. SNAPLOAD had occasional anomalous solutions. Nearer resonance, SEADYN models the data well, as shown on Figure 4-15. The cable was modeled with a definite slack interval in each cycle. On Figure 4-15, the proximity to resonance has exceeded the capacity of SNAPLOAD.

Figure 4-16 is not only far from resonance, but also the 0.1-pound load replaced the 0.25 pound sphere. Even though the excitation amplitude was doubled, the dynamic response is only half the mean value. Both programs were able to properly model this case.

4.1.6 DUAL CABLE SUSPENDED LOAD COMPARISONS. Test 133 used the small anchor. The two rubber cords hang in an L shape. Since the anchor hangs from the upper cord, the lower cord only provides "back tension". In Test 142, a buoy was used. That inverts the equilibrium catenary.

Figure 4-17 shows a sample of the tension in the lower link during Test 133. Intervals of constant tension indicate the anchor was swinging in an arc about the fixed end. Changing tension shows the anchor moving radially about the fixed end. Both SEADYN and SNAPLOAD over-responded to this case. This is because the tension in the lower end is sensitive to the terminal descent speed of the anchor. Both models show the lower link slack for fully half the cycle. This is another confirmation that the default cable drag coefficients in the models are too low.

Figure 4-18 shows the tension for Test 142. The plot is much smoother because the buoyancy force prevents the lower cable from going slack. In addition, the force required to displace the buoy laterally is less than the force required to lift the anchor vertically, so that cyclic variation in tension is less. The point-to-point variation in the test results reflects the natural period of buoy heave (vertical "bouncing") on the lower link. SEADYN modeled this case well, but SNAPLOAD appears to be barely stable. This may be because of the high frequency of the buoy heave (6 Hz).

4.2 THE 60-FOOT EXPERIMENT.
Of the 15 experimental cases performed, three were selected for comparison (Reference 13) with SEADYN and SNAPLOAD. Run 6 was a simulated anchor-last deployment using the 0.1-pound "light" anchor. Run 11 was a buoy relaxation, and Run 15 was another anchor-last simulation, using the heavier 0.25 pound anchor.

The two models, SEADYN and SNAPLOAD, are compared to the data from each of the three runs in three ways. First, the cable shape in a vertical plane is plotted for a sequence of instants during the run. "Snapshot" plots are the easiest to comprehend, because they show the experiment as the observer would see it: a sequence of shapes. Snapshot plots show whether the magnitude of dynamic forces are correctly modeled. Each part of the cable must follow its trajectory with the correct acceleration and velocity in order to maintain accurate shapes at subsequent times.

The second basis for evaluating models is to compare the trajectories of selected points on the cable with the trajectories measured for those points. Trajectory plots show whether the direction of dynamic force during the run is

4-23
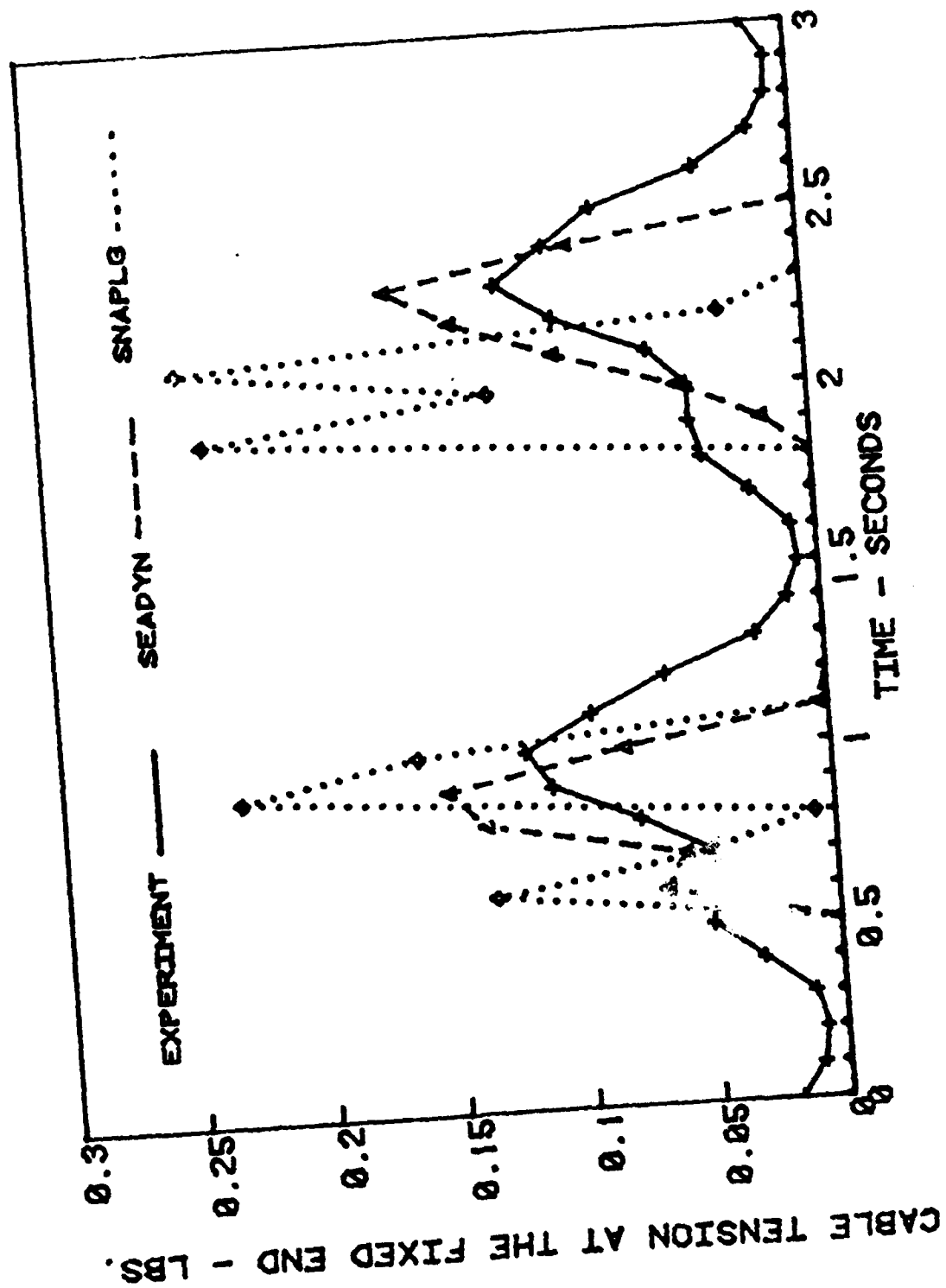
Figure 4-17. Tension Comparison For Test 133
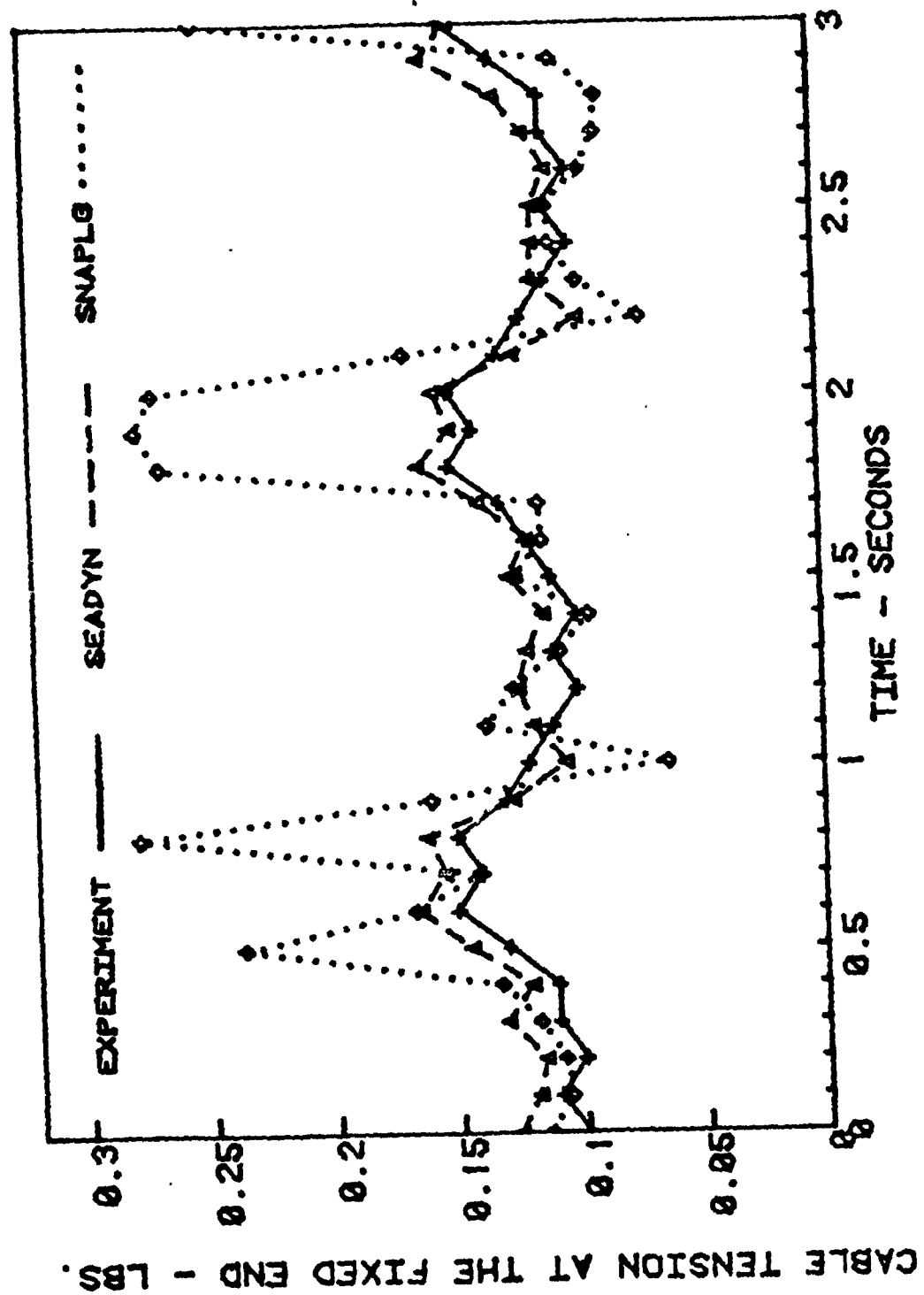
Figure 4-18. Tension Comparison For Test 142

modeled correctly. If the dynamic force is misaligned, a particle is accelerated into an improper trajectory.

The third portrayal compares the tension measured at the fixed end, plotted as a function of time during the run, with the corresponding calculated values.

4.2.1 RUN 6. Figure 4-19 is a diagram comparing the experimental cable with the physical models assumed for input to SEADYN and SNAPLOAD. Nineteen nodes were used for SEADYN; seventeen nodes is the maximum that SNAPLOAD can accommodate. Lamp 4 did not operate during Run 6. Figures 4-20 and 4-21 are images of the punched card data input for two programs.

Figures 4-22 and 4-23 show "snapshots" of the shape of the cable for a sequence of times during Run 6. The lamp locations for each time are connected by a dashed line to help visualize the shape of the cable. The actual shape of the cable was a smooth arc, not the articulated shape shown. The models, however, are also represented as articulated shapes, and it should be remembered that they approximate the smooth arc by a series of straight links.

The numbers at the tips of the curves show the time. The experimental times are circled for clarity.

The initial node locations computed by SEADYN are in close agreement with the experimental data, but the initial static shape computed by SNAPLOAD is in substantial error. Two nodes near the vertex are so far from their correct locations that the curvature of the cable is reversed. Both points are at or near the region of maximum curvature, where the error required to reverse the curvature is greatest.

Both plots show the extreme curvature of the cable as it inverts the catenary while being dragged down by the anchor. Both models produce corresponding shapes. This stage ends when the cable comes taut about 20 seconds after the release of the anchor. Both SEADYN and SNAPLOAD lag behind the data during the first 20 seconds, SEADYN places the anchor at t = 20 seconds, about where it was at t = 13.5 secconds - a time lag of about 6.5 seconds. SNAPLOAD shows a similar time lag, but only about 5 seconds. Both models "catch up" to the data by 40 seconds after release. Both models show erratic cable motion at the vertex of the catenary in the interval from 10 to 16 seconds after release, indicating slack cable.

In the second stage of the run, in which the anchor is suspended from the taut cable and swings toward the fixed support, SEADYN and SNAPLOAD calculate the velocity of the anchor node to be slightly faster than that experienced in Run 6. By t = 40 seconds, the lag of the first stage has been cancelled.

The model calculations lead the measured locations during the second stage of Run 6, especially for the portion of cable 30 to 50 feet from the fixed end. SNAPLOAD leads the data somewhat more than SEADYN on the average, even though the largest SNAPLOAD lead, 11 seconds, is only a little more than the maximum 10-second SEADYN lead.

Figures 4-24 and 4-25 show the path taken by each lamp during Run 6, as well as the path calculated by SEADYN and SNAPLOAD. The trajectories during stage two, when the anchor is suspended from the cable, are essentially circular arcs about

4-26

FEET	NODE		FEET	NODE		FEET	NODE*	
0.0	0	FIXED	0.0	19	FIXED	0.0	64	FIXED
6.6	1	LAMP	6.6	18	LAMP	6.6	60	LAMP
			9.7	17				
12.7	2	LAMP	12.7	16	LAMP	12.7	56	LAMP
			15.7	15				
18.8	3	LAMP	18.8	14	LAMP	18.8	52	LAMP
			21.8	13				
24.8	4	LAMP	24.8	12	LAMP	24.8	48	LAMP
			27.8	13		27.8	44	
30.8	5	LAMP	30.8	10	LAMP	30.8	40	LAMP
			33.8	9		33.8	36	
36.8	6	LAMP	36.8	8	LAMP	36.8	32	LAMP
			39.9	7		39.9	28	LAMP
42.9	7	LAMP	42.9	6	LAMP	42.9	24	LAMP
			45.9	5		45.9	20	
48.9	8	LAMP	48.9	4	LAMP	48.9	16	LAMP
			51.9	3		51.9	12	
						53.4	8	
54.9	9	LAMP	54.9	2	LAMP	54.9	4	LAMP
55.2	10	ANCHOR	55.2	1	ANCHOR	55.2	0	ANCHOR

EXPERIMENT   SEADYN   SNAPLOAD

* SNAPLOAD NODES ARE COUNTED BY 4. THIS MODEL HAS 17 NODES.

Figure 4-19. Node Assignments For Run 6

4-27

```
00001 CEL 60 FOOT EXPERIMENT-SEADYN MODEL-2, DILLON-RUN 5, ANCHOR LAST-SEPT 79      CASE TITLE
00002 19   1    2   18    1    3    1    1    1    3.   0.                            MASTER CONTROL
00003  2   0  32.1725 1.2017E-5  64.2394  1.6E-4  2.27529  0.   72.                  ENVIRONMENT
00004  1   0  55.15   0.    0.   0    1                                              ANCHOR NODE
00005  2   2  54.92   0.    0.   0    1                                              CABLE NODE 1
00006  4   1  48.92   0.    0.   0    1                                              CABLE NODE 2
00007  6   1  42.89   0.    0.   0    1                                              CABLE NODE 3
00008  8   1  36.85   0.    0.   0    1                                              CABLE NODE 4
00009 10   1  30.82   0.    0.   0    1                                              CABLE NODE 5
00010 12   1  24.84   0.    0.   0    1                                              CABLE NODE 7
00011 14   1  18.77   0.    0.   0    1                                              CABLE NODE 3
00012 16   1  12.72   0.    0.1  2.   1                                              CABLE NODE 3
00013 18   1   6.63   0.    0.   0    1                                              CABLE NODE 9
00014 19   1   0.00   0.    0.   1    1                                              FIXED NODE
00015  1   1   2      0     1    4    2.1      0.   2.                                ELEMENT
00016 18  18  19      1     1    0    2.1      0.   0                                ELEMENT
00017  1   0   2.014  0.0024      0    6    2.1                                      MATERIAL
00018  0.11   0.0169                                                                 STRAIN 2-1
00019  0.22   0.0375                                                                 STRAIN 2-2
00020  0.33   0.0602                                                                 STRAIN 2-3
00021  0.44   0.0845                                                                 STRAIN 2-4
00022  0.55   0.1060                                                                 STRAIN 2-5
00023  0.66   0.1289                                                                 STRAIN 2-5
00024  0  -0.1081  0.1666667   0    0    0    0.5   0.   3                            ANCHOR LOAD
00025 LIVE 20   2    4    0    1    2.   0    2    2   -1   200.   5                  SUBANALYSIS
00026  0.1   0.0001  0.0001   1.   1.                                               SOLUTION
00027  1    1  -33.916        1                       -1   90                        DISP.+ ANCHOR
00028  1    2   1.019         1                       -1   90   5                     DISP.+ ANCHOR
00029 DYN  0   1    5    0    0    0    0    0    2.1       5                         SUBANALYSIS
00030  0.01  -0.0002  -0.0032       0    0    2.   2.1   0.5                          SOLUTION
00031  0.01   1.      100.     0.5  0.0833333   2.1   2.   12.                        TIME
00032 END 0  1    1    0    2    3    4    5    6    7    7    8
00033 12345567890123456789012345678901234567890123456789012345678901234567892
```

Figure 4-20. Data Deck For SEADYN Model of Run 6

```
00010 COLUMNS: 1 123456789 2 123456789 3 123456789 4 123456789 5 123456789 6 123456789 7 123456789 8   COLUMN
00020           123456789   123456789   123456789   123456789   123456789   123456789   123456789       INDEX
00030 RUN 6 - ANCHOR LAST                                                                                TITLE
00040 SINGLE      FREE        FREEFALL            READ  .                                                OPTIONS
00050    0.01                                                                                            STATIC
00060    0.0      100.0        2.0                                                                       TIME SPEC
00070    1.0        0.5                        2.                                                        INSTABILITY
00080                                                                                                    SUPPORT
00090    0.0      -70.0                                                                                  BOUNDARY
00100 0                                                                                                  CURRENT POINTS
00110                                                                                                    PROFILE
00120    1    15                                                                                         NODES
00130   15    15                                                                                         SEGMENTS
00140  0.5   0.5                                                                                         ANCHOR
00150       0.23      0.2463     0.1081     0.0218     0.0218     218.                                   CABLE MATERIAL
00160     0.7500      0.022      0.168      0.0128     0.0024     0.0218    1.5000    1.5000             HALF-SEGMENT
00170     1.5000      0.7500     0.7500     1.5000     1.5000     1.5100    1.5080                       HALF-SEGMENT
00180     1.508       1.5000     1.5100     1.5100     1.495      1.495     3.035                        HALF-SEGMENT
00190     3.025       3.025      3.045      3.045      1.495      3.035                                   HALF-SEGMENT
00200    21.234      -1.019      6.630     -1.250                                                        ANCHOR NODE
00210    20.950      -2.7500    21.200     -4.2400                                                       NODE
00220    20.183      -7.2360    20.690    -10.200                                                        NODE
00230    18.830     -13.168     19.510    -16.030                                                        NODE
00240    16.832     -18.900     17.830    -21.300                                                        NODE
00250    13.258     -23.695     15.050    -23.544                                                        NODE
00260     7.7180    -23.373     10.4880   -18.399                                                        NODE
00270     2.4090    -12.626      4.3280    -6.6250                                                       NODE
00280     0.0         0.0        1.0840                                                                  NODE
00290                                                                                                    FIXED NODE
00300                                                                                                    PLOT-1
00310 COLUMNS: 1 123456789 2 123456789 3 123456789 4 123456789 5 123456789 6 123456789 7 123456789 8   END
00320           123456789   123456789   123456789   123456789   123456789   123456789   123456789       COLUMN
                                                                                                        INDEX
```

Figure 4-21. Data Deck For SNAPLOAD Model of Run 6
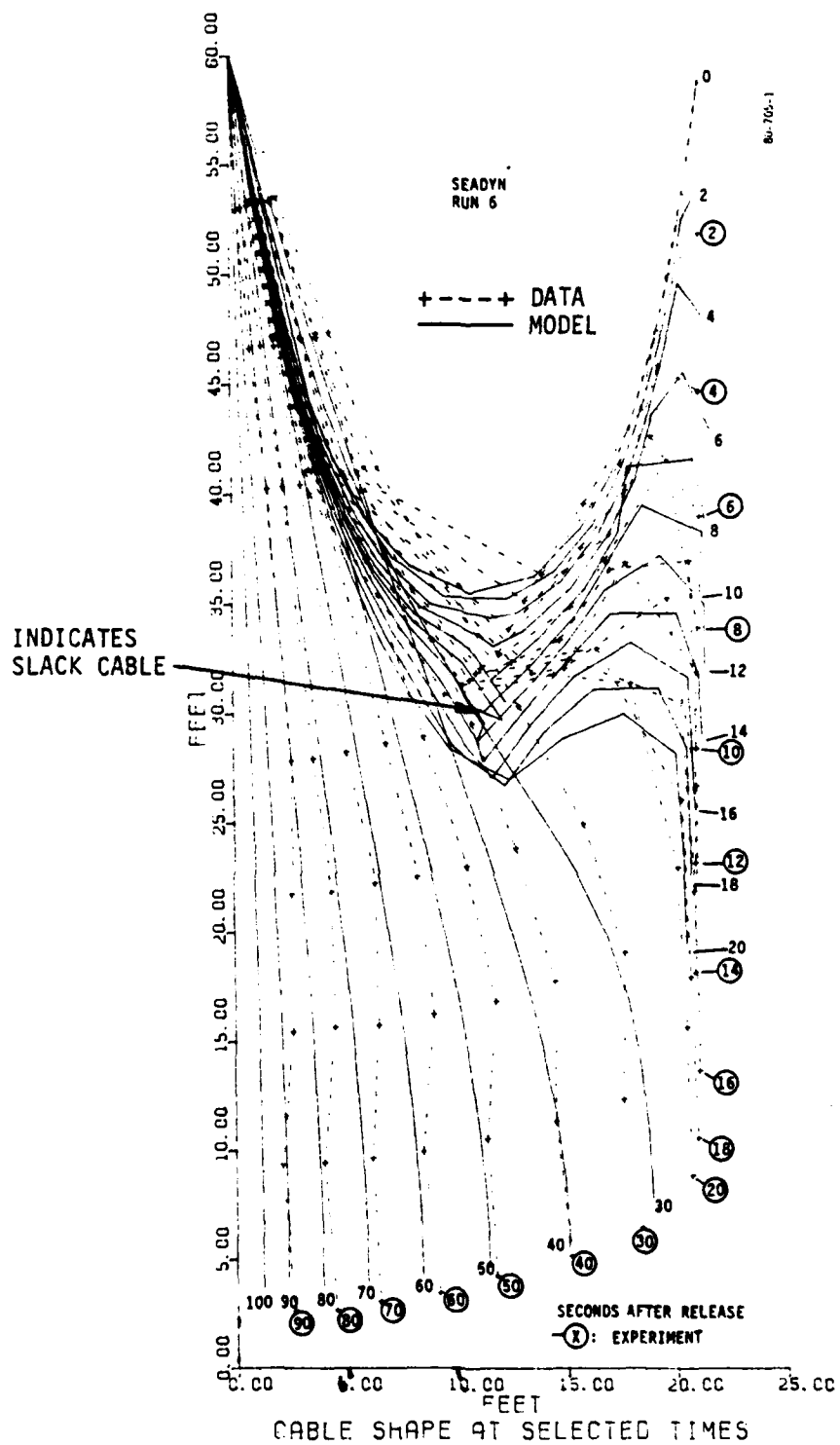
Figure 4-22.   SEADYN Snapshots of Run 6
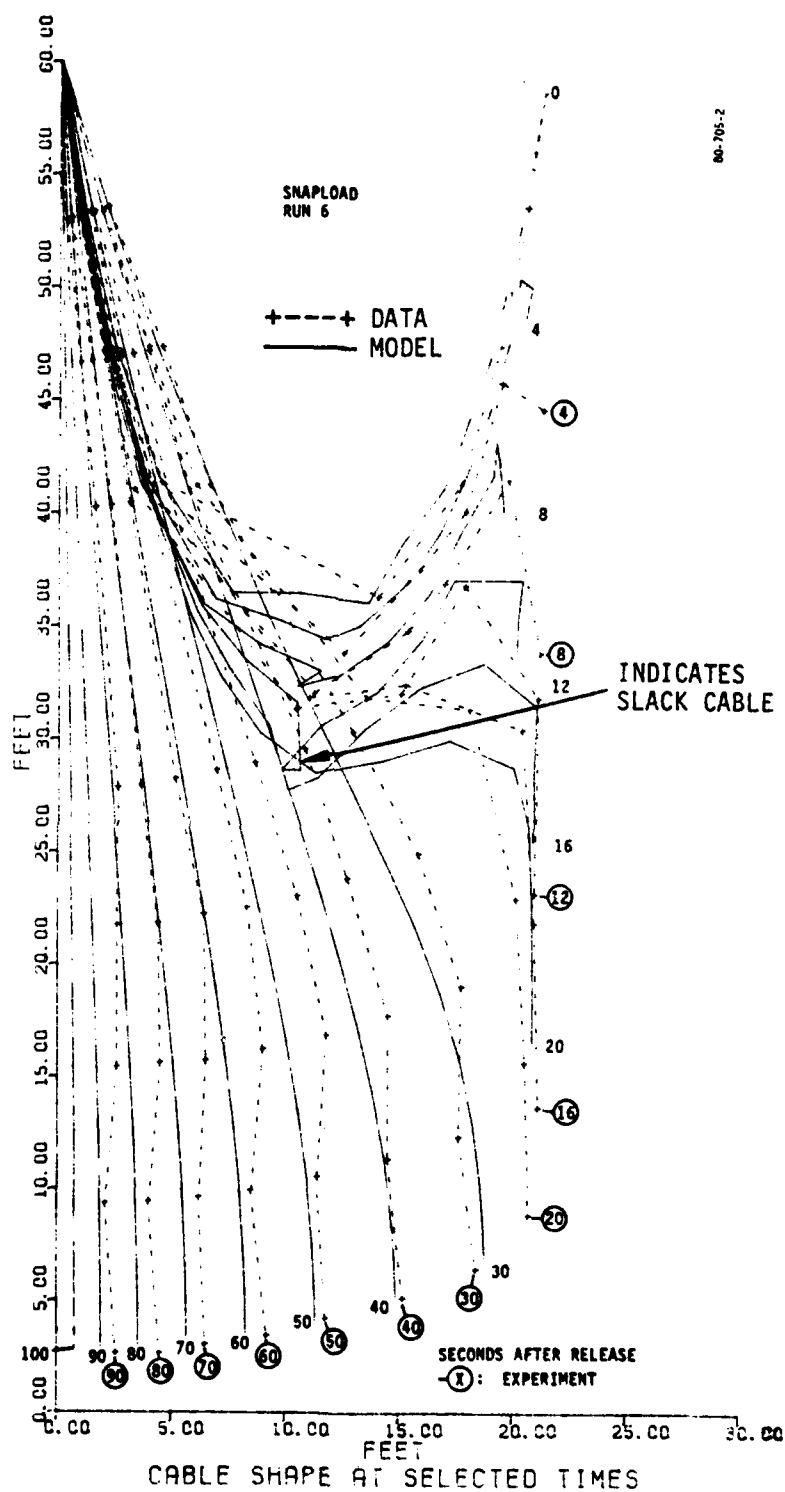
Figure 4-2: SNAPLOAD Snapshots of Run 6

4-31
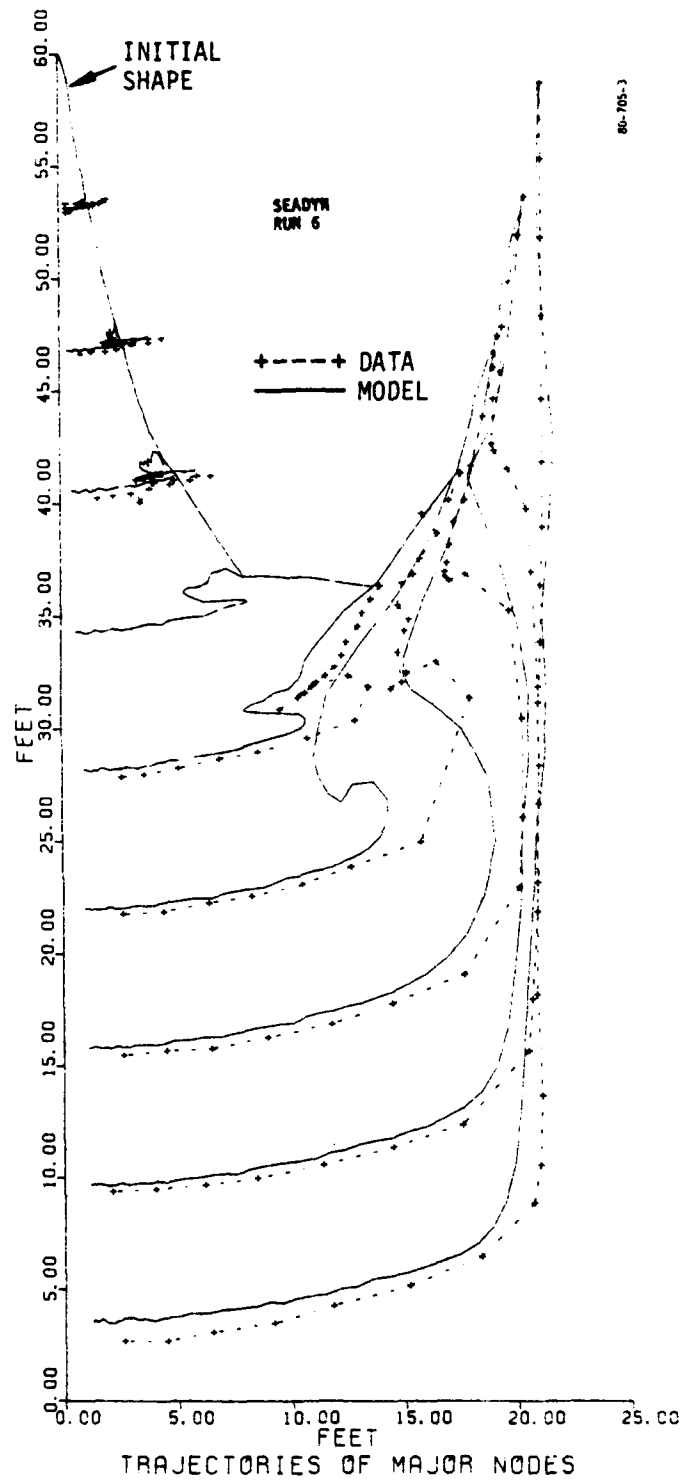
Figure 4-24. SEADYN Trajectories For Run 6
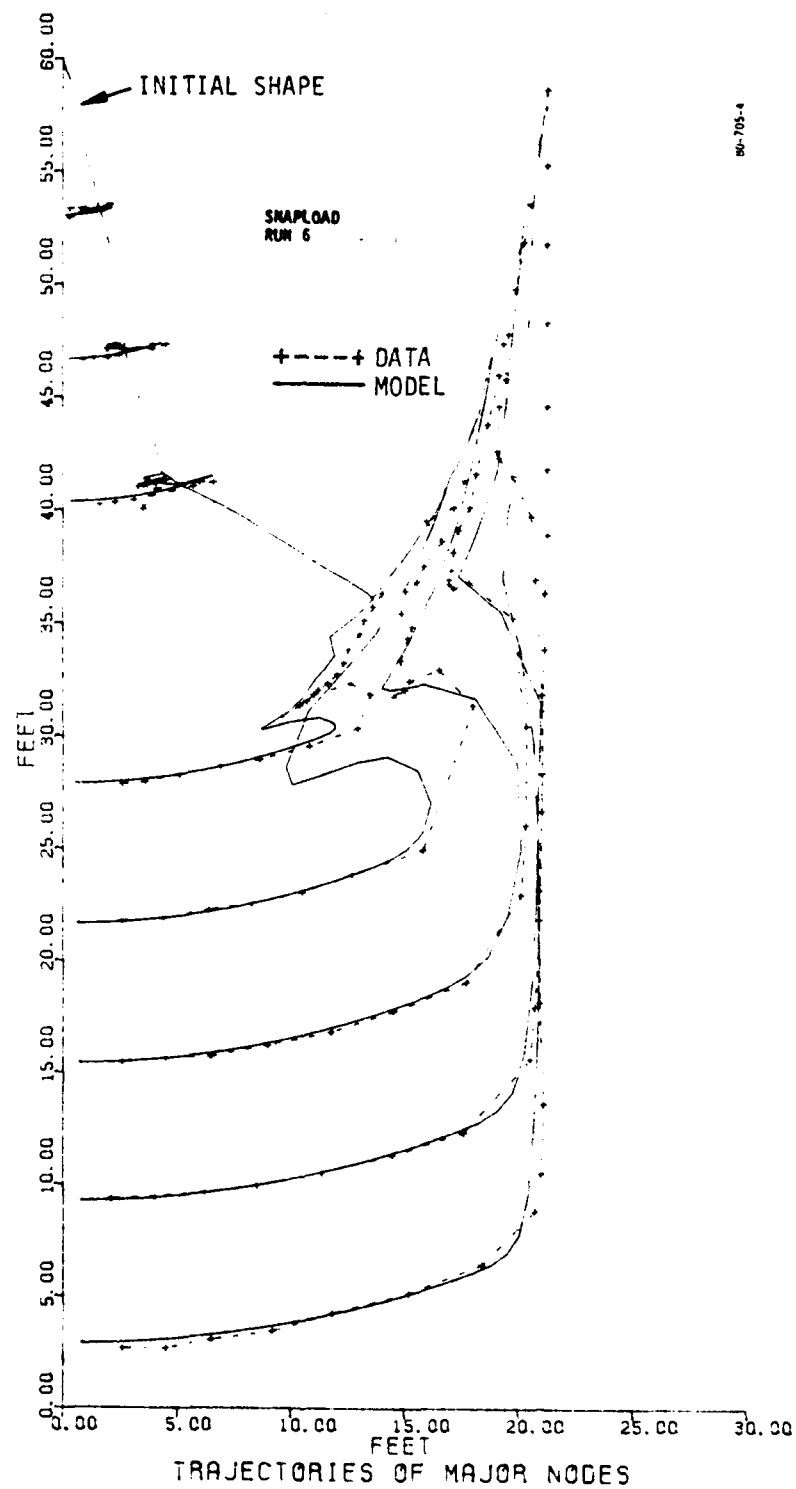
Figure 4-25. SNAPLOAD Tajectories For Run 6

4-33

the fixed point. Both models meet this simple criterion. SEADYN does not allow the silicon cord to stretch quite enough. This is attributable to the input parameters more than the computer model.

The most obvious discrepancies between the models and the data on the trajectory plots for Run 6 occur for nodes 7, 8, and 9 during stage one (anchor descent). Without support at the anchor end, these nodes fall down and away from the anchor path. A little later, after the anchor has passed by, the cable gets tighter and the nodes are jerked back towards the anchor path. The models allowed too much time for the anchor descent. This extra time allowed the nodes to deflect further before the anchor pulled them back.

The measured trajectory of the anchor is virtually a vertical fall until the cable snaps taut. But SEADYN shows the anchor oscillating slightly from side to side as it falls.* SNAPLOAD, on the other hand, calculates an anchor trajectory as much as 2.5 feet inside the measured path. This is sufficient to infer that the resultant force acting on the anchor calculated by SNAPLOAD is substantially misaligned.

Figures 4-26 and 4-27 show the tension at the fixed node as calculated by SEADYN and SNAPLOAD compared to the recorded values. The data record begins with the static value (0.06 pound) which drops slightly when the tension wave from the anchor release arrives. There is a slight steady growth as support for the weight of the lower half-cable shifts to the fixed node. Then the tension abruptly increases as the cable straightens, comes taut, and stretches to stop the plummeting anchor. This abrupt rise is damped smoothly into the steady value that represents the immersed weight of the cable and anchor.

The tension values calculated by SEADYN and plotted on Figure 4-26 follow the general trend of the recorded tension. However, large oscillations are calculated during stage one. They are attributed to inadequate dissipation of elastic energy in SEADYN because material damping was not modeled. The rise in tension is about 6.5 seconds late, corresponding to the lag noted on the snapshot plot. The final equilibrium tension is higher than the measured value, and still retains spurious

---

* These oscillations are an example of the interaction of the user with the model. The node spacing used to model these cases is about 10 percent of the cable length; the radius of the "gooseneck" that forms behind the anchor is somewhat less. In reality, only a small part of the cable is passing around the gooseneck at any time, and the motion is smooth. In the model with large elements, however, the motion is exaggerated and irregular as the links articulate around the sharp bend. The angular speed rises to a peak and falls back for each element. The resulting centrifugal force, which acts on the entire element, therefore oscillates exaggeratedly; its vertical component is restrained and results in negligible displacement, but its horizontal component produces the anomaly in the anchor trajectory.
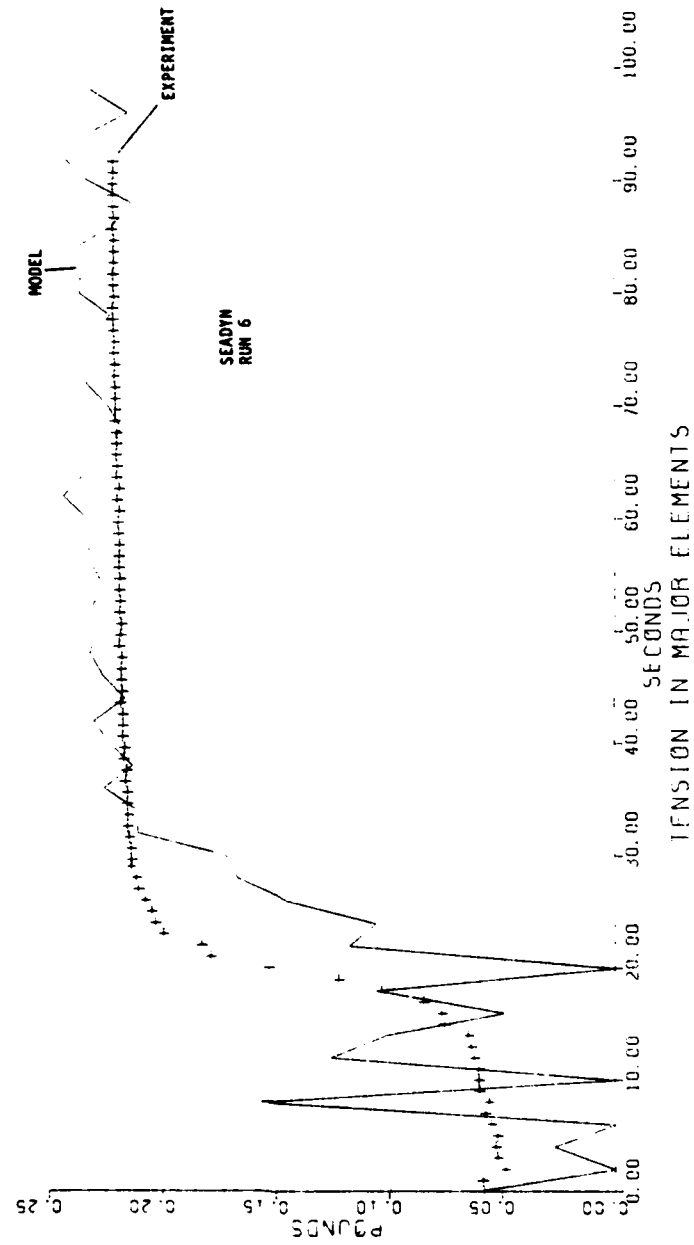
Figure 4-26. SEADYN Tension History During Run 6
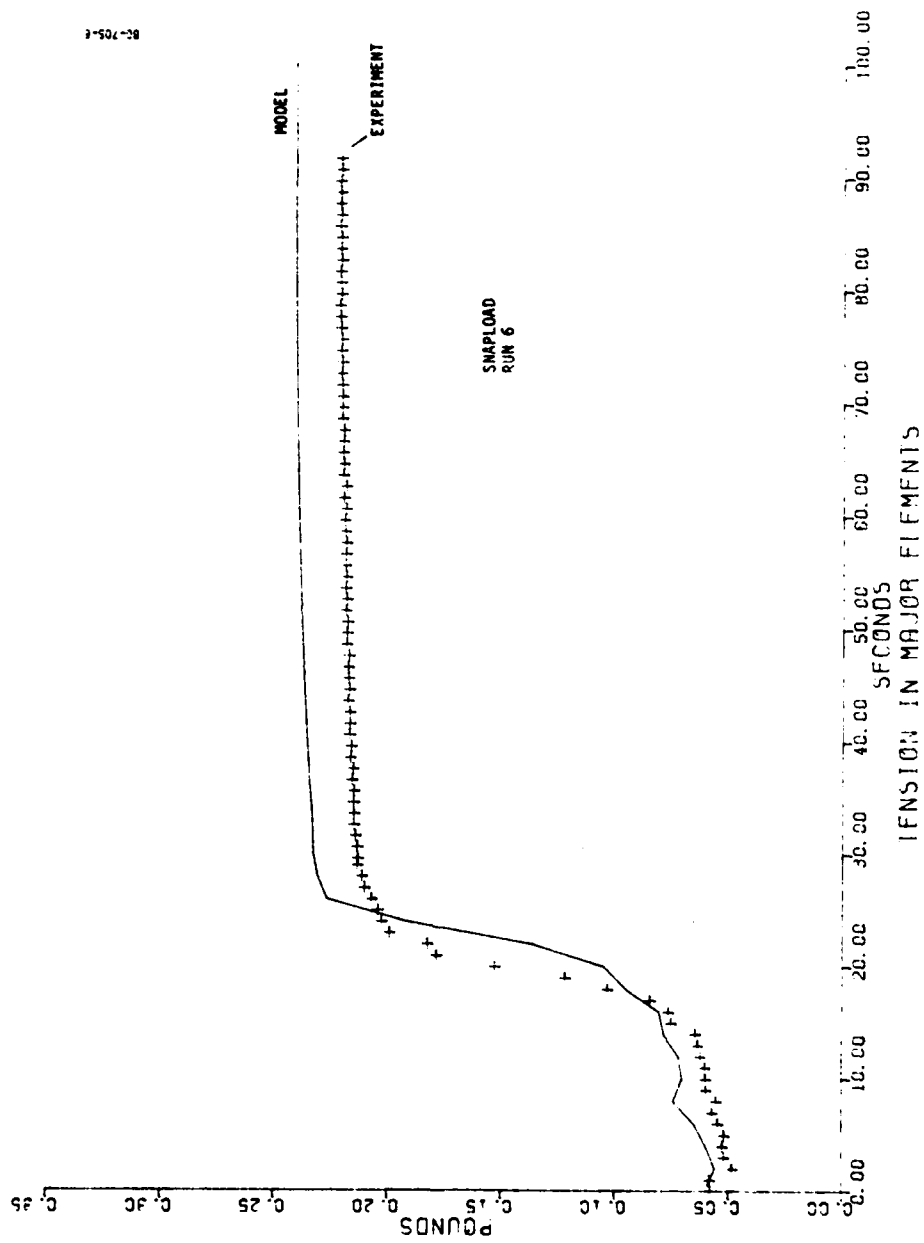
Figure 4-27. SNAPLOAD Tension History During Run 6

oscillations. SEADYN depends on measured values for the immersed weight of the anchor and cables. The discrepancy between the steady values on Figure 4-26 says more about the accuracy of the tensiometer used in the experiment vis-a-vis the scales used to weigh the anchor and cable. Figure 4-27 shows that SNAPLOAD modeled the tension smoothly throughout the event.

4.2.2 RUN 11 - BUOY RELAXATION. Figure 4-28 shows how SEADYN and SNAPLOAD were used to approximate the physical geometry of the 60-foot buoy relaxation experiment. The punch-card input decks are shown on Figures 4-29 and 4-30 for the two programs.

Run 11 is a buoy deflection experiment. The buoy is displaced to one side of the fixed anchorage, then released. It bobs up and drifts towards a position directly above the fixed anchorage. Figures 4-31 and 4-32 are the SEADYN and SNAP-LOAD snapshot plots for Run 11, respectively. This experiment is hydrodynamically identical to stage two of Run 6, with the exception of the inversion of the hydrostatic force on the cable. As in Run 6, both computer models lead the data. By the end of the run, SEADYN is roughly 11 seconds ahead, while SNAPLOAD is about 15 seconds ahead.

The measured data present an anomaly at the start of the run that will be shown more clearly on the trajectory plots: upon release, the anchor bobs up, as expected, but jumps away from the fixed point. This suggests that the release mechanism disturbed the buoy.

Figures 4-33 and 4-34 are the trajectory plots for Run 11. They show clearly the anomalous motion of the buoy at the start of the run. Otherwise, the node trajectories are a smooth progression from the initial point to the final point. Both SNAPLOAD and SEADYN calculate a final vertical shape in close agreement with the calculated static results.

Figures 4-35 and 4-36 show the SEADYN and SNAPLOAD comparisons to the measured fixed-end tension. Both models show the tension rising abruptly immediately upon buoy release. The data show a 2-second delay before the tension rises. Both models converge to a value of tension consistent with the measured weight and buoyancy of the components as provided in the input data for the models. SNAPLOAD shows the tension reading its final value within 15 seconds. The plot of the SEADYN results more nearly approximates an asymptomatic solution, although the curve is irregular from about 15 seconds through 30 seconds in the run.

4.2.3 RUN 15 - HEAVY ANCHOR DEPLOYMENT. Run 15 was a repeat of Run 6, with the 0.1-pound "light" anchor replaced by a heavier 0.25-pound sphere of the same size. Figure 4-37 shows the node assignments for SEADYN and SNAPLOAD. The data input cards are listed on Figures 4-38 and 4-39. The models performed about the same as they had for Run 6, so those comments will not be repeated in detail.

The snapshot plots for SEADYN and SNAPLOAD are presented as Figures 4-40 and 4-41. Both models show the anchor falling more slowly than measured in the experiment as was shown for Run 6. As in Run 6, the models overtake the experiment

FEET	NODE		FEET	NODE		FEET	NODE*	
51.2	0	BUOY	51.2	1	BUOY	51.2	0	BUOY
50.6	1	LAMP	50.6	2	LAMP			
			47.6	3				
44.5	2	LAMP	44.5	4	LAMP	44.5	4	LAMP
			41.4	5				
38.4	3	LAMP	38.4	6	LAMP	38.4	8	LAMP
			35.4	7				
32.4	4	LAMP	32.4	8	LAMP	32.4	12	LAMP
			29.4	9				
26.3	5	LAMP	26.3	10	LAMP	26.3	16	LAMP
			23.3	11				
20.3	6	LAMP	20.3	12	LAMP	20.3	20	LAMP
			17.2	13				
14.2	7	LAMP	14.2	14	LAMP	14.2	24	LAMP
			11.2	15				
8.2	8	LAMP	8.2	16	LAMP	8.2	28	LAMP
			4.1	17				
0.0	9	FIXED	0.0	18	FIXED	0.0	32	FIXED

EXPERIMENT   SEADYN   SNAPLOAD

FEET ABOVE ANCHORAGE

* SNAPLOAD NODES ARE COUNTED BY 4. THIS MODEL HAS 9 NODES

Figure 4-28. Node Assignments For Run 11

```
00001 COLUMNS: 1        2         3         4         5         6         7         8  COLUMN
00002 123456789 123456789 123456789 123456789 123456789 123456789 123456789  INDEX
00003 CEL 60 FOOT EXPERIMENT-SEADYN MODEL-RUN 11-AMENDED ORIGIN-OCT 81        CASE TITLE
00004 18    1    0    0    17    1    1    0    0     MASTER CONTROL
00005 2     0    32.1725 1.2817E-5 64.0394 1.6E-4 0.07528 60.   0.   ENVIRONMENT
00006 1     0    51.16   0.        0      1         0.              BUOY NODE
00007 2     0    50.57   0.        0      1                         CABLE NODE 1
00008 4     1    44.48   0.        0      1                         CABLE NODE 2
00009 6     1    38.42   0.        0      1                         CABLE NODE 3
00010 8     1    32.37   0.        0      1                         CABLE NODE 4
00011 10    1    26.32   0.        0      1                         CABLE NODE 5
00012 12    1    20.29   0.        0      1                         CABLE NODE 6
00013 14    1    14.21   0.        0      1                         CABLE NODE 7
00014 16    1    8.16    0.        0      1                         CABLE NODE 8
00015 18    1    0.      0.        1      1                         FIXED NODE
00016 1     2    0       0.350     1      0.              0.        ELEMENT
00017 17    18   1       0.        5      0.              0.        ELEMENT
00018 1     0.0147 0.0020 1.       0      1.                        MATERIAL
00019 0.11  0.0245                                                  STRAIN 1-1
00020 0.22  0.0509                                                  STRAIN 1-2
00021 0.33  0.0785                                                  STRAIN 1-3
00022 0.44  0.1060                                                  STRAIN 1-4
00023 0.55  0.1359                                                  STRAIN 1-5
00024 1     0.4060 0.2416667 0.    0      0.5       0.         0    BUOY LOAD
00025 LIVE  20   2    4      1   0   2   0   200    5               SUBANALYSIS
00026       0.1  0.0001 0.0001 1.  1.      0.        0.             SOLUTION
00027 1     28.859 1           0           1.                       DISP: BUOY X
00028 2     -11.276 1          0      -1    -1        90   0        DISP: BUOY Y
00029 DYN   0    1    5    0    0    0    0.          5             SUBANALYSIS
00030       0.01 -0.0002 -0.0002 0.  0.5 0.0833333 0. 0.5          SOLUTION
00031       0.01 1.   100.  0.5  5    6    7    2.         10.      TIME
00032 END 0 1    2    3    4    5    6    7    8
00033 12345678901234567890123456789012345678901234567890123456789012345678901234567890
READY.
```

Figure 4-29.   Data Deck for SEADYN Model of Run 11

4-40

```
00001 COLUMNS: 1         2         3         4         5         6         7         8 COLUMN
00002 123456789 123456789 123456789 123456789 123456789 123456789 123456789 INDEX
00003 60 FOOT TEST NUMBER 11 - BUOY RELAXATION                                       TITLE
00004 SINGLE    FREE                    FREEFALL        READ                          OPTIONS
00005           0.01 1000                                                             STATIC
00006     0.0        100.0     4.0                                                    TIME SPEC.
00007     1.0        0.5                                                              INSTABILITY
00008     0.0        0.0                                                              SUPPORT
00009     100.      -10.0                                                             BOUNDARY
00010    0                                                                            CURRENT POINTS
00011    0    0.0        0.0                                                          PROFILE
00012    1    7                                                                       NODES
00013    7    7                                                                       SEGMENTS
00014  0.5  0.5    0.047     -0.406    0.046                                          BUOY
00015  6.69 0.024  0.175      0.0128    0.0020    0.046                               CABLE MATERIAL
00016  3.03 3.03   3.03       3.03      3.03      161.96                              HALF-SEGMENT LENGTHS
00017  3.04 3.03   3.03       3.03      8.16      3.03      3.02                      HALF-SEGMENT LENGTHS
00018 28.859       39.884     27.803    35.720                                       BUOY NODE
00019 25.868       29.831     23.684    24.067                                       NODE
00020 19.773       15.733     16.581    10.535                                       NODE
00021 12.671       5.809      7.866     2.077                                         NODE
00022               0.0       0.0                                                     FIXED NODE
00023 ZXTENSION                                                                       PLOT-1
00024             10.         1                                                       PLOT-2
00025 32                      1                                                       PLOT-3
00026                                                                                 END
00027 COLUMNS: 1         2         3         4         5         6         7         8 COLUMN
00028 123456789 123456789 123456789 123456789 123456789 123456789 123456789 INDEX
READY.
```

Figure 4-30.   Data Deck for SNAPLOAD Model of Run 11

4-41
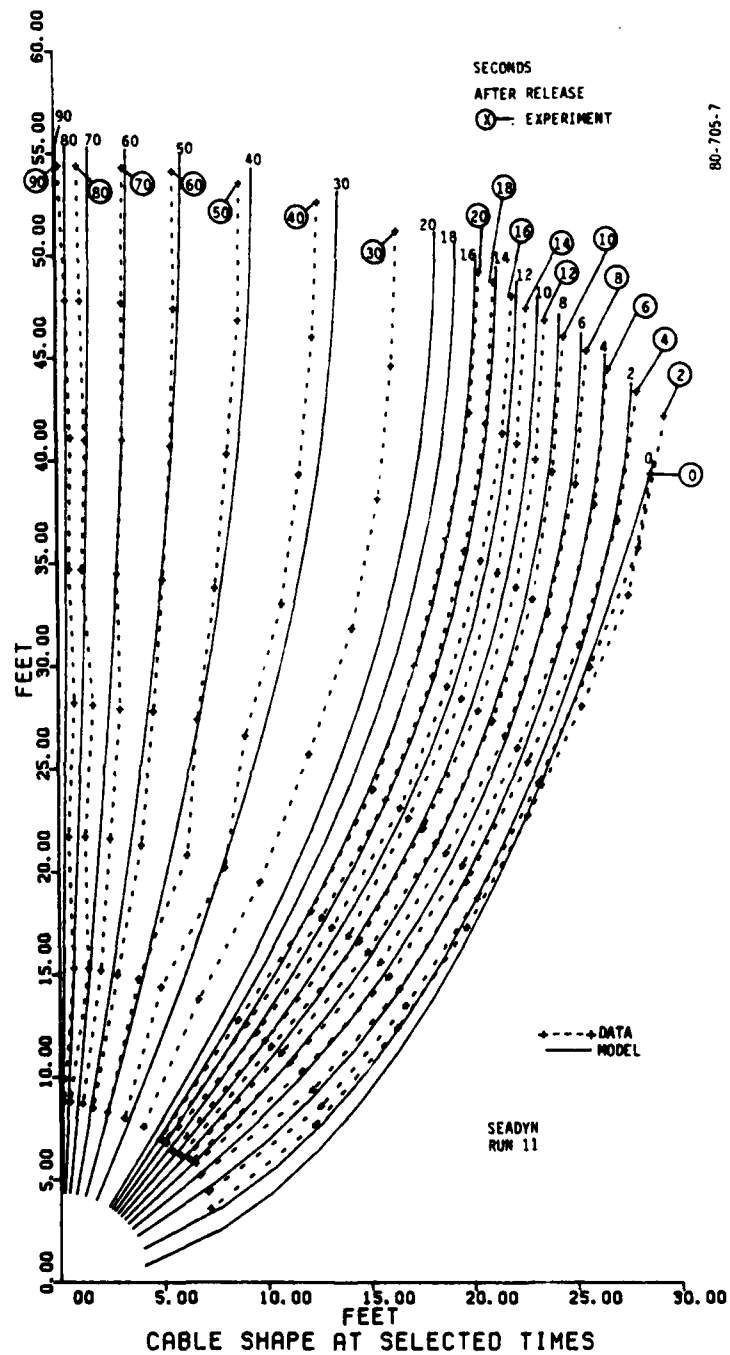
Figure 4-31. SEADYN Snapshots of Run 11
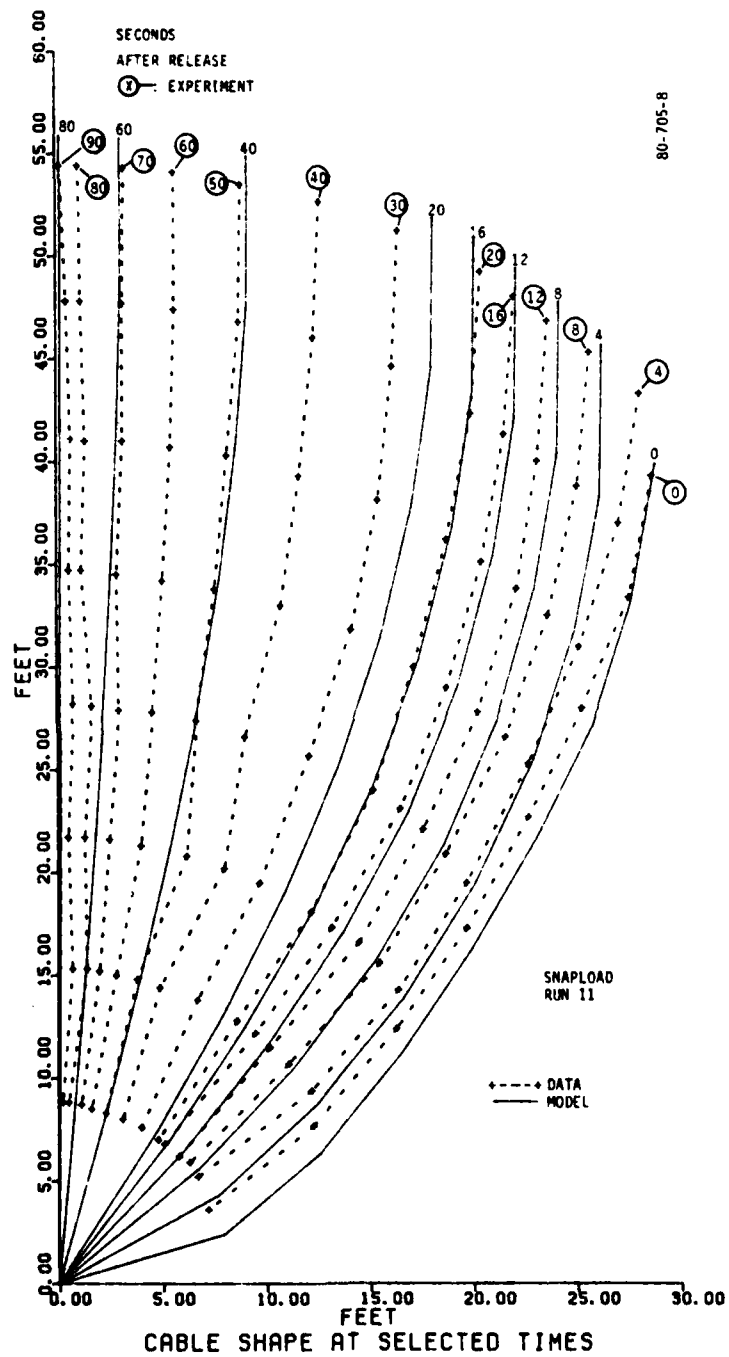
Figure 4-32. SNAPLOAD Snapshots of Run 11

4-43
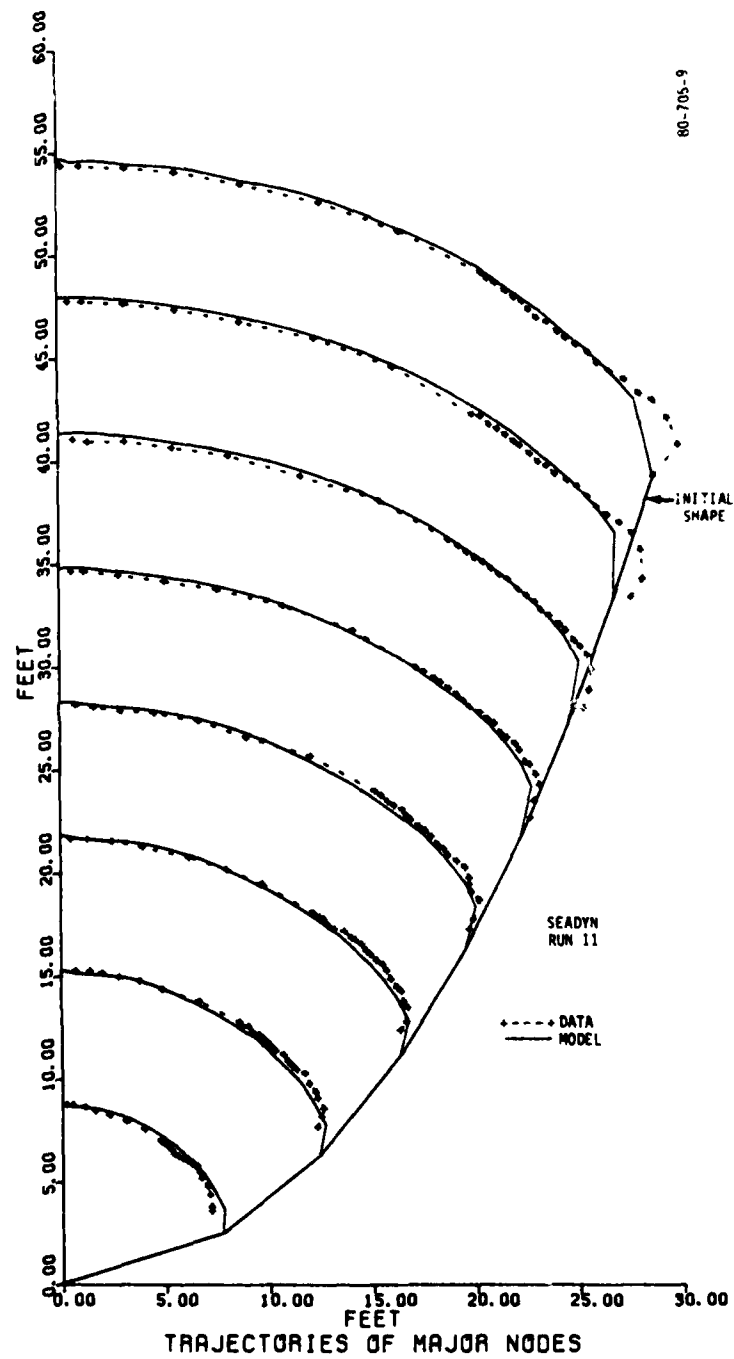
Figure 4-33. SEADYN Trajectories for Run 11

4-44
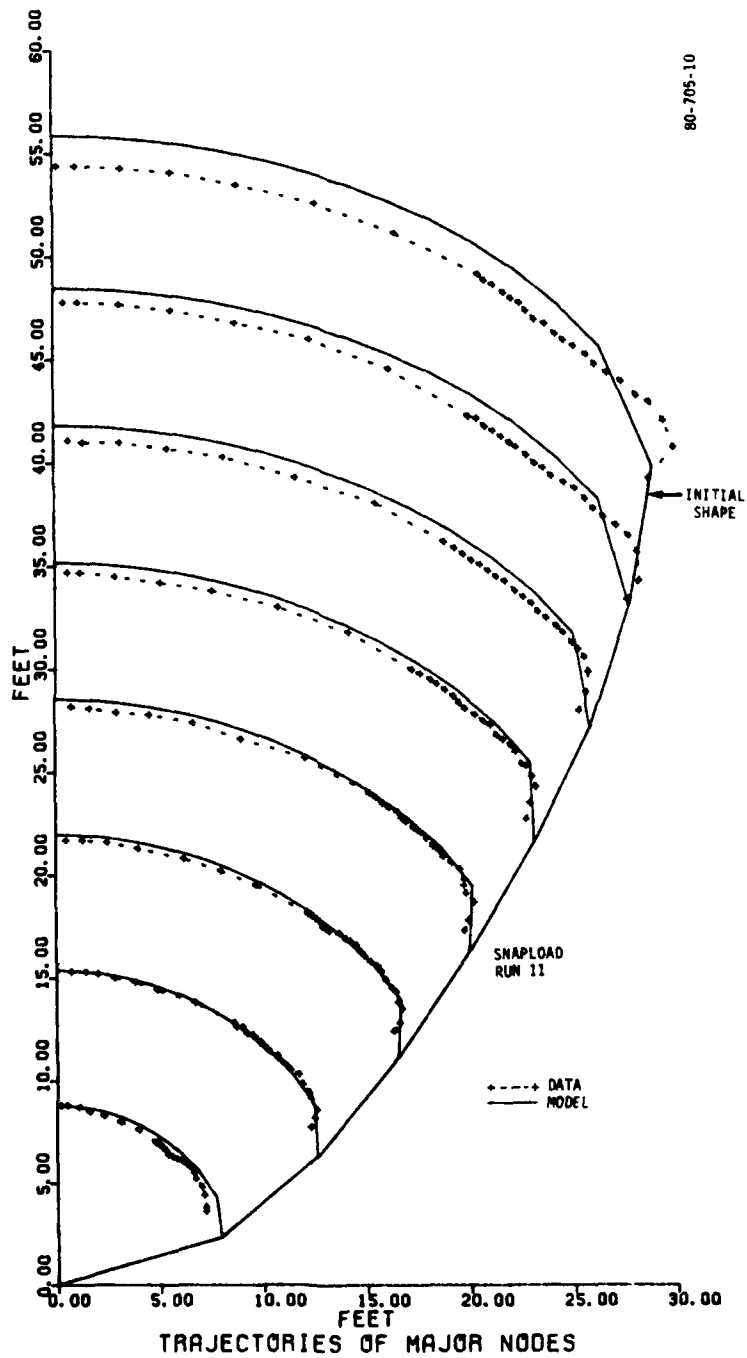
Figure 4-34. SNAPLOAD Trajectories for Run 11
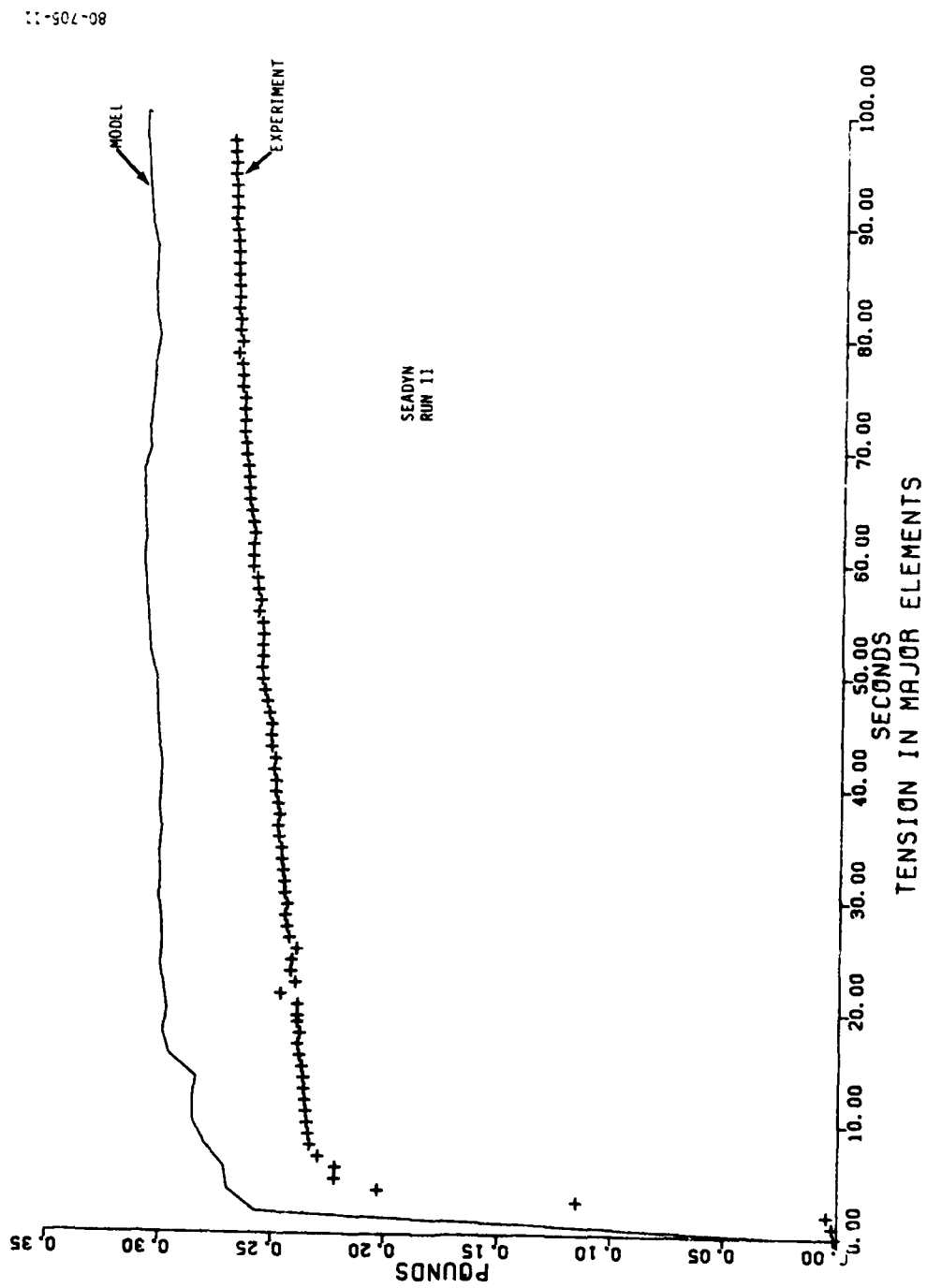
Figure 4-35. SEADYN Tension History During Run 11
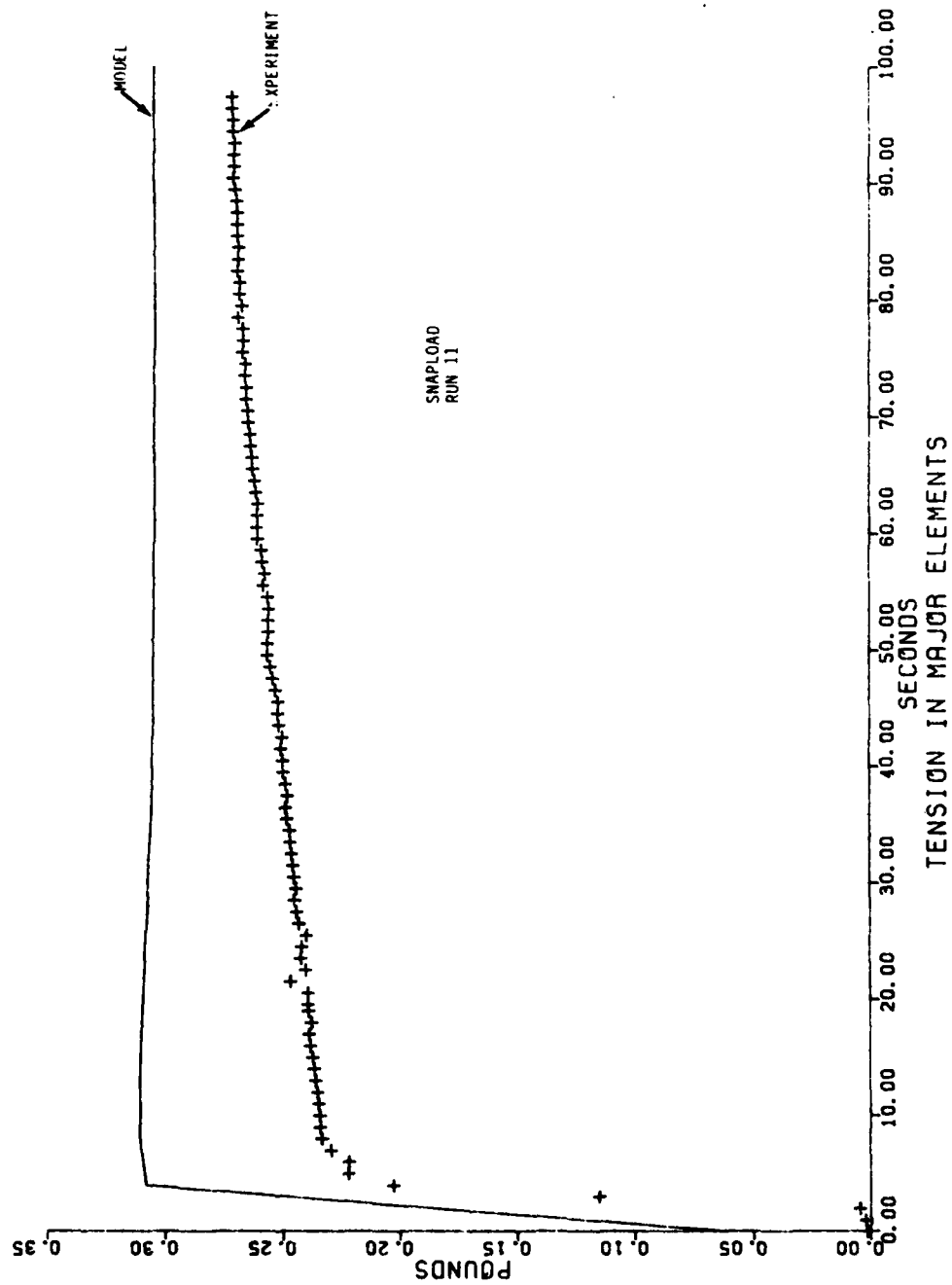
Figure 4-36. SNAPLOAD Tension History During Run 11

4-47

FEET	NODE			FEET	NODE			FEET	NODE*		
—0.0	10	FIXED		—0.9	19	FIXED		—0.0	64	FIXED	
—6.6	9	LAMP		—6.6	18	LAMP		—6.6	60	LAMP	
				9.7	17						
—12.7	8	LAMP		—12.7	16	LAMP		—12.7	54	LAMP	
				15.7	15						
—18.8	7	LAMP		—18.8	14	LAMP		—18.8	52	LAMP	
				21.8	13						
—24.8	6	LAMP		—24.8	12	LAMP		—24.8	48	LAMP	
				27.8	11			27.8	44		
—30.8	5	LAMP		—30.8	10	LAMP		—30.8	40	LAMP	
				33.8	9	LAMP		33.8	36		
—36.8	4	LAMP		—36.8	8	LAMP		—36.9	32	LAMP	
				39.9	7			39.9	28		
—42.9	3	LAMP		—42.9	6	LAMP		—42.9	24	LAMP	
				45.9	5			45.9	20		
—48.9	2	LAMP		—48.9	4	LAMP		—48.9	16	LAMP	
				51.9	3			51.9	12		
								53.4	8		
—54.9	1	LAMP		—54.9	2	LAMP		—54.9	4	LAMP	
—55.2	0	ANCHOR		—55.2	1	ANCHOR		—55.2	0	ANCHOR	

FEET BELOW FIXED SUPPORT

EXPERIMENT   SEADYN   SNAPLOAD

* SNAPLOAD NODES ARE COUNTED BY 4.   THIS MODEL HAS 17 NODES

Figure 4-37.   Node Assignments For Run 15

```
00001 CEL 60 FOOT EXPERIMENT-SEADYN MODEL-D.DILLON-RUN 15: ANCHOR LAST-SEPT.79      CASE TITLE
00002  19   1    0         18      1      0      1     0     3.     0    0           MASTER CONTROL
00003   2   0  32.1725  1.2817E-5  54.2396  1.6E-4  1   3.  2.2752R   0.
00004   1   0  55.15      0.                         72.                             ENVIRONMENT
00005   2   0  54.92      0.        0.      0    1                                   ANCHOR NODE
00006   4   1  48.92      0.        0.      0    1                                   CABLE NODE 1
00007   6   1  42.89      0.        0.      0    1                                   CABLE NODE 2
00008   8   1  36.85      0.        0.      0    1                                   CABLE NODE 3
00009  12   1  30.82      0.        2.1     0    1                                   CABLE NODE 4
00010  12   1  24.84      0.        0.      0    1                                   CABLE NODE 5
00011  14   1  18.77      0.        0.      0    1                                   CABLE NODE 6
00012  16   1  12.72      0.        0.      0    1                                   CABLE NODE 7
00013  18   1   6.63      0.        0.      0    1                                   CABLE NODE 8
00014  19   1   0.00      0.        0.      1    1                                   CABLE NODE 9
00015   1   1             0         2.1     1    3        2.1     0.                 FIXED NODE
00016  18  18   1         0         0.      3        2.1     0.                      ELEMENT
00017   1   0   2.014    0.0024     1.      6    0        2.1                        ELEMENT
                                                                                    MATERIAL
00018  0.11    0.0169                                                               STRAIN 2-1
00019  0.22    0.0375                                                               STRAIN 2-2
00020  0.33    0.0602                                                               STRAIN 2-3
00021  0.44    0.0845                                                               STRAIN 2-4
00022  0.55    0.1060                                                               STRAIN 2-5
00023  0.66    0.1289                                                               STRAIN 2-6
00024   1     -0.2518  0.1666667      0.     2     2        2.6    0.                ANCHOR LOAD
00025 LIVE    20     4         1      0      2     2       -1  200      2            SUBANALYSIS
00026  0.1     0.0001   0.0001        1.         2            2.                     SOLUTION
00027   1     -34.617                                                               DISP.1 ANCHOR
00028   1       1.019                                                               DISP.1 ANCHOR
00029 DYN      1      5        0       0      2     2        1    52      2          SUBANALYSIS
00030   0.01   -0.0002  -0.0002                    3.         2.1   0.5             SOLUTION
00031   0.01    1.      100.          0.5  0.0833333       2.1     2.               TIME
00032 END 0    1      2        3                5          6    7      8
00033 1234567890123456789012345678901234567890123456789012345678901234567890
```

Figure 4-38. Data Deck For SEADYN Model of Run 15

4-50

```
00010 COLUMNS: 1         2         3         4         5         6         7         8 COLUMN
00020 123456789 123456789 123456789 123456789 123456789 123456789 123456789           INDEX
00030 RUN 15 - ANCHOR LAST                                                             TITLE
00040 SINGLE   FREE                                                                    OPTIONS
00050 0.01                                                                             STATIC
00060 0.0    100.0    4.0          FREEFALL          READ                              TIME SPEC.
00070 1.0    0.5                    2.                                                 INSTABILITY
00080                                                                                  SUPPORT
00090 0.0    -70.0                                                                     BOUNDARY
00100 0                                                                                CURRENT POINTS
00110 0                                                                                PROFILE
00120 1  15                                                                            NODES
00130 15 15                                                                            SEGMENTS
00140 0.5   0.5    0.3980  0.2518  0.0218  0.0218                                       ANCHOR
00150 0.23   0.022   0.168   0.0128  0.0024  218.                                       CABLE MATERIAL
00160 0.7500 0.7500 0.7500 0.7500 1.5000 1.5000 1.5000                                  HALF-SEGMENT
00170 1.5000 1.5000 1.5100 1.5100 1.5100 1.5100 1.5080                                  HALF-SEGMENT
00180 1.508  1.495  1.495  1.495  3.035  3.035                                          HALF-SEGMENT
00190 3.025  3.045  3.045  6.630                                                        HALF-SEGMENT
00200 20.533  -1.019  20.500                                                            ANCHOR NODE
00210 20.259  -2.749  20.018  -4.248                                                    NODE
00220 19.535  -7.245  18.892  -10.218                                                   NODE
00230 18.249  -13.191 17.297  -16.074                                                   NODE
00240 16.344  -18.956 14.616  -21.397                                                   NODE
00250 12.887  -23.837 10.138  -23.682                                                   NODE
00260 7.388   -23.526 4.1170  -18.451                                                   NODE
00270 2.2880  -12.649 1.0290  -6.6330                                                   NODE
00280 0.0     0.0                                                                       FIXED NODE
00290 ZXTENSION                                                                         PLOT-1
00300 10.             1   1   1                                                         PLOT-2
00310 64                                                                               PLOT-3
00320                                                                                  END
00330 COLUMNS: 1         2         3         4         5         6         7         8 COLUMN
00340 123456789 123456789 123456789 123456789 123456789 123456789 123456789           INDEX
```

Figure 4-39. Data Deck For SNAPLOAD Model of Run 15

3-8
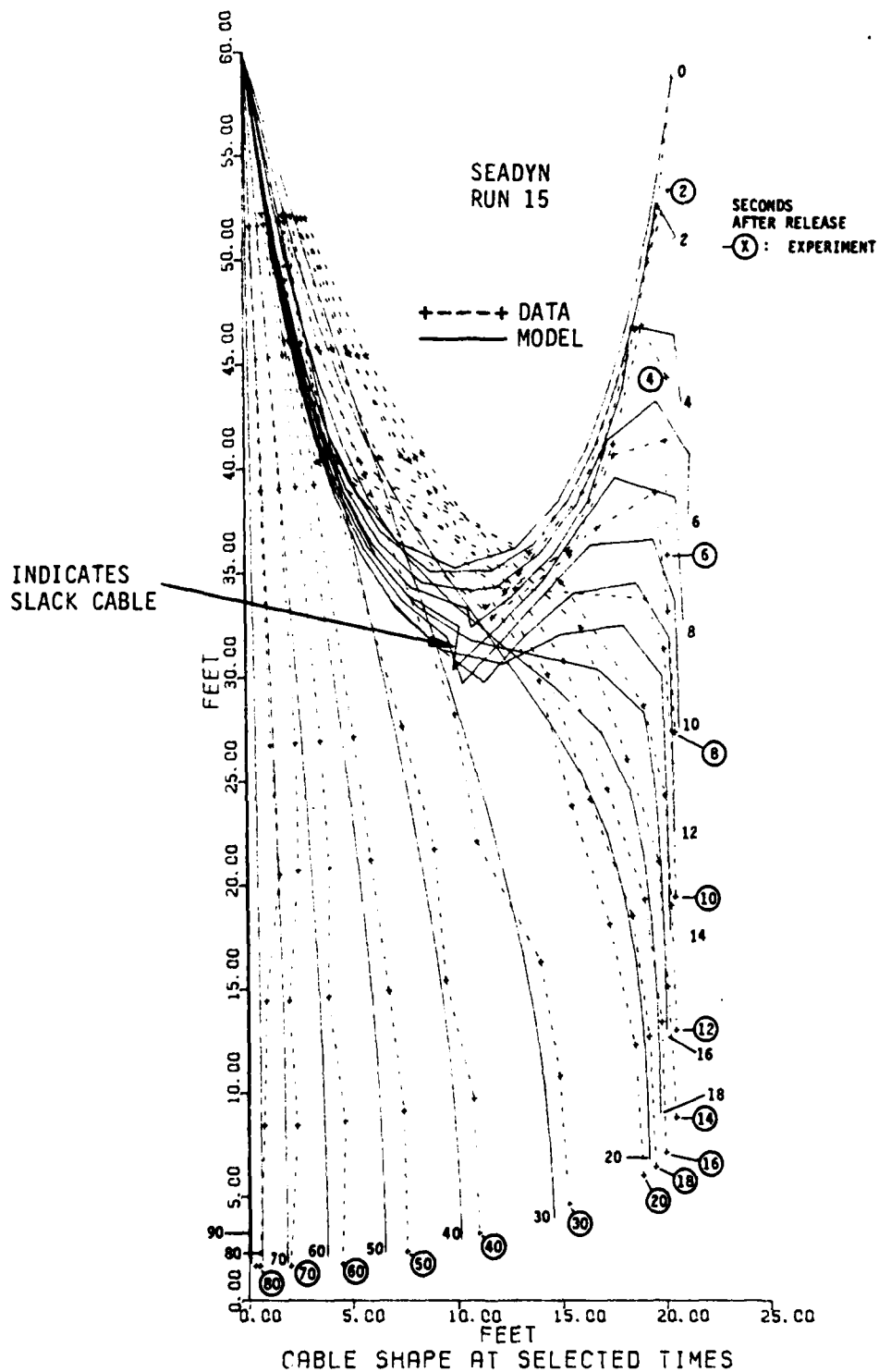
Figure 4-40. SEADYN Snapshots of Run 15

4-52
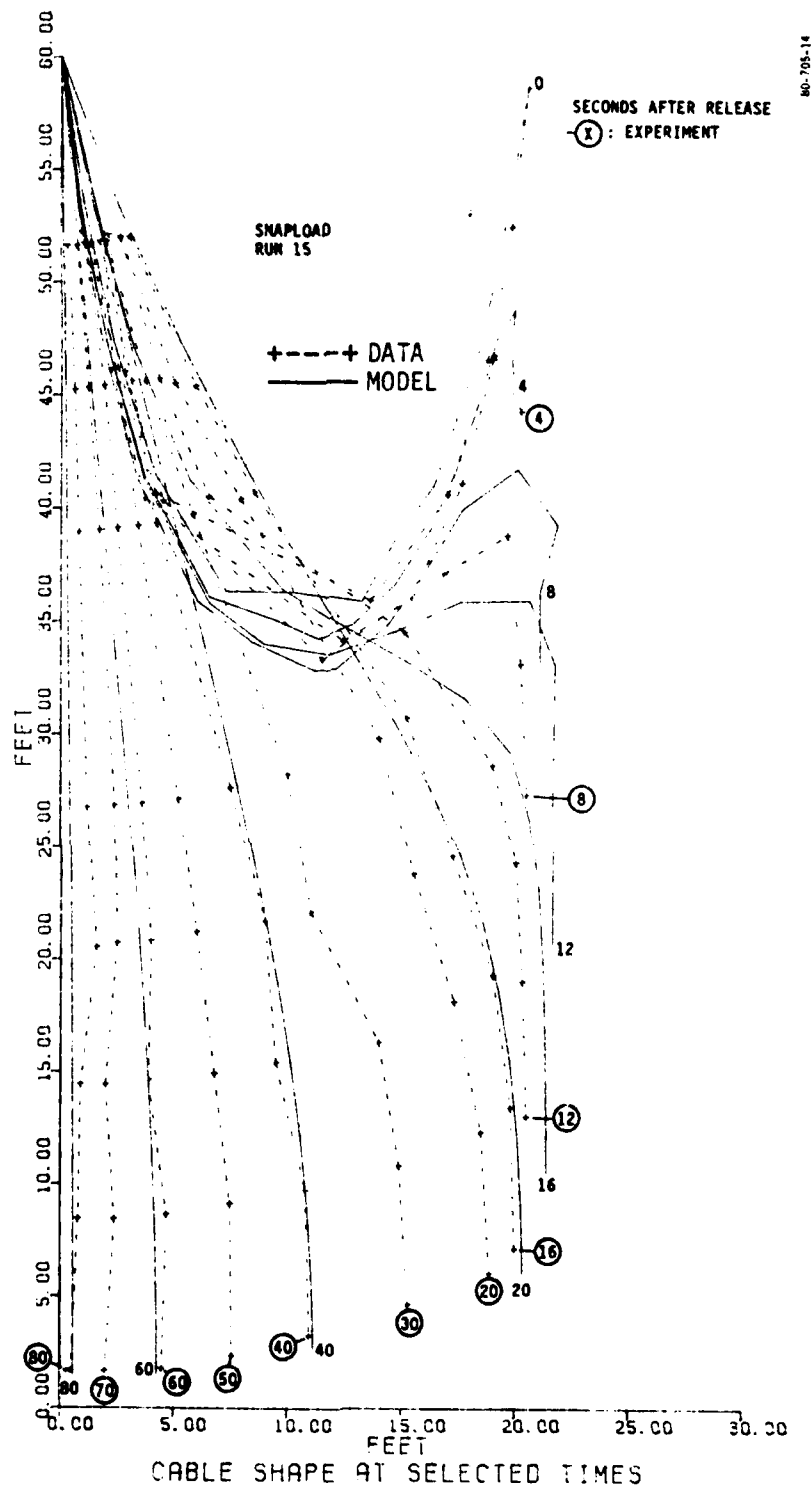
Figure 4-41. SNAPLOAD Snapshots of Run 15

during the pendulum stage. The anchor used in Run 15 was heavier than the anchor for Run 6. Less time is available for slack cable to develop at the vertex, and both models as well as the data reflect the smoother descent. This is also apparent in the trajectory plots (Figures 4-42 and 4-43) for SEADYN AND SNAPLOAD.

The fixed-end tension plots on Figures 4-44 and 4-45 show that both models and the data converged to the immersed weight of the anchor and cord with good accuracy. SEADYN gives somewhat erratic values, as in the other cases. SEADYN calculated the time for the anchor to jerk the cord taut about 5 seconds late; SNAPLOAD was 1.5 to 2 seconds late.

4.3 THE MOORING DYNAMICS EXPERIMENT MOORING SIX.

Mooring Six of the Mooring Dynamics Experiment is sketched in Figure 2-21. The deployment of this mooring by the anchor-last technique was modeled using the SEADYN computer program (Reference 14). SNAPLOAD was not compared to this experiment.

Figure 4-46 is a schematic diagram of the node model used to approximate the physical mooring. Images of the SEADYN input cards are shown on Figure 4-47. Appendix A reviews the development of the parameters describing each node. Other parameters were accepted as provided by default in the SEADYN model, with one exception. The drag coefficient of the sandbag anchor clump was selected by matching the terminal velocity of the anchor to the descent speed measured for pinger ALPHA during the deployment.

4.3.1 SNAPSHOT GEOMETRY COMPARISONS.

Figure 4-48 shows the shape of the MDE/CEL mooring calculated at selected times during the deployment. At time t = 0, the anchor is on the towship at the upper right corner of the figure, and the main buoy is on the water surface at the upper left corner of the figure.

Even though the ship is towing the mooring from left to right at 3.25 knots, the anchor does not coast an appreciable distance after release. Indeed, it swings back first, under the recovery buoys attached to the acoustic release. Then it falls nearly vertically down the right margin of the figures, until the main buoy is pulled under about 6 minutes (360 seconds) after release. Then the anchor begins a sedate pendulum-swing to the left under the main buoy until it impacts on the bottom during the eighth minute after release.

The actual anchor-last deployment differs from the 6- and 60-foot simulations not only in scale. The upper end of the simulated mooring was fixed, in order to enable the tension to be measured there. In the at-sea deployment, there is no fixed point. The buoy is towed along the water surface by the descending anchor, using the water as a great "sheave-wheel" (the "water-pulley"). This accounts for the different appearance of Figure 4-48 from snapshot plots of the simulated deployments, like Figure 4-41. Furthermore, the simulated anchor weights did not impact the bottom of the test tank.

It is easy to overlook another implication of the actual deployment. Once the anchor was "dropped" in the SEADYN model, there was no fixed point to restrain the overall position of the nodes in the computer model. Residual errors in the
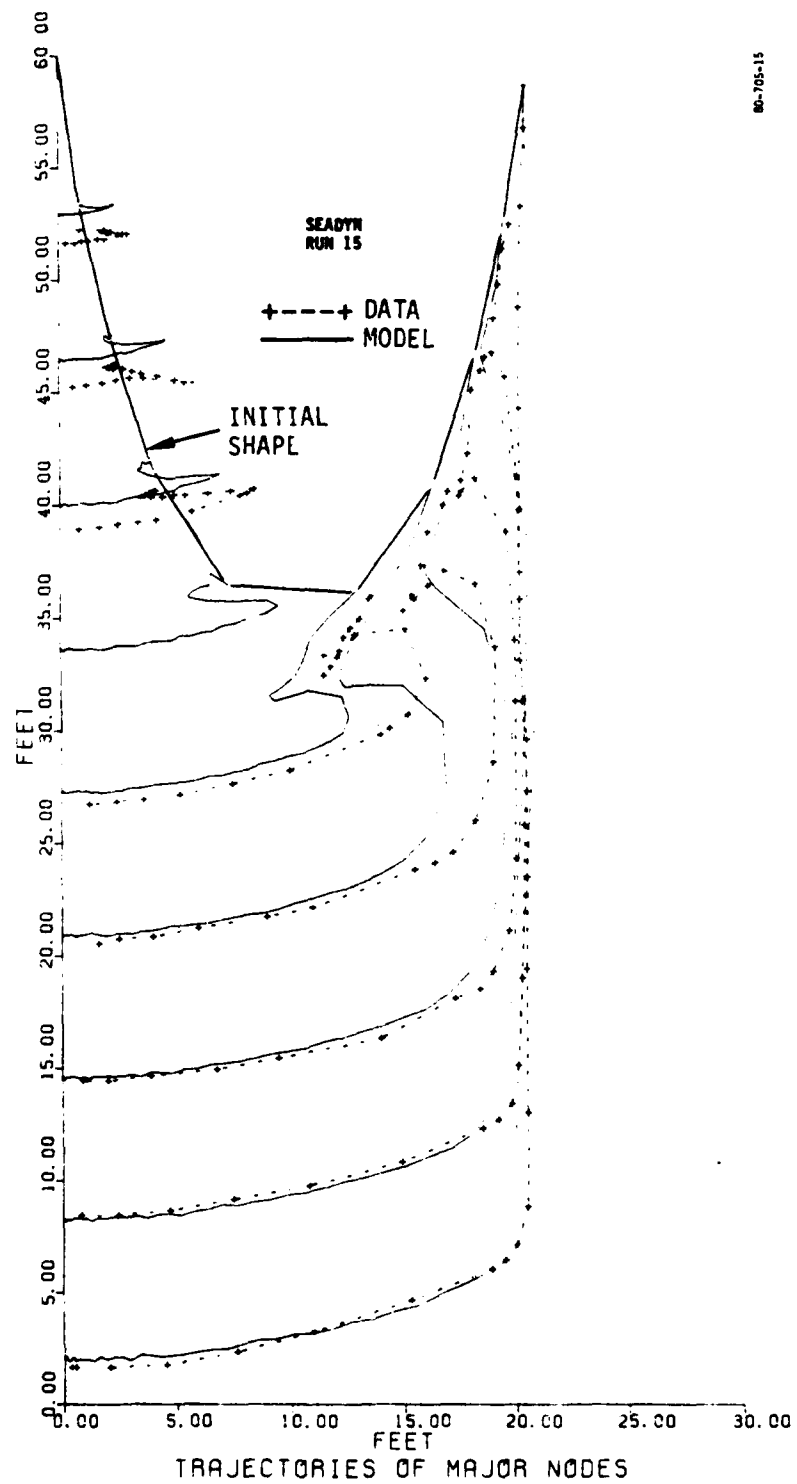
Figure 4-42. SEADYN Trajectories For Run 15
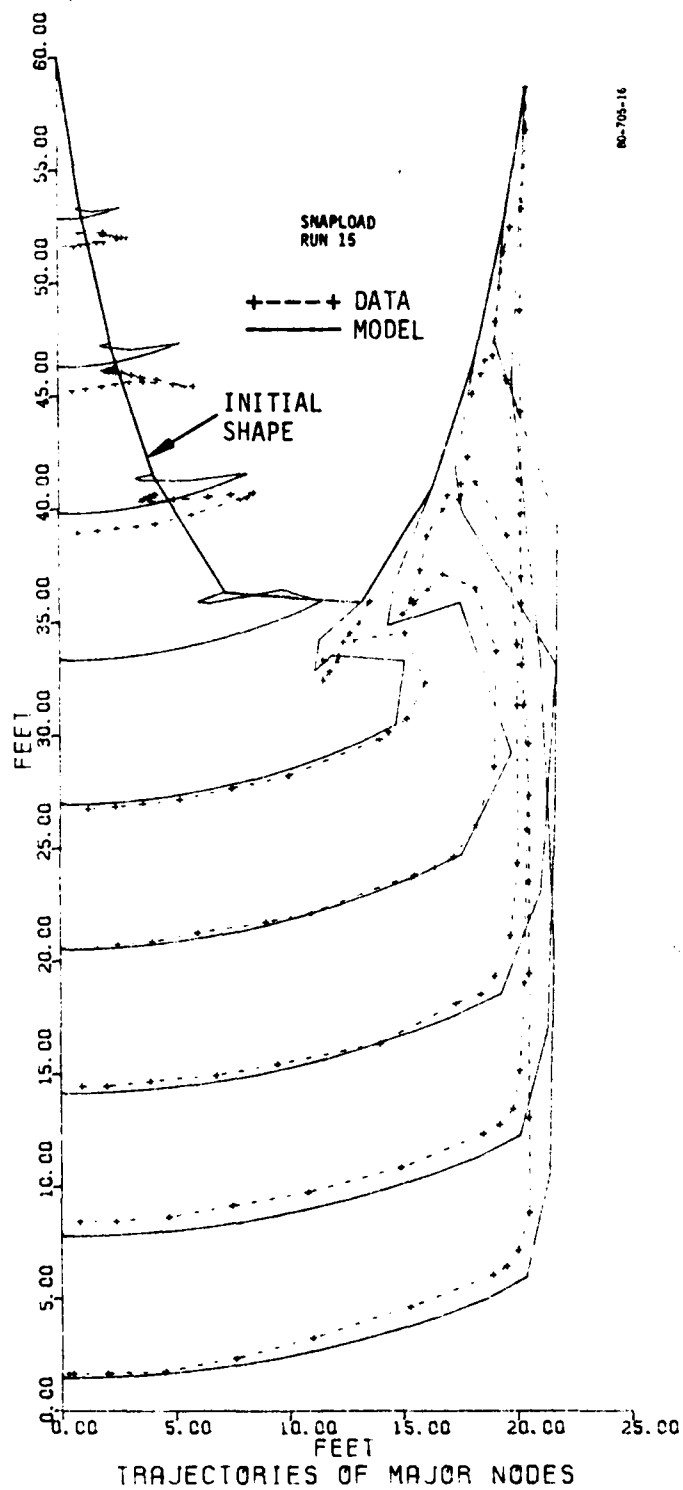
Figure 4-43. SNAPLOAD Trajectories For Run 15

4-57
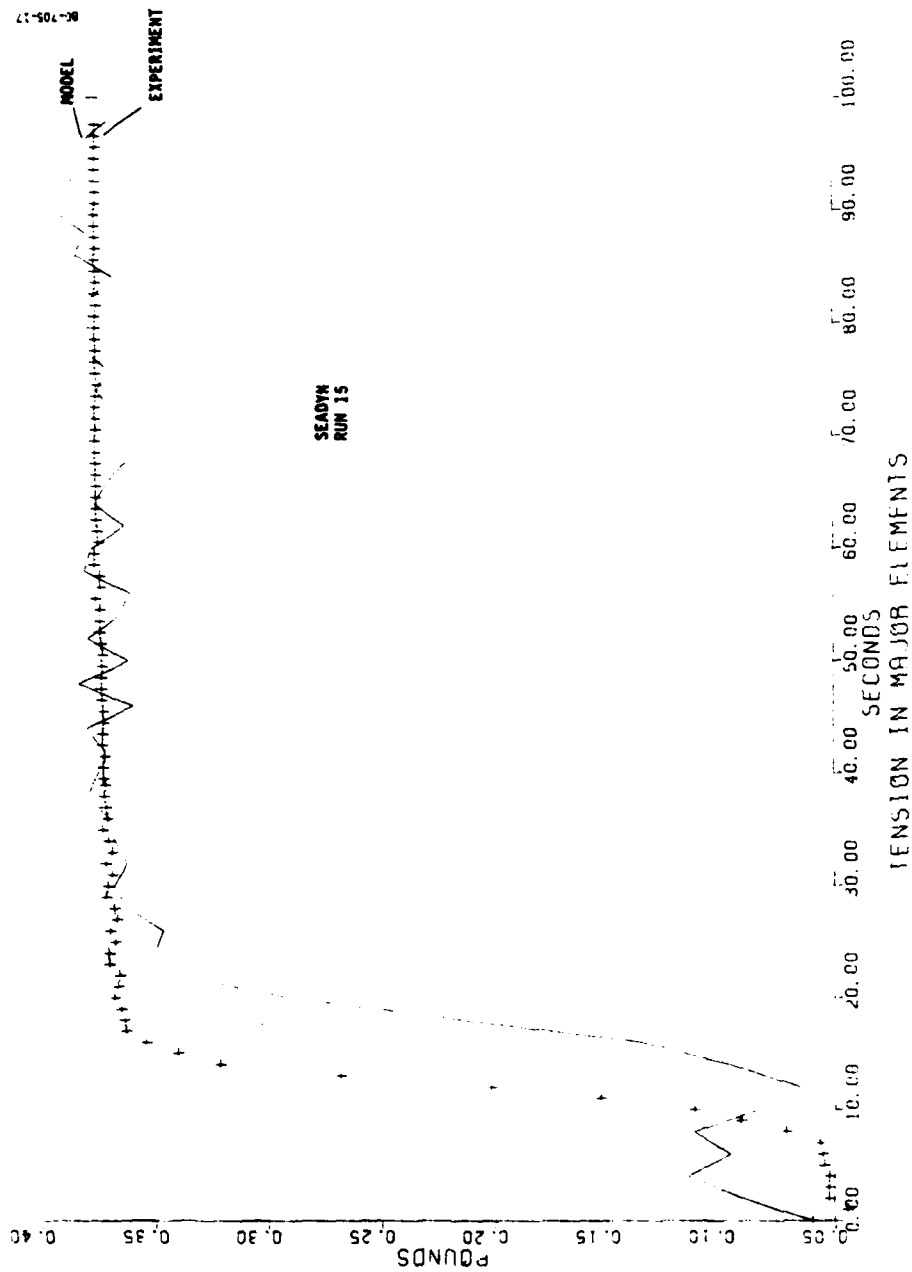
Figure 4-44. SEADYN Tension History During Run 15
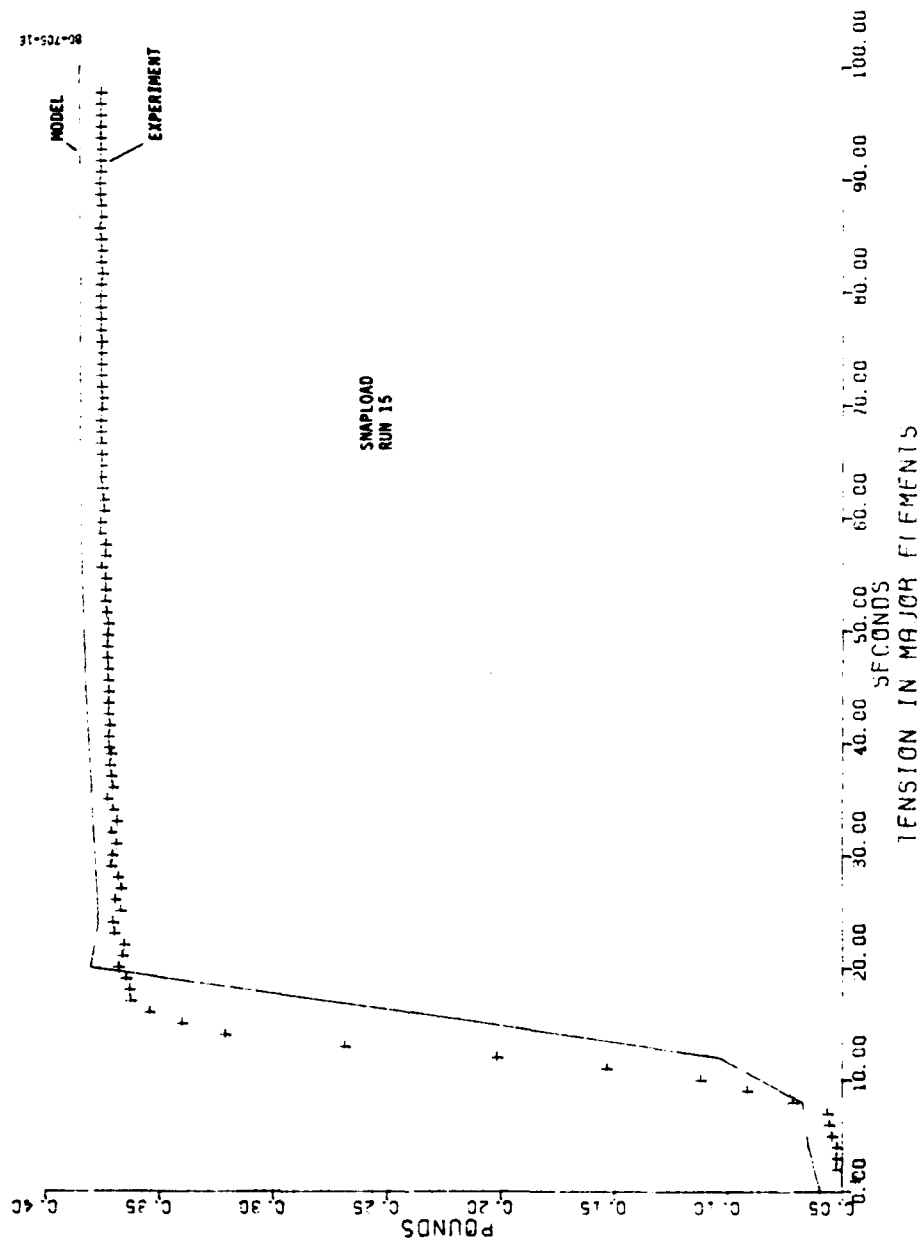
Figure 4-45. SNAPLOAD Tension History During Run 15

| NODAL POSITION (FT)	NODE	ELEMENT LENGTH (FT)	DIAMETER (IN)	WEIGHT (LB)	COMPONENTS
2323.6	22		44	-1046	SPHERE
		43.5	.375	1.55/FT	CHAIN
2280.2	21	26.5		59.7	PGR FVR T/P
2179.5	20				
2078.7	19				
1978.0	18				
1877.3	17	100.7	.39	.0537/FT.	WIRE ROPE
1776.6	16				
1675.8	15				
1575.1	14				
1474.4	13	25.8		50.0	PGR CHAIN FVR
1311.2	12	163.2	.39		
1148.0	11	11.5		19.9	T/P
997.6	10				
847.2	9	150.4	.39	.0537/FT.	WIRE ROPE
696.3	8	25.8		50.0	PGR CHAIN FVR
578.4	7				
459.8	6				
341.3	5	118.5	.39	.0537/FT.	WIRE ROPE
222.8	4				
104.3	3	47.0		-790.	SPHERE PGR FVR
		71.5	.375	1.55/FT.	CHAIN
32.8	2	54.3		-611.	SPHERE PGR 2 RELEASES
		32.8	.750	.017/FT.	NYLON
0	1	48.0		2600.	ANCHOR

Figure 4-46. The SEADYN Model of MDE Experiment Five

4-60

```
010  D.B. DILLON    ANALYSIS OF MDE EXPT 5 DEPLOYMENT USING SEADYN              PROBLEM TITLE
020  22  0     0   21   3        8   -1    1   1   3   0   0.                    MASTER CONTROL
030   2  1  32.1725  1.2872E-5  64.0394   0.   0.   2.1   1        2465.87       ENVIRONMENT
040   1  0    -0.00   0.   0.   0   0   1                                        ANCHOR NODE
050   2  0   -32.82   0.   0.   2.1   0   2   1                                  RELEASE NODE
060   3  0  -104.33   0.   0.   2.1   0   2   1                                  FWR-4 NODE
070   4  0  -222.83   0.   0.   2.1   0   2   1                                  WIRE NODE
080   5  0  -361.34   0.   0.   2.1   0   2   1                                  WIRE NODE
090   6  0  -459.84   0.   0.   2.1   0   2   1                                  WIRE NODE
100   7  0  -578.35   0.   0.   2.1   0   2   1                                  WIRE NODE
110   8  0  -696.85   0.   0.   2.1   0   2   1                                  FWR-3 NODE
120   9  0  -847.22   0.   0.   2.1   0   2   1                                  WIRE NODE
130  10  0  -997.59   0.   0.   2.1   0   2   1                                  WIRE NODE
140  11  0 -1147.96   0.   0.   2.1   0   2   1                                  T/P-5 NODE
150  12  0 -1311.18   0.   0.   2.1   0   2   1                                  WIRE NODE
160  13  0 -1474.40   0.   0.   2.1   0   2   1                                  FWR-2 NODE
170  14  0 -1575.12   0.   0.   2.1   0   2   1                                  WIRE NODE
180  15  0 -1575.84   0.   0.   2.1   0   2   1                                  WIRE NODE
190  16  0 -1776.56   0.   0.   2.1   0   2   1                                  WIRE NODE
200  17  0 -1877.29   0.   0.   2.1   0   2   1                                  WIRE NODE
210  18  0 -1978.01   0.   0.   2.1   0   2   1                                  WIRE NODE
220  19  0 -2078.73   0.   0.   2.1   0   2   1                                  WIRE NODE
230  20  0 -2179.45   0.   0.   2.1   0   2   1                                  WIRE NODE
240  21  0 -2280.17   0.   0.   2.1   0   2   1                                  FWR-1 NODE
250  22  0 -2323.64   0.   0.   0   2   1                                        SPHERE NODE
260   1  1    2   1   0  300.   2.1   0.   0                                     NYLON ELEMENT
270   2  2    3   2   0  300.   2.1   0.   0                                     CHAIN ELEMENT
280   3  3    4   3   0  300.   2.1   0.   0                                     WIRE ELEMENT
290  21 21   22   2   0  300.   2.1   0.   0                                     CHAIN ELEMENT
300   1  0  .0625     .017   1.   5   0                                          NYLON MATERIAL
310   4.     .001                                                               STRAIN 1-1
320  895.    .153                                                               STRAIN 1-2
330 1640.    .230                                                               STRAIN 1-3
340 4250.    .305                                                               STRAIN 1-4
350 6860.    .340                                                               STRAIN 1-5
```

Figure 4-47.   SEADYN Input Data Deck

Figure 4-47.   SEADYN Input Data Deck (Continued)

Line										Label
360	2	1							1	CHAIN MATERIAL
370	1.26E+6	1.	2.743	2.				2.1		STRAIN 2-1
380	3	0	.0325	1.	.05374			2.1		WIRE MATERIAL
390	3.44E+5	2	1.							STRAIN 3-1
400	1	-2600.	4.0	0.	0	0.	0.	0.7	1	ANCHOR SPECS
410	2	7.354	0.	1.0001	1			0.		EXTRA SPECS
420	2	511.1	4.562	0.	0	0	0.	0.7	1	RELEASE SPECS
430	0.	2.568	0.	1.0001	0			0.		EXTRA SPECS
440	3	790.3	3.917	0.	0	0	0.	0.6	1	FVR-4 SPECS
450	0.	7.051	0.	1.0001	0			0.		EXTRA SPECS
460	8	-49.95	2.149	0.	0	0	0.	0.7	1	FVR-3 SPECS
470	0.	2.123	0.	1.0001	0			0.		EXTRA SPECS
480	0	-19.92	0.958	0.	0	0	0.	0.6	1	T/P-5 SPECS
490	0.	0.270	0.	1.0001	0			0.		EXTRA SPECS
500	2	-49.95	2.149	0.	0	0	0.	0.7	1	FVR-2 SPECS
510	0.	2.123	0.	1.0001	0			0.		EXTRA SPECS
520	2	-59.75	2.210	0.	0	0	0.	0.6	1	FVR-1 SPECS
530	0.	2.245	0.	1.0001	0			0.		EXTRA SPECS
540	0	1046.2	3.667	0.	0	0	0.	0.6	1	SPHERE SPECS
550	0.	3.960	2.	1.0001	0			0.		EXTRA SPECS
560	LIVE	1	0	0		0	200	20	3	SUBANALYSIS
570	0.1	4	1	-2		-1	.5			SOLUTION
580	-5.483	.0001	.0001	1.						CURRENT
590	1	0.	0.							FIX ANCHOR-X
600	1	0.	1							FIX ANCHOR-Y
610	2	0.	1							FIX RELEASE-Y
620	3	0.	1							FIX FVR 4-Y
630	22	0.	1							FIX SPHERE-Y
640	DYN	1	5	0	0	0	1	-1	5	SUBANALYSIS
650	.01	-.0001	-.0001	0.	.08333333		2.	2.1		SOLUTION
660	.005	.5	10.	.5	.08333333		2.	2.1	10.1	TIME DATA
670	5.483	0.	0.						8	INITIAL VELOCITY
680	END	1	2	3	4	5	6	7		
690	123456789012345678901234567890123456789012345678901234567890123456789012345678901234567890123456789012									

4-62

TIME (SECONDS AFTER ANCHOR RELEASE)

120   180
0 30 60 90   150   240   300   360   540 WATER SURFACE   0*

4.00

8.00

FEET *10²

12.00

*SECONDS AFTER ANCHOR RELEASE

420 480

16.00

20.00

24.00

28.00

-24.00   -20.00   -16.00   -12.00   -8.00   -4.00   0.00
FEET *10²

0*
30
60
90
120
150
180
240
300
360
420
480
540

OCEAN BOTTOM

Figure 4-48.   Cable Shape at Selected Times

4-63

acceleration or velocity could introduce increasingly erroneous positions for the system. Even though no experimental data are plotted on Figure 4-48, it connotes a verification of the internal consistency of the model.

4.3.2 TRAJECTORY COMPARISONS. Figure 4-49 shows the paths taken by major nodes during the deployment. The trajectories should be viewed individually; viewed collectively, they can be confusing. Start with the anchor at node one. Upon release it swings under the recovery buoys, pulling them under one after the other, then plummets straight down the right margin of the plot until the main buoy pulls under, when the anchor begins to swing to the left. Finally, it impacts on the bottom at a depth of 2465 feet.

FVR 4 at node three coasts a moment after release, then is jerked under by the anchor and plummets down with it.

FVR 3 at node eight, the temperature/pressure (T/P) sensor at node 11, and FVR 2 at node 13 all coast a little while, then are pulled down in sweeping arcs following the "water pulley" principle (the drag on a cable perpendicular to it is much greater than the drag tangent to the cable. When a cable is pulled sideways in the water, it tends to bend as if the water were a great pulley wheel. The cable tends to pull "around the corner" more than it "cuts across" the corner). After the anchor hits bottom these three nodes abruptly stop falling and swing on arcs about the anchor as fixed point.

FVR 1 at node 21 and the main buoy at node 22 are towed along under or on the surface while the rest of the cable goes around the "water pulley". Then the anchor pulls the main buoy under, and shortly thereafter impacts. These nodes then pivot up and to the right about the anchor.

Figure 4-50 is a duplicate of Figure 4-49 with locations of the nodes measured during the MDE superimposed. It is easy to see the triangle symbols (pinger ECHO) closely paralleling the trajectory of node 21. The circle symbols (pinger ALPHA) follow node three behind the anchor. The square symbols (pinger DELTA) loosely follow node eight. The hexagons (pinger CHARLIE) clearly follow node 13.

4.3.3. TENSION COMPARISONS. Figures 4-51 through 4-54 show the calculated tension superimposed on Figures 2-27 through 2-30. The resemblance is striking, except for the large oscillations of tension. The large tension pulse produced by the anchor impact is shown on Figures 2-27 through 2-30 to have decayed fully within 30 seconds; one may infer that other inputs decay in a like time. Therefore, the tension oscillations on those plots are primarily due to continuous excitation, namely the action of ocean waves.

The SEADYN model contained no simulation of wave action. One would therefore expect smooth tension traces with discrete perturbations lasting about 30 seconds coincident with anchor release, anchor impact, and perhaps the immersion of the
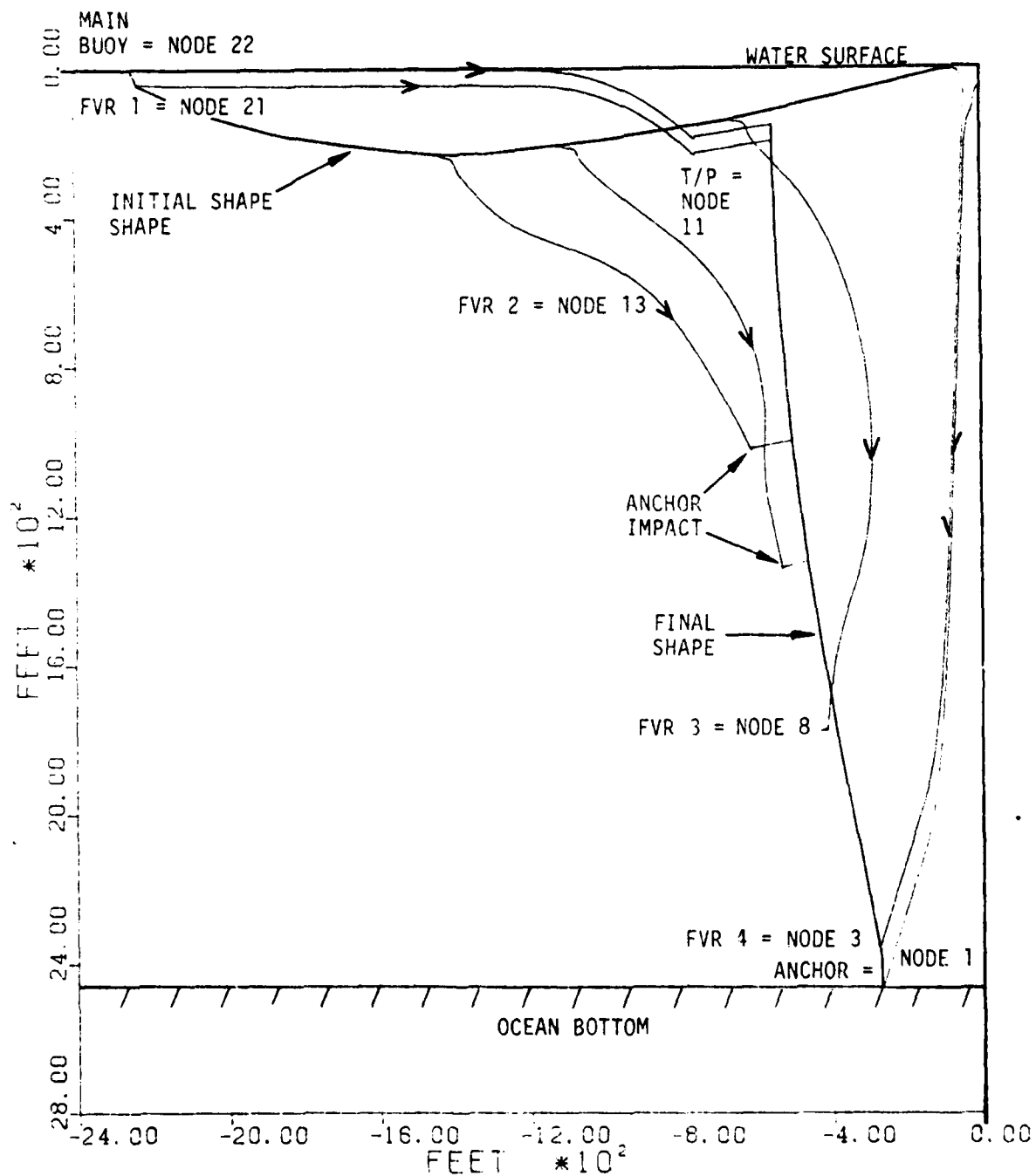
Figure 4-49. Modeled Trajectories of Major Nodes

4-65
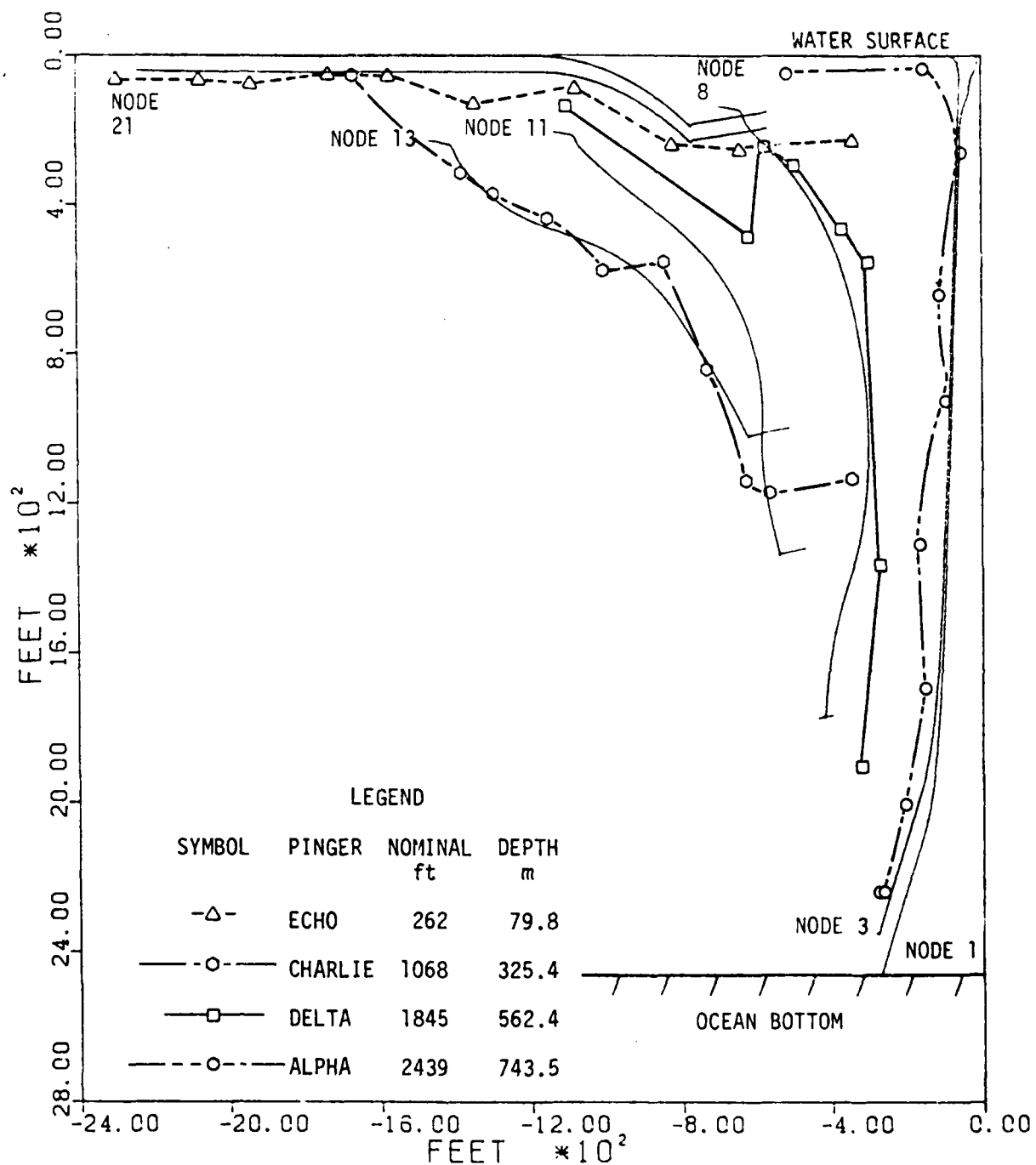
Figure 4-50.   Trajectories of Major Nodes (Composite)

4-66
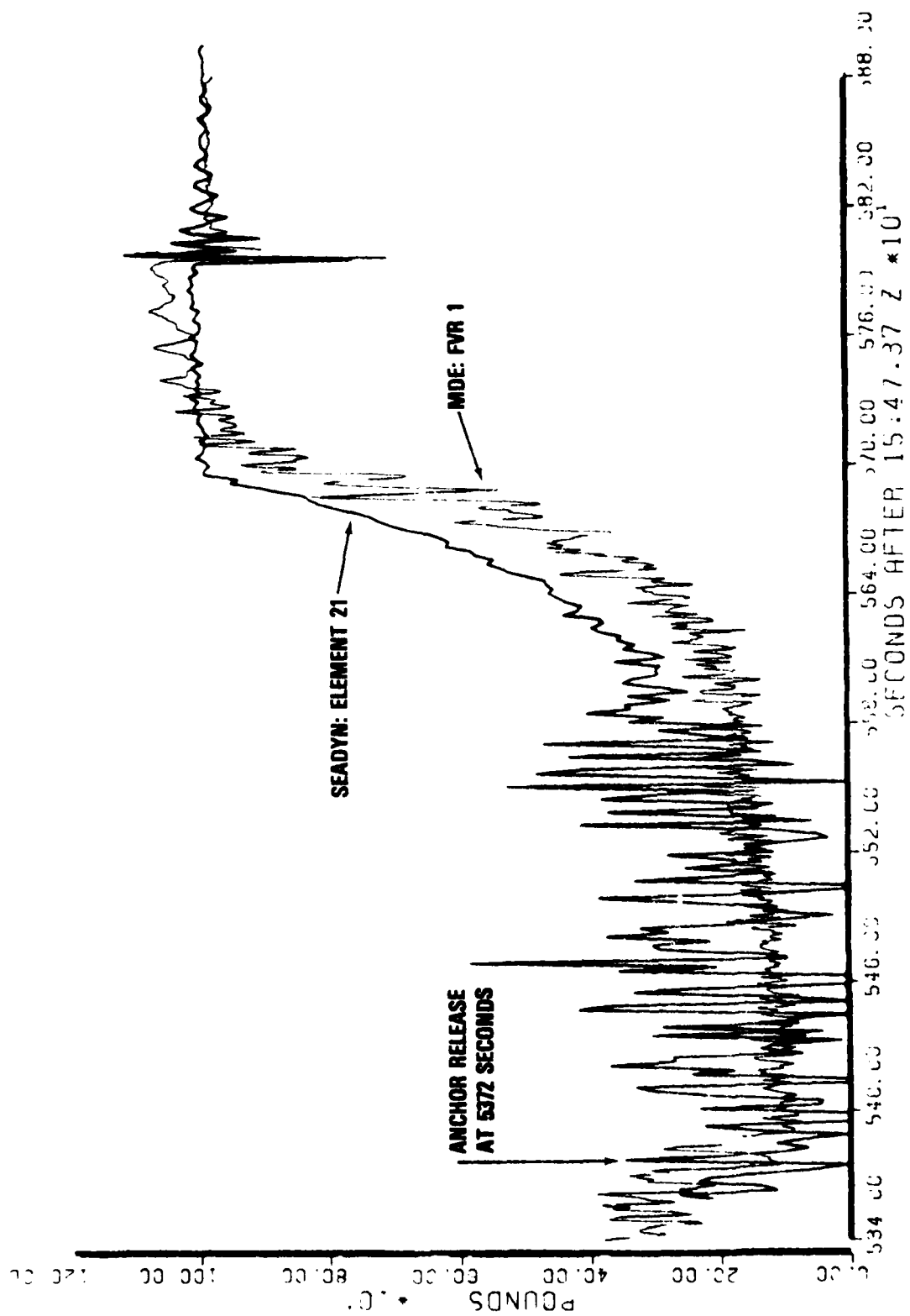
Figure 4-51. Tension Comparison For FVR 1
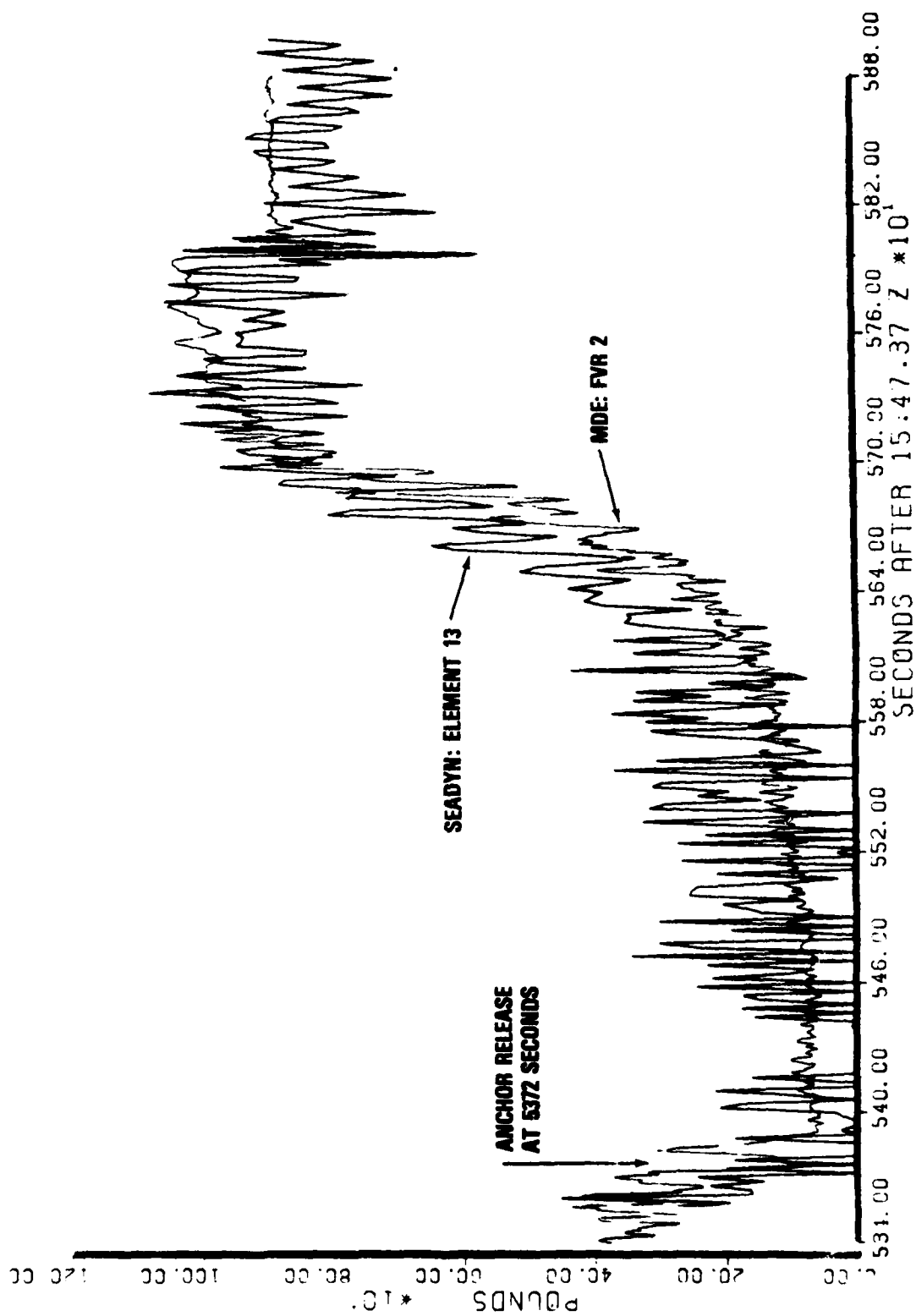
Figure 4-52. Tension Comparison For FVR 2
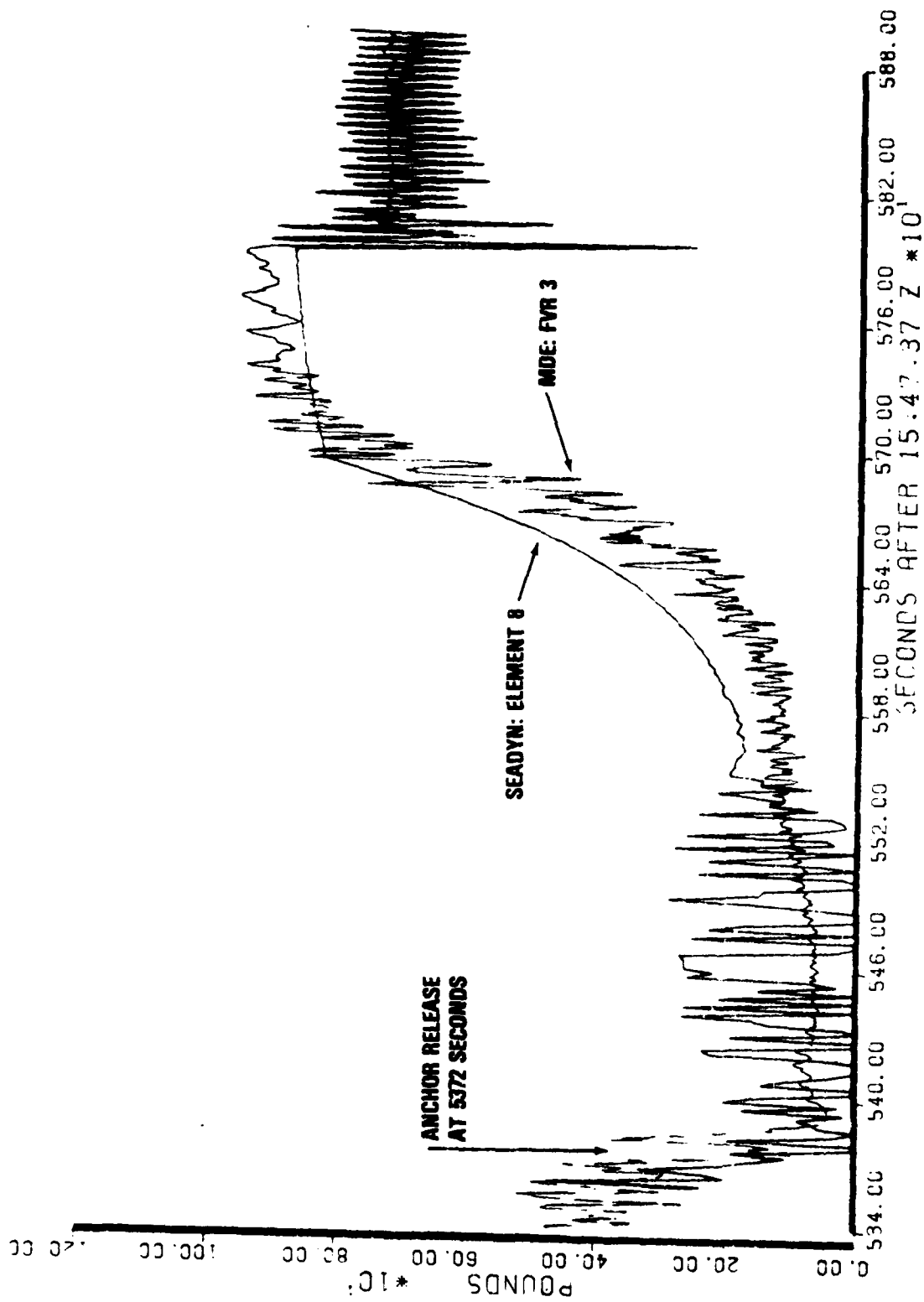
Figure 4-53. Tension Comparison For FVR 3
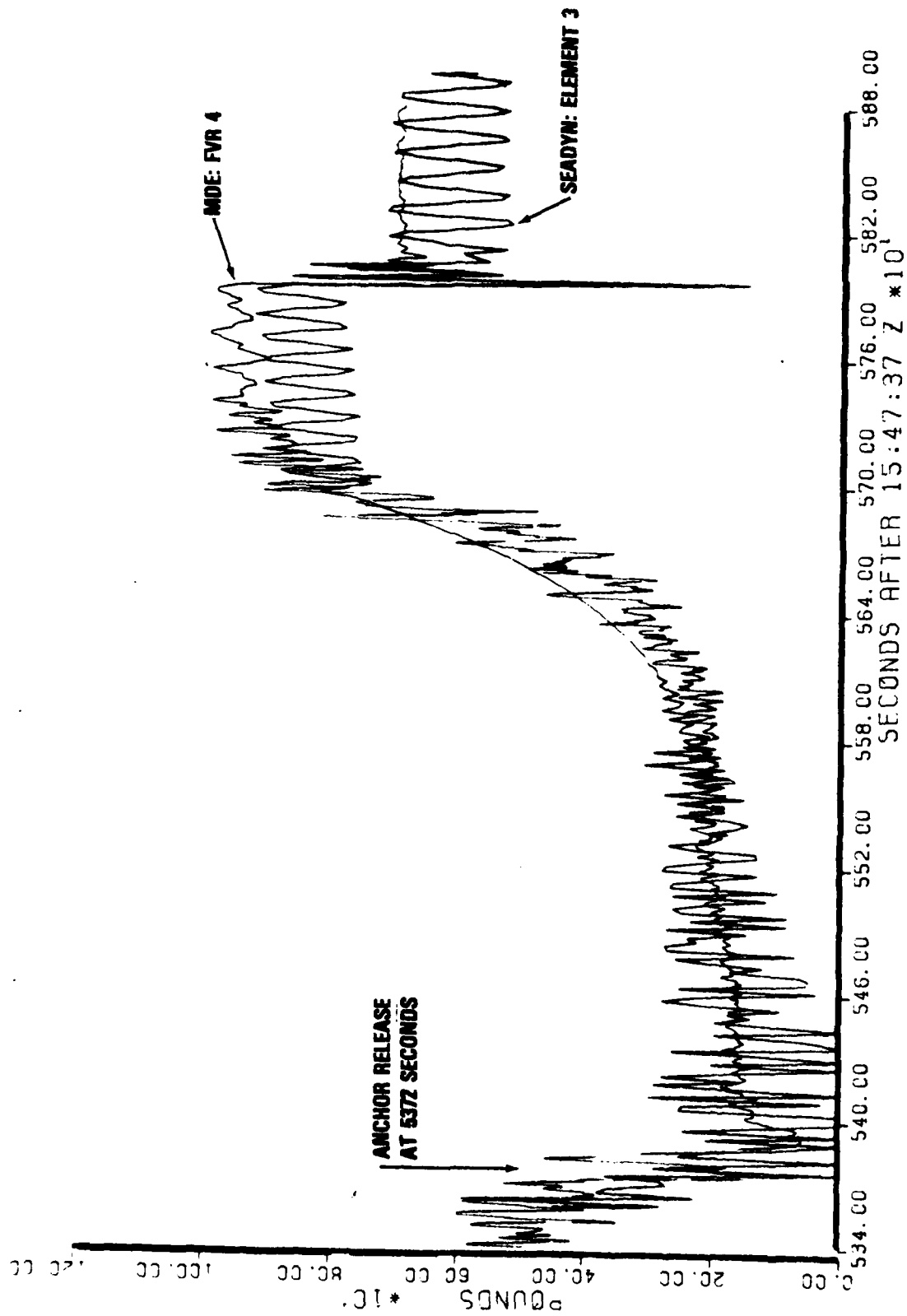
Figure 4-54. Tension Comparison For FVR 4

main buoy. This is found to be the case for some elements some of the time: element eight from about 3.5 to 7 minutes after anchor release, for example, on Figure 4-53. The large, undamped oscillations of tension shown on Figures 4-51 through 4-54 (especially Figure 4-52) are artifacts of the undamped SEADYN model.

These oscillations represent the resonant exchange of elastic energy between adjacent elements. This energy is dissipated in nature by material damping, i.e., hysteresis in the stress-strain curve of the element material. The SEADYN algorithm did not include material hysteresis when this comparison was performed.

The drag coefficient of the anchor and buoys was calculated (Appendix A) as part of the input model to produce terminal velocities equal to those measured in MDE, so the time from release to impact is, not surprisingly, nearly equal for the model and experiment.

However, the beginning and duration of sub-events may be usefully compared, after aligning the impact pulse. For example, both data and model indicate that a very low tension occurs 16 to 18 seconds after anchor release. Figure 2-29 shows the main buoy pulled under 97 seconds before impact. This is marked by the change from large, wave-induced tension pulses to smaller double pulses after immersion (tension waves echoing off the massive main buoy). Buoy immersion is shown as 96 seconds before impact on Figure 4-52 from the SEADYN results.

The post-impact "ringing" had a 4-second period, as shown on the FVR plots in Section 2. The corresponding plots in this section show a period of about 4.5 seconds for the first few oscillations after impact. This "ringing" dies out after 3-4 cycles on the FVR plots and either dies out or is replaced by a spurious oscillation on the SEADYN plots within four cycles of impact.

At the start of the anchor drop the vertical force exerted by the falling anchor is turned by the "water sheave" principle into a roughly horizontal force on the main buoy. The tension is defined primarily by the hydrodynamic drag tangent to the cable and nodes. But as the anchor falls deeper and the water sheave is worn away, the cable tends more and more towards the vertical. The main buoy is pulled deeper in the water until it comes awash and submerges. Both model and data reflect this smooth increase in tension followed by a period of roughly constant tension until the anchor impacts on the bottom.

4.4 VARIABLE LENGTH COMPARISONS.

A schematic diagram of the variable length experiment was sketched in Figure 2-16. Ninety-seven runs were performed using various combinations of an oscillation frequency and payout/reel-in rates. Two material types were used, an inelastic nylon line and a plastic rubber cord.

The two models, SEADYN and SNAPLOAD, are compared to the data by examining the tension vs time plots for each run. Tension was measured at the top node (payout/oscillation point). Visual scans of the output were made to check that the bottom node position appeared reasonable. Direct comparisons are not possible since the anchor position was not tracked during the experiment. Reference 15 describes the comparison of SNAPLOAD and SEADYN to the variable length experiment data in detail.

Appendix B lists the data input decks for each run. SEADYN used a standard node spacing of 5 feet for all runs. The SNAPLOAD spacing was adjusted to accommodate modeling deficiencies in the program. Very long segments were used with SNAPLOAD in order to avoid inserting nodes during payout.

In the actual experiment the oscillator was about 2 feet above the water surface. Neither program could model this set-up exactly so the approximation was made that the entire cable was underwater. The difference in total drag and weight of the cable/anchor system due to this approximation is insignificant.

Elasticity tests gave two tension/strain curves for nylon, one for loading and one for unloading. Neither curve seemed appropriate for SEADYN when the resonance peaks were compared with both payout and reel-in runs. A stiffness (EA) value of 133 lb was then computed for Run 23 by assuming resonance at 2.5 Hz and applying the formula for the natural period of a mass on a spring. This effective value gave good results for other runs, both payout and reel-in, and was within the experimentally determined range of 100 to 200 lb.

The nylon material damping was also adjusted to better correlate SEADYN with the data. The damping was increased to 1.0 lb-sec from a predetermined value of 0.05 lb-sec.

SNAPLOAD does not model material damping. Mathematical damping was eliminated by setting the artifical damping factor, DMAX, equal to 0.0001, and the ramp limit, TDE, to 99999. The smooth results were obtained using exceptionally small error limits: ABEBD = RGEBD = 0.0001. SNAPLOAD relies on hydrodynamic damping to limit resonant response.

All SEADYN runs ran to conclusion. SNAPLOAD encountered certain difficulties during Runs 12, 47 and 48. Run 12 is a reel-in run and it was discovered that SNAPLOAD stops when only two cable segments remain underwater. Since the run was two-thirds complete, it was not rerun.

During the SNAPLOAD model of Run 47, the time step decreased to a very small value. The program continued to execute until the computer time allotted was exhausted but the model time barely changed. SNAPLOAD does not limit the number of times the time step is decreased, so it is possible to waste computer resources on ineffective computation.

The SNAPLOAD code does not allow element strains greater than 0.5. Modeling Run 48 aborted when the soft rubber exceeded this limit.

4.4.1 <u>RUN 3</u>. Run 3 is a nylon payout without oscillation. Figure 4-55 is a ten-sion vs time plot of the SEADYN model and the data. Figure 4-56 is the correspond-ing SNAPLOAD plot. The SNAPLOAD plot contains anamolous spikes that represent instantaneous numerical instabilities in the program, perhaps due to too large a time step or error tolerance. SEADYN produces a smooth curve for the entire run. Previous experience using SEADYN without material damping resulted in tension plots containing many undamped oscillations. Tiny steps are visible on Figure 4-55 when SEADYN inserted nodes for the payout.

Both models almost identically reproduce the data. Both models have a slight tension offset of about 0.05 pound. This could be caused by drag modeling deficiencies in the models, an error in measuring payout rate, or simply a data collection error for the tension.

The first four and final six seconds of the run represent a cable accelera-tion and deceleration. SEADYN appears overdamped at the beginning and underdamped near the end. SNAPLOAD exhibits good initial transient response but is under-damped at the end.

4.4.2 <u>RUN 23</u>. Run 23 is a nylon payout with oscillation. Figures 4-57 and 4-58 show the corresponding plots. The data show an increase in peak to peak tension near the time at which the natural frequency of the cable/anchor system approached the oscillating frequency.

Both models exhibit this resonance near the proper time; the SNAPLOAD model peak is displaced by about 1.5 seconds. SNAPLOAD is slightly underdamped at reso-nance. The two models produce almost identical transient responses at the end of the run. Both models underpredict this response, perhaps due to incorrect damping at this point.

4.4.3 <u>RUN 12</u>. Run 12 is a nylon reel-in with oscillation. Figures 4-59 and 4-60 show the corresponding plots. SNAPLOAD terminated at the point where only two cable segments remained in the water. Up to this point the results of both SEADYN and SNAPLOAD are in excellent agreement with the data. The SNAPLOAD phase is offset slightly since SNAPLOAD does not allow for an initial phase shift in the input data.

SEADYN models the transient portion at the end of the run well, picking up the negative peak at 24.5 seconds. The SEADYN response perhaps is slightly under-damped towards the end of the run.

4.4.4 <u>RUN 29</u>. Run 29 is a rubber payout with no oscillation. Figures 4-61 and 4-62 show the corresponding plots. The SEADYN curve contains small discontinui-ties that represent cable tension interpolations at node insertions (mitosis points). These "steps", though small, are much larger than those noted on Fig-ure 4-55. An error has subsequently been corrected in the SEADYN code. Both models follow the transient shape at the beginning and end of the run with over-prediction in both models.
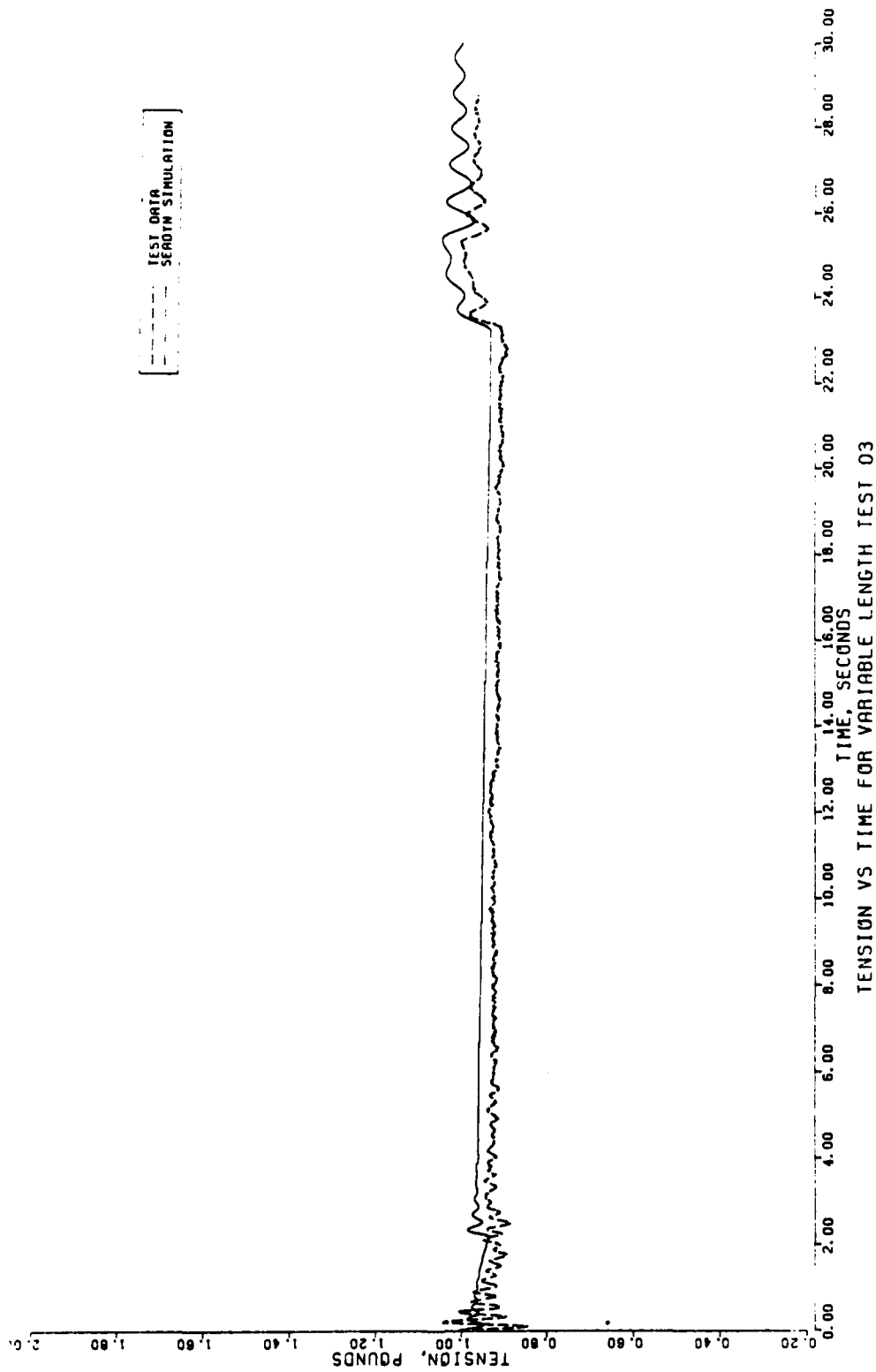
Figure 4-55. Tension Vs Time For Variable Length Test 03 (SEADYN)
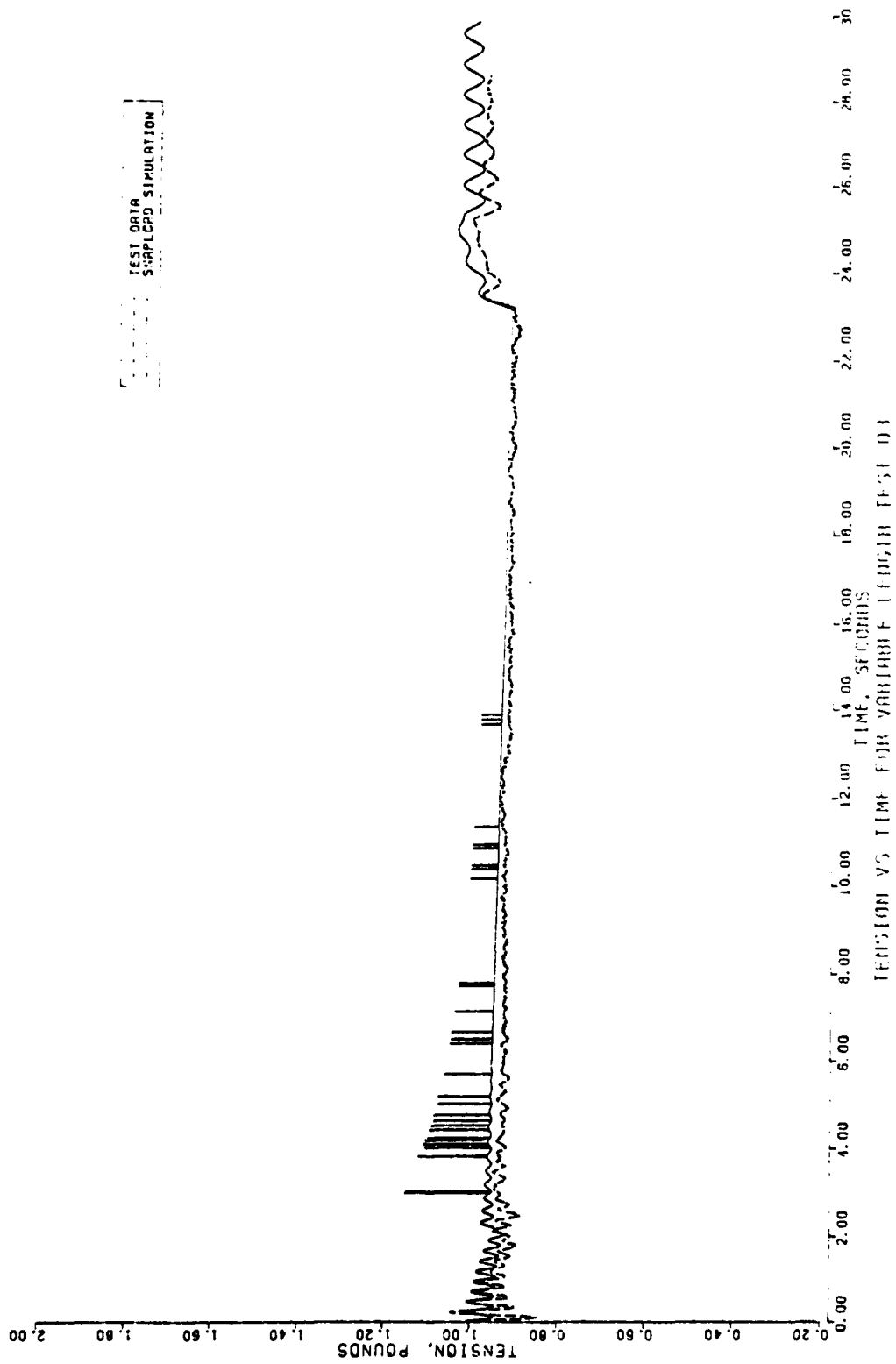
Figure 4-56. Tension Vs Time For Variable Length Test 03 (SNAPLOAD)

4-75
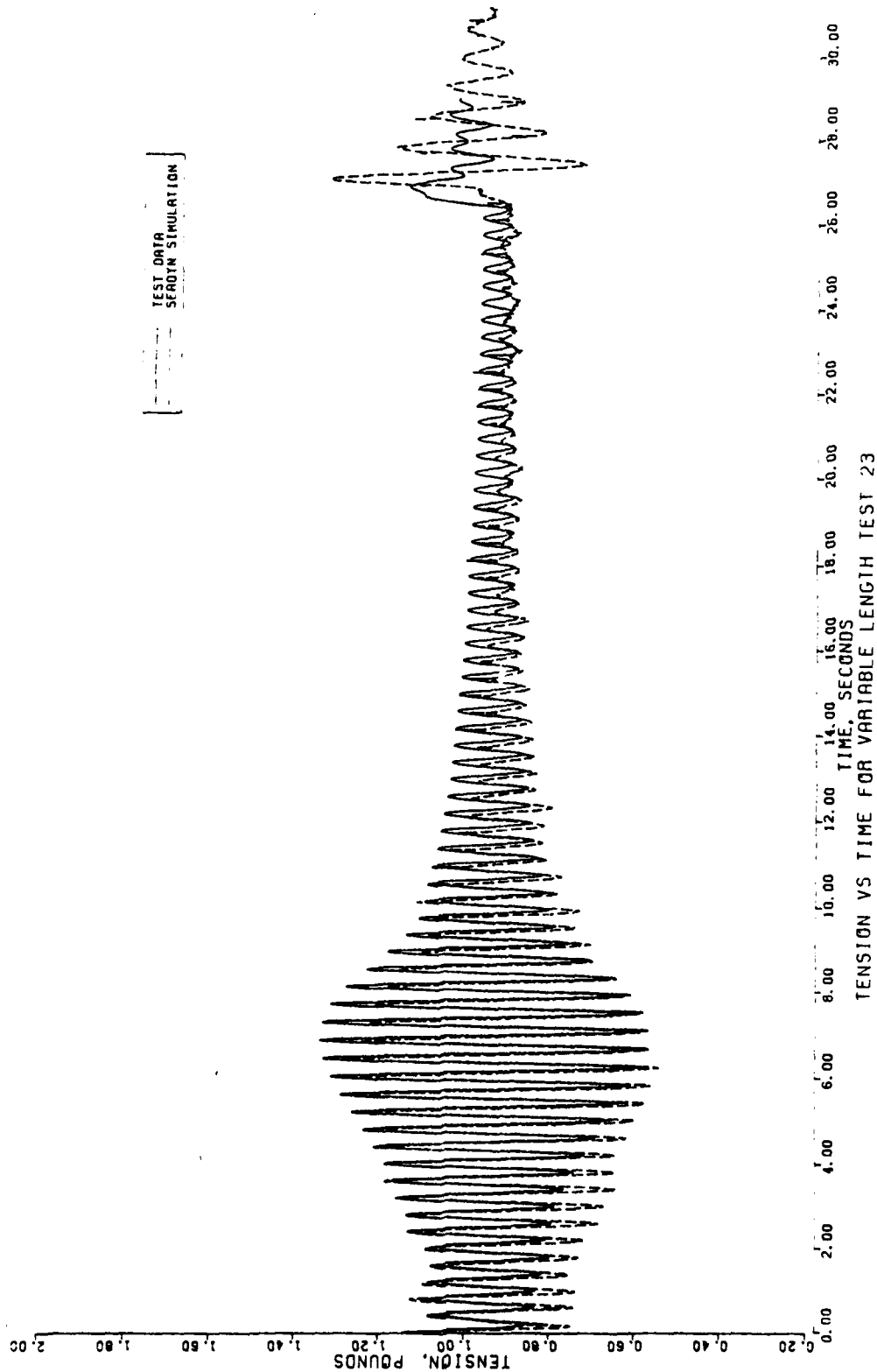
Figure 4-57. Tension Vs Time For Variable Length Test 23 (SEADYN)

4-76
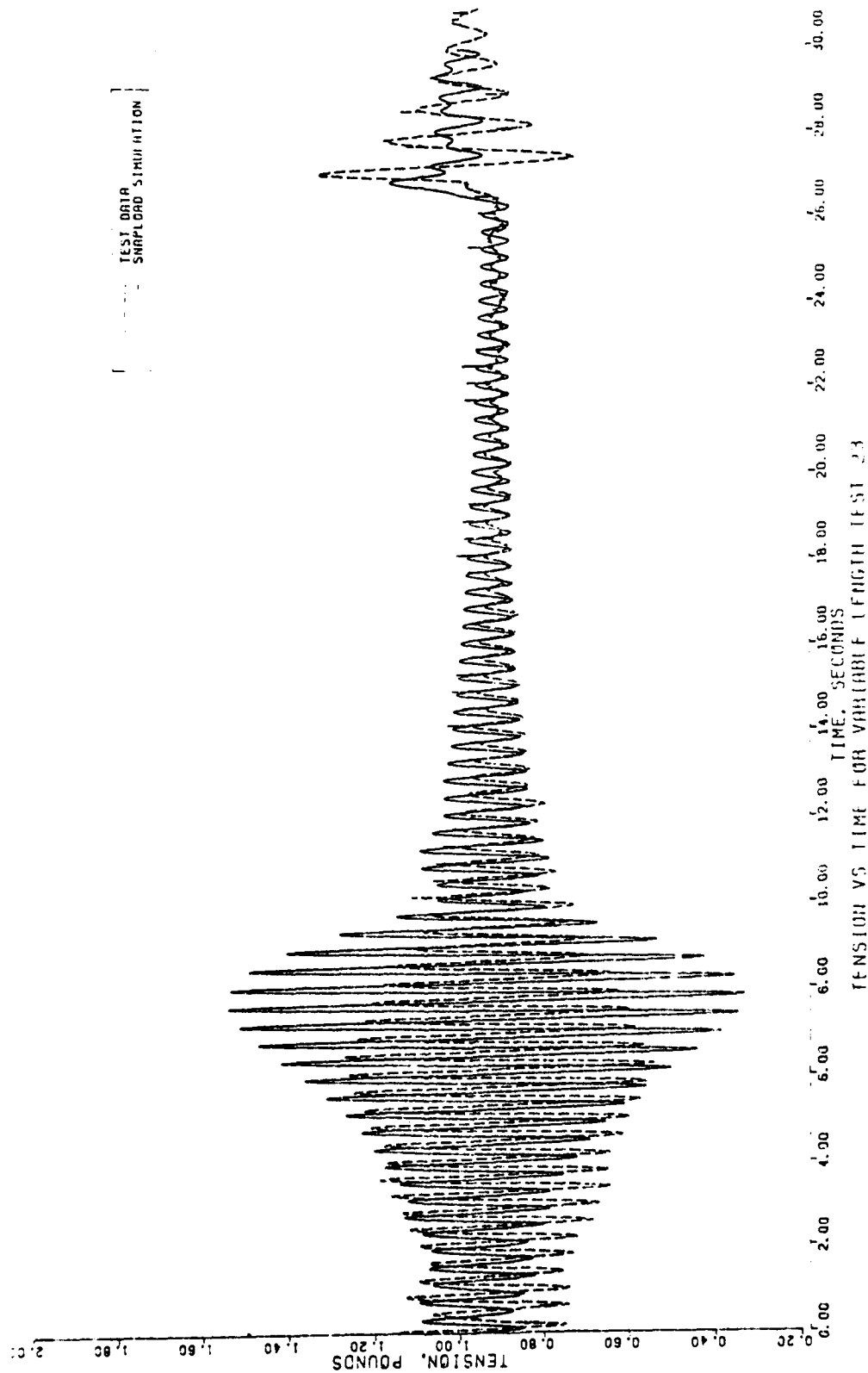
Figure 4-58. Tension Vs Time For Variable Length Test 23 (SNAPLOAD)
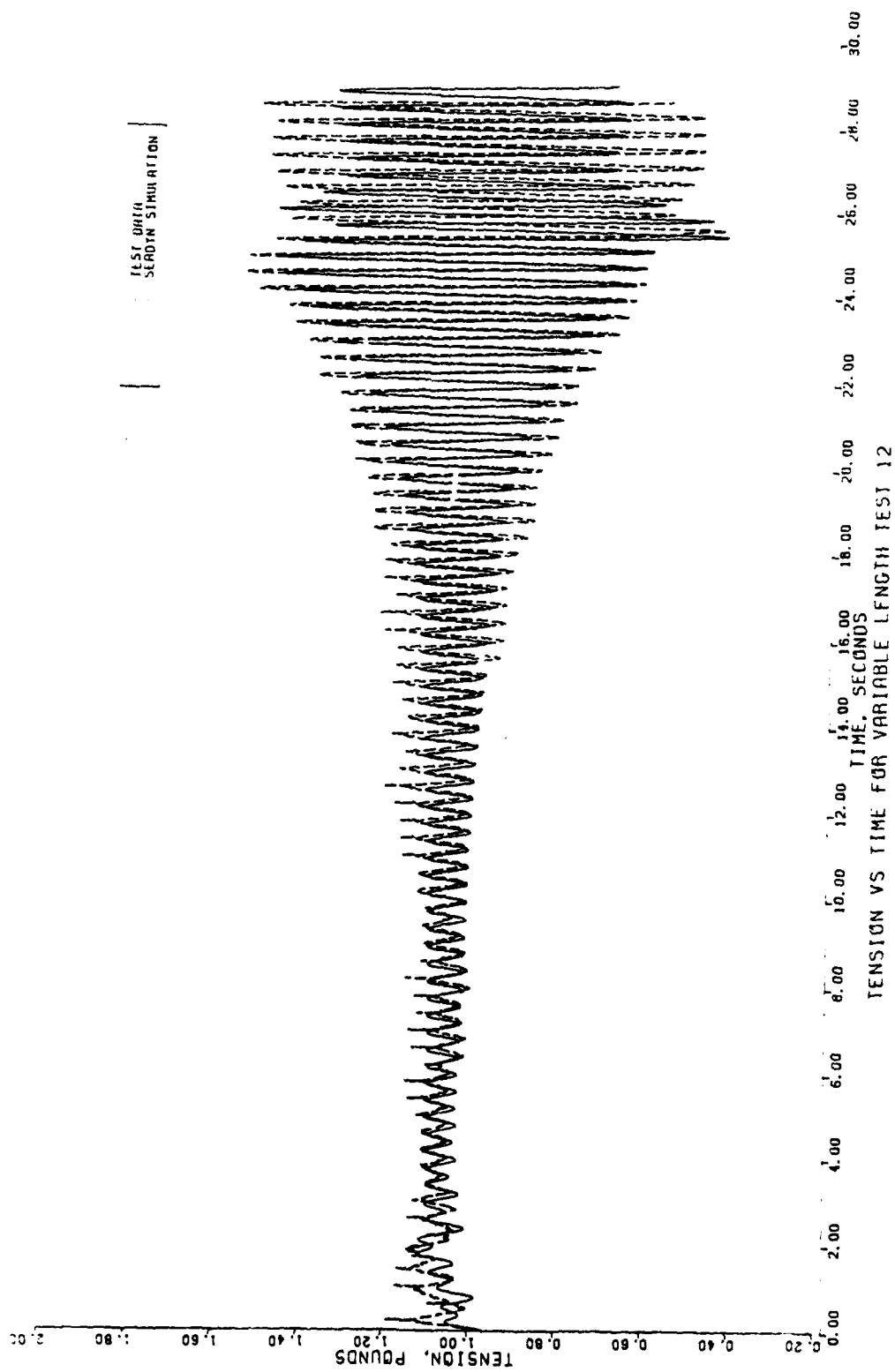
Figure 4-59. Tension Vs Time For Variable Length Test 12 (SEADYN)

TENSION VS TIME FOR VARIABLE LENGTH TEST 12

TIME, SECONDS

TENSION, POUNDS

TEST DATA
SEADYN SIMULATION

4-78
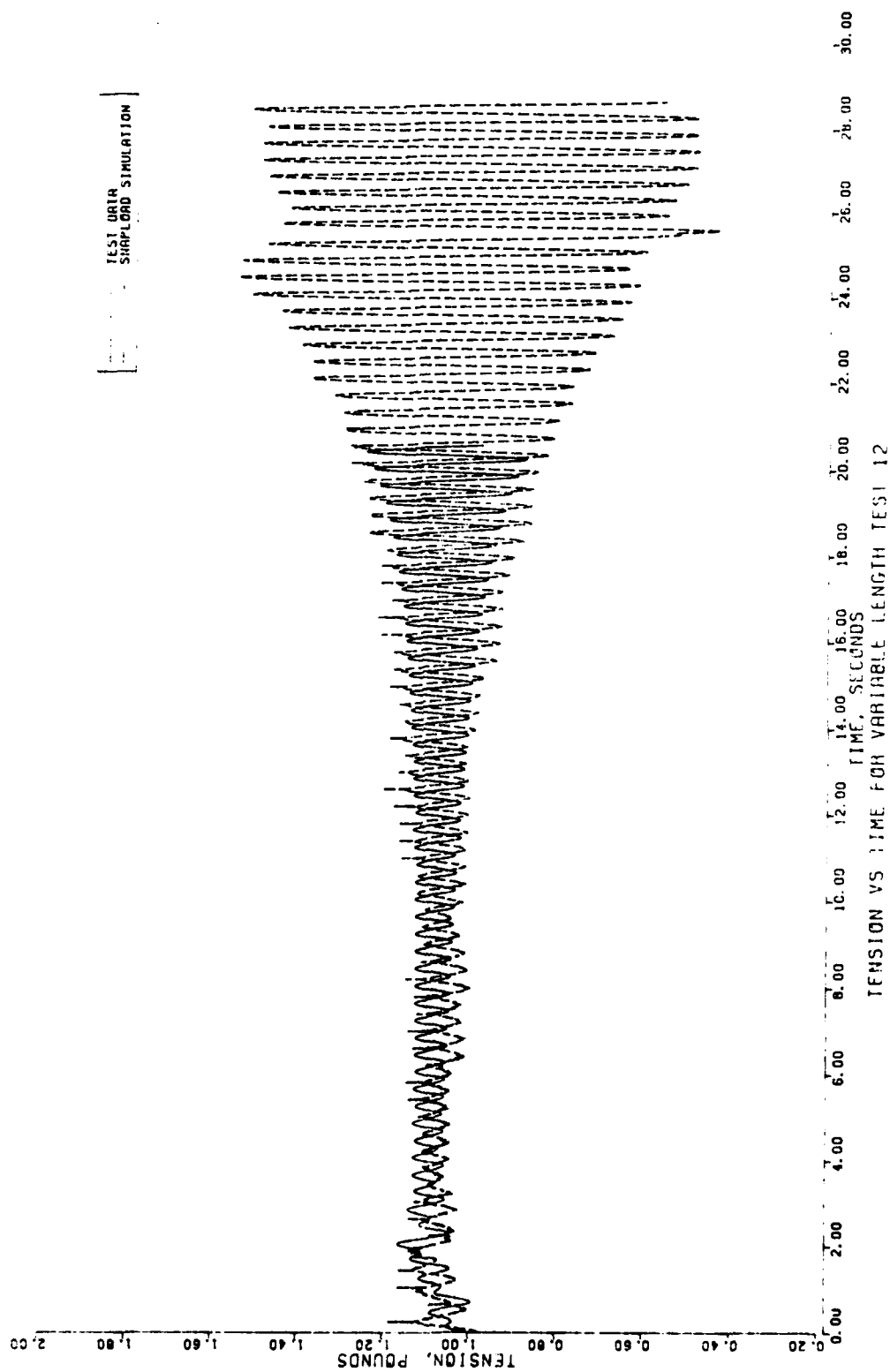
Figure 4-60. Tension Vs Time For Variable Length Test 12 (SNAPLOAD)
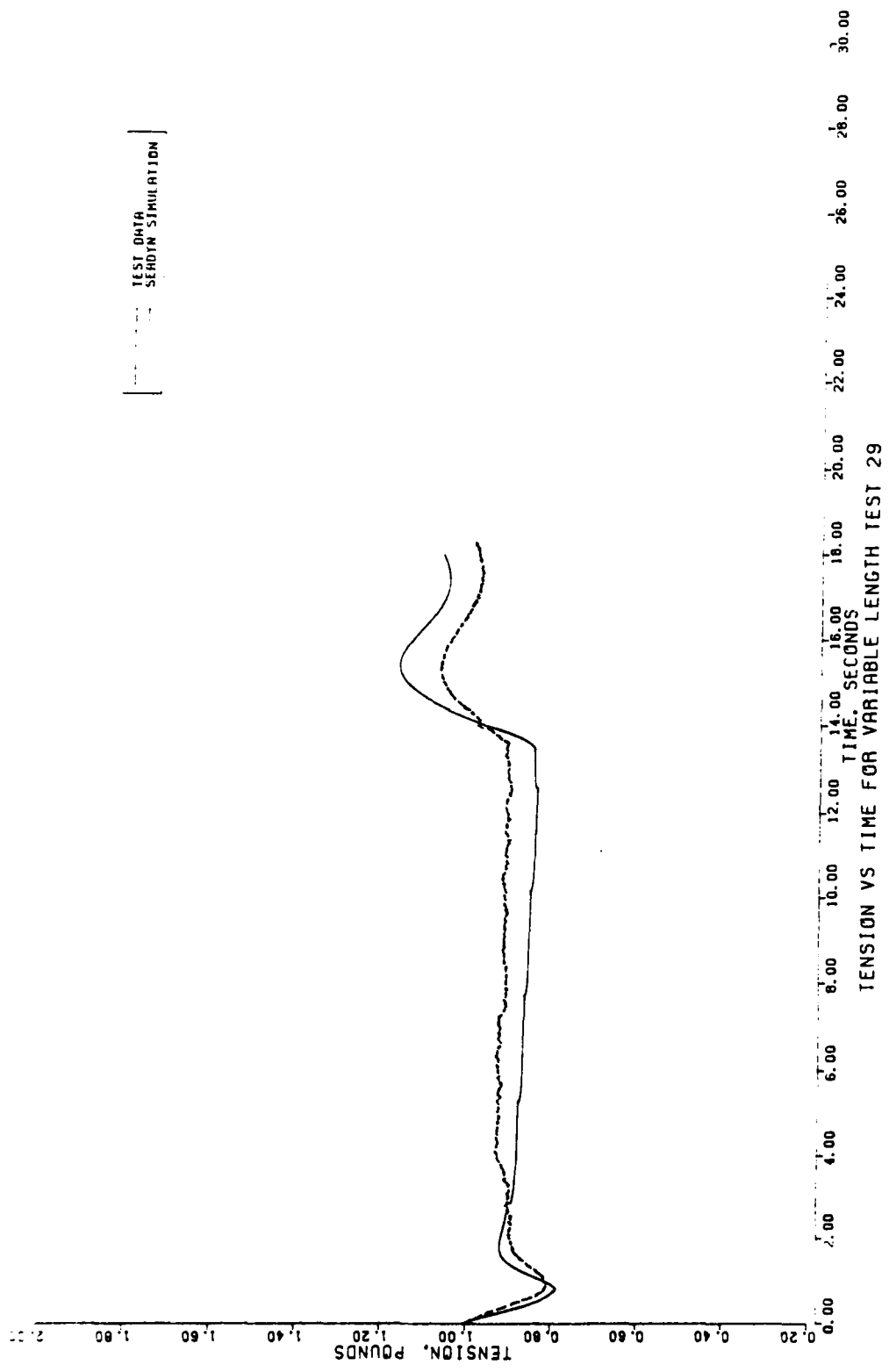
Figure 4-61. Tension Vs Time For Variable Length Test 29 (SEADYN)

4-80
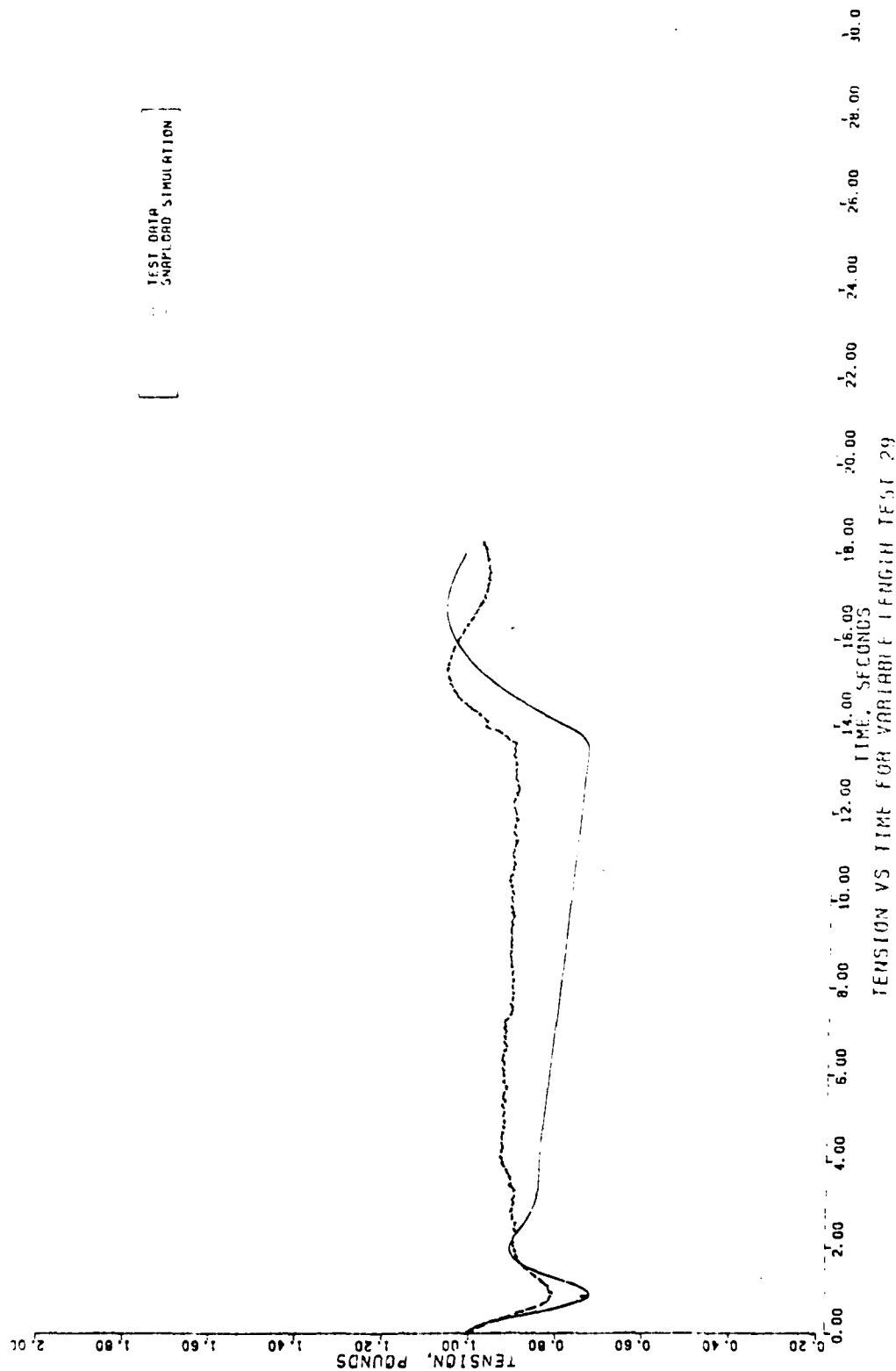
Figure 4-62. Tension Vs Time For Variable Length Test 29 (SNAPLOAD)

Both models show a tension/time slope in the constant velocity portion of the run. The SNAPLOAD slope is about twice that of the SEADYN slope. This slope is caused by the frictional drag on the cable; as more cable enters the water the frictional drag increases. The SNAPLOAD frictional drag coefficient is programmed as a fixed 0.025 while SEADYN uses a default value of about 0.018. Both values are above the normal range of 0.002-0.008, introducing an increasing error as cable is paid out.

Subsequent analysis of the nylon run showed the same trend, although it was not as evident since the nylon cable diameter was less than the rubber diameter.

4.4.5 <u>RUN 47.</u> Run 47 is a rubber payout with oscillation. Figures 4-63 and 4-64 show the corresponding plots. Again, the effect of the frictional drag error is evident. Discounting this error, both models give a good approximation of the data. SNAPLOAD did not complete the run within the allotted time.

Both models appear to underdamp the initial transient and overdamp the final transient. SNAPLOAD also overdamps the final half of the constant velocity portion. No explanation was determined for this difference in response. SEADYN models both the high frequency excitation and the low, natural frequency after the winch was braked. The modeling of the high frequency tension amplitude runs counter to the data when the two frequencies are superposed. The data show an increase in high frequency tension amplitude after the winch stops (from 0.06 lb before braking to 0.08 lb peak to peak after braking). SEADYN is virtually exact before braking, but models the tension as decreasing, instead of increasing, to 0.03 lb after braking. Ironically, this minor discrepancy suggests slightly excess material damping.

4.4.6 <u>RUN 48.</u> Run 48 is a rubber reel-in with oscillation. Figure 4-65 shows the SEADYN plot of this run. SNAPLOAD aborted Run 48 when the strain exceeded 0.5. Except for the frictional drag error, the SEADYN simulation is quite good. The transients appear overdamped at the beginning and underdamped near the end, but the trends exactly follow the data.

4.4.7 <u>SUMMARY OF VARIABLE LENGTH COMPARISONS.</u> SEADYN modeled the characteristic response of all runs accurately. Minor difficulties pertain to damping in the transient range, small time step sizes required by node mitosis, and a possible frictional drag coefficient error. The most striking results of these runs is seen when the SEADYN results are compared with the plots of modeled tension for the earlier experiments. The addition of material damping has eliminated the large tension abberrations that marred the earlier modeling, a significant improvement. Overdamping or underdamping occurred frequently because the material damping parameter was only crudely estimated.

SNAPLOAD could model some runs accurately, but the frictional drag coefficient error is significant. One run stopped due to an insufficient number of segments remaining in the water. A rerun with additional segments presumably would work. SNAPLOAD will not model cables in which the strain is greater than 0.5. Without artificial or material damping, overdamping or underdamping occur frequently. The excessive tangential cable drag coefficient replaces some of the lost damping. Tension spikes occurred during one run, possibly due to an improper error tolerance. The most serious problem was the failure of SNAPLOAD to abort an ineffective run.

4-83
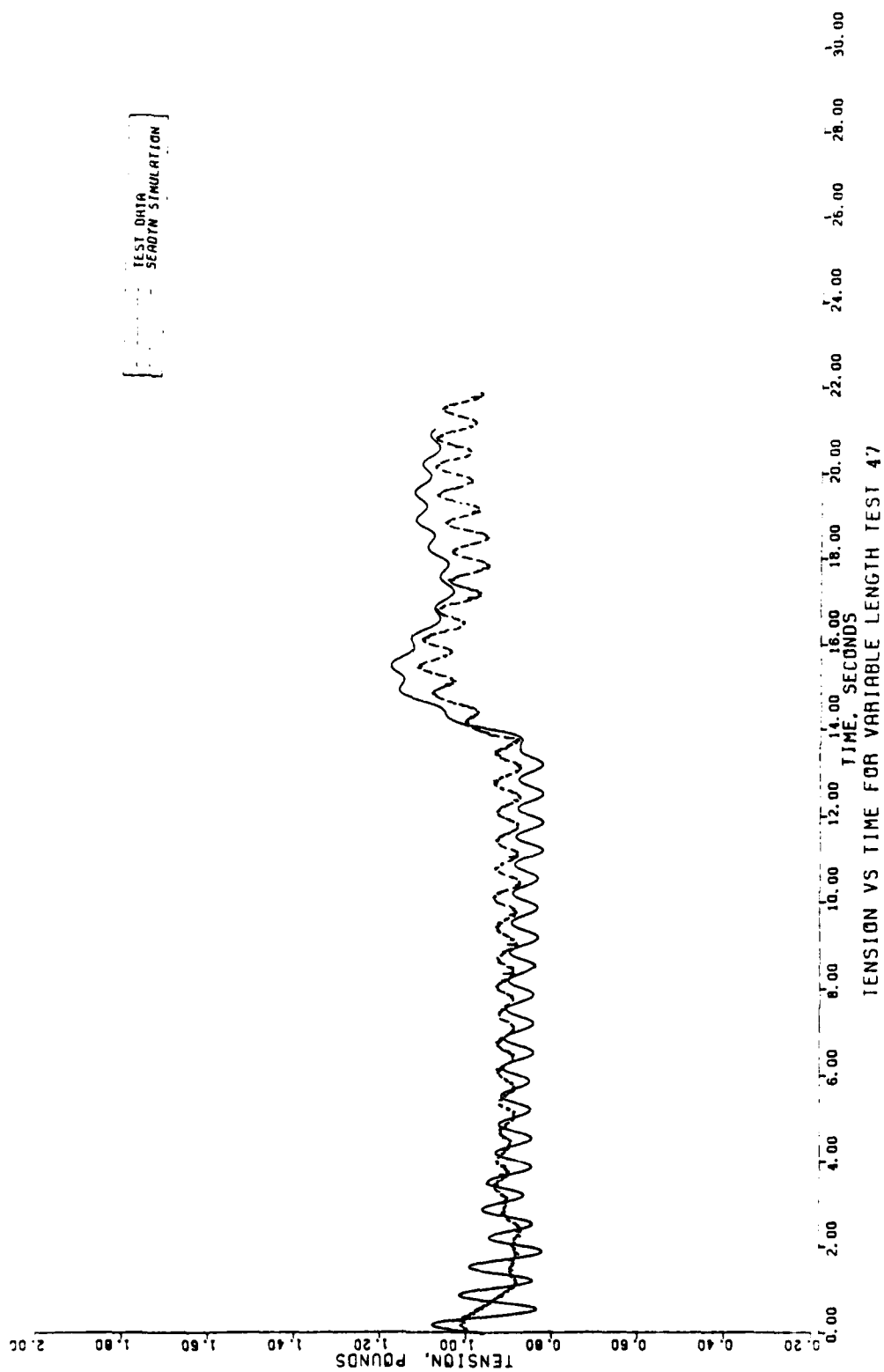
Figure 4-63. Tension Vs Time For Variable Length Test 47 (SEADYN)
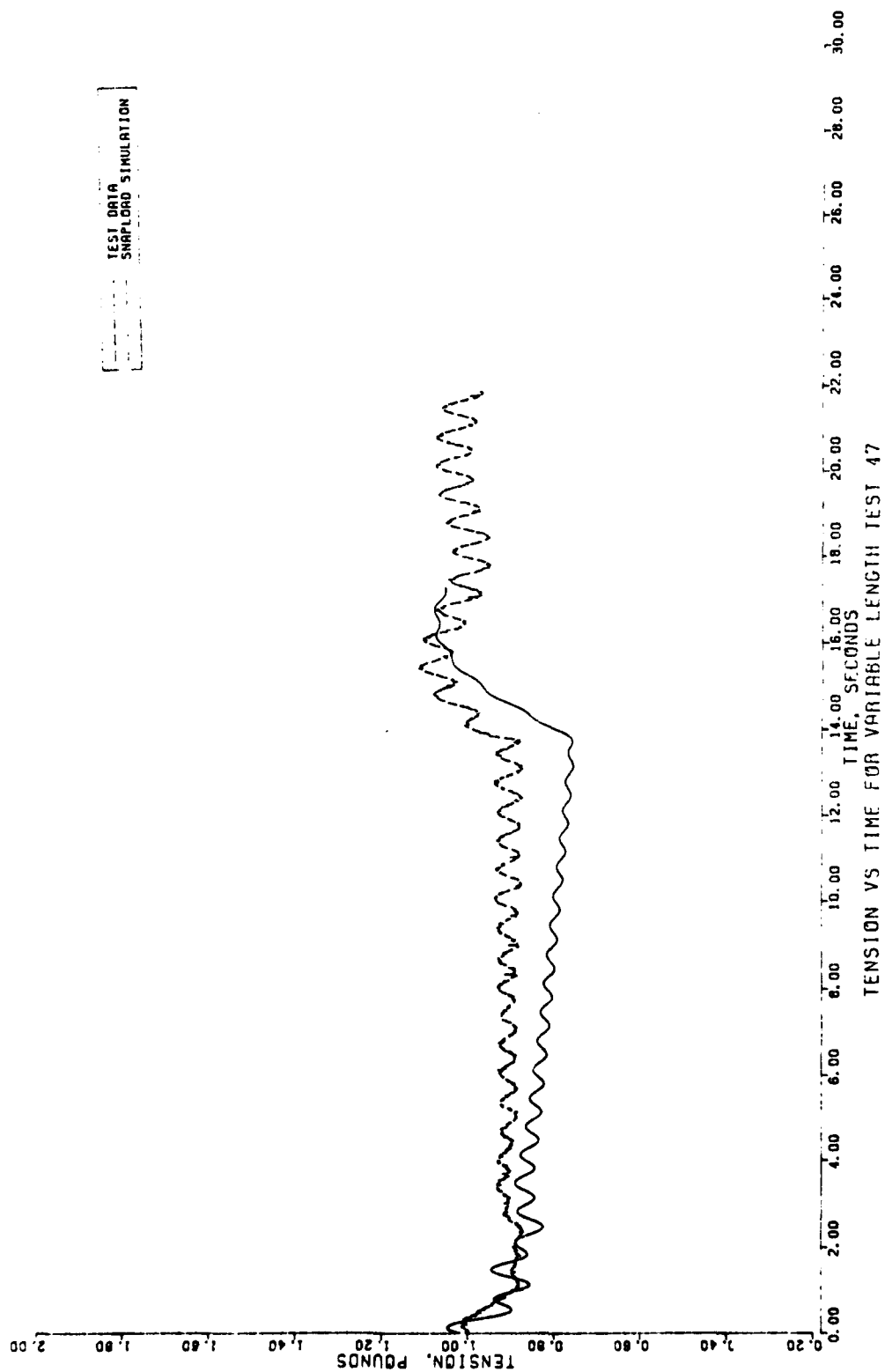
Figure 4-64. Tension Vs Time For Variable Length Test 47 (SNAPLOAD)

TEST DATA
SEADYN SIMULATION

TENSION VS TIME FOR VARIABLE LENGTH TEST 48

TIME, SECONDS

0.00 2.00 4.00 6.00 8.00 10.00 12.00 14.00 16.00 18.00 20.00 22.00 24.00 26.00 28.00 30.00

TENSION, POUNDS

0.20 0.40 0.60 0.80 1.00 1.20 1.40 1.60 1.80 2.00
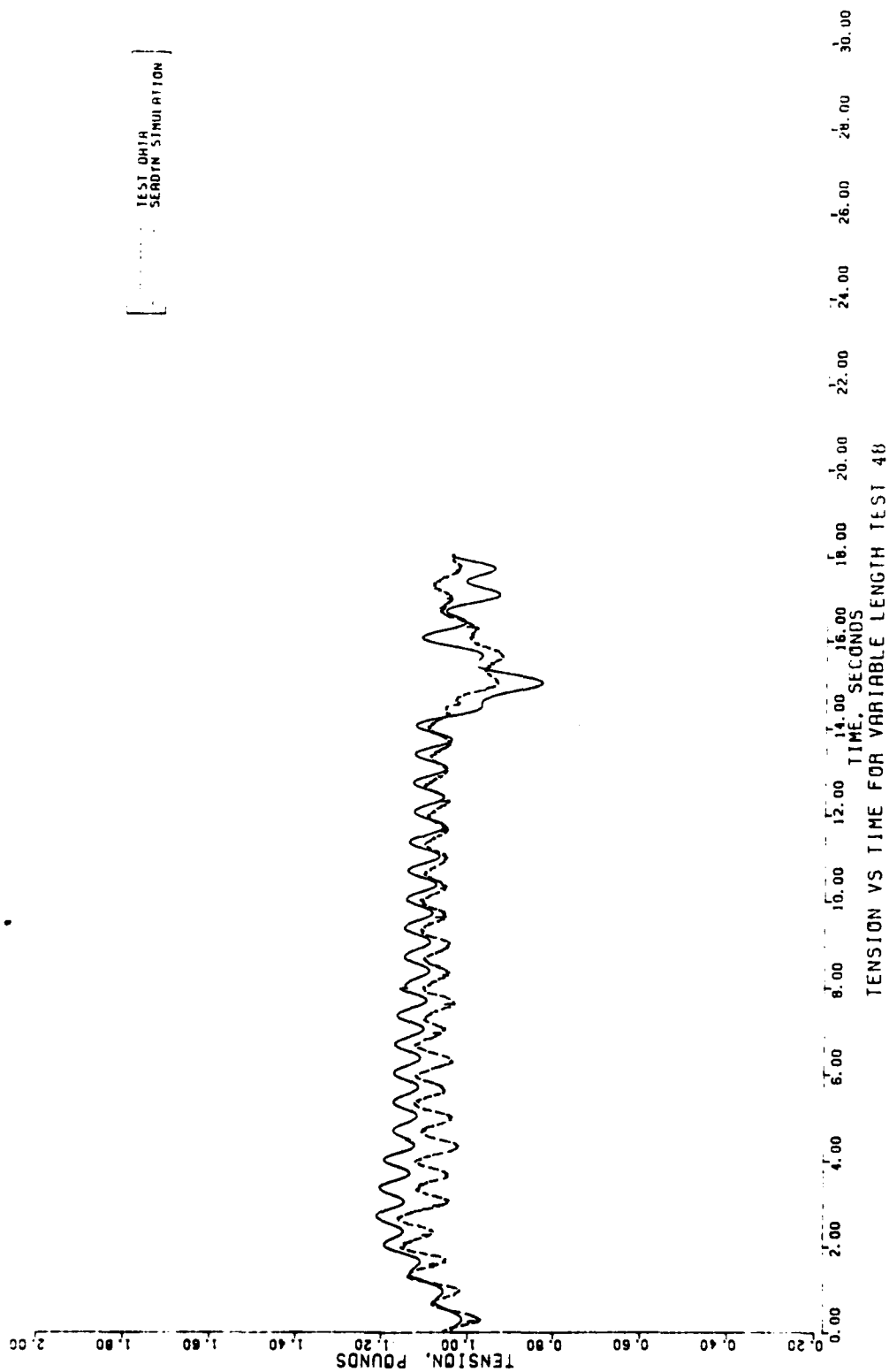
Figure 4-65. Tension Vs Time For Variable Length Test 48 (SEADYN)

SECTION 5

OBSERVATIONS AND CONCLUSIONS

5.1 EXPERIMENTS AND DATA.

Four experiments have been performed that measure the dynamic excitation and response of cable systems in water. These experiments are characterized by size: 6, 60, 2,500 feet, and variable length. The small size experiments are not scale models of their large size systems; they represent small systems in their own right. Each experiment has produced data suitable for evaluating computer models of cable systems. Simple shapes were used in order that the widest range of computer programs would be compatible with the geometry. For the same reason, all the cables were suspended in a vertical plane.

The data from each experiment series have been shown to be rigorous in that the computer models were severely taxed in order to obtain solutions. Some cases are less severe than others: buoy relaxations and simple payout/reel-in do not demand as much as the anchor drops or oscillation with payout or reel-in through a resonance.

Tracking the position of cable points throughout an event was a difficult measurement. The method used for the 6-foot experiment was accurate to within about 8 percent. Selected events in the 60-foot series were found with accuracies estimated to be within 1 or 3 percent of the cable length. Misalignment of the coordinate grid during data reduction could introduce larger errors that were hard to detect. The Mooring Dynamics Experiment (MDE), conducted at sea, relied on acoustic tracking of pingers attached to the mooring. Positions could be measured within about 6 feet when the tracker was "locked" onto a solution. However, the depth measurement could abruptly jump by several hundred feet if the tracker became undecided among multiple solutions.

Tension was the most accurate measurement in all four experiments. The errors seemed greatest in the laboratory tests when the cables were nearly slack. Then residual turbulence in the water and cable stiffness became perceptible. The direction of the tension force was affected more than the magnitude, based on comparing equilibrium measurements from the 60-foot experiment with the static, elastic catenary equations.

Measurement of the size and weight of components was essentially routine. However, the displacement of the model buoy and anchor spheres should not be estimated from their nominal shape.

The nylon and silicon rubber materials used for the laboratory experiments exhibited plastic properties: hysteresis in their load-deflection curves. Creep affected the rubber cable in the variable length experiments. Not only did the winch pay-out cable in a relaxed state and reel it in stretched, but the relaxed length after the reel-in was longer than before the deployment.

Linear cable models require the user to supply an equivalent elastic modulus for plastic cable materials. Furthermore, these experiments have amply demonstrated the importance of internal material damping to the stability of tension calculation in numerical models. Without material damping, the calculated tension shows large irregular variations that appear abruptly in some element and then abruptly shift to another element. For SEADYN, at least, even unrealistically small values of material damping are sufficient to eliminate the undulations. But larger (and, one hopes, correct) values allow the computer to portray the tension accurately even when the cable is oscillated near resonance. This was shown in the variable length cases.

For most ocean cable systems the goal is to avoid resonances. The internal damping of the cable has negligible effect on the design. But it is clear that a reasonably accurate value is important to the design process, enabling the computer models to operate efficiently and portray their results unmasked by spurious values.

The variable length experiments may be an effective procedure to measure material damping and equivalent elastic modulus. The cable length for which SEADYN models resonance is sensitive to the elastic modulus; the amplitude of the resonant tension oscillation computed by SEADYN is sensitive to the material damping parameter. Reference 16 reports the current knowledge of the properties of nylon line. Experiments like the variable length runs with oscillation could be performed for larger sizes in a deep test tank or lake. Very long lengths could be tested at sea, but the frequency analysis would be substantially complicated by the unavoidable wave spectrum.

5.2 THE SEADYN MODEL.

It should be stated at the start and perhaps repeated several times in the discussion below that solutions obtained from the SEADYN model have consistently modeled the major responses of cable systems. It is a point easily stated and easily forgotten in a discussion focussed on the errors of detail in the model comparisons.

SEADYN has been developed significantly during this series of comparisons. Early efforts were devoted to the determination of which solution algorithm applied to which problem. Then the ability of the algorithm to converge to the solution was strengthened. Material damping was added only in time for the last, variable length, series of comparisons; the dramatic improvement in the tension model is apparent. Even small amounts of material damping eliminate the "ringing" that masked the tension in earlier comparisons. The variable length results suggest that the "right" value of damping enables SEADYN to model the tension during resonant oscillation accurately.

There are several other areas of "unfinished business" for the SEADYN model. These do not affect the underlying accuracy of the model, but improve its ability

to model details of dynamic events, its efficiency in obtaining results, and reduce the technical skills required to use the program properly.

Variable length problems require the SEADYN model periodically to add or delete nodes by splitting or merging elements. This is done to keep the variable length elements from becoming too long or short. SEADYN requires a very small time step during this process of changing nodes, called mitosis. The time step size control algorithm in SEADYN does not properly account for this process. The current approach is simply to force the entire problem to run with a small time step. At press time, this problem had been confirmed by other SEADYN users. A coding error was identified and corrected.

A third approach to the mitosis problem was tried that may, with improvement, be useful. The time step algorithm can efficiently reduce the step size for a mitosis: it halves the time step iteratively; but after the mitosis is complete, the recovery to a larger step is very slow. In fact, the model takes as long or longer with this approach as it does when a small step is specified for the entire run. The improvement suggested is to increase the step size faster after a mitosis. This requires that the algoritnm be able to distinguish mitosis from other events requiring step changes. The recent correction may obviate this approach.

There is a small error in the tension that is inherent to the discretization of the continous cable to finite elements. The tension for an element is calculated as the average of the forces applied at its ends. When a node is inserted or removed during mitosis, this average is changed by the weight and drag of the length of cable split off or merged. Step changes in the tension are apparent in the variable length plots, marking the mitosis events. In a cable system of ocean engineering size, these discontinuities are negligible. They can be minimized by using shorter elements if necessary, but there is a cost penalty in execution time.

The algorithm that computes the equilibrium shape of a cable system can find the initial state from very simple approximations given by the user. The anchor last deployments were defined with the cable horizontal and under no tension; the buoy relaxation cables were input as vertical lines. This is a convenient form to define the element lengths.

The treatment of hydrodynamic drag on the cable elements is deficient. The default functions for the drag perpendicular to an element consistently produce insufficient normal drag. The result is that transverse cable motions are too rapid. The variable length experiment was the only series sensitive to tangential drag. It shows that the default functions overpredict these forces.

Examination of the SEADYN code shows that the default drag functions are not coded in the subroutine DRAGCO where they would be expected; indeed, an undocumented set of functions occur there. The only way to avoid the default functions is to write a substitute subroutine named DRAGCO and re-compile the program with it. This requires significant computer skills of the user as well as delays the solution. The user is required to know the FORTRAN computer language, understand the concepts of subroutine and argument, be able to compile the code and link it into the existing SEADYN program. While this procedure is a valid ultimate resource, it should not be required simply to change a drag coefficient.

5-3

These results have shown that SEADYN represents a sound mathematical analysis. Significant progress has been made in developing it from a prototype in the computer laboratory to a production code available for ocean engineers. Finally, repeating the first observation, SEADYN always displayed the characteristic behavior of the cable system in view.

5.3 THE SNAPLOAD MODEL.

SNAPLOAD was used successfuly to model most of the experimental cases studied. Each program should be viewed within its own context rather than by comparison to the results of the other program, because each program was written with different intentions. SNAPLOAD is an attempt to model serially-connected cables suspended in a vertical plane with reasonable accuracy and economy. Inasmuch as the majority of ocean cable systems fall in this class, the potential tradeoff of numerical sophistication against computer economy and user simplicity is attractive. It is "fair", however, to compare the actual cost of using the two programs in these baseline studies. The SEADYN program was steadily updated while these cases were modeled, but very little program maintenance was done on SNAPLOAD.

Although SNAPLOAD is based on a different mathematical analysis than SEADYN, the program demonstrated the same difficulty in modelling tension when inadequate damping was present. The model has a mathematical damping algorithm, but no formula is supplied to relate the mathematical damping parameter to cable properties. The algorithm was intended to stabilize the program during the early seconds of a run; it decays along a "ramp function" whose duration is specified by the user.

SNAPLOAD requires a good initial estimate of the shape of the cable system. Rough estimates require substantial computer time for SNAPLOAD to refine. The crudest estimates (entering the nodes in a horizontal or vertical row for convenience) may not converge at all. This is not a major problem because many programs are available to calculate the equilibrium shape of serial cables in a vertical plane.

One of the premises for SNAPLOAD is that it is easy to use. The node numbering scheme counts by four, and is divided among "major nodes", where cable properties may change and discrete loads inserted, and ordinary nodes that simply divide a cable into parts. A revision is in process to simplify the nomenclature for users.

The hydrodynamic drag coefficients are not specified by the SNAPLOAD user. The normal drag on cables was consistently understated in these runs, allowing both anchor-last deployment simulations and buoy relaxation cases to translate a little too rapidly transverse to the cable axis. The tangential drag coefficient was significant only in the variable length cases. The value coded in the program overpredicts the tangential drag in all these cases.

SNAPLOAD will only run until 170 solution times have been tabulated, because the solution tables are accumulated in the computer core memory. This can be increased by recompiling the program with larger DIMENSION arguments for the arrays used. A better approach involves recoding the program to write the arrays to a binary file.

Cable payout is restricted to cases in which the payout link can accommodate the entire payout length. In the variable length cases, SNAPLOAD computed an extremely small tension in the link adjacent to an inserted node. This abrupt error then destabilized the computation. The variable length cases were revised so that no nodes were inserted during a run. Other users have not reported this problem for "full size" ocean cable systems.

The second premise for SNAPLOAD is that it trades computation economy for reasonable accuracy. However, the algorithm for controlling the time step lacks a minimum step size. There is the risk in any run that an instability early in the run will stall the computation until the computer time allotted for the entire case is exhausted. This can be a substantial waste for long events.

Although SNAPLOAD obtained solutions that modeled the essential events with creditable accuracy in most cases, its potential for widespread use is limited until these drawbacks have been addressed.

One of the attractions for SNAPLOAD users is that it is more economical than SEADYN. Even in the variable length cases reported here, where SNAPLOAD was required to converge to extremely narrow error bounds, it used only one-fifth to one-third the computer time required by SEADYN for equivalent runs. One may expect a greater cost advantage for SNAPLOAD for "easier" cases.

SECTION 6

RECOMMENDATIONS

This series of four experiments provides a basis for evaluating dynamic models of ocean cable structures. The data have been checked by comparison to elementary theory at several points. The data base includes sizes of 6 feet, 60 feet, as well as variable length and the deployment of a scientific mooring in the ocean. The data base should be extended to include the massive components used in ship moorings and other large ocean structures. The value of dynamic modeling with computers is not realized for lightweight moorings. Some specialized scientific moorings may require sophisticated "tuned" moorings in order to make reliable measurements, but the major contribution of dynamic modeling is to reduce the risk of loss or damage to enormously expensive large ocean structures. It is essential that dynamic models be verified for full-size ocean structures.

The models studied in this report have shown that modeling the elastic properties of cables has an important effect on the stability of the models, even in cases where the elastic response of the cable has only a slight effect on the dynamic event itself. Load versus strain data for a wide variety of cable constructions may be available at modest cost from manufacturers willing to release sample results of their routine quality assurance load testing. Material damping data are scarce, and a program to measure the damping of various materials and cable constructions should be developed and implemented. The concept of the variable length experiment is suggested as a technique for finding both the effective elasticity (EA) and material damping factor. The limited experience gained in these few cases is impressive because the results correlated well with elementary spring-mass theory even though the materials used were nonlinear plastics. Furthermore, the method allows water absorbing materials like nylon to be immersed during the test measurement.

Both models have shown that they accurately compute the major features of an event. For both models, however, there is a clear need for a continuing program of maintenance. This does not require full-time attention, but it is essential that a protocol for correcting, completing, and adapting these codes be maintained. Both programs have minor errors that should be corrected. SNAPLOAD has lacked adequate maintenance in the past.

The time step algorithm in SEADYN needs to be adapted to recognize the onset of a "mitosis" event during variable length modeling.

The SEADYN manual is oriented towards the parameters that the user inputs to define a case and the way SEADYN will process it. Each parameter is listed and described in the manual. These descriptions should be expanded, giving the user more guidance in the selection of values to use. This may rely on cataloging what value has worked with which prior case.

An archive of SEADYN input decks for successful problems should be kept, along with annotations of critical parameters. A copy of this archive should accompany the manual sent to new users.

SEADYN is a very general model, both in its mathematical formulation and in the set of options programmed for it. This presents a formidable obstacle to the novice user. Once the basic algorithms have been verified for a suitable variety of problems, it is recommended that a series of programs be written that apply the verified method to smaller classes of problems. One of these should be serially connected cables in a vertical plane, because this is a very common ocean structure. There are several advantages to having a suite of smaller programs to augment the general code. First, the directed purpose reduces the number of options in the code. This results in simpler input, which means the manuals are easier to understand (as well as write). The code itself is more efficient, not only because it may be restricted to planar structures, but also because the time step and convergence limits can be optimized for the kind of problem addressed.

There are several recommendations about drag coefficients:

- Replace the present in-line default drag coefficient functions with calls to subroutine DRAGCO;

- Select new default functions that more closely predict the drag forces;

- Rewrite subroutine DRAGCO in a menu format. That is, provide a list of drag coefficient versus Reynolds Number functions (starting with A + B * (R**C)). Calling arguments include the function number as well as the function coefficients. The above function will handle the most common cases (A + B/R, and B * R**C) by setting C = -1 or A = 0, respectively. The default function number and its coefficients should be programmed in DATA statements using dummy arguments to prevent erasure.

- Provide additional input cards for each cable material. Each card provides the drag coefficient function number, function coefficients A, B, C, etc, as well as the Reynolds Number range limitation. A field on the cable material card itself would show how many drag function cards to read. A zero entry in this field would indicate the default functions. Separate cards would be needed for normal and tangential functions.

6-2

- Some cables generate a third component of hydrodynamic force, transverse to the cable plane. Addition of this detail would be convenient during this revision of the code.

The foremost recommendation for the SNAPLOAD program is that a protocol be established to maintain and update the code. Initial tasks include the following:

- Add an interpreter in the input and output stages so that nodes count by 1 and the ambiguity between links and segements is resolved.

- Provide a minimum time step or other "trigger" to stop the program when the algorithm gets stuck.

- Remove the 170 output table limit by using an extra I/O unit.

- Adjust the code so that payout nodes are inserted smoothly, even for laboratory-scale cases.

- Add material damping to the code or modify the mathematical damping so that it relates to the physical damping property.

- Add a new algorithm to calculate the initial cable equilibrium state accurately from an initial user definition as a straight horizontal or vertical line.

- Change the default drag coefficients and add a drag coefficient subroutine as recommended for SEADYN.

- Make other trivial parameters that are fixed constants in the present code user input variables. The fluid density is an example; SNAPLOAD models cables suspended in seawater only.

Finally, the material damping parameter has had such a striking affect in smoothing the tension response for the variable length comparisons, that certain of the comparison cases reported here should be remodeled. In particular, the dual cable suspended load run 133 from the 6-foot series, the deployment simulation run 6 from the 60-foot series, and the MDE deployment were badly affected by the lack of material damping in the initial comparison. The remodeling will verify this assertion. In addition, remodeling the 6-foot case will verify that the development of SEADYN since those comparisons were performed has been consistent with the earlier results.

REFERENCES

1. Dillon, D. B., "An Inventory of Current Mathematical Models of Scientific Data-Gathering Moors", Hydrospace-Challenger, Inc., Feb 1973

2. Meggitt, D. J., P. A. Palo, and E. F. Buck, "Small-Size Laboratory Experiments on the Large Displacement Dynamics of Cable Systems", Volume I, U.S. Navy Civil Engineering Laboratory Technical Memo No. M-44-78-11, June 1978.

    Meggitt, D. J., P. A. Palo, E. F. Buck, and P. Lacroce, "Small-Size Laboratory Experiments on the Large-Displacement Dynamics of Cable Systems", Volume II-A, "Single Point Mooring Relaxation Test Results (Test 1-15)", CEL TM No. M-44-79-1, Oct 1978.

    Meggit, D. J., P. A. Palo, E. F. Buck, and P. Lacroce, "Small-Size Laboratory Experiments on the Large-Displacement Dynamics of Cable Systems", Volume II-C, "Simulated Anchor Last Deployment Test Results (Tests 32-47)", Oct 1978.

    Meggitt, D. J., P. A. Palo, E. F. Buck, and P. Lacroce, "Small-Size Laboratory Experiment on the Large Displacement Dynamics of Cable Systems", Volume II-D, "Bi-Moor Relaxation and Single and Dual Cable Suspended Load Test Results (Tests 50-142)", CEL TM No. M-44-79-1, Oct 1978.

3. Buck, E. F., D. J. Meggitt, "Laboratory Experiments on the Large Displacement Dynamics of Cable Systems", U.S. Navy Civil Engineering Laboratory, Technical Memo No. M-44-78-6, Feb 1978.

4. Graduate Aeronautical Laboratories, California Institute of Technology, "Experimental Study of the Dynamics of Variable-Length Cable Systems", Supplement Volumes II and III, Apr 1979.

5. Meggitt, D. J. and D. B. Dillon, "At-Sea Measurements of the Dynamic Response of a Single-Point Mooring During an Anchor-Last Deployment", U.S. Navy Civil Engineering Laboratories, Technical Memo No. M-44-78-9, Mar 1978.

6. Webster, R. L. "An Application of the Finite Element Method to the Determination of Nonlinear Static and Dynamic Responses of Underwater Cable Structures", Ph.D. thesis, Cornell University, Ithica, N.Y., Jan 1976. Also available General Electric Co., Report TIS R76EMH2, Jan 1976.

7. Liu, F. C. "Snap Loads in Lifting and Mooring Cable Systems Induced by Surface Wave Conditions", U.S. Navy Civil Engineering Laboratories Technical Note Technical Note N-1288, Port Hueneme, Calif., Sep 1973.

8. Walden, E. G., D. H. DeBok, J. B. Gregory, D. J. Meggitt, and W. A. Vachon, "The Mooring Dynamics Experiment - A Major Study of the Dynamics of Buoys in the Deep Ocean", Offshore Technology Conference Paper 2883, May 1977.

9. Vachon, W. A., and J. R. Scholten, "Final Report on the C. S. Draper Laboratory Role in the Mooring Dynamics Experiment", C. S. Draper Laboratory Report R-1093, Apr 1977.

10. Webster, R. L. "Deep Sea Ship Moor User's Manual", Volume I, U.S. Navy Faciliity Engineering Command, Aug 1978.

    Webster, R. L. "Deep Sea Ship Moor User's Manual SEADYN/DSSM", Volume 2, Aug 1978.

    Webster, R. L. "Deep Sea Ship Moor Program Maintenance Manual, SEADYN/DSSM", Volume 3", Aug 1978.

    Webster, R. L. "Deep Sea Ship Moor Acceptance Report SEADYN/DSSM", Volume 4, Aug 1978.

    Webster, R. L. "Deep Sea Ship Moor Final Engineering Report", Volume 5, Aug 1978.

11. Liu, F. C., "SNAPLOAD User's Manual, A Computer Program for the Analysis of Oceanic Cable System", U.S. Navy Civil Engineering Laboratories Technical Memo No. M-44-80-1, Dec 1979.

12. Palo, P. A., "Comparison Between Small-Scale Cable Dynamics Experimental Results and Simulations Using SEADYN and SNAPLG Computer Models", U.S. Navy Civil Engineering Laboratory Technical Memo No. M-44-79-5, Jan 1979.

13. Dillon, D. B., "Mooring Dynamics: Computer Models and Experiments at a Sixty Foot Scale", EG&G Washington Analytical Services Center, Inc., Technical Report 49999-0004, July 1980.

14. Dillon, D. B., "Evaluating the SEADYN Model: Mooring Dynamics Experiment Final" EG&G Washington Analytical Services Center, Inc., Technical Report 4999-0003, Feb 1979.

15. Kahn, L. A. "Variable Length Cable Dynamics: Evaluating the SEADYN and SNAPLOAD Computer Models, EG&G Washington Analytical Services Center, Inc., Technical Report E950-0001, April 1981.

16. Bitting, K. R., "The Dynamic Behavior of Nylon and Polyester Line", U.S. Coast Guard Research and Development Center, Report No. CG-0-31-80, Apr 1980.

APPENDIX A

MODELING MDE EXPERIMENT 5 FOR SEADYN

APPENDIX A

MODELING MDE EXPERIMENT 5 FOR SEADYN

A.1 ASSIGNING THE NODES.

Given an overall length of cable in a system, the user must select the number and location of nodes to be included in his input model. There will usually be a fairly obvious minimum number of nodes, located at cable ends and Y's and where discrete bodies are attached. But more nodes will usually be required in order to express the dynamic curvature of the cable adequately.

However, there is a double penalty extracted for using more nodes. On the one hand, more nodes mean more computation in each "pass" along the cable. On the other hand, more nodes mean shorter elements. There is a direct relationship between element length and time step size. Shorter elements require shorter time steps. The number of time steps required to model a given time interval therefore increases with the number of nodes used in the model. When the user defines more nodes, the computer executes more passes requiring more computation.

The user relies on experience, intuition, and the results of trial runs to concentrate nodes in areas of sharpest curvature.

Figure 2-21 shows the CEL mooring as it was deployed during the MDE. Figure 4-46 shows the mooring as it was modeled for SEADYN. By comparing these figures, it will be seen that nodes were located where one or more instruments were clustered. Long wire rope spans were broken into uniform elements between 100 and 200 feet long.

The center spans were assigned longer elements than the spans near the upper and lower ends, because the cable curvature is greatest near the ends in this problem. Element lengths less than 100 feet were accepted when they could not be avoided, namely, elements 1, 2, and 21 where the node spacing defies the element. Element lengths were made long enough that the transit time for a tension wave along an element is at least 0.01 seconds. This allows a 0.005 second time step to be used in SEADYN without numerical instability.

A.2 NODAL DRAG COEFFICIENT.

The terminal velocity of the combination of nodes 1, 2, and 3 is shown on Figure A-1 by the slope of the depth trace for pinger ALPHA. During the first 2 minutes, the descent speed is 6.14 feet per second. Later in the descent, the drag and buoyancy of other nodes slow the descent perceptibly.
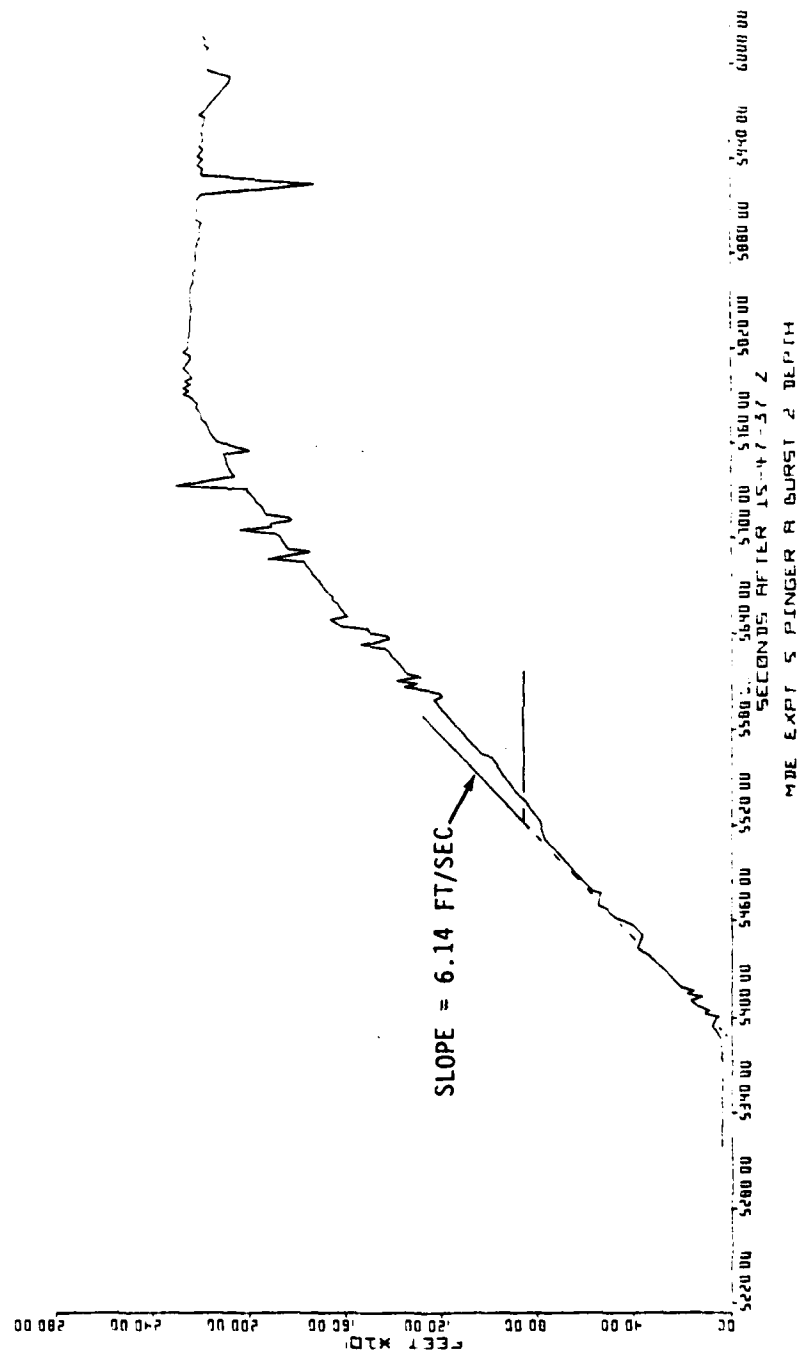
FIGURE A-1   MDE Experiment 5 PINGER A Burst 2 Depth

From Table A-1, the net weight of nodes 1, 2, and 3 is 2600-611-790 = 1199 pounds. Using a familiar hydrodynamic expression in the form

$$C_D \cdot A_T = F/Q,$$

where F is force and Q is dynamic pressure,

gives $\qquad\qquad C_D \cdot A_T = 32.0 \ Ft^2.$

The actual anchor was made of sandbags heaped on a wooden pallet and contained by a coarse net. This irregular shape was approximated by a sphere 4 feet in diameter. The diameter of the sphere was selected to coincide with the length of a side of the pallet. The spherical shape was assumed to approximate the shape of the sandbag pile. SEADYN is able to calculate the added mass coefficients for spheres. Combining the frontal area of the anchor, assumed to be a 4-foot diameter sphere, with the areas of the components in nodes two and three gives

$$A_T = 12.4 + 16.3 + 12.1 = 41 \ ft^2,$$

so that $\qquad\qquad C_D = 32/41 = 0.78.$

It is assumed that this coefficient applies to all the nodes, not only nodes 1, 2, and 3 as computed.

A.3 NODAL WEIGHT.
The weight of each node is simply the sum of the weights of the parts. The weights and dimensions of the MDE components were taken from Table 2-2. Table A-1 shows how these weights were assigned to each node.

An element in SEADYN extends from the center of one node to the center of the next. As shown on Figure 2-16, the actual instruments were inserted in the MDE mooring line, not clamped alongside. Thus, the element lengths tabulated in Figure 4-46 overlap the length of the instruments themselves. The weights of the nodes are adjusted downward to account for the weight of this extra length.

A.4 EQUIVALENT DIAMETERS.
Table A-1 also includes the frontal areas of each nodal component. The equivalent diameter for a spherical node is calculated to give the same frontal area. Note that this diameter must not be used to calculate the "equivalent displacement" volume. That is why the weights used in SEADYN are immersed values.

TABLE A-1. MDE NODAL PARAMETERS

NODE	COMPONENT	WEIGHT (LB.)	FRONTAL AREA (FT²)	EQUIVALENT DIAMETER (FT)
2	Release 1	70.	2.14	
	Release 2	70.	2.14	
	Frame (estimated)	20.	2.00	
	DC Pinger	76.	2.20	
	28" sphere	-847.	7.88	
		<u>611.</u>	<u>16.36</u>	4.56
3	38" Sphere	-847.	7.88	
	DC Pinger	76.	2.20	
	FVR	-4.	1.97	
	Chain Excess*	<u>-15.</u>		
		<u>-790.</u>	<u>12.05</u>	3.92
8, 13	SC Pinger	44.3	1.15	
	FVR	-4.	1.97	
	Chain	10.2	.51	
	Wire Excess*	<u>-.5</u>		
		<u>50.</u>	<u>3.63</u>	2.15
11	T/P	20.0		
	Wire Excess*	<u>.1</u>		
		<u>19.9</u>		.96
21	SC Pinger	44.3	1.15	
	FVR	-4.0	1.97	
	T/P	20.0	0.72	
	Wire Excess*	<u>-.5</u>		
		<u>59.8</u>	<u>3.84</u>	2.21
22	44" Sphere	-1050.		
	Chain Deficit*	<u>4.</u>		
		<u>1046</u>		3.67

* Corrects for excess/deficit in element lengths adjusted to reach center of spherical node.

APPENDIX B

INPUT DATA FOR SEADYN AND SNAPLOAD

VARIABLE LENGTH COMPARISONS

APPENDIX B

INPUT DATA FOR SEADYN AND SNAPLOAD
VARIABLE LENGTH COMPARISONS

Tables B-1 through B-6 show input data decks for the SEADYN comparison runs. The descriptions of the card images correspond to major card description headings in the SEADYN user's manual (Reference 10). Tables B-7 through B-9 show FORTRAN update decks for the SEADYN source code subroutine TVARY. This subroutine describes the time varying moving boundary and payout velocities.

Tables B-10 through B-15 show input data decks for SNAPLOAD. Reference 11 contains the SNAPLOAD user's guide.

Table B-16 is an input deck for SEADYN. It is used to estimate the material damping parameter. The event models a cable slightly stretched between fixed supports. The center node is displaced slightly and abruptly released at the start. The material damping parameter is adjusted in successive runs until the oscillation of the center node decays to half its initial displacement in a certain number of cycles.

TABLE B-1. SEADYN INPUT DECK FOR VARIABLE LENGTH TEST 3

```
VARIABLE LENGTH TEST 3                                         TITLE CARD
   11   0   1   0    10   1    1   0     1   0                  MASTER CONTROL
    2      32.17         .0000177 64.                           PARAMETER CARD
    1   0.          5.0000000 0.          0   0                 NODE CARD
    2   0.          0.0000000 0.          2   2                 NODE CARD
   11  10.          0.0000000 0.          2   2                 NODE CARD
    1   2       1        0   1 0.        -1                      ELEMENT CARD
   10  11       1        0   1 0.        -1                      ELEMENT CARD
    1   .004917 0.000792 1.               1   1                 MATERIAL DATA
 1.        .0075      1.                                        TENSION DATA
    1   0-1.003      .1675                                      ANCHOR DATA
 HEAT  1   1        4    0           0   0     1   0   0        SUBANALYSIS OPTION
 .001     .0001      .0001           0.00      .00             SOLUTION PARAMETERS
 DYN   0   1        5    0           0   0     1   0  -2   20   10   SUBANALYSIS OPTION
 .001     .00010     .00010          10   10  1    1         .01       .01   SOLUTION PARAMETERS
 .0010 0.         30.000                                       TIME DATA CARD
    2  1 1.       5.                                            PAYOUT DATA
 END                                                           END CARD
```

B-2

TABLE B-2. SEADYN INPUT DECK FOR VARIABLE LENGTH TEST 12

```
VARIABLE LENGTH TEST 12                                   TITLE CARD
13   0   1   0   12   1    1   0              MASTER CONTROL
 2  32.17      .0000177  64.                  PARAMETER CARD
 1   0.        55.00833330.    0    0   0     NODE CARD
 2   0.        50.00833330.    0    0   0     NODE CARD
12  10.        0.0083333 0.    2    2   2     NODE CARD
13  10.        0.0083333 0.    2    2   2     NODE CARD
 1   1   2   1            -1                  ELEMENT CARD
12  12  13   1            -1                  ELEMENT CARD
 1   0  .004917  0.000792  1.   1    1        MATERIAL DATA
 1.       0-1.003   1.                        TENSION DATA
 1  .0075   .1675                             ANCHOR DATA
DEAD  1   1   4   0        0    1    1   0     SUBANALYSIS OPTION
.001   .0001   0   .0001  .00   0         0   SOLUTION PARAMETERS
DYN   0   1   5   0        1    1    1   0  -2   20   10   SUBANALYSIS OPTION
.001   .00010       .00010 .01           .01  SOLUTION PARAMETERS
.001000   0.     33.000    2.0083333  1       TIME DATA CARD
12   0      00.    10   1   1                 MOVED NODE
12  11-1.   5.                                PAYOUT DATA
END                                           END CARD
```

B-3

TABLE B-3. SEADYN INPUT DECK FOR VARIABLE LENGTH TEST 23

```
VARIABLE LENGTH TEST 23                                          TITLE CARD
10   0   1   9   1   1   1   1   0                                MASTER CONTROL
2        32.17    .0000177   64.                                 PARAMETER CARD
1    0.     5.0083333   0.    0   0   0                          NODE CARD
2    0.     0.0083333   0.    2   2   2                          NODE CARD
10   10.    0.0083333   0.    2   2   2                          NODE CARD
1    1    2    1    0    10.   -1   -1                            ELEMENT CARD
9    9    10   1    0    10.   -1   -1                            ELEMENT CARD
1    0  .004917  0.000792   1.    1   1                          MATERIAL DATA
1.       .0075      1.0                                          TENSION DATA
1    0-1.003     .1675                                           ANCHOR DATA
HEAD  1    1    4    0    0    0    1    0                        SUBANALYSIS OPTION
.001     .0001    .0001                                          SOLUTION PARAMETERS
DYN   0    1    5    0    .00   0    1   -1   -2   20   3         SUBANALYSIS OPTION
.001     .00010    33.000   .00                                  SOLUTION PARAMETERS
.0005  0.      00.    2.0083333   .01       .01                  TIME DATA CARD
2    1    1.    5.     8    1                                    MOVED NODE
                                                                 PAYOUT DATA
END                                                              END CARD
```

B-4

TABLE B-4. SEADYN INPUT DECK FOR VARIABLE LENGTH TEST 29

```
VARIABLE LENGTH TEST 29                              TITLE CARD
7    0    1    0    6    1    1    0    1    1    0   MASTER CONTROL
2    32.17    .0000177  64.    1    0    0           PARAMETER CARD
1    0.    5.0000000   0.    2    2    2             NODE CARD
2    0.    0.0000000   0.    2    2    2             NODE CARD
7    10.    0.0000000   0.    1    0                 NODE CARD
1    1    2    1    0    1   0.   -1   -1            ELEMENT CARD
6    7    1    0    1   0.   -1   -1                 ELEMENT CARD
1    0   .013250  0.009200   1.    1    1            MATERIAL DATA
.33.5    .1355   0.40   .1675                        TENSION DATA
1    0-1.003                                         ANCHOR DATA
ILAD    1    1    4    0    0                         SUBANALYSIS OPTION
.001    .0001   .0001    0    -2   20   10           SOLUTION PARAMETERS
DYN     0    1    5    0    0    1   0   0            SUBANALYSIS OPTION
.001    .00010  .00010  .00  .00   .01               SOLUTION PARAMETERS
.0100   0.   18.000    5    1    1                   TIME DATA CARD
2    1 1.    5.                                       PAYOUT DATA
END                                                  END CARD
```

TABLE B-5. SEADYN INPUT DECK FOR VARIABLE LENGTH TEST 47

```
VARIABLE LENGTH TEST 47                                          TITLE CARD
7      0    1   0    6   1   1    1   0                          MASTER CONTROL
2    32.17      .0001177  64.                                    PARAMETER CARD
1    0.      5.0833333  0.         0   2   0                     NODE CARD
2    0.      0.0833333  0.         0   2   2                     NODE CARD
7    7.      0.0833333  0.         0   2   2                     NODE CARD
1     2     1     0    1   0.   -1                               ELEMENT CARD
6     7     1     0    1   0.   -1                               ELEMENT CARD
1   0  .01?50  0.009200  1.       1   1                          MATERIAL DATA
.333    .1355     .40                                            TENSION DATA
1   0-1.003     .1675                                            ANCHOR DATA
DEAD   1   1     4    0      0                                   SUBANALYSIS OPTION
.001    .0001      .0001                                         SOLUTION PARAMETERS
DYN    0   1     5    0    .00    0   1   1   0   -2   20   3     SUBANALYSIS OPTION
.001     .00010     .00010    .00   .00  2.0833333        .01    SOLUTION PARAMETERS
.0100   0.      25.000        1   5   1   1                      TIME DATA CARD
2   0      00.                                                   MOVED NODE
2   1  1.      5.                                                PAYOUT DATA
END                                                              END CARD
```

B-6

TABLE B-6.   SEADYN INPUT DECK FOR VARIABLE LENGTH TEST 48

```
VARIABLE LENGTH TEST 48
   8   0   1   0   7   1      1      0    1   1   0    TITLE CARD
   2  32.17      .0000177  64.             0           MASTER CONTROL
   1   0.      30.00000000.      0    0   0  0          PARAMETER CARD
   7  10.       0.0000000 0.     2    2   2  2          NODE CARD
   8  10.       0.0000000 0.     2    2   2  2          NODE CARD
   1   2       1      0  10.    -1                      NODE CARD
   7   8       1      0  10.    -1                      ELEMENT CARD
   1   0 .013250  0.009200  1.        1                 ELEMENT CARD
 .333   .1355     .4                                    MATERIAL DATA
   1   0-1.003  .16/5                                   TENSION DATA
 DLEN   1   1      4    0      0                         ANCHOR DATA
 .001      .0001  .0001                                 SUBANALYSIS OPTION
 DYR    0   1      5    0  .00      0    1  1   0  -2  20  10   SOLUTION PARAMETERS
 .001      .00010  22.000  .00          .01  .01        SUBANALYSIS OPTION
 .010000   0.      00.     2.0833333                    SOLUTION PARAMETERS
   1   5   1                                            TIME DATA CARD
   7   6-.714  5.          5    1                       MOVED NODE
 INH                                                    PAYOUT DATA
                                                        END CARD
```

B-7

TABLE B-7. SEADYN SUBROUTINE TVARY STATEMENTS FOR
VARIABLE LENGTH TESTS 3 AND 12

```
*IDENT LK1024
C    TVARY UPDATES FOR TEST 3
*D TVARY.6,8
       IF(I.EQ.2) GO TO 600
       IF(T.GE.0.0.AND.T.LE.2.2) F=.8136*T
       IF(T.GT.2.2.AND.T.LE.23.2) F=1.78992
       IF(T.GT.23.2.AND.T.LE.25.4) F=.8136*(25.4-T)
       IF(T.GT.25.4) F=0.
       RETURN
   600 F=COS(15.708*T)
       RETURN
   100 CONTINUE
```

```
*IDENT LK1024
C    TVARY UPDATES FOR TEST 12
*D TVARY.6,8
       IF(I.EQ.2) GO TO 600
       F=0.
       IF(T.GT.4.0.AND.T.LE.6.) F=.8925*T-3.57
       IF(T.GT.6.0.AND.T.LE.29.2) F=1.785
       IF(T.GT.29.2.AND.T.LE.29.8) F=2.98333*(29.8-T)
       IF(T.GT.29.8) F=0.
       RETURN
   600 F=COS(15.708*T)
       RETURN
   100 CONTINUE
```

TABLE B-8.   SEADYN SUBROUTINE TVARY STATEMENT FOR
VARIABLE LENGTH TESTS 23 AND 29

```
*IDENT LK1024
C    TVARY UPDATES FOR TEST 23
*D TVARY.6,8
       IF(I.EQ.2) GO TO 600
       F=0.
       IF(T.GT.4.0.AND.T.LE.6.) F=.8925*T-3.57
       IF(T.GT.6.0.AND.T.LE.30.4) F=1.785
       IF(T.GT.30.4.AND.T.LE.31.2) F=2.23125*(31.2-T)
       IF(T.GT.31.2) F=0.
       RETURN
   600 F=COS(15.708*T)
       RETURN
   100 CONTINUE
```

```
*IDENT LK1024
C    TVARY UPDATES FOR TEST 29
*D TVARY.6,8
       IF(I.EQ.2) GO TO 600
       IF(T.GE.0.0.AND.T.LE..8) F=2.57*T
       IF(T.GT..8.AND.T.LE.13.5) F=2.056
       IF(T.GT.13.5.AND.T.LE.14.0) F=4.112*(14.0-T)
       IF(T.GT.14.0) F=0.
       RETURN
   600 F=COS(15.708*T)
       RETURN
   100 CONTINUE
```

```
*IDENT LK1024
C    TVARY UPDATES FOR TEST 47
*D TVARY.6,8
      IF(I.EQ.2) GO TO 600
      F=0.
      IF(T.GT.4.0.AND.T.LE.6.) F=T-4.
      IF(T.GT.6.0.AND.T.LE.17.6) F=2.
      IF(T.GT.17.6.AND.T.LE.18.1) F=4.*(18.1-T)
      IF(T.GT.18.1) F=0.
      RETURN
  600 F=COS(9.4248*T)
      RETURN
  100 CONTINUE
```

```
*IDENT LK1024
C    TVARY UPDATES FOR TEST 48
*D TVARY.6,8
      IF(I.EQ.2) GO TO 600
      F=0.
      IF(T.GT.4.0.AND.T.LE.6.) F=T-4.
      IF(T.GT.6.0.AND.T.LE.18.2) F=2.
      IF(T.GT.18.2.AND.T.LE.18.7) F=4.*(18.7-T)
      IF(T.GT.18.7) F=0.
      RETURN
  600 F=-SIN(9.4248*T)
      RETURN
  100 CONTINUE
```

TABLE B-10. SNAPLOAD INPUT DECK FOR VARIABLE LENGTH TEST 3

VARIABLE LENGTH TEST 3

SINGLE	FREE	NONFF	READ	PAYOUT	
.00001					TITLE CARD
00.	30.	.01	.001	.00001	.00001	OPTION SELECT
.0001	99999.	0.	0.	5.		STATIC CONTROL
0.	100.	21.	0.			DYNAMIC TIME CARD
.8136	1.78992	-.8136				DYNAMIC INSTABILITY
100.	0.					SURFACE CARD
3	0					PAYOUT CARD
1	2					ELEVATION BOUNDARY
2	1					CURRENT POINTS
.5	.47	.47	1.1	1.003	.0218	.0218	0.	CURRENT PROFILE
2.5	.0027262	.059	.000792	0.	48785.	CABLE DIVISION CARD
2.5	50.	50.	0.	0.	97.5	NUMBER OF SEGMENTS
0.	0.	95.	0.	0.		END PAYLOAD
0.	0.	100.				SEGMENT DATA
						HALF SEGMENTS
						INITIAL POSITION
						INITIAL POSITION
						PLOT OUTPUT
						BLANK TITLE

B-11

TABLE B-11. SNAPLOAD INPUT DECK FOR VARIABLE LENGTH TEST 12

SINGLE	FREE	NONFF	READ	SINE	REELIN	Card
VARIABLE LENGTH TEST 12						TITLE CARD
SINGLE	FREE	NONFF	READ	SINE	REELIN	OPTION SELECT
.00001						STATIC CONTROL
00.	34.	.01	.001	.00001	.00001	DYNAMIC TIME CARD
.0001	99999.	00.	00.5	5.		DYNAMIC INSTABILITY
0.	100.					SURFACE CARD
-.8925	-1.785	2.98333	23.2	4.		REELIN CARD
100.	0.					ELEVATION BOUNDARY
0.	.00833333	15.708				EXCITATION CARD
0.						CURRENT POINTS
0.						CURRENT PROFILE
1	4					CABLE DIVISION CARD
4	4					NUMBER OF SEGMENTS
.5	.47	.47	1.1	1.003	.0218	0. 9.	END PAYLOAD
5.0	.0027262	.059	5.	.000792	48785.	8.75	SEGMENT DATA
5.	5.	45.	8.75	8.75	8.75	50.0	HALF SEGMENTS
0.	0.	60.	0.	0.	0.	73.75	INITIAL POSITION
0.	.	91.25	0.			100.	INITIAL POSITION
0.	0.		0.				INITIAL POSITION
						PLOT OUTPUT
						BLANK TITLE

TABLE B-12. SNAPLOAD INPUT DECK FOR VARIABLE LENGTH TEST 23

				NONFF	READ	SINE	PAYOUT	
VARIABLE LENGTH TEST 23								TITLE CARD
SINGLE	FREE							OPTION SELECT
.00001								STATIC CONTROL
00.	34.	.01		.001	.00001			DYNAMIC TIME CARD
.0001	99999.	00.		00.5	5.			DYNAMIC INSTABILITY
0.	100.							SURFACE CARD
.8925	1.785	-2.23125	15.708	24.4	4.			PAYOUT CARD
100.	0.							ELEVATION BOUNDARY
0.	.00833333	15.708						EXCITATION CARD
0								CURRENT POINTS
0								CURRENT PROFILE
1	2							CABLE DIVISION CARD
1								NUMBER OF SEGMENTS
.5	.47	.47		1.003	.0218	0.	0.	END PAYLOAD
2.5	.0027262	.059		.000792	48785.			SEGMENT DATA
2.5	50.	50.		0.				HALF SEGMENTS
0.	0.	95.		0.	0.	97.5		INITIAL POSITION
0.	0.	100.						INITIAL POSITION
								PLOT OUTPUT
								BLANK TITLE

B-13

TABLE B-13. SNAPLOAD INPUT DECK FOR VARIABLE LENGTH TEST 29

```
                                      NONFF      READ      PAYOUT
VARIABLE LENGTH TEST 29                                              TITLE CARD
SINGLE  FREE                                                         OPTION SELECT
.00001                                                               STATIC CONTROL
00.      18.       .01      .001      .00001    .00001              DYNAMIC TIME CARD
.0001    99999.    0.       0.        5.                            DYNAMIC INSTABILITY
0.       100.                                                        SURFACE CARD
2.57     2.056    -4.11     12.7      0.        0.                  PAYOUT CARD
100.     0.                                                          ELEVATION BOUNDARY
0    1    2                                                          CURRENT POINTS
0    2    1                                                          CURRENT PROFILE
                                                                     CABLE DIVISION CARD
                                                                     NUMBER OF SEGMENTS
.5     .47    1.1      1.003     .0218     .0218     0.             END PAYLOAD
2.5    .0198556   .159    .009200   .0006     123.77              SEGMENT DATA
2.5    50.    50.      0.        0.        0.        97.5          HALF SEGMENTS
0.     0.     95.                                                   INITIAL POSITION
0.     0.     100.                                                  INITIAL POSITION
                                                                     PLOT OUTPUT
                                                                     BLANK TITLE
```

B-14

TABLE B-14. SNAPLOAD INPUT DECK FOR VARIABLE LENGTH TEST 47

```
VARIABLE LENGTH TEST 47                                 TITLE CARD
SINGLE   FREE          NONFF   READ    SINE   PAYOUT    OPTION SELECT
.00001                                                  STATIC CONTROL
00.      26.     .01   .001    .00001                   DYNAMIC TIME CARD
.0001    99999.  00.   00.5    5.                        DYNAMIC INSTABILITY
0.       100.          0.                               SURFACE CARD
1.       2.000   -4.   11.6    4.                        FAYOUT CARD
100.     0.                                             ELEVATION BOUNDARY
0.   0.0833333 9.4248                                   EXCITATION CARD
0                                                       CURRENT POINTS
0                                                       CURRENT PROFILE
1    2                                                  CABLE DIVISION CARD
2    1                                                  NUMBER OF SEGMENTS
.5   .47      1.1    1.003   .0218    0.      0.         END PAYLOAD
2.5  .0198556 .159   .0092   .0006    123.77            SEGMENT DATA
2.5  50.      50.                                       HALF SEGMENTS
0.   0.       95.    0.      0.       97.5              INITIAL POSITION
0.   0.       100.                                      INITIAL POSITION
0.                                                      PLOT OUTPUT
0.                                                      BLANK TITLE
```

B-15

```
VARIABLE LENGTH TEST 48                                 TITLE CARD
SINGLE   FREE           NONFF     READ     SINE    REELIN   OPTION SELECT
.00001                                                  STATIC CONTROL
00.      22.    .01     .0001     .0001                 DYNAMIC TIME CARD
.0001    99999. 00.     00.5      5.       .0001        DYNAMIC INSTABILITY
0.       100.                                           SURFACE CARD
-1.      -2.000 4.      12.2      4.                    REELIN CARD
100.     0.0833333 9.4248                               ELEVATION BOUNDARY
0.                                                      EXCITATION CARD
0.                                                      CURRENT POINTS
0.                                                      CURRENT PROFILE
  1   5                                                 CABLE DIVISION CARD
  5   5                                                 NUMBER OF SEGMENTS
.5   .47  .47    1.003    .0218    0.       0.          END PAYLOAD
.5   .0198556 .159   .0092   123.77   7.     6.5        SEGMENT DATA
.5   .5   .5     .5      7.                             HALF SEGMENTS
3.5                                                     HALF SEGMENTS
0.   0.   70.    0.      0.       70.5                  INITIAL POSITION
0.   0.   71.5   0.      0.       72.5                  INITIAL POSITION
0.   0.   80.    0.      0.       93.5                  INITIAL POSITION
0.   0.   100.   0.      0.                             INITIAL POSITION
                                                        PLOT OUTPUT
                                                        BLANK TITLE
```

TABLE B-16. SEADYN INPUT DECK FOR ESTIMATING MATERIAL DAMPING

```
MATERIAL DAMPING RUN
3    0    1    0    2    1    0    0    0    1    1    0
2    032.17    0.    10.2    0.    .000168    1    .0765
1    0.    5.    0.    1    1    0    1
2         1    -2    5.
3    0.    0.    1    -2    5.
1    2    1    0    1    1    1
2    3    1    0
1    0    .000792    0.004917    1.
1.00    .0075    1.00
DEAD    1    1    4    0    1
.001    .0001    .0001
DEAD    1    1    4    0    1    0    0    1
.001    .0001    .0001
2    2.05
DYN    0    1    5    0    0    0    0    0    0    -1    20
.001    .00005    .00005    .00    .00
.0050    0.    2.50    .020
END
1234567890123456789012345678901234567890123456789012345678901234567890
         1         2         3         4         5         6         7
```

DATE
FILME
−8